EVALUATION OF ALGINATE MAGNETIC NANOPARTICLE BEADS FOR IMMOBILIZATION OF QUORUM QUENCHING BACTERIA ISOLATED FROM DAIRY INDUSTRY WASTEWATER TO ALLEVIATE BIOFOULING

Thesis Submitted to the Central University of Punjab

For the award of

Doctor of Philosophy

In

Centre for Environmental Science and Technology

By
Jaskiran Kaur

Supervisor

Dr. Yogalakshmi K.N.

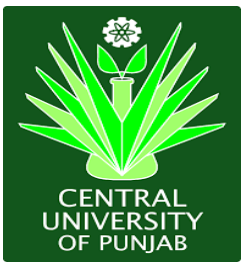

Centre for Environmental Science and Technology
School of Environment and Earth Sciences
Central University of Punjab, Bathinda

August, 2019

CERTIFICATE

I declare that the thesis entitled “Evaluation of alginate magnetic nanoparticle beads for immobilization of quorum quenching bacteria isolated from dairy industry wastewater to alleviate biofouling" has been prepared by me under the supervision of Dr. Yogalakshmi K.N., Assistant Professor, Centre for Environmental Science and Technology, School of Environment and Earth Sciences, Central University of Punjab, Bathinda. No part of this thesis has formed the basis for the award of any degree or fellowship previously.

Jaskiran Kaur
Centre for Environmental Science and Technology
School of Environment and Earth Sciences
Central University of Punjab, Bathinda - 151001
Date:

CERTIFICATE

I certify that JASKIRAN KAUR has prepared her thesis entitled “EVALUATION OF ALGINATE MAGNETIC NANOPARTICLE BEADS FOR IMMOBILIZATION OF QUORUM QUENCHING BACTERIA ISOLATED FROM DAIRY INDUSTRY WASTEWATER TO ALLEVIATE BIOFOULING”, for the award of Ph.D. degree of the Central University of Punjab, under my guidance. She has carried out this work at the Centre for Environmental Science and Technology, School of Environment and Earth Sciences, Central University of Punjab, Bathinda.

Dr. Yogalakshmi K.N.
Centre for Environmental Science and Technology
School of Environment and Earth Sciences
Central University of Punjab, Bathinda - 151001
Date:

ABSTRACT

Evaluation of alginate magnetic nanoparticle beads for immobilization of quorum quenching bacteria isolated from dairy industry wastewater to alleviate biofouling

Name of the student	: Jaskiran Kaur
Registration Number	: CUP/M.Ph-Ph.D/SEES/EVS/2010-11/02
Degree for which submitted	: Doctor of Philosophy
Name of the supervisor	: Dr. Yogalakshmi K.N.
Name of Centre	: Environmental Science and Technology
Name of School	: Environment and Earth Sciences
Key words	: Membrane bioreactor, Membrane biofouling, Quorum sensing, Acyl homoserine lactone, Quorum quenching, Immobilization, Magnetic iron nanoparticles

Membrane fouling is one of the prominent problem of membrane bioreactors (MBR) during wastewater treatment. Biofouling caused by the bacterial biofilm formation on the membrane surface is considered as one of the major contributor of the overall membrane fouling process. Reduction in hydraulic performance; increase in transmembrane pressure (TMP) and shortening of membrane's life span are some of the widely encountered adverse effects of biofouling on membrane systems. Various approaches including membrane backwashing, cleaning of membranes employing numerous chemicals, variation in hydrodynamic conditions and membrane modification have been explored to mitigate fouling. But membrane biofouling being a complex multistage process is not effectively eradicated by these approaches. Additionally, the problems of chemical toxicity, foulant accumulation within membrane pores also facilitates the need for development of effective technologies for biofouling control.

Bacterial acyl homoserine (AHL) based quorum sensing (QS) mechanism is considered as the regulatory phenomenon for biofilm formation. However, these signalling molecules are disrupted by a special group of bacteria termed the quorum quenching bacteria through the phenomena of quorum quenching (QQ). This phenomenon has been recognized as a promising method to control the problem of membrane biofouling. The QQ bacteria co-exist with the QS bacteria in a wide variety of habitats including rhizosphere, sewage, soil and many other sources but the occurrence of QQ bacteria in dairy waste activated sludge (WAS) remains unexplored. Keeping this in view, an attempt has been made to investigate the potential of QQ bacteria isolated from the dairy WAS collected from Verka milk industry effluent treatment plant situated in Bathinda, Punjab. The QQ bacteria showing higher AHL degrading potential was chosen to alleviate biofouling in MBR. Since, the bacteria are known to have low survival rate in the free-state, they were

immobilized onto the magnetic iron nanocomposite carriers. The nanoparticles in the magnetic nanocomposite beads possessed enough magnetic strength to enable their easy separation from the MBR during operation.

The QQ bacteria present in dairy WAS was enriched in the KG medium supplemented with n-hexanoyl homoserine lactone (C6-HSL) as a sole source of carbon and nitrogen. Five bacterial isolates obtained after enrichment were identified as *Klebsiella pneumoniae* (JYQ1 and JYQ5), *Acinetobacter baumannii* JYQ2, *Pseudomonas nitroreducens* JYQ3, and *Pseudomonas* JYQ4 through 16S ribosomal deoxyribonucleic acid (16S rDNA) analysis. These isolates were submitted in Genbank under accession numbers KP189202 (JYQ1), KP340458 (JYQ2), KP340459 (JYQ3), KU555415 (JYQ4), and KP780263 (JYQ5).

The C6-HSL degrading ability of the isolated QQ bacteria was determined quantitatively and qualitatively through biosensor (using *Chromobacterium violaceum* CV026) assay and GC-MS analysis, respectively. All the five isolates exhibited decolourization zone around the *Chromobacterium violaceum* CV026 spotted lawns indicating C6-HSL degradation. Maximum degradation percentage of 83.8% was shown by *Pseudomonas* JYQ4 within 6 h of incubation. Other isolates *Klebsiella pneumoniae* JYQ1 and JYQ5 showed around 81.5% and 81.4% of C6-HSL degradation, respectively within 24 h of incubation. *Pseudomonas nitroreducens* JYQ3 degraded 68.4% of C6-HSL in 12 h of exposure. The isolate *Acinetobacter baumannii* JYQ2 possessed both QS and QQ activity which is evident from its degradation percentage. The isolates *Klebsiella pneumoniae* JYQ1 and JYQ5 due to their pathogenic nature were exempted and the other three QQ bacterial isolates (*Acinetobacter baumannii* JYQ2, *Pseudomonas nitroreducens* JYQ3 and *Pseudomonas* JYQ4) were immobilized onto the IMN beads by encapsulating magnetic iron nanoparticles and QQ bacteria in sodium alginate mixture.

The magnetic iron nanoparticles prepared by co-precipitation method were cubical in shape and ranged in size from 5-19 nm. The FTIR analysis indicated the presence of Fe and O functional groups in the nanoparticles. The nanoparticles exhibited polycrystalline structure with crystallite size of around 6.9 nm and saturation magnetization of 39 emu g^{-1}. The successful immobilization of QQ bacteria onto the magnetic nanocomposite beads was confirmed through the SEM analysis. The QQ bacteria IMN beads also showed C6-HSL degradation potential. Confirming the preliminary studies, the *Pseudomonas* JYQ4 IMN beads exhibited the maximum C6-HSL degradation of 90% within 6 h of incubation when compared to other isolates whose degradation percentage varied in the range between 73- 90%. The IMN beads of bacterial consortium (prepared by mixing JYQ2, JYQ3 and JYQ4) showed degradation percentage of 73.9%.

The efficiency of QQ bacteria IMN beads in controlling the biofilm developed by *Pseudomonas aeruginosa* 3541 was then assessed. The SEM analysis demonstrated the growth of less number of bacterial cells on the surface of QQ IMN beads incubated membranes when compared to control. Among the different QQ IMN beads, *Pseudomonas* JYQ4 IMN beads indicated better biofilm reduction ability. Furthermore, the CLSM analysis confirmed the efficiency of QQ bacteria IMN beads in controlling the biofilm growth and development when compared to control which exhibited signs of *Pseudomonas aeruginosa* 3541 biofilm maturation in 10

days. Among the different QQ bacteria and consortium IMN beads incubated membranes, *Pseudomonas* JYQ4 IMN beads incubated membranes showed no signs of biofilm maturation till 30 days of incubation. The isolates *Acinetobacter baumannii* JYQ2 and consortium incubated membrane showed signs of biofilm maturation within 20 days, respectively unlike *Pseudomonas nitroreducens* JYQ3 that showed biofilm maturation in 30 days. The biofilm structural elucidation by COMSTAT software further supported the results of CLSM analysis by showing less biomass (0.015± 0.001 $\mu m^3/\mu^2$) and more surface to biovolume ratio (0.93± 0.003 $\mu m^2/\mu^3$) for biofilm developed by *Pseudomonas aeruginosa* 3541 in 30 days incubation period with *Pseudomonas* JYQ4 IMN beads when compared to control membrane that showed biomass volume of 0.06± 0.003 $\mu m^3/\mu^2$ and surface to biovolume ratio of 0.21± 0.005 $\mu m^2/\mu^3$. Microcolony development and biofilm growth is indicated by more biomass volume and lesser surface to biovolume ratio. Further, the flux measurement of the incubated membranes confirmed the delayed biofilm formation in membranes incubated with *Acinetobacter baumannii* JYQ2, *Pseudomonas nitroreducens* JYQ3, *Pseudomonas* JYQ4 and consortium IMN beads that showed 10.4%, 17.7%, 20.3% and 8.1% higher flux, respectively compared to control.

The potential of QQ bacteria IMN beads in controlling the biofilm formation by the sludge bacteria was also tested. The light microscopy analysis of glass slides incubated with QQ bacteria IMN beads revealed a significant reduction in the number of sludge bacterial cells when compared with the control slide (without IMN beads). *Pseudomonas* JYQ4 IMN beads were more efficient in controlling biofilm formation followed by *Pseudomonas nitroreducens* JYQ3, *Acinetobacter baumannii* JYQ2 and consortium. The CLSM analysis of the QQ bacteria IMN beads incubated membranes exhibited the less amount of biofilm on the membranes compared to control. Similar to *Pseudomonas aeruginosa* 3541 studies, *Pseudomonas* JYQ4 delayed the biofilm maturation up to 30 days showing better biofilm controlling ability compared to other isolates. The biomass volume and surface to biovolume ratio of sludge bacteria biofilm developed on the *Pseudomonas* JYQ4 IMN beads incubated membrane was calculated to be around 0.019± 0.015 $\mu m^3/\mu^2$ and 0.85± 0.65 $\mu m^2/\mu^3$, respectively. The control 1 (without IMN beads) incubated membranes however, showed biomass volume of 0.065± 0.061 $\mu m^3/\mu^2$ and surface to biovolume ratio of 0.18± 0.14 $\mu m^2/\mu^3$, respectively whereas control 2 (blank nanoparticle beads) incubated membranes showed biomass volume of 0.06± 0.02 $\mu m^3/\mu^2$ and surface to biovolume ratio of 0.16± 0.38 $\mu m^2/\mu^3$, respectively. The flux studies showed that *Pseudomonas* JYQ4 IMN beads incubated membranes showed 22% higher flux followed by *Pseudomonas nitroreducens* JYQ3 (19% higher), *Acinetobacter baumannii* JYQ2 (16% higher) and consortium (12.6% higher) compared to control membranes within 30 days incubation.

The efficiency of the QQ bacteria IMN beads in biofouling control was also investigated in MBR. A submerged aerobic MBR with polyethersulfone hollow fiber membrane of pore size 0.4 µm and working volume of 4.5 L was used for the study. The MBR was operated at hydraulic retention time (HRT) and flux of 8h and 12.5 L/(m^2h), respectively. Synthetic dairy industry wastewater with COD of 4800± 40 mg/L was used as substrate in MBR. The MBR performance was evaluated at three different MLSS (i.e.) 4000, 7000 and 10,000 mg/L. The MBR showed removal efficiencies in the range of 95.6- 99.2% for COD removal; 55.7- 88.4% for TSS removal; 93.6- 94.6% for NH_3-N removal and 25.5- 33.2% for phosphate removal at

the MLSS 4000, 7000 and 10,000 mg/L. The performance of MBR in terms of effluent quality remained the same in QQ-MBR and showed no significant change in removal efficiencies.

The membrane fouling potential at three different MLSS (i.e.) 4000, 7000 and 10,000 mg/L were assessed through tightly bound (TB-EPS), loosely bound (LB-EPS) and soluble EPS polysaccharides and proteins. At MLSS of 4000 mg/L, the polysaccharides and protein fraction in TB-EPS varied between 32- 42.6 mg/L and 34.2- 50.7 mg/L, respectively which increased to 59.9- 71.3 mg/L and 61.6- 80.3 mg/L at 7000 mg/L MLSS; and 76.6- 92.6 mg/L and 85.9- 115.9 mg/L at 10,000 mg/L MLSS. Likewise, the LB-EPS polysaccharides and proteins were in the range of 11.7- 17.7 mg/L and 38.5- 56.1 mg/L at 4000 mg/L MLSS; 25.5- 36.2 mg/L and 81.1- 115.9 mg/L at 7000 mg/L MLSS; and 40.4- 58.5 mg/L and 124.6- 186.5 mg/L at 10,000 mg/L MLSS. The polysaccharides and proteins in soluble EPS also increased with increase in MLSS and was observed to be 23.4- 31.8 mg/L and 30.3- 48.1 mg/L at 4000 mg/L MLSS; 40.2- 53.2 mg/L and 56.3- 75 mg/L at 7000 mg/L MLSS; and 56.4- 72.3 mg/L and 77.9- 101.1 mg/L at MLSS 10,000 mg/L. Among all the EPS, TB-EPS and LB-EPS showed higher levels of polysaccharides and proteins, respectively. TMP also showed continuous increase and reached 29.8 kPa during MLSS 10,000 mg/L.

When the QQ-MBR (*Pseudomonas nitroreducens* JYQ3 and *Pseudomonas* JYQ4 IMN beads) was assessed, it showed decreased EPS production in terms of polysaccharide and protein fractions of TB-EPS, LB-EPS and soluble EPS. During the operation of QQ-MBR at 4000 mg/L, 75.3% and 63.2% decrease in polysaccharide and proteins fractions of TB-EPS was observed compared to that of control MBR. Likewise, the QQ-MBR showed 64% and 77% lower LB-EPS and soluble EPS polysaccharides, respectively. The protein of LB-EPS and soluble EPS decreased by 62.2% and 68.7%, respectively in QQ-MBR at MLSS of 4000 mg/L. At MLSS 7000 mg/L, the polysaccharide in TB-EPS, LB-EPS and soluble EPS reduced by 69.7%, 63.1% and 72.3% when compared to control MBR. Similarly, around 57.3%, 63.4% and 61.7% reduction in the protein fraction of TB-EPS, LB-EPS and soluble EPS, respectively was attained in the QQ-MBR. At MLSS 10,000 mg/L, the QQ-MBR showed a decrease of around 57.3% and 42.7% in TB polysaccharides and proteins fractions, respectively. LB polysaccharides and proteins reduced by 52.2% and 59.5% and soluble polysaccharides and proteins showed a decrease of around 60.7% and 40.3% in the QQ-MBR at 10,000 mg/L MLSS compared to control. Also, the QQ-MBR showed comparatively slower TMP rise than control MBR.
The results concluded that the QQ bacteria *Pseudomonas nitroreducens* JYQ3 and *Pseudomonas* JYQ4 can be used effectively for interrupting the QS mechanism in bacteria for controlling the membrane biofouling problem in MBR.

Jaskiran kaur **Dr. Yogalakshmi K.N.**

ACKNOWLEDGEMENT

First and foremost I pay my heartful thanks to the great Almighty and His guardian angels for being with me throughout and whose blessings provided me the vigorous passion, uninterrupted strength and indispensible help needed to complete my research work successfully.

It's my privilege and honor to express my sincere gratitude to my debonair and energetic supervisor Dr. Yogalakshmi K.N. for her peer support, inexhaustible inspiration and constructive criticism for the accomplishment of the present endeavor. I will remain indebted to her for pruning my personality and giving new dimension in the scientific field through her analytical scientific outlook. I salute her great wisdom and personality. I am also gratified to University Grants Commission for providing me Maulana Azad National Fellowship during whole tenure of my study.

I would like to pay my sincere thanks to Prof. R.K. Kohli, the honorable Vice Chancellor of CUPB, for providing me the entire infrastructure for my research work. It's my proud privilege to express my deep gratitude to Prof. P. Rama Rao, Dean Academic Affairs, Central University of Punjab, Bathinda for his valuable suggestions.

I empathetically extend my sincere thanks to Prof. V.K. Garg, COC, Centre for Environmental Sciences and Technology and the entire faculty of the department Dr. Puneeta Pandey, Dr. MS Dhanya and Dr. Sunil Mittal for their valuable suggestions and tremendous cooperation. I would also thank Dr. J. Nagendra Babu, Assistant Professor, Centre for Chemical Sciences for his help in GC-MS sample analysis. I thank Verka Milk Plant, Bathinda, Punjab for the waste activated sludge sample. I also extend my thanks to Mr. Ashish Pandey for confocal laser scanning microscopy. I pay my regards to Institute Instrumentation Centre, IIT Roorkee for TEM analysis and Sophisticated Analytical Instrumentation Facility, IIT Madras for VSM analysis.

I would like to thank all my lab mates and my friends Manohari, Ravishankar, Gini, Jatinder, Vijay, Rajveer, Satveer, Pooja, Lovlesh, Kanwaljeet, Anu, Anil, Navrattan, Sandeep, Rakesh for their help. I also want to thank Nilesh for his help in XRD and SAED data interpretation.

At last but not the least with generous humbleness, I thank almighty for bestowing me a supportive family, my parents, Sh. Surinder Mohan Singh, Smt. Gurdeep Kaur and my younger sister, Jasmeen Kaur whose extreme sacrifice, support and inspiration is inexplicable which enabled me to pursue and accomplish this work.

Jaskiran Kaur

TABLE OF CONTENTS

LIST OF TABLES

LIST OF FIGURES

LIST OF ABBREVIATIONS

Sr. No.	Full Form	Abbreviation
1.	Ammonical nitrogen	NH_3-N
2.	Ammonium chloride	NH_4Cl
3.	Basic Local Alignment Search Tool	BLAST
4.	Biochemical Oxygen Demand	BOD
5.	Biopolymer clusters	BPC
6.	Bovine serum albumin	BSA
7.	Calcium chloride	$CaCl_2$
8.	Chemical Oxygen Demand	COD
9.	*Chromobacterium violaceum* 2656	*CV*2656
10.	Cleaning Enhanced Backwashing	CEB
11.	Cleaning in place	CIP
12.	Confocal laser scanning microscope	CLSM
13.	Conventional Activated Sludge	CAS
14.	Deoxyribonucleic acid	DNA
15.	Dissolved oxygen	DO
16.	Effluent Treatment Plant	ETP
17.	Extracellular polymeric substances	EPS
18.	Food to microorganism ratio	F/M
19.	Fourier transform infrared spectroscopy	FTIR
20.	Gas Chromatography- Mass Spectrometry	GC-MS
21.	Hydraulic retention time	HRT
22.	Immobilized magnetic nanocomposites	IMN
23.	Institute of Microbial Technology	IMTECH

24.	Kilo pascal	kPa
25.	Kok-Gan	KG
26.	Loosely bound extracellular polymeric substances	LB-EPS
27.	Luria Bertani	LB
28.	Magnesium chloride	$MgCl_2$
29.	Membrane Bioreactor	MBR
30.	Microbial Type Culture Collection	MTCC
31.	Milligram	mg
32.	Milliliter	mL
33.	Million liter per day	MLD
34.	Minute	min
35.	Mixed Liquor Suspended Solids	MLSS
36.	Mixed liquor volatile suspended solids	MLVSS
37.	Natural organic matter	NOM
38.	N-hexanoyl homoserine lactone	C6-HSL
39.	Nitrate nitrogen	NO_3-N
40.	Nitrite nitrogen	NO_2-N
41.	Ortho-nitrophenyl-β-D-galactoside	ONPG
42.	Phosphate buffer saline	PBS
43.	Polyacrylonitrile-graft-poly (ethylene oxide)	PAN-*g*-PEO
44.	Polydopamine	PDA
45.	Polyether sulfone	PES
46.	Polyferric chloride	PFC
47.	Polymerase chain reaction	PCR
48.	Potassium dihydrogen phosphate	KH_2PO_4

49.	Powdered activated carbon	PAC
50.	Protein to polysaccharide ratio	PN/PS
51.	Quorum Quenching	QQ
52.	Quorum quenching membrane bioreactor	QQ-MBR
53.	Quorum Sensing	QS
54.	Revolutions per minute	RPM
55.	Saturation magnetization	Ms
56.	Scanning electron microscope	SEM
57.	Sludge volume index	SVI
58.	Sodium bicarbonate	$NaHCO_3$
59.	Sodium chloride	NaCl
60.	Sodium hydroxide	NaOH
61.	Sodium hypochlorite	NaOCl
62.	Sodium sulfate	Na_2SO_4
63.	Solid Retention Time	SRT
64.	Soluble microbial products	SMP
65.	Suspended Solids	SS
66.	Tightly bound extracellular polymeric substances	TB-EPS
67.	Titanium dioxide	TiO_2
68.	Total dissolved solids	TDS
69.	Total kjeldahl nitrogen	TKN
70.	Total phosphorus	TP
71.	Total solids	TS
72.	Total suspended solids	TSS
73.	Transmembrane Pressure	TMP

74.	Transmission electron microscope	TEM
75.	Tris Hydrochloride	Tris HCl
76.	Vibrating Sample Magnetometer	VSM
77.	Waste Activated Sludge	WAS
78.	Water	H_2O
79.	X ray Diffraction	XRD

CHAPTER I

INTRODUCTION

1.0 General

The growing need to meet the stringent discharge standards imposes the industries to adopt advanced treatment technologies that has the great potential to generate high quality effluent. Of the prevailing water and wastewater treatment technologies, membrane bioreactor (MBR) has emerged as a promising solution for advanced wastewater treatment (Meng *et al.*, 2009). MBR is a modification of conventional activated sludge (CAS) process that couples the aeration tank with secondary clarifier. In CAS systems, flocs of active micro-organisms are used for degradation of aerobically biodegradable organic substances. However, the problems of high energy consumption and poor effluent quality limits its applicability (Stypka *et al.*, 2002). In addition, the process suffers from problems of excess sludge generation and the requirement of large space for secondary clarifiers along with the problem of solid - liquid separation. Therefore, the MBR has been developed as an alternative technology to CAS where the biological stage is integrated with the membrane filtration (Cicek, 2003; Marrot *et al.*, 2004). In this process, an active biomass is maintained in the aeration tank and the treated effluent is withdrawn through the membrane module. The membranes perform the function of solid - liquid separation and act as a filter that rejects the solid material developed during the biological process, thereby resulting in a high quality effluent. Other benefits of MBR over the CAS includes compact footprint, higher volumetric loading rate, less sludge production, short hydraulic retention time (HRT) and longer sludge retention time (SRT) (Judd, 2006; Meng *et al.*, 2009).

MBR exists in two configurations: internal/ submerged MBR where the membrane is placed inside the bioreactor; and external/ sidestream MBR where the location of the membrane unit is outside the biological tank. Over the past two decades, the MBR technology has become an attractive option to treat wastewater. Henceforth, MBR is increasingly employed for municipal and industrial wastewater treatment around the world (Meng *et al.*, 2009; Fallah *et al.*, 2010). In Industrial sectors, this advanced technology has been applied for treating different types of wastewater viz. dairy,

petrochemical, urban, bamboo, oily, food processing, leachate and many more (Farizoglu and Uzuner, 2011; Alnaizy *et al.*, 2011; Lin *et al.*, 2011; Wang *et al.*, 2013). As mentioned earlier, the widespread application of MBR in the treatment of wide variety of wastewater is due to its high effluent quality. MBR shows almost 100% suspended solid (SS) removal, 95-97% chemical oxygen demand (COD) removal and 99% Biochemical oxygen demand (BOD) removal. It also reduces the sludge production by 48.3% (Bouhabila *et al.*, 2001). Besides their prevalent application, the use of MBR technology suffers from certain disadvantages such as membrane fouling, high capital and operating cost (Iorhemen *et al.*, 2016). Membrane fouling is considered as a major limitation for the MBR process efficiency as it leads to decreased flux, increased transmembrane pressure (TMP) and high energy consumption (Nagaoka *et al.*, 1996; Davies *et al.*, 1998; Wisniewski and Grasmick, 1998; Kimura *et al.*, 2005; Tu *et al.*, 2010).

Membrane fouling occurs as a result of the deposition of suspended or dissolved substances on the membrane surface or within the membrane pores (Drews, 2010). The foulants that cause membrane fouling include colloids, solutes, micro-organisms and cell debris. Depending on the foulants, membrane fouling is categorized into colloidal fouling (suspended solids and flocs), organic fouling (EPS and humics), scaling (sparingly soluble inorganic substances) and biofouling (micro-organisms). The accumulation of EPS and formation of biofilm that results in biofouling is considered as the most persistent form of fouling as they play a significant role in degrading the membrane's life.

The mechanism of membrane fouling involves 1) adsorption of solute particles or colloids onto the membrane surface or within its pores 2) accretion of sludge flocs on the membrane surface and 3) precipitation of dissolved components such as iron, silica and manganese on the membrane. The mechanism of membrane fouling is influenced by factors such as biomass characteristics (extracellular polymeric substances; EPS, soluble microbial products; SMP, floc size, Mixed liquor suspended solids; MLSS); operating conditions (SRT, HRT); feed water characteristics and membrane properties

(pore size, zeta potential, membrane material, roughness) (Fan *et al.*, 2013; Iorhemen *et al.*, 2016). .

Membrane fouling is an inevitable phenomenon of MBR process. To make MBR as an economically viable option for advanced wastewater treatment, it is essential to mitigate the problem of membrane fouling. So far, researchers have explored various methods such as physical and chemical cleaning (backwashing; membrane relaxation; air flushing; use of ultrasonic, electrical and magnetic fields; use of chemicals such as sodium hydroxide, sodium hypochlorite, oxalic acid); membrane modification (membrane surface coating, modification using hydrophilic additives) and optimization of operating conditions (suction pressure, feed flux, filtration duration, air flow rate, high shear, force fields) (Campbell *et al.*, 1999; Gander *et al.* 2000; Laitinen *et al.*, 2001; Asatekin *et al.*, 2007; Ahmed *et al.*, 2007; Madaeni *et al.*, 2011). Studies also focused on modifying sludge characteristics through the addition of powdered activated carbon, plastic media, adsorbents, organic and inorganic flocculants into the MBR to control membrane biofouling (Widjaja *et al.*, 2010; Zhang *et al.*, 2014; Skouteris *et al.*, 2015). However, these control techniques were not so effective due to an array of disadvantages such as operational cost, toxic nature of chemicals, slow accumulation of foulants within the membrane pores and increased membrane resistance (Xi *et al.*, 2009; Madaeni *et al.*, 2011). Though, the biocides effectively reduced the viable organisms, but the micro-organisms change their physiological responses through gene regulation and metabolism and become resistant to the cleaning procedure (Mahendran *et al.*, 2010; Malaeb *et al.*, 2013). With time, these micro-organisms adhere to the membrane surface and form biofilm.

The formation of biofilm on a substrate is coordinated by a phenomenon termed as quorum sensing (QS). QS is a mode through which the individual bacterial cells communicate to exchange information by means of signal molecules termed as autoinducers. Every individual bacterium secretes an inducer (signalling molecule) and contains a receptor capable of detecting the signaling molecule. The transcription of certain genes including those responsible for the synthesis of inducer itself, is stimulated on binding of inducer to the receptor. Thus, these auto-inducers play a

noteworthy role in QS (Fuqua and Greenberg, 2002). The signalling molecules (autoinducer) diffuse into the surrounding environment through the bacterial membrane. Every individual bacteria produces a very petite amount of inducer. The quantity of inducer increases with increase in the bacterial population. Consequently, a positive feedback loop is formed which results in increasing concentration of these signalling molecules. On attaining the threshold concentration, the receptor becomes activated and triggers the expression of specific genes in the bacterial cells which regulate various physiological functions (Lal, 2009). Generally bacteria make use of acylhomoserine lactone (AHL) as signalling molecule for biofilm formation. It has been found that the QS mechanisms influence all stages of the process from establishment to maturity of biofilm on the membrane surfaces (Davies *et al.*, 1998; Kjelleberg and Molin, 2002). Hence, it is vital to develop an effective and sustainable solution to embark upon the biofouling problem.

Recently a new phenomenon, the bacterial quorum quenching (QQ) has been introduced by various research groups as an innovative approach for mitigating the hostile effects of membrane biofouling (Chan *et al.*, 2011; Christiaen *et al.*, 2011). Inhibition of AHL production, interference with the signal receptor proteins and enzymatic degradation of AHL are some of the QQ strategies employed for the disruption of QS mechanisms among micro-organisms (Dong *et al.*, 2002; Lee *et al.*, 2014; Lee *et al.*, 2016b). Of these, targeting the AHL molecule via enzymatic activity has received great attention among the scientific communities. The mechanism to inactivate AHL through enzymatic action is reported in certain bacteria termed as QQ bacteria that are known to co-exist with QS bacteria. These bacteria express variety of enzymes such as lactonases, acylases and oxidoreductases that can carry out AHL inactivation. Numerous studies focused on the mitigation of membrane biofouling in MBRs through enzymatic AHL inactivation have been carried out in the recent years (Yeon *et al.*, 2009b; Lee *et al.*, 2014). Nevertheless, enzymatic QQ approach has issues of enzyme production cost, enzyme purification requirement and stability problem which hamper its application in the MBR. Due to the above mentioned problems, the area of research has shifted towards the use of whole cell immobilized bacteria for biofouling control.

Several QQ bacteria including *Bacillus*, *Pseudomonas*, *Rhodococcus*, *Enterobacter cloaca*, *Delftia* sp. have been used in MBRs (Gul and Koyuncu, 2017; Nahm *et al.*, 2017a; Waheed *et al.*, 2017). Since, these micro-organisms have low survival rates in the new environment, cell immobilization can be a suitable option. Various immobilization media such as fixed membrane vessels, free-moving alginate beads, polymeric membrane layer coated alginate beads and QQ sheets have been successfully used for immobilization of QQ bacteria (Kim *et al.*, 2013; Oh *et al.*, 2012; Nahm *et al.*, 2017a; Waheed *et al.*, 2017). It has been reported that the immobilized QQ bacteria have showed considerable biofilm control potential in laboratory as well as in pilot MBRs (Oh *et al.*, 2012; Cheong *et al.*, 2013; Cheong *et al.*, 2014; Lee *et al.*, 2016b).

The QQ bacteria commonly exists in diverse habitats. The existing literatures have proven the presence of QQ bacteria in wide array of sources like soil, sewage, Chinese soya sauce brine, *Pterocarpus santalinus* plant and pond water (Chan *et al.*, 2009; Christiaen *et al.*, 2011; Chong *et al.*, 2012; Yin *et al.*, 2012; Rajesh and Rai, 2014). The presence of QQ bacteria in wastewater other than sewage remains unexplored. Punjab state in India is dominated with a number of dairy industries that generates huge amount of organically rich wastewater. MBR technology can be used to treat the dairy industry wastewater and provide an effluent of reusable standards. However, their application in the dairy industry might be limited due to fouling. In view of this, the current study aims to combat membrane biofouling in laboratory scale MBR operated with dairy industry wastewater using the QQ bacteria immobilized alginate magnetic iron nanoparticle beads isolated from dairy waste activated sludge (WAS).

1.1 Significance of the study

Membrane biofouling caused by the QS bacteria through the production of signalling molecules, reduces the membrane shelf life that ultimately increases the cost factor in terms of membrane replacement and operational cost. One of the best approaches for biofouling control is the disruption of signalling molecules by QQ bacteria. The current study basically aims to isolate indigenous QQ bacteria from WAS sample of dairy industry and evaluate the efficiency of isolated QQ bacteria by immobilizing them in

alginate magnetic iron nanoparticle beads to control biofouling in MBR's. The magnetic iron nanoparticles permit the separation of QQ bacteria immobilized beads using strong magnet.

1.2 Hypothesis

The present research is carried out on the basis of the following hypothesis:

- It is hypothesized that the activated sludge sample contains QQ bacteria that can mitigate biofouling problem on the membrane surfaces.
- It is hypothesized that the alginate magnetic beads are the appropriate carriers for immobilizing QQ bacteria.

1.3 Objectives of the study

For the purpose of accomplishing the research targets, the present study was done under the following objectives:

- To isolate and identify the QQ bacteria from the waste activated sludge (WAS) of dairy industry
- To evaluate the feasibility of alginate magnetic iron nanoparticle beads for immobilizing QQ bacteria
- To determine the QQ activity of immobilized alginate magnetic iron nanoparticle beads in batch studies
- To investigate the efficiency of Immobilized QQ bacteria in mitigating membrane biofouling in MBR treating dairy wastewater

CHAPTER II

REVIEW OF LITERATURE

2.0 General

Membrane Bioreactor (MBR) is an advanced wastewater treatment process where membrane processes for instance, microfiltration and ultrafiltration is integrated with the suspended growth processes such as activated sludge process (Meng *et al.*, 2009). High quality effluent, nutrient removal, compact footprint, excellent disinfection ability, high volumetric loading, sludge minimization, uncoupling of solid and hydraulic retention time are some of the merits associated with this recent technology over conventional treatment processes (Judd, 2006; Meng *et al.*, 2009; Le-Clech, 2010). Attributable to these advantages, the MBR technology has been increasingly applied for treating industrial and municipal wastewater. During the past 15 years, there is a massive growth in MBR market. Figure 2.1 depicts the growth trend of MBR in global market. The MBR in the market was estimated to be around US$ 337 in 2010 that rose to US$ 627 by 2015 (Fig 2.1). The total installed capacity of MBRs in 2017 exceeded 12,000 MLD (TMS, 2016).

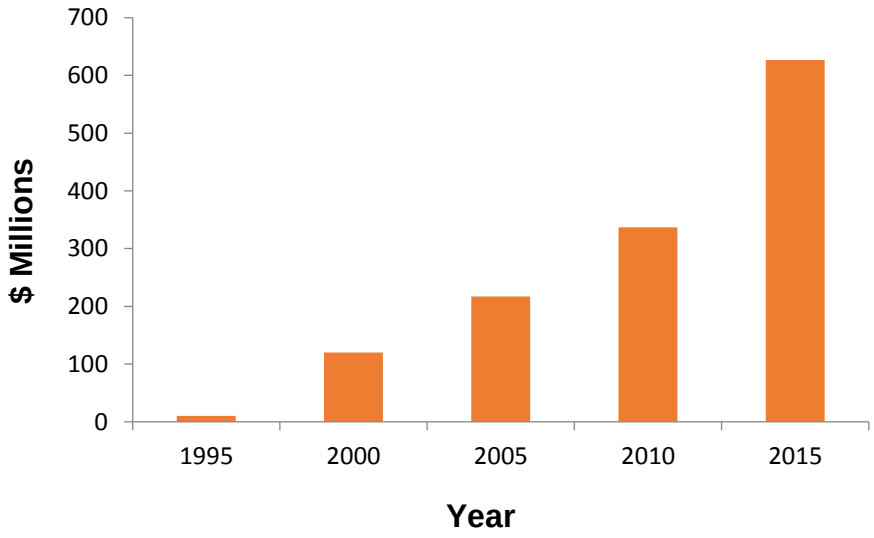

Figure 2.1 Membrane Bioreactors (1995-2015) in global market

Source: Hanft, S. (2011)

Despite the widespread advantages, applications and growth in global market, the MBR technology faced certain challenges that limit its usage. One of the major drawback of this technology is membrane fouling which declines membrane

permeability as a result of accumulation of colloidal and particulate matter, organic foulants, sparingly soluble inorganic compounds and microorganisms on the membrane surfaces (Tang *et al.*, 2011). This affects the performance of treatment process, operation costs and membrane life. Rapid permeate flux decline as a result of fouling is a key hurdle in wider implementation of MBR. In order to enhance the performance of MBR in wastewater treatment, a number of fouling control strategies such as membrane cleaning (physical and chemical cleaning), membrane relaxation, sludge disintegration (using ultrasound treatment, ozonation, electric fields, carriers), membrane surface coating, membrane modification with hydrophilic additives etc. were adopted by the researchers (Drews, 2010; Xiong and Liu, 2010). In recent times, the biological based approach via enzymatic disruption using quorum quenching (QQ) bacteria has garnered attention for fouling mitigation. This chapter reviews the various aspects of MBR including its configurations and its applications. The chapter also throws light on the problem of membrane fouling faced by the MBR and its contributing factors. The chapter also discusses the various mitigation strategies viz. membrane cleaning, sludge disintegration, membrane modification and other methods adopted to control membrane fouling.

2.1 MBR fundamental aspects and its application

Membrane bioreactor is state-of-the-art technology which combine biological treatment process, the activated sludge system with the membrane filtration process. Activated sludge process is one of the oldest biological treatment process that has been applied successfully to treat different wastewaters. A typical activated sludge process is a suspended growth process system. The basic activated sludge treatment process comprise of three key elements: (a) an aeration tank where the microorganisms accountable for wastewater treatment are suspended and aerated; (b) sedimentation tank for the separation of liquid and solid; and (c) a recycle system for recycling the voluminous fraction of biomass (Figure 2.2).

The aerobic treatment of wastewater is carried out in an aeration basin where the active mass of micro-organisms oxidize the organic matter into CO_2 and H_2O, NH_4, and new cell biomass. The aeration tank is provided with diffused or mechanical aeration system so as to transfer oxygen to the biomass. From the aeration tank, the aerated mixed liquor passes to the secondary clarifier for the removal of finer

suspended solids while the treated effluent is discharged to the receiving waters (Bitton, 2005). Though it is efficient enough to remove 97% BOD and suspended solids, the problems of high energy consumption, high capital and operation costs limits its application (Stypka *et al.*, 2002). Also, in activated sludge system, the sedimentation tank's hydrodynamic conditions and the sludge settling characteristics play a key role in determining the quality of sludge. Moreover, it also requires huge capacity sedimentation tank to obtain sufficient solid/ liquid separation. Moreover, close control of the biological treatment system is needed to prevent the conditions that cause poor settleability or sludge bulking. Even with such controls, the activated sludge process requires further treatment to produce high quality effluent. The MBR can overcome the disadvantages of the activated sludge process (Visvanathan *et al.*, 2000).

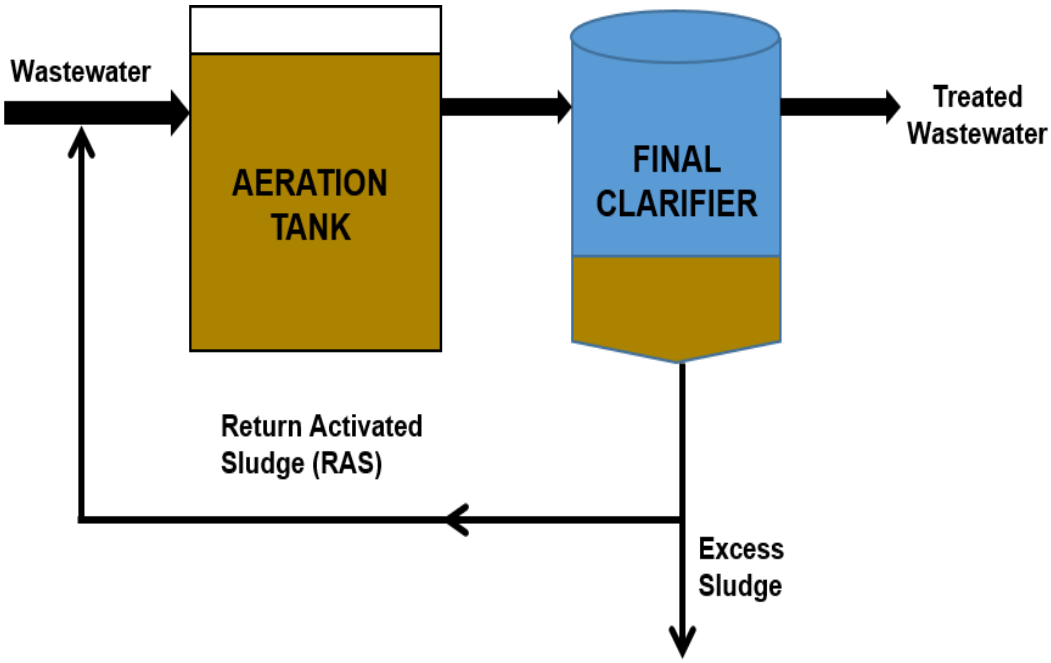

Figure 2.2 Activated sludge process

MBR can be classified as submerged and side stream configuration depending upon the location of membrane module in bioreactor (Figure 2.3). In submerged MBR, the membrane unit is installed into the biological tank. The effluent is extracted from the MBR by suction or by pressurizing the MBR. In side-stream configuration of MBR, the pressure - driven membrane unit is located outside the reactor. The submerged

MBR is operated in dead-end mode compared to the side-stream MBR which is operated in cross-flow mode (Radjenovic *et al.*, 2008).

Now a days, MBR has proven an attractive option for optimal treatment of industrial wastewater such as dairy, urban, bamboo, sludge, petrochemical, hospital, bathing and municipal wastewater (Gander *et al.*, 2000; Wen *et al.*, 2004; Xia *et al.*, 2008; Fallah *et al.*, 2010; Farizoglu and Uzuner, 2011; Alnaizy *et al.*, 2011; Wang *et al.*, 2013; Meabe *et al.*, 2013).

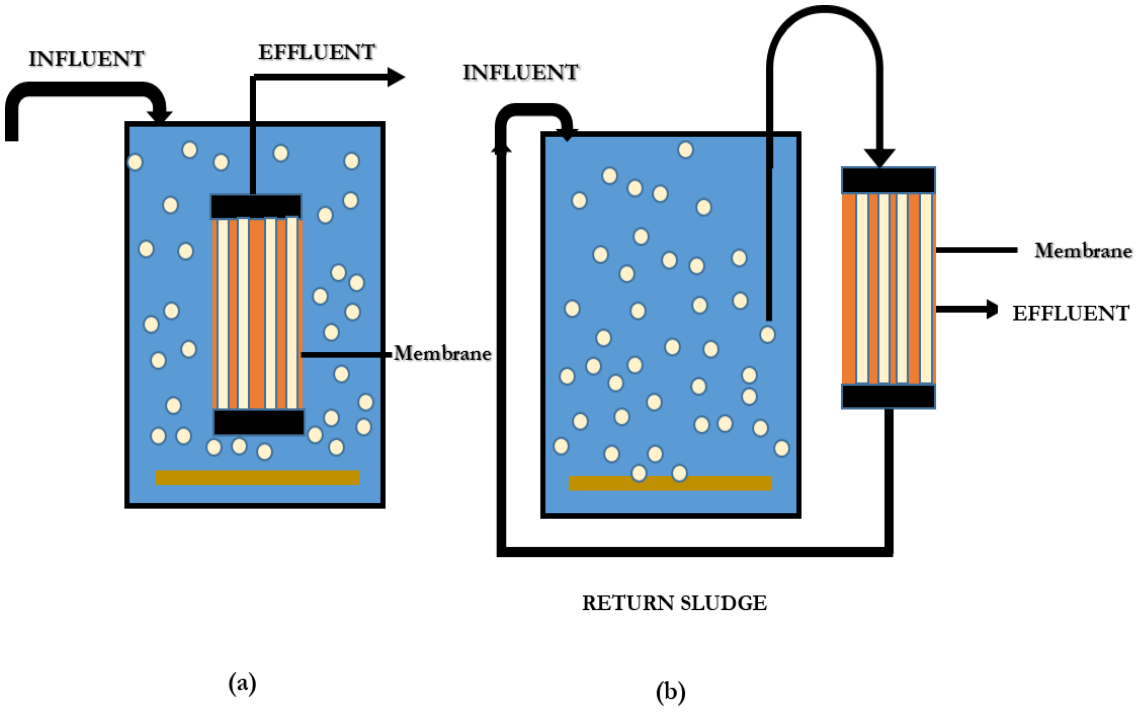

Figure 2.3 Submerged MBR (a) and side stream MBR (b)

Table 2.1 summarizes the application of MBR in the treatment of different types of wastewater with information on configuration of membrane module and treatment efficiency. From the Table, it is clearly evident that hollow fiber membrane module with microfiltration process are commonly used in fabrication of MBR. The pore size of the membrane ranged from 0.1 - 0.4 µm and lead to generation of high quality effluent. The COD removal efficiency of MBR varied in the range of 82.7- 99.4% (Lyko *et al.*, 2008; Naghizadeh *et al.*, 2008; Wiszniowski *et al.*, 2009; Zhidong *et al.*, 2009; Wang *et al.*, 2013). Alnaizy *et al.* (2011) reported COD removal of 99.4% during operation of vacuum rotation MBR for treatment of urban wastewater. Since the efficient nutrient removal by MBR required the prevalence

Table 2.1 Application of MBR in treating different wastewaters

S.No.	MBR Configuration	Membrane configuration	Type of wastewater treated	Treatment efficiency	Reference
1.	Submerged MBR	Hollow fibre microfiltration	Landfill leachate	90% COD removal	Bouhabila *et al.* (1998)
2.		Hollow fibre ultrafiltration	Municipal wastewater	>95% COD removal	Rosenberger *et al.* (2002b)
3.		Hollow fibre		99.3% COD, 98.1% TKN, 85.5% TN and 52% phosphorus removals	Naghizadeh *et al.* (2008)
4.		Hollow fibre ultrafiltration		98% COD, 90% total nitrogen and 98% total phosphorus removals	Lyko *et al.* (2008)
5.		Hollow fibre		92.3% of COD and 98.5% of BOD removals	Matosic *et al.* (2009)
6.		Flat sheet		98.5% NH_4-N, 82.7% COD and 65.5% total phosphorus removals	Yang *et al.* (2011)
7.		Flat sheet microfiltration	Mixture of municipal, hospital and industrial wastewater	90.4% COD removal	Radjenovic *et al.* (2007)
8.		Hollow fibre microfiltration	Bathing wastewater	93% COD removal	Xia *et al.* (2008)
9.		Hollow fibre membrane	Synthetic wastewater	97% DOC, 99.5% NH_4-N and 97% COD removals	Ngo *et al.* (2008)
10.		Flat sheet	Domestic wastewater	80% total nitrogen, 90% COD and 99% NH_3-N removals	Zhidong *et al.* (2009)
11.		Hollow fibre	Tapoica starch wastewater	97.9% COD removal	Wenten *et al.* (2009)
12.		Microfiltration	Petrochemical industrial wastewater	93% COD, 99.7% BOD and 99.9% NH_4-N removals	Wiszniowski *et al.* (2009)

13.		Flat sheet		99% COD removal	Fallah *et al.* (2010)
14.		Hollow fibre microfiltration	Hospital wastewater	80% COD removal	Wen *et al.* (2004)
15.		Flat sheet ultrafiltration		COD and DOC removal of 92% and 94%, respectively	Kovalova *et al.* (2012)
16.		Hollow fibre microfiltration	Dairy wastewater	99% COD, 96% NH_3-N and 100% BOD removals	Andrade *et al.* (2013)
17.		Polyvinylidene fluoride hollow fibre		93% COD and 92% BOD removals	Praneeth *et al.* (2014)
		Polyacrylonitrile hollow fiber		91% COD and 86% BOD removals	
18.		Hollow fiber		95.4% NH_3-N, 98.2% COD and 88.9% PO_4-P removals	Erkan *et al.* (2018)
19.	External	Ultrafiltration	Human excrement	>99% BOD removal	Magara and Itoh (1991)
20.	External	Ultrafiltration	Maize/ egg processing	>97% COD removal	Ross *et al.* (1992)
21.	External	Ultrafiltration	Dairy wastewater	95.4% COD and 62.3% TDS removals	Chandrasekhar *et al.* (2017)
22.	External anaerobic	Ultrafiltration	Brewery wastewater	>97% TOC removal	Strohwald and Ross (1992)
23.	Vacuum rotation MBR	Flat sheet ultrafiltration	Urban wastewater	99.4% COD removal	Alnaizy *et al.* (2011)
24.	Jet loop MBR	Tubular type ultrafiltration	Dairy wastewater	97-98% COD removal	Farizoglu and Uzuner (2011)
25.	Anaerobic MBR	Hollow fibre	Bamboo industry wastewater	91% COD removal	Wang *et al.* (2013)
26.	Anaerobic MBR	Hollow fibre	Bamboo industry wastewater	89.1% COD removal	Xia *et al.* (2016)

of anaerobic conditions in the reactor, anaerobic MBR was considered as an effective choice. Anaerobic MBR improves the treatment efficiency and is also capable of producing methane and less sludge. They are widely applied for the treatment of industrial wastewater (Xia *et al.*, 2016).

In some cases, the MBR is combined with some other technology for efficient wastewater treatment, energy recovery and sludge reduction (Xiao *et al.*, 2011; Wang *et al.*, 2011b). Su *et al.* (2013) combined microbial fuel cell with MBR and reported more than 90% of ammonical nitrogen (NH_3-N) and COD removal. In addition, the average voltage of 430mV and maximum power production of about 51mWm^{-2} was obtained with this combined system.

2.2 Membrane fouling

The application of MBR for wastewater treatment is affected by the problem of membrane fouling. Operationally, fouling can be defined as the accumulation of substances in the feed water on or within the membrane surface that leads to drop in water transport per unit area of membrane (Paul and Abanmy, 1990). The membrane fouling occurs as a result of interactions between the components of mixed liquor and the membrane material. The former includes colloidal particles, suspended solids, inorganic substances, microbial cells, extracellular polymeric substances (EPS), soluble microbial products (SMP). It occurs in a stepwise manner and comprises of pore narrowing, pore plugging and cake formation (Ahn *et al.*, 1998). Lim and Bai (2003) also reported the occurrence of initial pore blocking chased by cake formation. As a result of pore blocking, a decrease in flow area of the permeate was seen resulting in greater transmembrane pressure (TMP) so as to achieve the same flux (Liao *et al.*, 2004).

The membrane fouling is divided into two categories- reversible and irreversible fouling on the basis of size of particle and method employed for foulant removal. Large particles and flocs that deposited on membrane surfaces and can be removed by physical means like air scouring and backwashing fall under the category of reversible fouling whereas small colloids and solute that plug the membrane pores which can only be removed by chemical cleaning is considered irreversible fouling. Depending on the causative agents of fouling, the membrane fouling can be

classified into particulate, organic, inorganic and biofouling. Table 2.2 summarizes various foulants and fouling factors involved in membrane fouling.

2.2.1 Colloidal fouling: The colloidal fouling is caused by the deposition and building up of particulate matter either on the membrane surface or within the membrane pores (Cheryan, 1998). The colloidal particles are expected to be accountable for pore blocking of membrane while the suspended solids are responsible for cake layer resistance (Itonaga *et al.*, 2004). Fan *et al.* (2013) reported a linear relationship between the amount of colloidal particles in the MBR and membrane filtration resistance change. However, according to Teychene *et al.* (2008), the colloids contributed only 10% of total organic loading, indicating a minor contribution of colloidal particles in membrane fouling.

2.2.2 Organic fouling: Organic fouling is caused by the binding of certain organic substances (oil, proteins and humic substances) to the surface. The natural organic matter (NOM) is the foremost organic foulant of membranes in treatment processes (Hong and Elimelech, 1997; Taniguchi *et al.*, 2003). It was reported that the high hydrophilic fraction content of NOM in feed waters caused a significant flux decline (Lee *et al.*, 2004). Seidel and Elimelech (2002) illustrated that the permeation drag and calcium binding to NOM facilitate the development of a densely compacted fouling layer on the membrane surface that leads to severe flux decline. The divalent calcium ions facilitate NOM fouling through complexation and consequent formation of intermolecular bridges among organic foulant molecules (Li and Elimelech, 2004).

2.2.3 Scaling: Scaling is related to precipitation of dissolved metal salts present in the feed water on the surface of membrane. After the removal of salt free water from permeate, the concentration of ions in the feed increases. At some point, the salt concentration in the feed exceeded their solubility limit. At this point, the salt precipitates on the membrane surface as scale (Pervov, 1991; Heldman and Moraru, 2014). Though scaling is most commonly occurred in reverse osmosis membrane but it is not a significant foulant in MBR fouling. Nevertheless, iron or calcium precipitation could happen in some cases.

2.2.4 Biofouling: The fourth type of fouling i.e., biofouling is mainly caused by the biofilm formation (formed by intercellular communication between bacteria through the phenomenon of QS) or accretion of biological material such as EPS on the membrane surface. The deposition of cells or its aggregates leads to formation of

Table 2.2 Fouling types and their characteristics

S. No.	Fouling type	Foulant	Foulant examples	Fouling causing factors	Fouling indicating parameters	Impact	Reference
1.	Particulate	Colloids and suspended solids	Silica, aluminium silicate, aluminium oxide, manganese oxide, elemental sulphur, large molecular weight polysaccharides, fulvic acid, humic acid, proteins etc.	Concentration polarization	Silt density index, modified fouling index	Higher membrane filtration resistance, TMP increase	Paul and Abanmy (1990); Liao *et al.* (2004); Tang *et al.* (2011); Gao *et al.* (2013)
2.	Organic	Natural organic matter	Humic acids, extracellular polymeric substance	Divalent calcium, concentration polarization, pH, electrolyte concentration, molecule or membrane surface charge, hydrophobicity	Dissolved organic compounds	Flux decline	Hong and Elimelech (1997); Amoudi and Lovitt (2007)

3.	Scaling or inorganic	Metal salts	Magnesium, silicon, iron, phosphorus, calcium carbonate, $CaSO_4.2H_2O$, silica, $BaSO_4$, $SrSO_4$, ferric and aluminium hydroxides	Co-precipitation, pH, temperature, pressure, concentration polarization, surface morphology	Solubility	Physical damage of membranes, flux decline	Faller (1999); Schafer *et al*. (2005); Amoudi and Lovitt (2007); Zhang *et al.* (2012a)
4.	Biofouling	Microorganism	*Pseudomonas* sp., *Ochrobactrum anthropi* sp., *Enterobacter* sp., *Brevundimonas, Asticcacaulis*, *Acinetobacter*, *Clostridium*	Mixed liquor suspended solids, food to microorganism ratio, hydraulic and solid retention time, temperature and nutrients	Assimilable organic carbon and Biofilm formation rate	Augment in pressure drop across membrane elements, decline in membrane permeability, permeate flux decline, shortening of membrane performance, increased energy consumption.	Zhang *et al.* (2006); Xia *et al.* (2008); Vrouwenvelder *et al.* (2010); Guo *et al.* (2012)

gel or cake on the membrane surface which results in biofouling of membranes (Holman and Ohlinger, 2007). It has been found that these four types of fouling might occur simultaneously in MBRs (te Poele and van der Graaf, 2005). Wang *et al.* (2008) characterized the membrane foulants and gel layer formed on membrane surfaces under sub-critical flux operation. On the basis of mean oxidation state of organic carbons and Fourier transform infrared spectroscopy, it was demonstrated that the gel layer on membrane surfaces were comprised of EPS (proteins, polysaccharides etc.) and other kinds of organic substances. Also, certain inorganic elements like Mg, Al, Fe, Ca, Si etc. enhanced the gel layer formation along with the organic foulants. But, biofouling has more than 45% contribution to the overall membrane fouling (Komlenic, 2010).

2.3 Mechanism of fouling

The membrane fouling is a complex phenomenon as it involves interaction of different foulants. Fouling involves three mechanisms- particle deposition, particle adsorption on membrane surface and pore blocking mechanism. These mechanisms prevail through different stages (conditioning fouling, steady fouling and TMP jump) of fouling. Figure 2.4 depicts the schematic representation of mechanism of membrane fouling.

Stage 1 Conditioning fouling

Fouling begins with the adsorption of the mixed liquor constituents in the feed onto the pores of the membrane material (Chang and Lee, 1998; Mukai *et al.*, 1999). It involves complex physical and chemical interactions between the membrane surface and the mixed liquor constituents such as the EPS, SMP, colloids and particulates (Nuengjamnong *et al.*, 2005; Drews *et al.*, 2006). However, these interactions are aggravated by the concentration polarization, a process where the concentration of foulants is increased at the membrane solution interface.

Pressure acts as a major driving force in pulling the foulants towards the membrane (Guo *et al.*, 2012). Passive adsorption of colloids and organics on the membrane has been reported to occur even at zero flux operation (Ognier *et al.*, 2002a). In another elaborative study conducted by Ognier *et al.* (2002b) on passive adsorption, they concluded that hydraulic resistance was independent of tangential shear and

initial adsorption contributed to about 20-2000% of the clean membrane resistance (depending on the pore size). However, once filtration occurs, its contribution to overall resistance is negligible (Choi *et al.*, 2005).

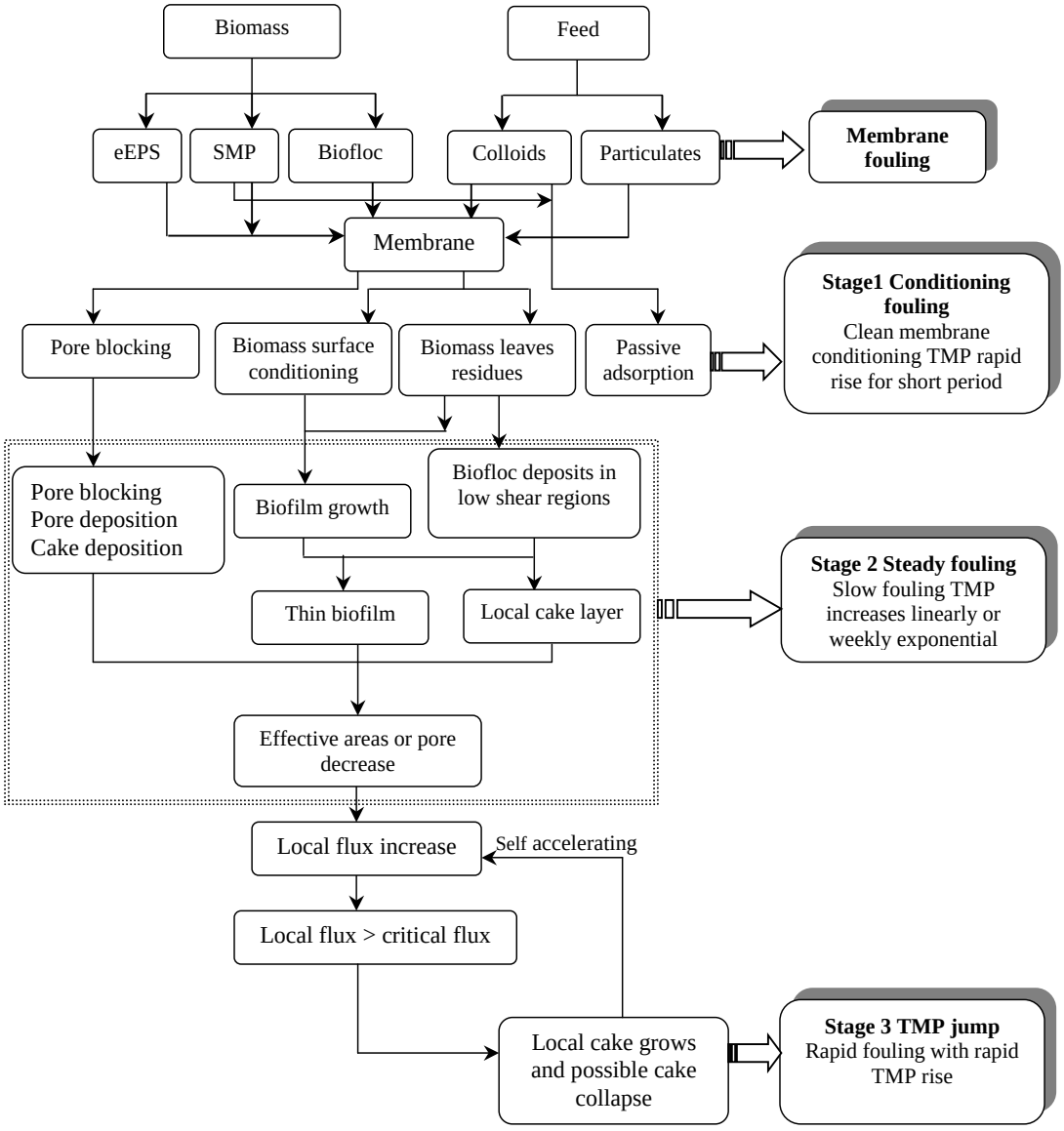

Figure 2.4 Mechanism of membrane fouling (Adapted from Yogalakshmi, 2008)

The flow rate or flow regime inside the MBR decides the contact time of the foulants at the membrane solution interface. Higher flow rate creates turbulence or eddies on the retentate side thereby producing a scouring effect at the membrane solution interface and reducing the contact time of the foulants on the membrane surface. Ma *et al.* (2005) were able to reduce colloidal adsorption onto the membrane by using filtration cycle of 10 min vacuum pump dragging with 5 min air back washing. Succeeding adsorption, deposition of foulants occurs on the side of the membrane

pore walls resulting in pore narrowing and blocking. These investigations suggest that pore narrowing (through colloidal adsorption) and pore blocking may occur in MBR (Jiang *et al.*, 2005). Pore narrowing takes place when the particles having size smaller than the molecular weight cut off of the membrane gets attached to the interior surface of the pore whereas pore blocking occurs through particles with size similar to the molecular weight cut off of the membrane (Karr and Keinath, 1978; Urbain *et al.*, 1993). Figure 2.5 provides a diagrammatic representation of pore narrowing and pore blocking. As a consequence, the flow area of the permeate decreases resulting in greater TMP to achieve the similar flux. Some flocs loosely roll and slide over the membrane without getting attached while some bioflocs leaves a footprint through deposition of smaller flocs or EPS material on the membrane. Further this facilitates the attachment and colonization of biomass on the membrane surface contributing to stage 2 (Gkotsis *et al.*, 2014).

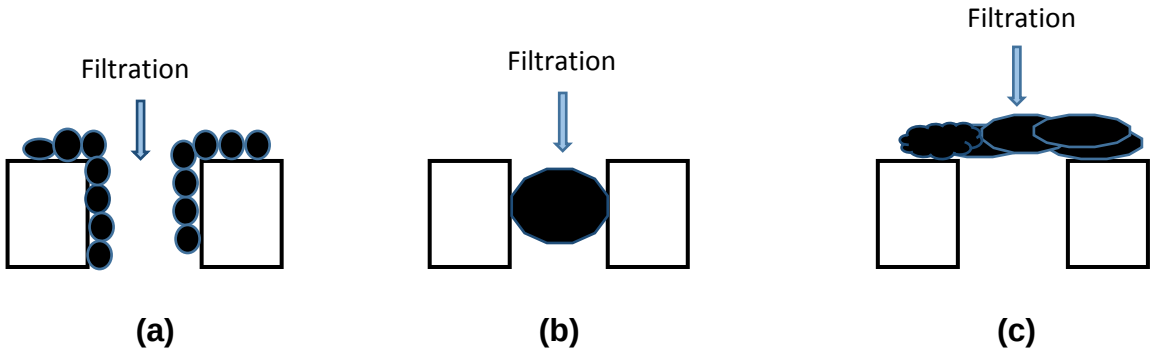

Figure 2.5 Membrane fouling mechanisms: (a) Pore narrowing; (b) Pore blocking and (c) Gel cake formation

Stage 2 Steady fouling

At the end of stage 1, the SMP is expected to cover the membrane surface. Further this would act as the nucleation site to promote the attachment of biomass, particulates and other colloids on the membrane at a steady rate (under conditions of constant flux). Slow or weakly exponential TMP rise takes place during this step. Adsorption of these mixed liquor constituents occurs on the entire membrane surface promoting the biofilm growth and local cake layer formation on the membrane surface. Certain studies reported that the biopolymer clusters (BPC) play a vital role in gel cake formation (Wang *et al.*, 2007; Sun *et al.*, 2008; Wang *et al.*,

2011a). BPCs neither belong to biomass flocs nor to SMP or EPS. These are much larger in size than SMP and are formed by the clustering of SMP and loose EPS within the sludge cake layer deposited on the membrane surface (Wang and Li, 2008; Wang *et al.*, 2011a). The BPCs accumulate on the membrane surface resulting in high filtration resistance of the cake layer on fouled membranes (Wang *et al.*, 2011a). These attached bioflocs ultimately initiate the formation of biofilm. Biofilm is an assemblage of community of microorganisms in the extracellular polymeric matrix attached to the surface commonly known as slime (Liao *et al.*, 2004; Kokare *et al.*, 2009). The formation of biofilm involves various steps including formation of conditioning layer, bacterial attachment, bacterial growth and maturation, biofilm expansion and dissolution (Figure 2.6). Initially a conditioning layer is formed through coating of polymers on the surface. It facilitates adhesion of bacteria on to the surface. However, adhesion of bacteria is controlled by both environmental (nutrient availability, pH and temperature) as well as genetic (presence of genes encoding motility functions, adhesions etc.) factors. As long as fresh nutrients are provided, the microbes undergo a transition from planktonic cells to sessile surface attached cells and the biofilm continue to develop. Under nutrient starvation conditions, they disengage from the surface and return to the planktonic method of growth. Apparently, these starvation responses permit the cell to search for a new nutrients source and are determined by well-studied adaptations that bacteria experience, when nutrients become scarce (Kolter *et al.*, 1993).

Due to uneven distribution of liquid flow and air, biofilm is irregularly distributed over the membrane area. This forms the foundation of stage 3. Over time the thickness of biofilm increases resulting in decreased effective pore area. The EPS produced by biofilm attracts more sludge particles initiating the formation of thin cake layer. It is to be noted that biofilm formation, expansion and maturation takes place in stage 2 while the initial conditioning process occurs in stage 1.

Stage 3 TMP jump

Fouling is not uniform throughout the membrane surface. Certain regions of the membrane are more fouled, resulting in decreased flux. Apparently, pressure builds up on the less fouled regions in order to maintain the permeate production. Further continued operation at constant flux increases the critical flux. Once the membrane

working regions achieves the critical flux an exponential increase in TMP will be observed. This TMP rise is eventually termed as 'TMP jump'. The mechanisms accelerating the TMP jump can be explained through the following models.

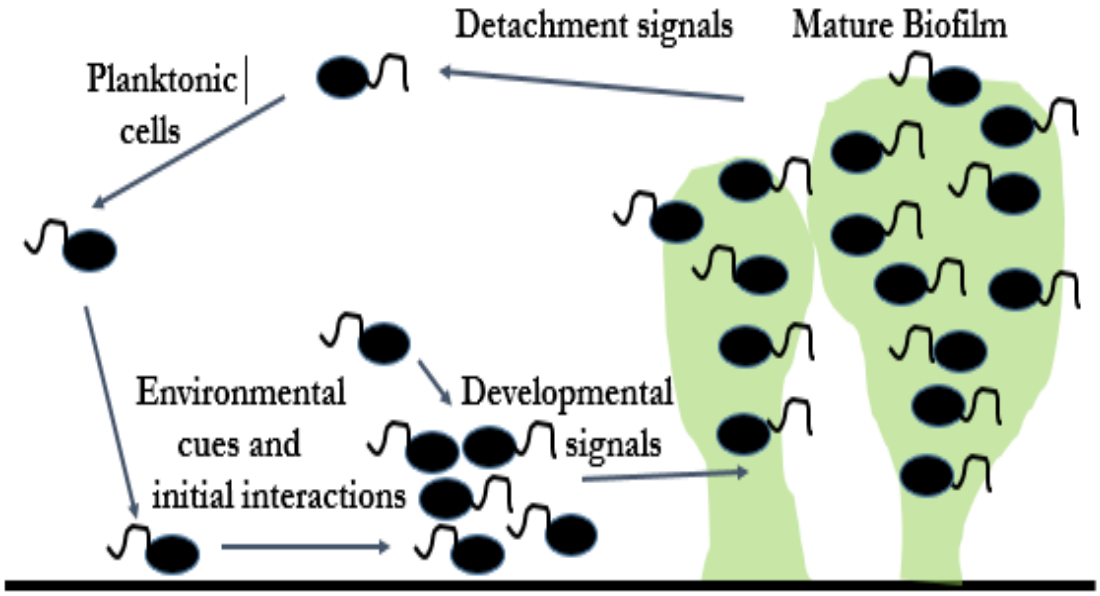

Figure 2.6 Biofilm formation mechanism

(a) Inhomogeneous fouling (area loss) model: This model was proposed by Cho and Fane (2002) to explain the TMP profiles of a cross flow filtration membrane operated with anaerobic liquor. According to this model, fouling is not always homogenous. Inhomogeneous fouling results in irregular distribution of flux. To maintain a constant permeate flow, the local flux has to compensate for the non-productive areas. The TMP begins to show a steep rise if the adjustment results in increased local fluxes above the critical flux of a dominant foulant. This model focusses on the TMP profiles at a fixed flux lower than the critical flux. Two stage TMP profile was witnessed- the extended period of slow TMP rise at the start which is followed by the rapid TMP rise. The initial slow TMP rise is attributed to the deposition of EPS whereas the rapid TMP rise is caused by increase in local flux in some membrane areas and local flux is found to even exceed the critical flux of the dominant foulant.

(b) Inhomogeneous fouling (pore narrowing) model: The model proposed by Ye *et al.* (2005) focuses on the microscopic redistribution of flux while the area loss

model on macroscopic redistribution. After initial fouling, a further increase in the imposed flux will lead to a rapid increase in TMP. Redistribution of flux occurs at the open pores and the local flux at the pore level exceeds the critical flux (Ognier *et al.*, 2002b).

(c) Inhomogeneous fouling (pore loss model): Pore narrowing will subsequently lead to pore blocking and closure of the pores. Loss of pores increases the local flux above critical flux inducing a sharp increase in TMP (Ognier *et al.*, 2002b).

(d) Critical suction pressure model: According to this model, the base of filter cake collapse when critical suction pressure is reached, resulting in formation of less permeable layer. This causes a severe drop in total permeability (Chang *et al.*, 2005).

(e) Percolation theory: This model is based on cake layer porosity and is applicable to membrane filtration of biological suspension. Porosity and connectivity determines the permeability of the cake layer. The cake layer formed over the membrane keeps changing during the filtration process due to complex particle size distribution. It generates a resistance that increases the TMP. According to the model, the porosity of the cake layer reduces with filtration and at a critical point the cake layer loses its connectivity and resistance. As a result, a dramatic drop in permeability of cake layer was observed (Hermanowicz, 2004).

(f) Inhomogeneous fiber bundle model: This model explained the TMP increase pattern in modules with fiber bundle geometry. The effect of individual fibers in TMP rise through blockage and membrane fouling has been explained in this model. Bundles operated at constant permeate flow and suction pressure showed an average flux resulting in uniform flow across the fibers of the bundle.

Thus it is evident that the TMP rise in a MBR is due to several phenomena discussed above. They may act in a sequence or simultaneously ending up in drastic TMP rise. According to Fane (2007), MBR operation at constant flux instead of constant pressure is the driving factor for unsustainable TMP rise.

2.4 Factors affecting membrane biofouling

The fouling of membrane in MBR is affected by various factors including SRT, HRT, EPS, MLSS, membrane pore size and many other (Table 2.3). The details of each factor with respect to its contribution to membrane fouling is discussed below

2.4.1 Pore size

Pore size of membrane play a significant role in causing membrane fouling. It has been observed that the membrane pore blocking mechanism increases with the increase in pore size. Increase in membrane porosity increases the permeate flux decline (Hong *et al.*, 2002). According to Hong *et al.* (2002), microfiltration membranes suffer faster reduction rates in permeate flux in comparison to ultrafiltration membranes because of higher porosity of the former.

2.4.2 Membrane material and module configuration

The membrane material exhibits varying in fouling propensity depending on the characteristics of membrane such as membrane pore size, hydrophobicity and many others (Meng *et al.*, 2009). Choi *et al.* (2002) while performing filtration tests with cellulose acetate, sulfonated polyetherulfone (PES) and polyethersulfone membranes concluded that hydrophobic PES membranes fouled more seriously rather than hydrophilic CA membranes. In addition, it has been found that the polymeric membranes are more prone to membrane fouling compared to ceramic membranes. The low volume/ area ratio of the former is the reason behind the increased rate of membrane fouling in the polymeric membrane.

Module design plays an indispensable part in determining performance of MBR. Increasing packing density of hollow fibers results in more varied permeate profile along the fibre length, subsequently lessening the filtration flux per surface area of the membrane (Braak *et al.*, 2011).

2.4.3 Sludge retention time (SRT)

SRT is one of the vital operational parameter that affects the sludge characteristics and hence influences membrane fouling (Huang *et al.*, 2001). Operating the MBR at long SRT increase the sludge concentration and organic loading which make the

process more efficient in pollutant degradation. However, the prolonged SRT is known to affect the behaviour of microbes in the MBR thus, affecting the quality of effluent. Huang *et al.* (2001) reported an increase in pollutant degradation ability of MBR with increasing SRT. However, with increasing SRT, the sludge particles tend to severely deposit on the surface of the membrane thereby causing membrane fouling (Han *et al.*, 2005). Conversely, certain studies reported the negative impact of low SRT in terms of membrane fouling (Grelier *et al.*, 2006; Malamis and Andreadakis, 2009). A study by Hao *et al.* (2017) reported an increase in the amount of total bound EPS when the MBR is operated at low SRT of 7 days. The EPS is considered as one of the cause of fouling. Ahmed *et al.* (2007) while studying the effect of SRT on membrane biofouling observed that decrease in SRT to 20 days resulted in increase in bound-EPS per unit of biomass and therefore, value of specific cake resistance increases which resulted in rise of TMP.

There are many fouling causing factors that are influenced by SRT. It was reported that the concentration of MLSS increases with increase in SRT which elevate the chances of membrane fouling through rapid deposition of particles of sludge on the surface of the membrane (Sato and Ishii, 1991). Mixed liquor properties, for instance, sludge viscosity and cell surface properties are also affected by the operation of MBR at longer SRT (Shin and Kang, 2003). Long SRT results in an increase in sludge viscosity. As a result of increased sludge viscosity, the mixing reduces thereby causing settling of biomass on the membrane surface. This leads to rise in thickness of cake layer (Meng *et al.*, 2006).

2.4.4 Hydraulic retention time (HRT)

HRT is an important parameter in biological treatment which is also known to affect the biomass characteristics. Shariati *et al.* (2011) observed that the decrease in HRT from 24 h to 8h resulted in an increased fouling rate. Isma *et al.* (2014) reported lower membrane fouling and slow TMP rise at the longest HRT of 12h along with the SRT of 30 days. The HRT induced increase in SMP thereby causing fouling (Zonoozi *et al.*, 2017). Huang *et al.* (2011) while investigating the effect of HRT on the SMP concluded that the decrease in HRT from 12 to 8h enhanced the membrane fouling in anaerobic MBR. In addition, the HRT also affects the biomass activity. It was reported that the growth of filamentous bacteria was more with

decreasing HRT. As a result of excessive growth of filamentous bacteria, the sludge viscosity and EPS concentration increases (Meng *et al.*, 2007b).

2.4.5 Extracellular polymeric substances (EPS)

EPS is one of the fundamental constituent that play a role in determining the physicochemical properties of bacterial biofilm (Jiao *et al.*, 2010). It is considered as a biofilm construction material. EPS is secreted by the microbial cells for attachment to the surface. EPS is usually synthesized during the endogenous phase of growth (Chang and Lee, 1998). They facilitate bacterial cell aggregation, cell adhesion to the surfaces and biofilm formation (Cescutti *et al.*, 1999; Burdman *et al.*, 2000; Frank and Belfort, 2003). The carbohydrates and proteins are the main components of EPS, although its chemical composition also includes other macromolecules such as lipids, DNA and humic substances (Dignac *et al.*, 1998; Donlan, 2002; Flemming *et al.*, 2007; Sheng *et al.*, 2010).

The content of EPS affects the morphological characteristics of biological aggregates (granular sludge, flocculent sludge and biofilms) which further affects the membrane filtration performance (Abdessemed *et al.*, 1998; Tay *et al.*, 2002). Xuan *et al.* (2010) concluded that the increase in content of EPS in flocculated sludge causes a decrease in membrane filtration. EPS also governed the gel layer formation which again affected the membrane filtration performance. According to Bin *et al.* (2008), decrease in membrane flux from 2.6 to 1.0 L/ $(m^2h)^{-1}$ was observed as a result of formation of gel layer produced by EPS.

Depending on the nature of EPS association with the bacterial cells, it can be categorized into tightly bound (TB) and loosely bound (LB) EPS. While the TB-EPS represent the inner layer that clings tightly to the cell surface, the LB-EPS is the outer layer that is a slime layer which is attached loosely to the cell (Flemming and Wingender, 2001; Sheng *et al.*, 2010). Both TB-EPS and LB-EPS also contribute to membrane fouling. Among both fractions, TB-EPS significantly affect membrane fouling while the other fraction i.e. LB-EPS results in filtration resistance and is also responsible for irreversible fouling (Ramesh *et al.*, 2007).

2.4.6 Soluble microbial products (SMP)

SMP which are the major organic foulant are released by substrate metabolism and biomass decay (Barker and Stuckey, 1999). Several researchers reported that the SMP cause internal membrane fouling due to which the permeate flux reduced (Drews *et al.*, 2007). Geng and Hall (2007) detected that the quantity of SMP in the mixed liquor significantly influence the sludge fouling propensity. It has been found that the SMP showed strongest relationship with membrane fouling compared to other sludge characteristics (Zhang *et al.*, 2007a). Due to their low back transport velocity, they readily adsorbed on the membrane surface. Hence, they induce the formation of gel layer thereby causing membrane pore blocking. They also penetrate the membrane pores and the spaces between the cake layers (Jarusutthirak and Amy, 2006; Wang *et al.*, 2012). SMP generally offers high filtration resistance. Further, the effect of SMP on the filtration resistances is affected by the organic loading rate. According to Chen *et al.* (2017), SMP induced pore blocking is seen when the reactor is operated at OLR of 0.7 gCOD/L/d.

Like EPS, SMP also is composed of polysaccharides and proteins. The polysaccharides like substances have been shown to contribute more to membrane fouling when compared to protein like substances (Yigit *et al.*, 2008). However, in a state of unsteady MBR operation, the nature and fouling propensity of SMP's polysaccharide fraction changes, so it is impossible to correlate the membrane fouling to the SMP polysaccharides (Drews *et al.*, 2006). Apart from polysaccharides, Rojas *et al.* (2005) reported that an increase in protein fraction of SMP from 30 to 100 mg/L causes a corresponding increase in specific resistance by a factor of 10.

2.4.7 Mixed liquor suspended solids

MLSS is considered as one of the possible fouling causing factor. Controversial findings regarding the effect of MLSS on the membrane fouling is found in literature including positive correlation with fouling, negative relationship and minor impact. Chang and Kim (2005) reported rapid membrane fouling at higher MLSS concentrations. An increase in MLSS concentration corresponded to higher TMP or a lower permeate flux (Adham *et al.*, 2001). Dvorak *et al.* (2011) observed an increase in EPS content at MLSS of 6000 mg/L. However, according to Hong *et al.*

Table 2.3 Factors governing membrane biofouling

S.No.	Fouling parameters		Relation with membrane fouling	Reference
1.	Module configuration	Packing density	Increased packing density promotes solids accumulation in the space between fibers.	Liao *et al.* (2004)
2.	Membrane materials and properties	Membrane surface roughness	Membrane surface roughness favours attachment of colloids and particulate matters on membrane surface.	Gupta *et al.* (2008)
		Pore size	Larger pore size results in accumulation of foulants in membrane pores.	Hong *et al.* (2002)
		Membrane material	Fouling is less prevalent in the ceramic membranes than the polymeric membranes. This is due to the hydrophobic nature of polymeric membrane as a result of which they are more prone to fouling	Jin *et al.* (2010); Hofs *et al.* (2011)
3.	Operating conditions	Sludge retention time	Decreased SRT promotes accumulation of carbohydrates and proteins fraction of SMPs. Increased SRT results in deposition of large	Han *et al.* (2005); Liang *et al.* (2007)

			amount of sludge particles on the membrane and increases fluid viscosity.	
		Hydraulic retention time	Decrease in HRT results in decrease in EPS, thus causing sludge deflocculation. Also, decreased HRT facilitates overgrowth of filamentous bacteria and leads to formation of larger and irregular flocs. However, increased HRT beyond optimum too results in foulants accumulation.	Meng *et al.* (2007b); Wang *et al.* (2009a); Fallah *et al.* (2010)
		Suction pressure	With TMP increase, accumulation of particles in cake layer increases.	Hong *et al.* (2002)
		Permeate flux	At unsustainable flux conditions, fouling resistance increases exponentially as filtration progresses.	Nywening *et al.* (2005)
		Food to microorganism ratio	An increase in F/M ratio results in an increase in active biomass due to high food utilisation. This results in an increase in EPS production.	Huang *et al.* (2008a)

		Temperature	Low temperature causes increase in sludge viscosity, thereby promoting membrane fouling.	Sozanski *et al.* (1997); Wilen *et al.* (2000); Lin and Shien (2001); Jiang *et al.* (2005)
4.	Sludge properties	Extracellular polymeric substances	Increase in EPS causes an increase in filtration resistance of membrane.	Nagaoka *et al.* (1996); Nagaoka *et al.* (1998)
		Mixed liquor suspended solids	Increase in MLSS increases the membrane fouling because of severe sludge cake formation on the membrane surfaces. As a result of which membrane resistance increases.	Fane *et al.* (1980); Adham *et al.* (2001)
		Soluble microbial products	Increase in SMP increases viscosity and decreases the flux.	Nagaoka *et al.* (1996)

(2002), fouling was independent of MLSS concentrations ranging between 3600-8400 mg/L. Rosenberger *et al.* (2005) conducted a detailed study on the impact of MLSS on membrane fouling and reported that for low MLSS of less than 6000 mg/L, membrane fouling decreases but when MLSS levels increase above 15,000 mg/L, an increase in fouling was observed. However, according to them, no impact was observed at MLSS 8000- 12,000 mg/L. Ross *et al.* (1990) observed a sharp decline in permeate flux during operation of MBR at 40,000 mg/L MLSS. Nevertheless, MLSS alone is not considered a significant indicator of membrane fouling (Le-Clech *et al.*, 2006).

2.5 Fouling mitigation strategies

The strategies for controlling biofouling fall under the following categories: 1) Modification of sludge characteristics; 2) Membrane cleaning; 3) Disintegration of sludge flocs; 4) Membrane modification approaches and 5) Biological approaches. The details of each category along with the method employed are mentioned in the following section.

2.5.1 Modification of sludge characteristics

The deposition of colloids and organics on the membrane in MBR can be controlled by changing the biological state of biomass. Hence, sludge modification is explored as an alternative in controlling the production and release of EPS. Table 2.4 summarizes the different methods used for the modification of sludge characteristics. From the Table, it can be seen that the adjustment of SRT is one of the approach for sludge characteristic modification. The SRT adjustment approach is rarely employed. To control production of foulants particularly organic foulants, addition of flocculants and adsorbents is done (Judd and Judd, 2010).

Ferrous sulphate and ferric chloride coagulants are used in MBRs for membrane fouling minimization via sludge modification (Wu *et al.*, 2006; Zhang *et al.*, 2008b; Ivanovic and Leiknes, 2011). Coagulants improve filtration ability of mixed liquor via charge neutralization (Wu *et al.*, 2006). Zhang *et al.* (2008b) reported that ferric chloride promotes bio flocculation of small particles in the activated sludge via interaction with the negatively charged group in EPS. According to Yang *et al.* (2011), during continuous addition of polyferric chloride (PFC), ferric phosphate complex are formed and gets deposited on the membrane surfaces. This blocks

Table 2.4 Methods for modification of sludge characteristics

S.No.	Method employed	Conditions used	Outcomes	Reference
1.	Addition of coagulant or flocculent	• Flux- 18 L/m^2/h • Air flow- 0.4 m^3/h • MLSS- 11-12 g/L, • PFS (polymeric ferrous sulphate) optimal dose-1.05mM as Fe	Decrease in TMP from 24.9 kPa to 24.1 kPa during PFS addition at the middle of experiment. Also the increase rate of TMP reached 0 at dose of 1.05 mM Fe.	Wu *et al.* (2006)
		• Flux- 13L/m^2h • Air flow- 5L/ min • Operational mode- 13 min on and 2 min off • TMP- till 30 kPa • HRT- 6h • SRT- 30 days • Ferric chloride concentrations- 0-1.6 mM.	>65% cleaning efficiency in Hybrid membrane bioreactor was seen with ferric chloride concentration of 1.2 mM.	Zhang *et al.* (2008b)
		• Constant flux of 25L/m^2/h^{-1} • Constant aeration of SAD_m of app. 1.8 Nm^3/m^2/h	Seven times reduction in fouling rate using iron chloride coagulant (dosage of 22.5 ppm).	Ivanovic and Leiknes (2011)

		• HRT- 1h • SRT- 10.1 h • TMP upto 0.3 bar.		
		• Flux- 10L/m^2h • Air flow- 5L/ min • HRT- 6h • SRT- 30 days • MLSS - 10-13 g/L • MLVSS - 8-10.5 g/L • Membrane Performance Enhancer (MPE50) - 600 mg/L	Average removal of COD, NH_4^+-N and TP increased by 4.1%, 13.2% and 21.2%, respectively as compared to control. A significant reduction in soluble microbial products (i.e.) proteins was seen.	Zhang *et al.* (2014)
2.	Addition of adsorbents	• MLSS- 8000 and 15000 mg/L • COD- 1500 and 2500 mg/L • SRT- 10, 20 and 30 days • Activated carbon concentrations-0%, 2.5%, 5%, 7.5% and 10%.	32-66% reduction in SMP, 90-95% COD removal efficiency and 72% reduction in microorganisms in the reactor were observed at 10% addition of PAC.	Widjaja *et al.* (2010)
		• Intermittent mode (10 min on, 2 min off) at constant flux • HRT- 8 h	40% reduction in average concentration of soluble EPS with 66% reduction in carbohydrate	Khan *et al.* (2012).

		• Aeration at flow rate of 10.6 m^3/m^2h • Powdered activated carbon dosage- 1000 mg/L.	content of soluble EPS in MBR_{PAC} than $MBR_{control}$ was observed. Also, decrease in fouling rate by 71-77% was seen in MBR_{PAC} compared to $MBR_{control}$	
		• Reactor volume- 5L • HRT-10 h • SRT- 50 days • MLSS- 4 mg/L • Average temperature- 12˚C (January) and 22˚C (July).	Low dosage of PAC (2 and 5 mg/L) reduced the permeate flux loss from 16% up to 27%, respectively as compared to high dosage (10 and 20 mg/L).	Torretta *et al.* (2013)
		• HRT- 24 h • Activated carbon- 715 mg/L.	Two times TMP decrease, irrecoverable fouling rate was 2 times lower and foulant was 9.12% lower in Hybrid MBR (MBR with added activated carbon) as compared to control MBR	Boonyungyuen and Wichitsathian (2014)

the membrane pores, thus exacerbating membrane fouling. Due to these limitations, the research focus has been shifted towards the use of adsorbents for modification of sludge.

The addition of adsorbents is beneficial because it augments the adsorption of low molecular organics and henceforth leads to the reduction of membrane fouling. Also, it removes the total organic carbon in the supernatant (Wu *et al.*, 2006). In addition, they restrained the formation of gel layer which in turn causes reduction of anaerobic conditions in the reactor, anaerobic MBR was considered as an effective choice. Anaerobic MBR improves the treatment efficiency and is also of TMP increase rate thereby enhancing the filtration performances. Usually low PAC dosage is beneficial for fouling mitigation (Torretta et al., 2013). Ying and Ping (2006) reported a decrease in EPS content inside the microbial floc at PAC dosage of 0.75 g/L. In another study by Li *et al.* (2005), 32% higher flux in MBR containing 1.2 g/L of PAC was observed.

2.5.2 Membrane cleaning

Membranes are usually taken for cleaning when there is a rapid increase in TMP with simultaneous drop in flux. Several approaches (physical and chemical) are employed for effectively cleaning the fouled membranes. These methods are used in order to recover the permeate flux. The details of these methods are given below.

2.5.2.1 Physical cleaning

Backwashing and membrane relaxation methods fall under the category of physical cleaning methods. Backwashing is considered as an efficient way of membrane's physical cleaning for moderately recovering the membrane performance (Laitinen *et al.*, 2001). Backwashing, a process where permeate is pumped through membrane in the reverse direction, effectively removes most of the reversible fouling. It pushes the colloidal particles and cell debris from the pore structure into the mixed liquor and partially removes sludge cake from membrane surfaces of MBR's (Liao *et al.*, 2004). But, the problem of product loss confines its application. To deal with this problem, a combination of backflushing and air sparging is used. Moreover, using this approach, higher fluxes can be attained even at significantly

higher MLSS concentrations (Psoch and Schiewer, 2006). Conditions used and the outcomes of backwashing method is summarized in Table 2.5.

Membrane relaxation or non-continuous operation of membrane is another fouling control method which appreciably advances membrane efficiency (Chua *et al.*, 2002). During the membrane relaxation, an enhanced back transport of foulants is observed. The foulants gets diffused away from the membrane surface because of concentration gradient during the non-suction periods. Moreover, the efficacy of air scouring is superior in absence of transmembrane suction pressure. This improves the removal efficiency of foulants from membrane surfaces (Hong *et al.*, 2002). At certain times, long and recurrent relaxation may perhaps cause fouling because of high instantaneous fluxes required to maintain water production (Metzger *et al.*, 2007).

2.5.2.2 Chemical cleaning

With time, more irreversible fouling accumulates on the membrane surface, thereby decreasing the efficacy of backflushing and membrane relaxation processes (Le-Clech, 2010).To overcome these problems, membrane cleaning methods are used. Only limited studies are there in mitigation of membrane fouling by chemical cleaning agents (Table 2.6).

Chemical cleaning methods are mostly used in combination with backflushing (Woo *et al.*, 2013). Chemical cleaning agents affects the flux recovery rate. It was found that sodium hypochlorite (NaOCl) was superior to sodium hydroxide (NaOH) in cleaning efficiency. According to Woo *et al.* (2013), flux recovery rate of 44% was obtained using NaOCl in comparison to NaOH (23.6%) at 1% concentration and cleaning time of 4 hours. Further, among acidic chemicals, oxalic acid showed a recovery rate of 38.1% at 1% of its concentration. For chemical cleaning combinations, oxalic acid - NaOCl-oxalic acid was more effective at cleaning time of 8 h with recovery rate of 64.8%.

Woo *et al.* (2013) investigated fouling characteristics of microfiltration membranes and evaluated the flux recovery by chemical cleaning. They tested raw water with

Table 2.5 Physical methods of fouling control

S.No.	Methods used	Conditions used	Outcomes	Reference
1.	Backwashing	• 15s backwash period during every 5 min	Total resistance decreased by 3.5-fold	Bouhabila *et al.* (2001)
		• 600s filtration and 45s backwashing duration	Rate of irreversible resistance can be minimized by 33.8% as compared to more frequent backwashing (200s/ 15s).	Jiang *et al.* (2005)
2.	Air sparging and backflushing	• Temperature- around 20˚C • MLSS- app. 10 g/L • TMP- 38 kPa	Flux can be maintained at about 40% of the limiting flux.	Psoch and Schiewer (2005)
		• SRT- 35 days • TMP- between 1-2 bar • Cross flow velocities of water within membrane tubes- between 1.3 and 3.5 m/s • Air pressure- 60 to 70 kPa above TMP • Air injection ratio- 0.53 for air sparging and backflushing • Backflush pressure- app. 60 kPa above the TMP	The total resistance decreased by 75% when air sparging and backflush was used. Highest permeate yield was observed when compared to non-enhanced or conventional operation (NON)	Psoch and Schiewer (2006)

Table 2.6 Chemicals used for fouling control

S. No.	Cleaning agent	Concentration (%)	Method of cleaning	Cleaning time	Nature of foulant to be mitigated	Reference
1.	Sodium hypochlorite	1	CEB and CIP	4 h	NOM	Woo *et al.* (2013)
2.	Oxalic acid	1	CEB and CIP	4 h	NOM	Woo *et al.* (2013)
3.	Sodium hydroxide	1	-	5 min	NOM, Fe and Mn	Woo *et al.* (2014)
4.	Nitric acid	2	-	5 min	NOM, Fe and Mn	Woo *et al.* (2014)

CEB: Cleaning Enhanced Backwashing; CIP: Cleaning In Place

organic matter (15mg/L), inorganic matter [1 mg/L Fe and 1 mg/L Mn]) and a mixture of organic and inorganic matter (humic acid, Fe and Mn). Nitric acid (HNO_3) and NaOH were tested as cleaning agents. They observed 83.5% and 100% of filtration index values, respectively while cleaning with combinations of 1% sodium hydroxide initially and 2% nitric acid later. Conversely, cleaning with combinations of 2% HNO_3 and 1% NaOH resulted in filtration index values of 40.8% and 85%, respectively. On the basis of their findings, it can be concluded that acid/base sequence is more proficient than base/acid sequence in cleaning of membranes. Zhang *et al.* (2011) observed that irreversible fouling can be removed efficiently by using NaOCl and hydrochloric acid (HCl). NaOCl oxidized the gel layer and HCl caused removal of inorganic particles that are formed by Ca^{2+}, Mg^{2+} ions.

2.5.3 Sludge disintegration methods of fouling control

Sludge concentrations in terms of MLSS and viscosity could affect membrane fouling and membrane permeability during membrane filtration (Rosenberger *et al.*, 2002a; Meng *et al.*, 2007a; Wu *et al.*, 2009). So, sludge disintegration is considered as reasonable approach for fouling control. This treatment disrupts the EPS and decreases sludge viscosity (Pham *et al.*, 2010). Array of methods are generally used for sludge disintegration namely ultrasonication, ozonation and application of electric fields (Jagannadh and Muralidhara, 1996; Neis *et al.*, 2000; Sui *et al.*, 2007; Huang and Wu, 2008; Zhang *et al.*, 2008a; Wu and Huang, 2010), the details of which are discussed in following sections

2.5.3.1 Ultrasound method

Ultrasonic treatment is a simple and effective approach for disintegrating sludge flocs and disrupting bacterial cells' walls (Wang *et al.*, 2006). Ultrasonic cavitation and acoustic streaming destroy the sludge floc structure and reduces the average particle size and viscosity in mixed liquor, hence improving filtration process (Luther *et al.*, 2001; Lamminen *et al.*, 2004; Zhang *et al.*, 2008a). Cavitation detaches particles away from membrane surfaces whereas acoustic streaming causes turbulence which facilitates transport of particles away from membrane surface (Muthukumaran *et al.*, 2005). Table 2.7 summarizes the studies related to the sludge disintegration method of fouling control. Zhang *et al.* (2007b) observed that sonication at 25 kHz for 30 minutes disintegrated the sludge flocs by 30%, reduced the solid mass by 23.9% and decreased the sludge viability by 95.5%. It has been found that ultrasonic irradiation induces various physical and chemical changes in the liquid which further depends on ultrasonic frequency, power intensity and characteristics of the liquid medium. Usually, low frequency and high intensity ultrasonic conditions are the preferable one for sludge disintegration (Aydin and Civelekoglu, 2010; Zhang *et al.*, 2008a). Zhang *et al.* (2008a) observed an increase in oxygen uptake rate, biomass growth rate and wastewater COD by 28%, 12.5% and 5-6% by employing sonication conditions with frequency of 25kHz, power intensity of 0.2 W/ml and duration of 30 s. Sui *et al.* (2007) reported that high power intensity of 150 W is efficient in controlling membrane fouling with a cross flow velocity of 0.75 m/s.

In another study by Xu *et al.* (2010b), while working on online ultrasonic equipment in an anaerobic membrane bioreactor for digestion of waste activated sludge concluded that ultrasonic power intensity of 0.18 W/cm^2 at 3 min/h was efficient in membrane fouling control with no membrane damage. Although ultrasound treatment effectively controlled membrane fouling, it suffers from certain drawbacks that limit its use. Major drawback is the membrane damage that is caused by collision of micro particle on membrane surface and also through chemical interaction between membrane materials and hydroxyl radicals produced by acoustic cavitations (Wen *et al.*, 2008).

2.5.3.2 Ozonation

Ozonation of sludge is considered as a promising technology because of its high sludge disintegration and solubilization capability. It also improves membrane permeability of mixed liquor (Oh et al., 2007; Huang and Wu, 2008; Hwang et al., 2010). Ozone, being a strong chemical oxidant is used in membrane bioreactors for sludge disintegration for breaking down cell walls. By applying ozone, refractory organic substances are oxidized and converted into biodegradable low molecular compounds. Zhang *et al.* (2009a) studied the effect of ozonation on sludge disintegration and supernatant changes and concluded that ozone dose of 50 mgO3/g DS decreased the sludge solid concentration and volatile solid concentration by 49.1% and 45.7%, respectively whereas supernatant soluble chemical oxygen demand, total nitrogen, total phosphorus, protein, polysaccharide and deoxyribonucleic acid increased by 699%, 169%, 2379%, 602%, 528% and 556%, respectively. As ozone is beneficial in preventing membrane fouling by bringing about sludge disintegration, researchers used this technology in MBRs for treating sludge. Oh *et al.* (2007) investigated the effects of disintegration treatment by ozone and NaOH on the excess sludge production in MBR by operating two MBRs, one with disintegration and other without it. They observed relatively constant TMP for more than 6 months in the bioreactor with disintegrated sludge.

Hwang *et al.* (2010) combined turbulent jet flow ozone contactor (TJC) with MBR to study the effect of disintegrated sludge on EPS, membrane's bio-cake formation and permeability of membrane. TJC generated ozonated sludge with negligible amount of LB-EPS and a positive zeta potential, the recycling of such sludge resulted in increased average sludge particle size, greater bio-cake porosity that ultimately resulted in increased membrane permeability. Wu and Huang (2010) studied the effect of ozonation on fouling mitigation in long-term MBR's. They supplied ozone at dosage of 0.25 mg g^{-1} –SS at 1 day intervals and found that ozonation is effective in removing colloidal and macro-molecular organics in supernatant, reducing eEPS content and enlarging sludge flocs by decreasing zeta potential and increasing hydrophobicity. Certain researchers compare the ozonation and ultrasonic treatment methods of sludge disintegration (Bougrier *et al.*, 2006; Erden *et al.*, 2010; Braguglia *et al.*, 2012). Erden *et al.* (2010) while applying specific energy of 9690 kJ/kg TS for ultrasonication and ozone dosage of0.1 g O_3/ kg TS to sludge samples,

Table 2.7 Ultrasonication method for sludge disintegration

S.No.	Operating Conditions	Outcomes	Reference
1.	• Permeate flux- 10 L/m^2h • BOD_5- 3630mg/L • COD- 4036 mg/L • HRT- 4 days • Organic loading rate- 0.91 Kg BOD_5/m^3 per day • Power output- 600W • Ultrasonic frequency- 20 kHz.	28% reduction in average sludge particle size and around 25-30% of phosphorus removal was achieved.	Yoon *et al.* (2004a)
2.	• Permeate flux- 24 L/m^2h • Ultrasonic frequency-28 kHz • Power output ranges- 30, 45, 60, 75, 90 and 150 W • Cross flow velocity- 0.75 m/s.	Ultrasound is efficient in maintaining membrane filtration resistance at 5 X 10^{11} m^{-1} for more than a week with cross flow velocity of 0.75 m/s same as that of effect of cross flow velocity of more than 1.0 m/s without ultrasound.	Sui *et al.* (2007)

3.	• Cross flow velocity- 0.75 m/s • Power intensity- 0.1222 W/cm^2 • Sonication on/off time-1 min/60 min and 3 min/ 60 min, respectively	With ultrasonic treatment , only 30% filtration resistance is observed	Sui *et al.* (2008)
4.	• Ultrasonic frequency- 28 kHz • Power intensity-0.12 W/cm^2 and 0.18W/cm^2	Volatile solids reduced by 52% and about 92% of cake layer was controlled with ultrasonic power intensity of 0.18 W/cm^2.	Xu *et al.* (2010b)
5.	• Flux- 7.5L/m^2h • Ultrasonic frequency- 25 KHz and 50KHz • Power intensity- 200 W	Delay in TMP rise and decrease in MLSS concentration, average particle size, EPS and sludge viscosity and also 51.85% decrease in total membrane filtration resistance was observed.	Li *et al.* (2013a)

observed that ultrasonication method is more efficient in terms of volatile solids reduction and protein degradation. However, it resulted in reduction of dewatering potential of sludge. In order to improve solubilization and anaerobic biodegradability of waste activated sludge, Xu *et al.* (2010a) applied both ozonation and ultrasonic treatment in combination. They observed 66.9% increases in soluble chemical oxygen demand as a result of sludge disintegration due to synergistic action of both the methods.

2.5.3.3 Use of Electric fields

External field approach where dc electric field is employed is recognized as a mean for managing membrane fouling. During the application of external electric field, phenomena like electrophoresis, electroosmosis, electrolysis, Joule's heating, ion migration occur. The membrane performance is improved by one or more of these mechanisms (Jagannadh and Muralidhara, 1996). Chen *et al.* (2007) built an antifouling MBR in order to investigate the effect of appending direct electric field on the membrane flux. They concluded that appending electric fields results in increased membrane flux. According to Liu *et al.* (2012), a very small electric field of 0.2 V/cm resulted in increase in flux and improvement in effluent water quality. Application of electric field induces electrophoresis of negatively charged foulants such as sludge and EPS away from the membrane surfaces and hence mitigating fouling. Lee and Chang (2014) studied the effectiveness of high voltage impulse (HVI) electric fields in membrane fouling mitigation. Higher flux recoveries after HVI induction were observed. Also, decrease in MLSS concentrations and increase in SCOD, total nitrogen, total phosphorus in bulk solution was seen. This was due to the damage of flocs and cells, caused by HVI.

2.5.3.4 Use of Carriers

Carrier addition to MBR's was explored as an attempt to control membrane fouling. Carriers mitigate membrane fouling through cake layer reduction as a result of collision between them and membrane surface and it also affects the sludge characteristics. Yang *et al.* (2006) studied the effect of porous flexible suspended carriers on membrane fouling mitigation. Critical flux increased by 20% and cake resistance decreased by 86% in short term trials. Huang *et al.* (2008b) while

studying the mechanism of membrane fouling control by suspended carriers came to the conclusion that they have two effects, positive effect leading to mechanical scouring on the membrane surface and negative effects of breaking up sludge flocs. The carriers effects on fouling mitigation depended upon the relative intensity of these two effects. According to Wei *et al.* (2006), higher MLSS concentration of 8 g/L and lower carrier dosage (v/v= 1%) resulted in retardation of TMP increase thereby retarding the negative effects of carriers.

Hu *et al.* (2012) employed hollow cylinder with internal cross-support and external gears as carriers in MBR and studied its effect on membrane fouling. He found that membrane biofouling problem in attached growth MBR was mitigated by biochemical effects of carriers on sludge characteristics.

2.5.4 Membrane modification approaches

Interaction of foulants with the membrane surface results in fouling. Aeration or turbulence can delay but cannot avoid the contact of foulants with membrane. The membrane surface properties such as hydrophobicity, charge and roughness are considered the major factors for fouling (Choi *et al.*, 2002; Deng *et al.*, 2014; Zhang *et al.*, 2014). Their modification/ alteration can minimize the intensity of fouling. Very few research is done in the field of membrane modification in MBR. Mostly microfiltration and ultrafiltration membranes are used in MBR for fouling studies. These membranes are made from polymers like cellulose, PES, polysulfone, polypropylene, polyacrylonitrile, polyethylene, polyvinylidenefluoride which because of their hydrophobic property are more prone to fouling (Huisman *et al.*, 2000; Choi *et al.*, 2002; Chan and Chen, 2004; Meng *et al.*, 2009; Sun *et al.*, 2013; Kochkodan *et al.*, 2014). Organic foulants, being hydrophobic tend to adsorb to the membrane surface through the attraction of foulants to the polymer surface of membrane. So, in order to minimize fouling by foulants adsorption, best way is the hydrophilic membrane modification which is done by either introduction of oxygen containing radical groups or hydrophilic polymers to the surface. This ultimately reduces the attractive force between the membrane surface and foulant. Many attempts have been made to minimize fouling through the process of surface coating and modification using hydrophilic monomers (grafting and blending) which is explained in following sections.

2.5.4.1 Membrane surface coating

Surface coating reduces the adhesion of foulants on the membrane surface and is considered to be one of the best methods to counter fouling. The surface coated membranes repel the bacteria and other foulants, but do not act as a toxicant. Modification through surface coating alters the membrane surface and pore size. However, the physical characteristics and stability of the source material is not affected. Molecular surface engineering is also done to develop an antifouling membrane (Yang *et al.*, 2011). A wide range of combinations from morphology, source material (substrate) and functional groups is possible. Any functional group can be covalently bonded to the substrates without affecting the physical characteristics (Tolwinska *et al.*, 1998; Park *et al.*, 2006; Asatekin *et al.*, 2007; Xi *et al.*, 2009). The coating can be done by casting (Asatekin *et al.*, 2007) and filtration (Boributh *et al.*, 2009) techniques. Casting involves addition of an amphiphilic copolymer to the membrane casting solution along with base material. The additive segregates in a water-based interfaces and hence creates a hydrophilic surface. Asatekin *et al.* (2007) prepared an anti-fouling ultrafiltration membranes containing polyacrylonitrile-graft-poly (ethylene oxide) PAN-g-PEO) comb copolymer additives via casting method. PAN-*g*-PEO additives segregates during casting so as to form PEO brush layer on all membrane surfaces. PAN-*g*-PEO imparts improved flux, wettability and fouling resistance to the membrane. From 24 h dead-end filtration studies, it was shown that the blend membranes prepared with 20 wt% PAN-*g*-PEO (comb PEO content: 39 wt%) exhibited complete resistance to irreversible fouling by 1g/L solutions of bovine serum albumin (BSA), sodium alginate and humic acid.

Boributh *et al.* (2009) modified polyvinylidenefluoride membrane with chitosan by three different methods, i.e. immersion method, flow through method and the combined flow through and surface flow methods to reduce BSA fouling. Among these methods, it was found that combined flow through and surface method showed best anti-fouling properties. This might be due to the deposition of chitosan both on the membrane surface and into the pores which might prevent adsorption of BSA.

Xi *et al.* (2009) designed a facile method for surface modification of polyethylene, poly(vinylidene fluoride) and polytetrafluoroethylene based on the adhesive

behavior of poly((3,4-dihydroxyphenylalanine) and dopamine. Water contact angle for polyethylene, poly(vinylidene fluoride) and polytetrafluoroethylene decreased by 27%, 45% and 35% indicating the successful introduction of hydrophilic groups onto the membrane surface. From the water flux studies, it has been found that, the relative water flux increased with increasing coating time. It reached a maximum value of 1.64 before coating for 20 hours and then decreased to a value less than 1. This might be due to the formation of polymer layer on the porous membrane surface because of exceeding poly(dopamine) which ultimately blocked the membrane pores. This results in increased resistance and decreased water flux.

Liu *et al.* (2013) modified the surface of polyester filter cloth by coating with polydopamine (PDA). The results showed approximately 36% increase in the stable flux in short-term test in MBR after PDA coating. Although, PDA coating increased the membrane surface hydrophilicity but it decreased the membrane fouling resistance thereby resulting in high transmembrane pressure during constant flux operation. So, it is recommended to apply the PDA coating to the membrane of high native permeance (Miller *et al.*, 2014).

2.5.4.2 Modification using hydrophilic additives

Besides coating the hydrophilic polymers on membrane surface, addition of hydrophilic additives to the membrane is also used for membrane modification. This can be done either by adding hydrophilic particles to the membrane surface (Madaeni *et al.*, 2011; Luo *et al.* ; 2011; Ng *et al.*, 2013) or by graft polymerization (Zhang *et al.*, 2009c; Sawada *et al.*, 2012)

2.5.4.2.1 Membrane surface modification with nanoparticles

In the current era, hydrophilic particles have been widely studied for counteracting membrane fouling (Kim and Bruggen, 2010; Ng *et al.*, 2013). The most useful hydrophilic additives that grab much attention is metal oxide nanoparticles (Son *et al.*, 2004; Bae and Tak, 2005a; Luo *et al.*, 2005; Li *et al.*, 2009a and b). Two different approaches are followed for preparing nanoparticle based membranes; one involves the deposition of nanoparticles on membrane surface (Li *et al.*, 2009b; Madaeni *et al.*, 2011) and second involves entrapment of nanoparticles in polymer matrix via

phase inversion method (Luo *et al.*, 2011; Zhang *et al.*, 2012b; Dulebohn *et al.* (2014).

(i) Modification with deposited nanoparticles: Titanium dioxide (TiO_2), being photocatalytic in nature remains a topic of research. It can decompose organic chemicals and also kill bacteria (Mills and Hunte, 1997). Thus, it has been applied to membrane surfaces for modification. Certain researchers studied the influence of TiO_2 nanoparticles in membrane fouling mitigation. Bae and Tak (2005a) prepared TiO_2 entrapped as well asTiO_2 deposited ultrafiltration membranes and applied them to activated sludge filtration so as to assess their fouling mitigation effect. The slower flux decline was seen in TiO_2 entrapped membrane when compared to neat polymeric membrane. However, greater fouling mitigation was observed in TiO_2 deposited membranes rather than entrapped membranes. The degree of fouling mitigation is related to surface area of TiO_2 nanoparticles, which are located on the membrane surface and exposed to feed solution. In case of TiO_2 entrapped membranes, nanoparticles are uniformly distributed through the membrane cross section whereas in TiO_2 deposited membranes, the nanoparticles are located only on the membrane surface. So in this case, degree of surface modification is more than that of entrapped membranes and thus resulting in greater fouling mitigation. But stability of deposited nanoparticles is still a matter of concern. To overcome this drawback, Bae and Tak (2005b) prepared composite membrane by self-assembly between TiO_2 particles and sulfonic acid groups. It was found that the self–assembled polymeric nanocomposite membranes 1, 2 and 3 showed about 10%, 39% and 65.7% decrease in filtration resistance as compared to neat membranes. Decrease in filtration resistance strongly suggested that the adsorbed foulants on the nanocomposite membranes could be more readily dislodged by shear force (Chang *et al.*, 2002; Choi *et al.*, 2002). Li *et al.* (2009b) also prepared TiO_2 nanoparticle self-assembly membrane which shows better permeability and anti-fouling ability in comparison to poly(styrenealtmaleic anhydride)/ poly(vinylidene fluoride) (SMA/PVDF) blend membrane. It was shown that the relative flux was decreased from 83.5% to 58.7% and flux recovery ratio improved and increased from 28.2% to 80.5% in case of modified membrane.

Antifouling potential of TiO_2 modified membranes has been improved with the application of UV irradiation. It has been found that when TiO_2 nanoparticles are

irradiated with UV light, a pair of holes and electrons is created on the particles surface. The electrons generated by this photocatalysis reaction tend to reduce Ti(IV) cations to the Ti(III) state and the holes oxidize O^{2-}anions. Oxygen atoms are removed which produces a group of oxygen vacancies on the surface. The water molecules in the environment tend to occupy the empty sites and adsorbed hydroxyl groups are created on the surface which ultimately increases the membrane surface hydrophilicity (Diebold, 2003; Carp *et al.*, 2004; Guan, 2005; Langlet *et al.*, 2006). Madaeni *et al.* (2011) deposited TiO_2 nanoparticles on the ultrafiltration membrane surface and irradiate it with ultraviolet light. Significant decrease in water contact angle from 48˚ to 12˚ was seen which indicates a considerable increase in membrane hydrophilicity. However, blockage of membrane pores was observed at high TiO_2 nanoparticles concentration which ultimately reduces flux.

(ii) Phase Inversion method: Phase inversion is an eminent process for the membrane modification where initially homogenous polymer is converted in a controlled manner from liquid to soild state (Gkotsis *et al.*, 2014). Luo *et al.* (2011) prepared a sulfonated polyethersulfone/ nano-TiO_2 nanocomposite ultrafiltration membrane by phase inversion and assembly methods. They observed decreased mean pore size, increased surface roughness and decreased contact angles of the composite membranes. Silver nanoparticles are also known to possess anti-bacterial properties (Choi *et al.*, 2008; Kim *et al.*, 2008; Marius *et al.*, 2011). Silver ions interact with the thiol group of cysteine that normally present in the bacterial cell membrane (Matsumura *et al.*, 2003). They react with the thiol groups to form S-Ag complex, thus hindering the enzymatic function of protease (Kim *et al.*, 2008). Keeping this in view, certain researchers modified the membranes using silver nanoparticles.

Zodrow *et al.* (2009) incorporated silver nanoparticle into polysulfone ultrafiltration membranes. The modified membrane exhibited antimicrobial properties against *Escherichia coli* K12 and *Pseudomonas mendocina* KR1 and MS2 bacteriophage. However, silver nanoparticles suffer from leaching problem. X-ray photoelectron spectroscopy analysis showed that after a relatively short filtration period of 0.4 L/cm^2, there occurred a significant loss of silver from the membrane surface. To overcome this problem, Basri *et al.* (2010) applied polyvinylpyrrolidone (PVP) and

2,4,6-triaminopyrimidine (TAP) as dispersant in silver-filled polyethersulfone membranes. Using inductively coupled plasma mass spectrometry (ICP-MS), up to 57% and 63% reduction in silver leaching was seen upon addition of PVP and TAP, respectively. This improved silver dispersion on membrane surfaces. The attachment of silver particles is related to the coordination bonds between nitrogen atoms in PVP or TAP (Wang *et al.*, 2005). PVP structure contains only one nitrogen atom whereas TAP contains two nitrogen atoms from aromatic ring and another three atoms from the amine groups. This results in higher content of silver attachment (Basri *et al.*, 2010). From antibacterial activity studies, it was shown that PES-$AgNO_3$ with TAP as dispersant inhibited almost 100% bacterial growth in rich medium.

Zhang *et al.* (2012b) embedded biogenic silver nanoparticles into polyethersulfone membranes using phase inversion method. The anti-bacterial and anti-biofouling properties of this nanocomposites membrane have been tested with pure cultures of *Escherichia coli* and *Pseudomonas aeruginosa* and a mixed culture (an activated sludge bioreactor), respectively. It has been seen that even the lowest silver content of 140 mgbio-Ag^0 m^{-2} is capable of preventing the bacterial attachment to the membrane surface and decreased the biofilm formation during a 9 weeks test.

Huang *et al.* (2014) fabricated Ag-SiO_2 nanocomposite polyethersulfone (PES) membranes by phase inversion method. It was found that the contact angle decreased from 67.7˚ to 52.6˚ with the increase of Ag-SiO_2 loading indicating the increased hydrophilic characteristic of membrane. Anti-bacterial property of the membrane was studied with pure cultures of *Escherichia coli* and *Pseudomonas* sp. Results showed that the surfaces of membranes containing 0.48% and 0.96% silver were clean and free of bacteria growth. However, silver nanoparticles suffer from leaching problem. During phase inversion, some Ag-SiO_2 particles may leach into water with the diffusion flow of solvent and non-solvent which might be due to the physical incompatibilities between polymeric and inorganic materials.

Besides silver nanoparticles, alumina nanoparticles are also used for modifying membrane because of its intrinsic properties, for instance mechanical resistance and hydrophilicity (Yan *et al.*, 2005; Maximous *et al.*, 2009). Homayoonfal *et al.* (2015) prepared polysulfone/ alumina nanocomposite membranes via phase

inversion method. It was shown that polysulfone membrane impregnated with 0.03 wt.% Al_2O_3 nanoparticles resulted in 4 times increase in water flux and 83% reduction in membrane fouling. On the other hand, Dulebohn *et al.* (2014) prepared polymeric mesocomposite membranes by incorporating surfactant-templated mesoporous silica particles (MSP) into polysulfone matrices formed with and without PEG as a molecular porogen. Results showed that mesoporous membrane with 10 wt% initial loading of MSP-1 exhibited filtration performance that is higher by the factor of 2.8 (for membranes cast with a porogen) and 6.3 (in the absence of porogen) as compared to MSP-free controls. Also, the addition of MSP-1 even at high loading of 10 wt% did not affect the membranes mechanical strength.

2.5.4.2.2 Graft polymerization

Graft polymerization is a process of surface modification to develop a fouling resistant polymeric membrane. A polymer carrying the reactive group is covalently bonded to the surface of the membrane. Grafting is well known for its multiple advantages such as long term chemical stability due to covalent bonding of graft chains, specific choice of different monomers and controlled introduction of high density graft polymers without affecting the base membrane (sa and Misra, 2004). Grafting improved the flux rates.

(i) Radiation Grafting polymerization: Radiation grafting polymerization employ usage of ultraviolet and ionization radiation to create active sites on the membrane surface on which monomers are then grafted. This step is followed by polymerization of the monomer thereby forming a hydrophillic layer on membrane surface. Zhang *et al.* (2009c) grafted N-vinyl-2-pyrrolidinone onto the poly (vinylidene fluoride)-based microporous membrane containing a small quantity of PES with UV irradiation and then treated the modified membrane with BSA. They observed that the modified membrane exhibited fouling reduction by 66% and 32% flux recovery compared to non-modified PVDF membrane. Susanto *et al.* (2008) tested the antifouling efficiency of new thin layer hydrogel composite ultrafiltration membranes based on commercial PES membranes prepared via photo-initiated grafting method. Results shows that the ultrafiltration fluxes were much higher than with the unmodified PES membrane.

(ii) Plasma treatment: Plasma treatment have been carried out over the last few decades to modify membrane surface (Chen and Belfort, 1999; Vidaurre *et al.*, 2002; Yu *et al.*, 2005a; Yu *et al.*, 2005b; Tran *et al.*, 2007). Plasma treatment involves usage of plasma (a low pressure gas containing electron, photons, ions, and other charged particles) in presence of oxygen so as to form peroxides on the membrane surface which then decompose to form oxygen containing radical groups for instance, hydroxyls, carbonyls, or carboxyls and hence make the surface hydrophilic. By employing plasma treatment, specific surface chemistries can be created that reduces the attractive forces between protein and membrane surfaces. This ultimately minimize protein adsorption and hence counteract membrane fouling (Wavhal and Fisher, 2002).

Steen *et al.* (2001) modified polysulfone membranes with low temperature plasma treatment. The contact angle measurements confirmed improvement in the wettability of membranes that would be more than 16 months indicating permanent hydrophilic modification of membranes. Also, the plasma modified membranes are shown to be less susceptible to protein fouling as compared to unmodified membrane. Bryjak *et al.* (2002) modified ultrafiltration polysulfone membranes with NH_3 and NH_3/ Ar plasma. An enlargement in membrane pore diameter was observed in treated membrane. Although, argon plasma might increase the membrane hydrophilicity, it also decreased the pore diameter resulting in redeposition of etched material on the pores wall. In contrast, the pure ammonia plasma cleaned the membrane surface and demonstrated better flux recovery after cleaning (Yu *et al.* 2005a).

Besides ammonia and argon gases, CO_2 plasma is also used to improve the hydrophilicity of the membrane. CO_2 plasma treatment introduces oxygen containing polar groups onto the membrane surfaces ultimately increasing the hydrophilicity of treated membranes and hence improving the filtration performance (Yu *et al.*, 2005b). Still, plasma treatment of membranes with non-polymerizing gases has a severe problem. Membrane hydrophilicity on membranes is not permanent and vanishes after treatment. Due to segmental mobility of conventional polymers, rearrangement of their surface composition occurs in response to interfacial forces which results in time dependency of surface properties of plasma treated polymers. This significantly affects the membrane performance. However,

grafting and polymerizing monomers onto a plasma treated membrane can provide more stable and long lasting surface.

In a study by Wavhal and Fisher (2002), complete and permanent hydrophilic modification of polyethersulfone membranes has been done with argon plasma followed by polyacrylic acid grafting in vapor phase. The membrane showed resistance to protein fouling. A change in pore diameter is observed in plasma modified membranes. Tran *et al.* (2007) modified polyacrylonitrile ultrafiltration membranes by using oxygen plasma and then grafted acrylic acid monomer on the membrane surface effectively. The results showed that the modified membrane had larger pure water flux than the original membrane.

2.5.5 Biological methods of fouling control

Biofilm formation occurs when aggregates of micro-organisms attach themselves onto the surface and build up their colonies. These aggregates along with EPS become the principle reason for membrane biofouling. Formation of biofilm is a behaviour reported due to QS mechanism. QS is the mechanism of intercellular communication which is used by the bacteria for regulating various group behaviours including biofilm formation. The bacteria though are unicellular microorganisms but they do not exist as individual cells and live in colonies. They exhibit intercellular communication that allows them to perform a particular function. Signalling molecules such as AHL, furanosyl borate diester, 4,5-dihydroxy-2,3-pentanedoine, methyl dodecenoic acid and diketopiperazines are required in QS mechanism (Parsek *et al.*, 1999; Chen *et al.*, 2002; Zhu *et al.*, 2003; Li *et al.*, 2009c; Gu *et al.*, 2013). To date, the QS communication circuits were used by both gram-positive and gram-negative bacteria (Diggle *et al.*, 2007; Williams *et al.*, 2007) to regulate different physiological activities such as symbiosis (e.g.,*Vibrio fischeri* LuxI/ LuxR Bioluminescence system), virulence (e.g., *Staphylococcus aureus* AgrC/ AgrA Virulence system), antibiotic production (e.g., *Erwinia carotovora* ExpI/ExpR-CarI/CarR Virulence/ Antibiotic system), competence (e.g., *Streptococcus pneumonia* ComD/ComE competence system), sporulation (e.g., *Bacillus subtilis* ComP/ComA Competence/Sporulation system), conjugation (e.g., *Agrobacterium tumefaciens* TraI/TraR virulence system), motility and biofilm formation (Miller and Bassler, 2001; Diggle *et al.*, 2007; Williams *et al.*, 2007).

The detection of AHL molecules in biofilm point out the involvement of QS mechanisms in biofilm formation. For instance, in the formation of *Vibrio cholera* biofilm, QS mechanisms play central role in directing the expression of genes responsible for EPS biosynthesis (Hammer and Bassler, 2003). Researchers also witnessed the role of QS signals in the development of *Pseudomonas aeruginosa* biofilms (Davies *et al.*, 1998; Brooun *et al.*, 2000). So, with the relation of QS with the biofilm formation, it is crucial to develop some strategies which can disrupt these communication systems in bacteria. One such approach is 'QQ' which is under limelight for biofouling control on membrane surfaces (Choudhary and Schmidt-Dannert, 2010). QQ involves obstruction of QS mechanism through degradation of signalling molecules which lead to biofilms disruption resulting in biofouling control. The anti-QS activity is common in bacteria, fungi and certain plants (Yin *et al.*, 2012; Zhu *et al.*, 2011; Zahin *et al.*, 2010). Besides this, biofouling can also be controlled through inhibition of ATP synthesis by a method of chemical uncoupling of energy metabolism (Xu and Liu, 2011). Since, the research focuses on biofouling control using QQ bacteria, the biological method of fouling control will be covered in detail in the following section.

2.5.5.1 QQ activity in Plants, Fungi and Yeast

Wide array of plants have been reported to possess QQ activity (Zahin *et al.*, 2010; Balakumar *et al.*, 2010; Siddiqui *et al.*, 2012a; Song *et al.*, 2012; Anitha and Mahalakshmi, 2012). List of plants along with their parts possessing QQ activities is summarized in Table 2.8. Zahin *et al.* (2010) screened 24 plants for their anti QS activity using biosensor strain *Chromobacterium violaceum* (CV12472 and CV026) and found that out of these 24 medicinal plants, five plants (Table 2.8) showed varying level of inhibition of purple pigment, violacein in the reporter strains. Also, at elevated concentrations, except *P. corylifolia*, all the rest four exhibited antibacterial activity together with anti-QS activity. Certain herbal plants are also known to hold QQ activity (Al-Hussaini and Mahasneh, 2009; Chu *et al.*, 2013). Zhu *et al.* (2011) isolated pigments from fungi *Auricularia auricular* and revealed that these pigments reduced violacein production in *Chromobacterium violaceum*. Certain yeast are also found to possess QQ activity. Wong *et al.* (2013) reported degradation of signalling molecules N-butanoyl homoserine lactone (C4-HSL), N-hexanoyl homoserine

Table 2.8 List of plants with quorum quenching activity

S.No.	Plant used	Part of plant possessing QQ activity	Specific role	Reference
1.	*Vanilla planifolia* Andrews extract	Beans	Violacein reduction in *Chromobacterium violaceum* CV026 in a concentration dependent manner indicating quorum sensing inhibition	Choo *et al.* (2006)
2.	*Laurus nobilis*	Fruits, leaves, flowers and bark extract	QQ activity against *Staphylococcus aureus*, Methicillin Resistant *Staphylococcus aureus*, *Bacillus cereus*, *Bacillus subtilis*, *Klebsiella pneumonia*, *Aspergillus niger*, *Chromobacterium violaceum*, *Salmonella typhimurium*, *Pseudomonas aeruginosa*	Al-Hussaini and Mahasneh (2009)
3.	*Sonchus oleraceus*	Aerial part extract	QQ activity against *Staphylococcus aureus* , Methicillin Resistant *Staphylococcus aureus*, *Bacillus*	

			subtilis, *Klebsiella pneumonia*, *Aspergillus niger*, *Chromobacterium violaceum*, *Salmonella typhimurium*, *Pseudomonas aeruginosa*	
4.	*Hemidesmus indicus* (L.) Schult	Root	Inhibition of purple pigment, violacein in *Chromobacterium violaceum* (CV12472 and CV026)	Zahin *et al.* (2010)
5.	*Holarrhena antidysenterica* (Roth) A.DC.	Bark		
6.	*Mangifera indica* L.	Leaves		
7.	*Punica granatum* L.	Pericarp		
8.	*Psoraleacorylifolia* L.	Seeds		
9.	*Phyllanthus emblica*	Fruit aqueous and ethanol extract	Decreased proteolytic, Las B elastase, pyocyanin activity and biofilm formation in *Pseudomonas aeruginosa*	Balakumar *et al.* (2010)
10.	*Quercus infectoria*	Galls aqueous extract		
11.	*Piper betle*	Leaves extract	Inhibition of autoinducers (AIs)	Siddiqui *et al.* (2012a)
12.		Hexane, methanol and chloroform extract	Cessation of pyocyanin production in *Pseudomonas aeruginosa* PAO1	Tan *et al.* (2013)

13.	*Piper nigrum*		Quorum quenching activity against *Chromobacterium violaceum* CV026 and against *E. coli* pSB 401 bioluminescence in *E. coli* pSB 401 and *E. coli* pSB 1075	
14.	*Gnetum gnemon*		Interruption of bioluminescence in *E. coli* pSB 401 and *E. coli* pSB 1075	
15.	*Scutellaria baicalensis* Georgi	Plant ethanol extract	Inhibition of violacein production in *Chromobacterium violaceum* CV026 and reticence of QS-regulated virulence in *Pectobacterium carotovorum* subsp. *carotovorum*.	Song *et al.* (2012)
16.	*Rhubarb*	Whole plant	Reduction in pyocyanin pigment, protease, elastase production and biofilm formation in *Pseudomonas aeruginosa* PAO1	Chu *et al.* (2013)
17.	*Fructus gardeniae*			
18.	*Andrographis paniculata*			

lactone (C6-HSL), N-(3-oxohexanoyl) homoserine lactone (3-oxo-C6-HSL), N-heptanoyl homoserine lactone (C7-HSL), N-octanoyl homoserine lactone (C8-HSL) and N-(3-oxooctanoyl) homoserine lactone (3-oxo-C8-HSL) by the yeast *Trichosporon loubieri* WW1C isolated from the tropical wetland waters of Malaysia. Ghani *et al.* (2014) in his study on saprophytic yeast *Rhodotorula mucilaginosa* isolated from tropical shoreline found that the yeast possessed an enzyme lactonase that was capable to degrade C6-HSL, 3-oxo-C6-HSL and 3-hydroxy-C6-HSL.

2.5.5.2 QQ activity in bacteria

The bacterial isolates are more explored for quenching quorum sensing regulated functions. Table 2.9 summarizes a directory of bacteria along with the quencher and the function which is known to be quenched by these bacterial isolates.

The diversity of bacteria producing QQ enzymes ranges slightly (i) Proteobacteria- *Pseudomonas*, *Acinetobacter*, *Burkholderia*, *Klebsiella*, *Aeromonas*, *Comamonas*, *Shewanella*, *Enterobacter asburiae* (ii) Firmicutes- *Bacillus*, *Arthrobacter*, (iii) Actinobacteria- *Rhodococcus erythropolis, Kocuria rhizophila* (Chan *et al.*, 2007; Uroz *et al.*, 2009; Chan *et al.*, 2011; Christiaen *et al.*, 2011; Mahmoudi and Ahmadi, 2012).

These bacterial isolates were obtained from wide array of sources like soil, sewage, rhizosphere of different plants including potato, *Zingiber officinale* etc, red sea sediments, fouled RO membrane and many more. Table 2.10 enlists certain QQ bacteria along with their source.

2.5.5.3 Quorum quenching mechanism and biofouling control

The plants and bacteria were tested for their biofouling control potential in MBR.

2.5.5.3.1 Plants

Out of the reported plants in Table 2.8, Piper betel extract (PBE) was tested for biofouling mitigation (Siddiqui *et al.*, 2012b). Its leaves extract possessed anti-

bacterial activity (Nair and Chanda, 2008) thereby reported as membrane biofouling reducer (Siddiqui *et al.*, 2012a).

Table 2.9 List of quorum quenching as a result of introduction of bacteria capable of degrading AHLs

S.No.	Quenched	Quencher	Function quenched
1.	*Agrobacterium tumefaciens*	*Rhodococcus erythropolis* W2, *Bacillus spA24*	pTi transfer
2.	*Aeromonas*	*Shewanella* sp.	Exoprotease production
3.	*Chromobacterium violaceum*	*Rhodococcus erythropolis* W2 *Comamonas* sp. D1 B*acillus* sp. A24	Violacein production
4.	*Pseudomonas chlororaphis* PCL1391	*Bacillus* sp. A24 *Acinetobacter* sp. C1010	Phenazine production

(**Source**: Uroz *et al.*, 2009)

According to Siddiqui *et al.* (2012b), PBE decreased the TMP rise in MBR via blocking the production of AHLs. Certain plants produce compound that possess anti biofouling activity. Curcumin is one such compound which is found in turmeric that is known to inhibit biofilm formation in gram positive as well as gram negative bacteria (Lade *et al.*, 2015; Lade *et al.*, 2017). Lade *et al.* (2017) reported delay in TMP and a 17% reduction in EPS in the curcumin incorporated MBR which is attributed to its biofilm inhibition ability.

2.5.5.3.2 Bacteria and others

The bacteria exhibited QQ mechanism to control biofilm formation on membranes which can be achieved through degradation of Acyl Homoserine Lactone (AHL) molecules. This degradation can be brought about by AHL-inactivating enzyme possessed by bacteria that causes enzymatic inactivation of signalling (AHL) molecules. Dong *et al.* (2002) reported that the strains *B. thuringiensis*, *B. cereus*,

Table 2.10 QQ bacteria isolated from different sources

S.No.	Source	Quorum Quenching bacteria	Reference
1.	Sewage	*Proteobacterium*	Chan *et al.* (2009)
2.	*Zingiber officinale* rhizosphere	*Acinetobacter, Burkholderia* and *Klebsiella*	Chan *et al.* (2011)
3.	*Potato* rhizosphere	*Bacillus, Arthrobacter* and *Pseudomonas*	Mahmoudi and Ahmadi (2012)
4.	Soil	*Arthrobacter* and *Pseudomonas* sp.	Chong *et al.* (2012)
		Bacillus cereus and Bacillus thuringiensis	Chan *et al.* (2007); Dong *et al.* (2002)
5.	Ant lion	*Aeromonas*	Christianto and Yogiara (2011)
6.	Rhizosphere (*Cactaceae*)	*Microbacterium shrimpcida, Leifsonia sp.*, *Kocuria rhizophila*	Christiaen *et al.* (2011)
	Rhizosphere (*Araceae*)	*Arthrobacter* sp., *Comamonas* sp., *Advenella incenata*	
	Pond water (indoor)	*Aeromonas media*, *Delftia* sp., *Citrobacter* sp, *Aeromonas* sp.	
	Rhizosphere (*Plumbaginaceae*)	*Staphylococcus* sp., *Delftia* sp., *Arthrobacter nicotinovorans*, *Arthrobacter aurescens*	
	Rhizosphere (*Brassicaceae*)	*Arthrobacter* sp., *Achromobacter xylosoxidans*, *Delftia* sp., *Kocuria* sp.	
7.	Chinese Soya sauce brine	*Bacillus sonorensis*	Yin *et al.* (2012)
8.	*Pterocarpus santalinus* Linn.	Endophytic bacteria such as *Bacillus firmus* PT18 and *Enterobacter asburiae* PT39	Rajesh and Rai (2014)

9.	Sludge of wastewater treatment plant	*Acinetobacter, Pseudomonas*, *Micrococcus*	Kim *et al.* (2014)
10.	Fouling RO membrane	*Pseudomonas, Bacillus*, *Delftia tsuruhatensis*, *Stenotrophomonas maltophilia*	Zhang *et al.* (2017)
11.	Red sea sediments	*Erythrobacter*, *Labrenzia*, *Bacterioplanes*	Rehman and Leiknes (2018)

and *B. mycoides*, produces AHL inactivating enzyme AHL-lactonase which is known to hydrolyse the homoserine lactone ring of AHL signals while other enzyme AHL acylase encoded by certain bacterial species like *Varivorax paradoxus, Pseudomonas aeruginosa* PAO1 and *Streptomyces* sp. is known to carry out the hydrolysis of amide bond of AHLs, thereby producing fatty acids and homoserine lactone (Leadbetter and Greenberg, 2000; Huang *et al.*, 2003; Park *et al.*, 2005).

These enzymes are found to play an indispensable role in biofouling control in wastewater treatment processes like MBR. Table 2.11 enlists the studies related to the control of membrane biofouling in the MBR. Yeon *et al.* (2009a) utilizes porcine kidney acylase I enzyme for biofouling control in MBR. They applied the acylase enzyme to the batch type of MBR and noticed retardation in TMP in comparison to control thereby concluding that acylase abridged the membrane biofouling via quenching of AHL autoinducers. However, the diminutive catalytic time and complications in recovering free enzymes limits its application for long term continuous operation.

The best alternative to overcome the limitation would be enzyme immobilization on a suitable support system. Yeon *et al.* (2009b) immobilized free acylase enzyme in magnetic enzyme carrier and found them to be more stable when compared to free enzymes in terms of its ability to degrade AHL autoinducers as they reside in MBR for more time because of their large size than the membrane pores and can be easily recovered and reused.

Kim *et al.* (2011) immobilized free acylase enzyme on to a nanofiltration membrane. They observed that acylase immobilized membrane prevent the formation of mature

biofilm due to reduction in secretion of EPS. In addition, 90% of initial enzyme activity are maintained by the membranes for more than 20 iterative cycles of reaction and washing process.

Lee *et al.* (2014) immobilized acylase enzyme into magnetically separable mesoporous silica. They found that NER-AC (nanoscale enzyme reactor with acylase) alleviate the biofilm maturation on the surface, thereby enhancing the membrane permeability at a very low effective dosage level of 0.5 mg/L.

Although enzymatic QQ is considered to be a novel approach for biofouling mitigation in MBR but the enzyme cost, stability and need of enzyme purification restricts its use. This setback can be overcome by usage of intact bacterial cell. A number of studies are there where immobilized bacteria were used.

Oh *et al.* (2012) encapsulated recombinant *E.coli* that produce N-acyl homoserine lactone and real MBR plant isolated *Rhodococcus sp.* inside the microporous hollow fiber membrane lumen. The hollow fiber membrane module was put in the submerged MBR and assessed for 80 days. A delay in the increase of TMP was observed indicating the control of biofouling by QQ bacteria. However, internal submerged MBR equipped with microbial vessel had much lesser biofouling propensity as compared to conventional MBR. So, Cheong *et al.* (2013) encapsulated the lab scale MBR isolated *Pseudomonas* sp. 1A1 in a microbial vessel (made of hollow fiber microporous membrane) and concluded that this bacterium has extracellular QQ activity and produced AHL-acylase capable of degrading N-acyl homoserine lactones.

Kim *et al.* (2013) entrapped QQ bacteria *Rhodococcus* sp. BH4 into the microstructural pores of the alginate beads. Reduction in generation of EPS by microbial cells in biofilm was observed. The biofilm formed during this study was loosely bound which can be easily sloughed off from the surface of the membrane. Also, the moving cell entrapping beads and membranes collide with each other and as a result of frictional forces create disconnection between biofilm and the membrane surface.

Similarly, the *Rhodococcus* sp. BH4 entrapped in the other immobilization media such as hollow cylinder and polymer membrane layer coated microcapsules also

exhibited an excellent biofouling control in MBR (Kim *et al.*, 2015; Lee *et al.*, 2016b). Mutlu *et al.* (2016) carried out the detailed study on the biofouling control efficiencies of three different QQ immobilization media (Microbial vessel, Cell entrapping alginate beads, and rotating microbial carrier frame). Among the three immobilization media, cell entrapping alginate beads (CEB) is more effective in controlling biofouling (biofouling prevention efficiency of 99.3%). They also studied the effect of flux increase on the biofouling controlling potential of CEB and observed a decrease in biofouling control potential with increase in flux from 20 to 50 L/m^2/h. Certain researchers also evaluated the QQ activity of QQ bacteria consortium on the biofilm control (Waheed *et al.*, 2017). Recently, polymeric beads encapsulated with QQ bacteria consortium (*Enterobacter cloaca*, *Delftia* sp. and *Pseudomonas* sp.) has been used successfully to control biofouling in MBR (Waheed *et al.*, 2018). It has been found that the consortium containing MBR showed slightly lower bound EPS than the control MBR.

Now a days, researchers have applied an integrated approach to enhance the MBR performance by retarding both the membrane biofouling and pore blockage. Hasnain *et al.* (2017) demonstrated the combined effect of the use of QQ bacteria *Rhodococcus sp.* immobilized in polysulfone coated sodium alginate beads and backwashing (1 min) as a method to control membrane fouling in MBR. Compared to conventional MBR, three times longer filtration cycle was observed. Also, 61% reduction in soluble EPS was reported in QQ-MBR with backwashing. While the presence of QQ bacteria extended the filtration cycle due to mitigation of biofouling, the backwashing inhibited pore narrowing and pore blocking mechanism, thereby delaying the TMP jump. Waheed and Hashmi (2017) investigated the combined effect of QQ consortium (*Microbacterium* sp., *Pseudomonas* sp. and *Rhodococcus* RBH4) immobilized into alginate-polysulfone mixture and extended backwashing (backwash mode of 2 min) on the membrane biofouling control. They observed seven and three times longer filtration cycle when compared to conventional MBR and MBR with backwash, respectively. In another study by Weerasekara *et al.* (2016), combined effect of QQ bacteria *Rhodococcus* BH4 immobilized in microbial vessel and chemically enhanced backwashing (chlorine dose of 100 mg/L) was

Table 2.11 Biological methods of biofouling control

S.No.	Immobilization carrier use	Quorum quenching bacteria or enzyme	Reactor volume	Mixed liquor suspended solids (mg/L)	Hydraulic retention time (h)	Sludge retention time (days)	Flux ($L/m^2/h$)	Outcomes	References
1.	Magnetic enzyme carrier	Enzyme acylase	1 L	24,000 (± 3500)	10	50	15	In Continuous QQ-MBR, EPS production in biocake layer was retarded by nine times and TMP value is maintained at 10 kPa in both operations by the addition of MEC whereas in control, TMP rise	Yeon *et al.* (2009b)

								above 30 kPa in 48 h.	
2.	Hollow fiber microbial vessel	*Rhodococcus* sp. BH4	2 L	Recirculation rate of 7.5-30 mL/min	12	50	30	At higher recirculation rate of 30 mL/min of mixed liquor, more biofilm inhibition was seen. In addition, slower TMP rise (30 kPa in 68 h) was observed compared to control MBR (34 h).	Jahangir *et al.* (2012)
3.	Microporous hollow fiber membrane	Recombinant *E. coli* producing enzyme AHL lactonase,	1.2 L	4500-5000	12	40	18- 20	TMP increased to 25 kPa in 39 h in QQ-MBR and in 28 h in control.	Oh *et al.* (2012)

		Rhodococcus sp. BH4							
4.	Hollow fiber microbial vessel	*Pseudomonas* sp. 1A1	2.5 L	7600-8000	8	30	25	TMP rise to 50 kPa took 5.5 days in QQ-MBR when compared to control (2.2 days), extracellular QQ activity showing degradation of longer chain AHL molecules.	Cheong *et al.* (2013)
5.	Cell entrapping alginate beads	*Rhodococcus* sp. BH4	1.6 L	12,500-13,000	5.3	25	28.7	Exhibited maximum TMP of 70 KPa in 18.8 days in QQ-MBR as compared to 1.8 days in control.	Kim *et al.* (2013)

6.	Microbial vessel made of monolithic ceramic microporous membrane	*Pseudomonas* sp. 1A1	3 L	11,000-13,000	6	60	25, 30 and 35	62.2% reduction in polysaccharides content of mixed liquor, 37.7% and 43.4% reduction in polysaccharide and proteins, respectively in EPS was seen.	Cheong *et al.* (2014)
7.	Cell entrapping alginate beads	*Rhodococcus* sp. BH4	35 L	10,000-11,000	4	20	15	Higher pore blockage resistance (R_p) (32.5% of total hydraulic resistance) and 7 times increased filtration duration, delay in TMP rise, lesser EPS	Maqbool *et al.* (2015)

								production in QQ-MBR as compared to control MBR (19.7% of total hydraulic resistance), TMP took 95 days in QQ-MBR to reach its terminal value of 30 kPa as compared to 12 days in control.	
8.	Alginate beads and hollow cylinder (HC)	*Rhodococcus* sp. BH4	3 L	4720- 6240	8	30	21	QQ hollow cylinder and QQ-beads mitigate membrane fouling by 4.5 and 2.3 times,	Lee *et al.* (2016b)

								respectively compared to control-MBR.	
9.	Cell entrapping alginate beads Microbial vessel Rotating microbial carrier frame	*Rhodococcus* sp. BH4	5 L	12,000-13,000	13	30	50	Around 44% and 59.7% TMP decrease was observed during operation of MBR with microbial vessel and rotating microbial carrier frame, respectively compared to control. However, the cell entrapping alginate beads were found to be most successful	Mutlu *et al.* (2016)

								in controlling membrane biofouling as compared to other two immobilization media.	
10.	Polymer-coated alginate beads	A QQ consortium comprising of AHLs degrading strains *Enterobacter cloaca*, *Microbacterium* sp. and *Pseudomonas* sp.	450 mL	-	12	30	8.5	The QQ Consortium resulted in more than 66% reduction in overall fouling rate when compared with control MBR	Waheed *et al.* (2017)

11.	Cell entrapping alginate beads	*Undibacterium* sp. DM-1	2.5 L	3600- 4400	10	30	20	Around 2.2 times biofouling was mitigated by the QQ bacteria entrapped beads in the QQ-MBR as compared to control MBR with vacant beads.	Nahm *et al.* (2017a)
12.	Hollow fiber sheets Cell entrapping beads	*Rhodococcus* sp. BH4	2.5 L	4500- 5000	8	30	23	The QQ sheets were more effective in controlling membrane biofouling showing 2.5 fold greater QQ activity when compared to QQ beads.	Nahm *et al.* (2017 b)

evaluated for biofouling control. The QQ bacteria and chemically enhanced backwashing caused reduction in physically reversible filtration resistance and chemically reversible resistance, respectively.

Instead of using QQ bacteria for biofouling control, Lee *et al.* (2016a) investigated the effect of fungus *Candida albicans* entrapped in alginate beads coated with poly(vinyl alcohol). It has been observed that the QQ-MBR operated with *Candida albicans* entrapped beads took 41.5 days to reach the TMP of 30 kPa whereas the conventional MBR and vacant MBR took 1.7 and 11.7 days, respectively to reach the same TMP. The QQ potential of *Candida albicans* is attributed to its farnesol secreting ability which is a compound known to inhibit biofilm formation (Koo *et al.*, 2003; Unnanuntana *et al.*, 2009).

2.6 Summary

The application of MBR in wastewater treatment is limited by the problems of membrane fouling. Different factors like hydrodynamic conditions, operating conditions of membrane reactors such as SRT, HRT, membrane flux, F/M ratio, nutrient conditions, and sludge characteristics like MLSS, EPS, SMP governs fouling. To overcome fouling problem, fouling limitation methods like optimization of operating conditions, sludge modification and number of physical (Backwashing and Membrane Relaxation), chemical (NaOCl, NaOH) as well as biological methods (QQ approach) are used to tackle with this severe problem. Out of these approaches biological approach via QQ mechanism is considered to be the best. So, more work is needed in this area. Certain other sources of wastewater like dairy industry and also more plants should be tested for their QQ mechanism and also their fouling mitigation capability in MBRs.

CHAPTER III

MATERIALS AND METHODS

The outline of methodology followed in the present study is given in Figure 3.1. All the experiments were conducted in Laboratory AL051 of Department for Environmental Sciences and Technology at Central University of Punjab, Bathinda.

3.1 Chemicals used

The key chemicals used in the present study include N-hexanoylhomoserine lactone (C6-HSL), acetonitrile, Tris hydrochloride (Tris HCl), crystal violet, acridine orange, glutaraldehyde and sodium hypochlorite (NaOCl). All the chemicals were of high quality and purchased from Sigma aldrich, Loba chemie, Sisco research laboratories and Merck Pvt. Ltd.

3.2 Bacterial strains required

The bacterial strains used were *Chromobacterium violaceum* CV026, *Chromobacterium violaceum* 2656 (*CV*2656), *Pseudomonas aeruginosa* 3541 and *Bacillus cereus* 1306. Excluding *Chromobacterium violaceum* CV026, all the three strains were purchased from Microbial Type Culture Collection (MTCC), Institute of Microbial Technology (IMTECH), Chandigarh, India. The strain CV026, a gram negative proteobacteria was used as a biosensor strain. The strain uses exogenously supplied signalling molecules, acyl homoserine lactone such as n-hexanoyl homoserine lactone (C6-HSL) to produce violacein (Mani *et al.*, 2012; Devaraj *et al.*, 2017). So, CV026 strain was selected as a biosensor strain for isolating the bacteria that can consume C6-HSL. The strains *Bacillus cereus* 1306 and *Pseudomonas aeruginosa* 3541 were used as positive and negative controls, respectively in biofilm inhibition studies. All the bacterial strains were grown in Luria bertani (LB) broth at 28°C and 220 rpm for 24 hours.

3.3 Instruments

Gas chromatography - Mass spectrometry (SHIMADZU GC-MS-Model QP 2010 Ultra), UV-visible spectrophotometer (SHIMADZU 02539), rotary evaporator (ILMVAC S87), COD digester (Khera 4189), water bath (Nuve NB-20), laminar air

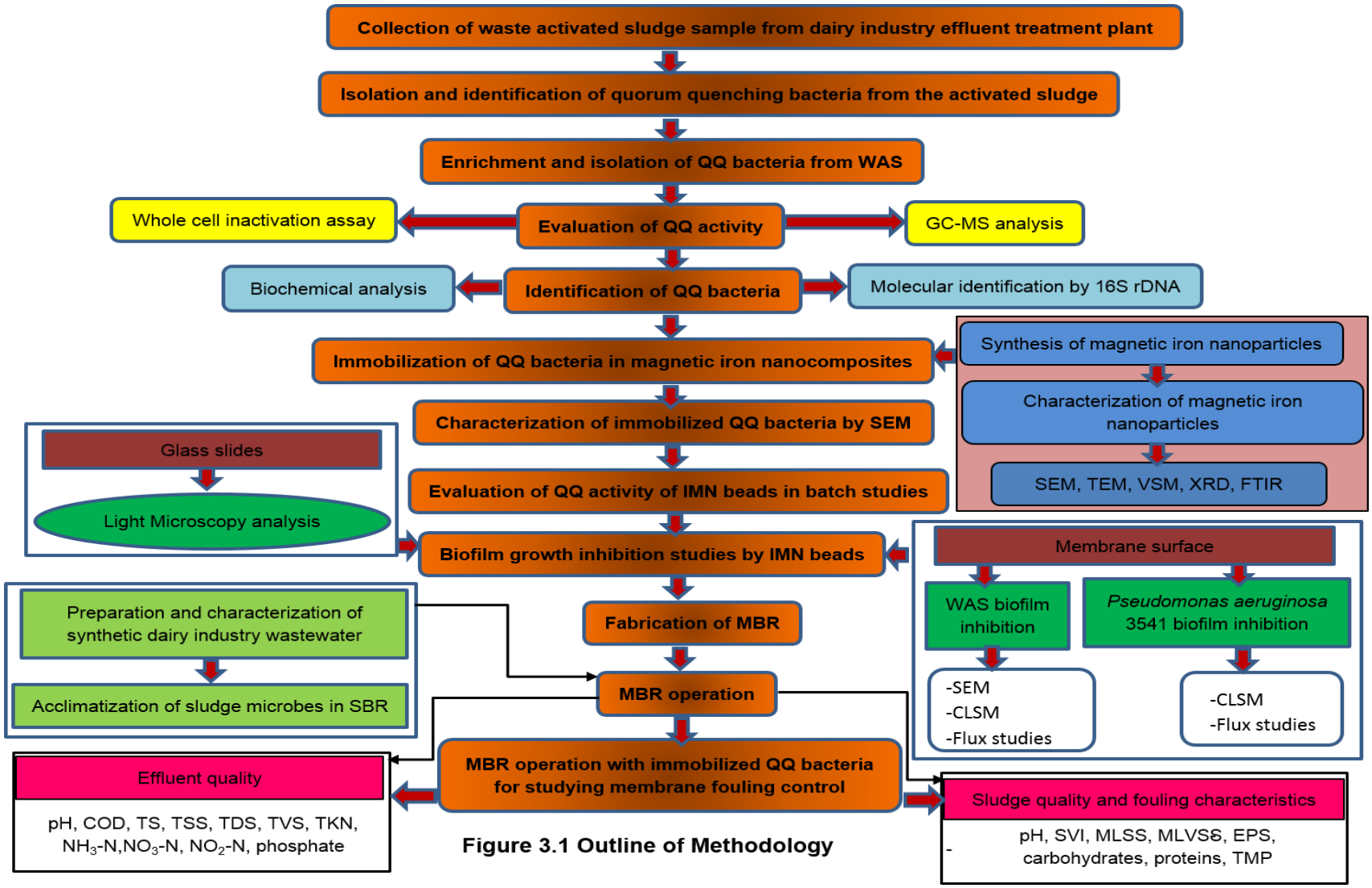

Figure 3.1 Outline of Methodology

flow (KLENZ FLO 1272), incubater shaker (INNOVA 42), vortex mixer (Labnet Z2050694), autoclave, microscope (OLYMPUS CX21FS1), automatic nitrogen/ estimation system KES (KELPLUS KES06LRTS), Scanning electron microscope (Merlin Compact 6073), Transmission electron microscope (Model TECNAI G^2 2S-TWIN),Vibrating Sample Magnetometer (Lakeshore Model 7410), peristaltic pump (Masterflex, Cole Parmer), confocal laser scanning microscope (Olympus FV 1200).

3.4 Collection of waste activated Sludge

The dairy waste activated sludge (WAS) used in the present study was collected from Effluent Treatment Plant (ETP) situated at Verka Milk Plant, Dabwali Road, Bathinda, India (N30˚11”086’ and E74˚56”356’). Figure 3.2 depicts the photographic view of the activated sludge plant located at Verka Milk Plant, Bathinda. The activated sludge was collected in cans of 1L capacity and transported to the laboratory. The cans were preserved in deep freezer at -40 °C till further analysis.

Figure 3.2 (a) Effluent treatment plant at Verka milk plant, Bathinda. (a) Aeration tank (b) close view of aeration tank (c) Return sludge.

3.5 Isolation and identification of QQ bacteria

In this section, bacterial species displaying QQ activity were isolated from the dairy WAS. The whole cell inactivation assay and GC-MS analysis was carried out to

investigate the QQ activity of the isolated bacteria. Further, the QQ bacteria screened from the dairy WAS sample was identified by biochemical and molecular analysis. The details are summarized in the following sections.

3.5.1 Preparation of medium

The QQ bacteria from dairy waste activated sludge were screened using KG medium as per the enrichment method described by Chan *et al.* (2009). The constituents in the KG medium are summarized in Table 3.1.

Table 3.1 Composition of KG medium

Constituents	Amount (g/L)
Sodium chloride	1
Potassium chloride	0.5
Magnesium chloride	0.4
Calcium chloride	0.1
Na_2SO_4	0.15
KH_2PO_4	5.0
2-(N-morpholino)-ethanesulfonic acid (MES)	1.0

Source: Chan *et al.* (2009)

The pH of the medium was maintained at 5.5 with 1M NaOH. After autoclaving, the basal medium was cooled and mixed with sterile stock solution of trace elements. The trace elements included 1 mg $FeCl_3$, 0.1 g of $MnCl_2$ and 0.46 g of $ZnCl_2$ per litre of basal medium. All mixing was done under aseptic conditions.

AHL molecule C6-HSL was used as the sole source of carbon and nitrogen for liquid KG medium. The rationale behind using C6-HSL is based on the fact that majority of gram-negative bacteria utilize C6-HSL as a signalling molecule (Swift *et al.*, 2001). The stock solution of C6-HSL was prepared in acetonitrile in an autoclaved tube. The acetonitrile was removed by rotary evaporator under a stream of cool air. Later, the

sterile KG medium was added to rehydrate the remaining C6-HSL to a final concentration of 500 µg/mL.

3.5.2 Enrichment of QQ bacteria

About 1 g of dairy WAS sludge was suspended in 10 mL of KG medium and vortexed vigorously on a vortex mixer for 10 min. The suspension (2 mL) was taken and spun at 7000Xg to remove any particles. The supernatant was further centrifuged at 13000Xg and the pellet obtained after centrifugation was washed with KG medium followed by resuspension in KG medium (2mL). To 3 mL of C6-HSL containing KG medium (500 µg/mL), about 100 µL of suspension was inoculated in test tube and incubated at 28˚C and 220 rpm for 48 h. 10% (v/v) of the cultured broth was transferred to fresh KG medium containing C6-HSL after 48 hours of incubation. The transfer procedure was repeated six times to enrich C6-HSL metabolizing bacteria. After the sixth enrichment cycle, a diluted suspension of the culture was plated onto the LB agar plate and incubated at 28˚C for 24 h. Every single colony of different morphology was picked and streaked repeatedly on LB agar for obtaining pure culture.

3.5.3 Evaluation of QQ activity

The ability of QQ bacteria to degrade C6-HSL signalling molecule was assessed qualitatively and quantitatively using biosensor strain *Chromobacterium violaceum* CV026 and GC-MS analysis, respectively.

3.5.3.1 Whole cell AHL inactivation assay

The bacterial isolates grown in LB broth at 28˚C in an orbital shaker at 220rpm for 24 hours was centrifuged at 9400 rpm, 4°C for 10 min. The pellet was washed twice with phosphate buffer saline (PBS) and suspended in 10 mL of 100mM PBS (pH 6.5). The cell suspension having 1.0 OD_{600} was used as resting cell for studying *in vitro* AHL-inactivation assay.

The whole cell inactivation assay was done according to the procedure given by Chan *et al.* (2011). C6-HSL dissolved in acetonitrile was taken in sterile tube and acetonitrile

was evaporated to dryness. The C6-HSL was then rehydrated using resting cell suspension to 0.025 µg/µL final concentration. The reaction mixture was incubated at 28˚C, 220 rpm for 24 hours. 10 µL of samples were withdrawn after 0, 6, 12, 18 and 24 hours. The samples were heated to stop the reaction and then allowed to cool at room temperature. Reaction mixtures (10 µL) were spotted onto the LB agar plates seeded with CV026. The agar plates with well-spaced reaction mixtures were incubated overnight in an inverted position at 28˚C. The diameter of decolourization of purple pigment was measured for each isolate to evaluate the C6-HSL degradation.

3.5.3.2 GC-MS analysis

The samples for GC-MS analysis were prepared as per the protocol reported for whole cell inactivation. The concentration of C6-HSL used was 25 mg/L. Every 6 h over a 24 h time period, 1 mL of sample was extracted with similar volume of ethyl acetate. The C6-HSL and ethyl acetate was mixed properly for 30 seconds on vortex mixer. The mixture was allowed to stand till it separated out into two phases. The upper layer containing C6-HSL was collected and the extraction procedure was repeated thrice. The extract was quantified for C6-HSL degradation compounds according to the method recommended by Rani *et al.* (2011) using GC-MS. GC capillary column (RTxi-1ms) having dimensions of 30 m X 1 mm X 0.1 µm was injected with 2µL of extracted sample. Helium gas at 1 mL/min flow rate was used as a carrier gas. The conditions of GC were: GC injector temperature, 280 ˚C; column oven temperature held at 100˚C followed by 10˚C/min increase up to 200˚C. Second immediate increase was 15˚C/min up to 260˚C and finally by 30˚C/ min up to 300˚C. The operating conditions of mass spectra were: electron ionization source set at 70 eV, MS ion source temperature was set at 200˚C with solvent cut time of 3.5 minutes. A mass spectrum was achieved in Selected Ion Monitoring (SIM) mode having fragment ion at m/z 143. The GC-MS spectral peaks obtained for the retention time of 9.5 min were compared with the standard C6-HSL to calculate the degradation percentage.

3.5.4 Identification of the bacterial isolates

The isolated QQ bacteria were identified by biochemical and molecular characterization (16S rDNA).

3.5.4.1 Biochemical characterization

The biochemical identification of the bacterial isolates was done using tests such as Ortho-nitrophenyl-β-D-galactoside (ONPG), lysine utilization, ornithine utilization, urease, phenylalanine deamination, nitrate reduction, H_2S production, citrate utilization, voges proskauer's, methyl red, indole, malonate utilization, esculin hydrolysis, arabinose, xylose, adonitol, rhamnose, cellobiose, melibiose, saccharose, raffinose, trehalose, glucose, lactose, oxidase and catalase. The unknown bacterial isolate was identified to the genus level using Bergey's Manual of Systematic Bacteriology (Krieg and Holt, 1984).

3.5.4.2 Molecular analysis of bacterial isolate

The bacterial nomenclature was further confirmed by molecular analysis. The bacterial colonies of isolates were picked up from the LB agar plate with sterilized toothpick, suspended in centrifuge tube filled with 0.5 mL of sterilized saline water and centrifuged at 10,000 rpm for 10 minutes. The pellet so obtained was further suspended in 0.5 mL of InstaGene Matrix (Bio-Rad- USA) and mixture was incubated at temperature of 56°C for a period of 30 minutes. The mixture was then heated on hot plate at 100°C for 10 minute. After heating, the supernatant was collected and used in polymerase chain reaction (PCR) for amplification of 16S rDNA gene. For PCR reaction, about 1 µL DNA template was added to PCR reaction solution of volume 20 µL. Using primers 27F (5' AGAGTTTGATCMTGGCTCAG 3') and 1525R (5' AAGGAGGTGWTCCARCC 3'), the reaction mixture was amplified. The DNA amplification was continued for 35 cycles at 94 °C for 45 sec, 55 °C and 72 °C for 60 sec each. After removing unincorporated PCR primers and dNTPs using Montage PCR Clean up kit (Millipore), the sequencing of purified PCR products of size approximately 1,400 bp was done with Big Dye terminator cycle sequencing kit (Applied BioSystems, USA). The sequencing products were resolved using M13 forward and reverse primers on an automated DNA sequencing system (Applied BioSystems, model 3730XL USA). The sequences were aligned and low quality sequences were trimmed from both the ends by software CodonCode Aligner (version 5.1.5). The nucleotide sequences of the isolated DNA were identified using nucleotide Basic Local Alignment Search Tool (BLAST) at NCBI.

3.6 Immobilization of QQ bacteria in magnetic iron nanocomposites

The bacteria in the free-state was known to have low survival rates. Keeping this in view, the isolated QQ bacteria were immobilized individually and as in consortium onto the magnetic iron nanocomposites. In this section, the preparation of carrier i.e. magnetic iron nanoparticles and immobilization of QQ bacteria onto the magnetic iron nanocomposite beads is explained.

3.6.1 Preparation and characterization of magnetic iron nanoparticles

Magnetic iron nanoparticles (Fe_3O_4) were prepared using co-precipitation method suggested by Kouassi *et al.* (2005). Salts of ferrous and ferric chloride (25M concentration each) in 1:2 ratio were amalgamated in the basic solution of NaOH of 3M concentration at room temperature (25 °C) and at pH 10. The precipitates were heated for 35 minutes at 35 °C on the hot plate under stirring conditions. Nanoparticles so formed were washed several times with distilled water and ethanol. During washing, the magnetic iron nanoparticles were separated from the supernatant using a magnetic separator of strength greater than 20 megaoersted. The particles were finally dried in a vacuum oven at 70 °C. The morphology and size of the magnetic iron nanoparticles was characterized using SEM (Merlin Compact 6073) and transmission electron microscopy (TEM; Model TECNAI G^2 2S-TWIN). The saturation magnetization (M_S) was measured by vibrating sample magnetometer (VSM; Lakeshore Model 7410). For studying the crystalline structure and the sample phase, X-ray diffraction (XRD) was performed. The functional groups present in the magnetic iron nanoparticles was analysed with Fourier transform infrared spectroscopy (FTIR Model- Bruker) using sample pellets prepared with KBr.

3.6.2 Immobilization of QQ bacteria in magnetic nanocomposite beads

The QQ bacteria was immobilized in the magnetic nanocomposites according to the technique proposed by Ivanova *et al.* (2011). Figure 3.3 (a) and (b) depicts the schematic representation of the experimental setup used in the preparation of QQ bacteria immobilized magnetic nanocomposites (IMN) beads. The sodium alginate/

magnetic iron nanoparticles was used for immobilizing QQ bacteria because of their non-toxic nature and low cost. The isolated QQ bacteria *Acinetobacter baumannii* JYQ2, *Pseudomonas nitroreducens* JYQ3 and *Pseudomonas* JYQ4 were grown overnight in 50 mL LB broth medium at 220 rpm and 28 °C.

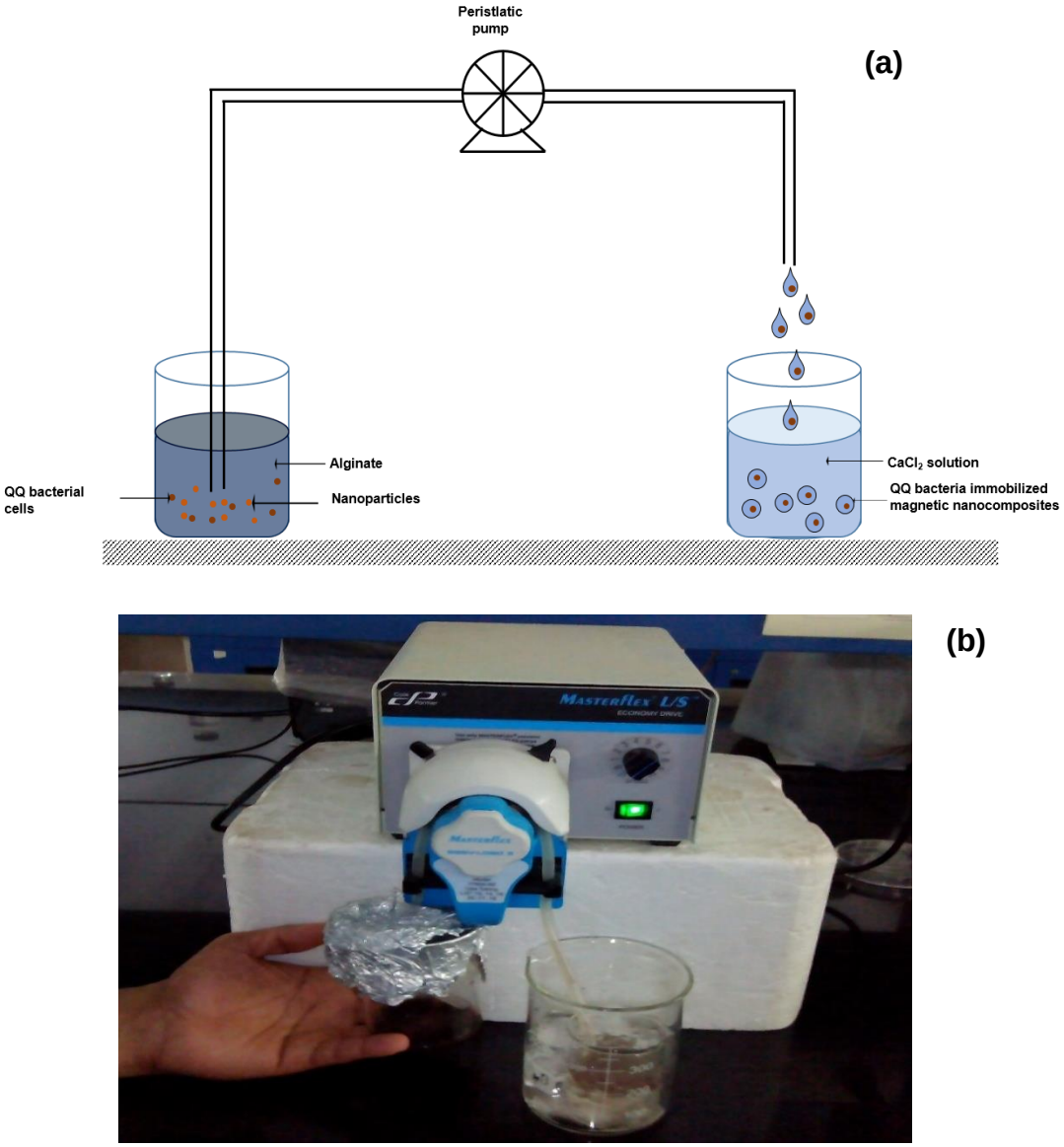

Figure 3.3 Preparation of immobilized magnetic nanocomposite beads (a) Schematic representation of experimental set up (b) Photographic view

Simultaneously, QQ consortium comprising of *Acinetobacter baumannii* JYQ2, *Pseudomonas nitroreducens* JYQ3, and *Pseudomonas* JYQ4 was prepared by co-

culturing each bacterial isolate in LB broth (50 mL) with an OD_{600} of 1 and incubated for 24 hours at 28°C and 220 rpm. Individual QQ bacteria as well as consortium were centrifuged at 9400 rpm and 4 °C for 10 minutes. 1 g of each bacterial pellet left after centrifugation were mixed with 20 mL of sterile sodium alginate (2%). About 100 mg of magnetic iron nanoparticles were added to the suspension for the preparation of magnetic nanocomposite beads. The mixed suspension (QQ/ alginate/ Fe_3O_4) was dripped into 2% (w/v) chilled $CaCl_2.H_2O$ using silicone tube (ID 3.5 mm/OD 7 mm) and peristaltic pump.

The blank beads i.e. beads devoid of QQ bacteria were prepared in the similar manner. Both IMN and blank beads were kept at room temperature for a period of 2h for hardening and then at 4 °C for 12 h. The beads were then filtered, thoroughly washed with distilled water and used for further studies. The bead size was measured with screw gauge and it ranged from 4 to 5 mm.

3.6.3 Characterization of QQ bacteria IMN beads

Morphological examinations of blank beads and QQ bacteria IMN beads were performed using SEM. The samples for the SEM analysis were prepared following the method given by Chen *et al.* (2012). Both the blank and IMN beads were washed three times with distilled water and kept in glutaraldehyde solution (3%) for 2 hours at room temperature for fixing. After fixing, the beads were once again washed in distilled water to remove residual glutaraldehyde. The beads were dehydrated with series of ethanol (30%, 50%, 70%, 90% and 100%). The dehydrated samples were freeze dried and coated with gold and observed using SEM.

3.7 Evaluation of QQ activity of IMN beads in Batch studies

The QQ activity of the IMN beads was studied qualitatively using biosensor strain *CV* 2656. 50 mL of LB broth was added to 1 mL of *CV* 2656 culture (OD_{600} to 1) in five flasks labelled as A_1, A_2, A_3, A_4 and A_5. Around 10 blank beads were added to the flask A_1 and maintained as control. To flasks A_2, A_3, A_4 and A_5, 10 beads of *Acinetobacter baumannii* JYQ2, *Pseudomonas nitroreducens* JYQ3, *Pseudomonas* JYQ4 and

consortium of the three bacteria IMN beads, respectively were added. All the flasks were incubated for 24 hours at 28 °C and 220 rpm in an incubator shaker. The QQ activity of IMN beads was evaluated by the loss of purple pigment indicated by the decolourization of colour developed by *CV* 2656.

The quantitative analysis of C6-HSL degradation was done as per the method given by Kim *et al.* (2013). The QQ activity was assessed by the degradation rate of standard C6-HSL. C6-HSL was added to 30 mL of 50 mM Tris HCl buffer (pH 7) in six flasks (A_1, A_2, A_3, A_4, A_5 and A_6) to prepare a concentration of 25 mg/L. To each of the flasks designated as A_3, A_4, A_5 and A_6, about 10 QQ IMN beads of *Acinetobacter baumannii* JYQ2, *Pseudomonas nitroreducens* JYQ3, *Pseudomonas* JYQ4 and consortium, respectively were added and incubated at 28˚C and 220 rpm. The flask A_1 (without any IMN beads) and A_2 (with blank nanoparticle beads devoid of QQ bacteria) were served as controls. The control A_1 was run for examining the self-degradation of C6-HSL in the Tris HCl buffer in the absence of IMN beads. Likewise, control A_2 was run for investigating the removal of C6-HSL by the virgin nanoparticle beads (without bacteria). Both the controls were executed for the purpose of elucidating the mechanism behind the degradation of signalling molecule C6-HSL. The flasks were incubated for 6 hours at 150 rpm in an incubator shaker. The samples were collected at every one hour interval up to 6 hours. All the collected samples were extracted according to the method explained in section 3.5.3.2 and C6-HSL degradation was measured by GC-MS analysis according to the equation 3.1. The experiment was performed in triplicates.

$$\text{Amount of C6-HSL degraded (\%)} = \frac{Ai - Af}{Ai} \times 100 \qquad (3.1)$$

where Ai= initial concentration of C6-HSL and Af= C6-HSL concentration after degradation.

3.8 Biofilm growth inhibition studies by QQ bacteria IMN beads

The ability of QQ bacteria IMN beads in preventing quorum sensing (QS) associated biofilm formation was assessed in terms of biofilm growth inhibition on glass slides and membrane surface. The results of biofilm growth inhibition studies are summarized in the following sections.

3.8.1 Biofilm growth inhibition studies on glass slides

The ability of QQ bacteria IMN beads to inhibit the growth of biofilm on glass slides was studied as per the protocol suggested by Kim *et al.* (2014). The experiment was carried out in triplicates in the beakers designated as B_1, B_2, B_3, B_4, B_5 and B_6. Sterile glass slides (76.2 X 25.4 mm) about eighteen in numbers (three in each beaker) were suspended in all the six beakers. To each beaker, about 50 mL acclimatized sludge and 150 mL synthetic dairy industry wastewater in the ratio of 1:3 was added. The beaker B_1 without QQ bacteria IMN beads and B_2 with blank nanoparticle beads were maintained as control 1 and control 2, respectively. 20 IMN beads of *Acinetobacter baumannii* JYQ2; *Pseudomonas nitroreducens* JYQ3; *Pseudomonas* JYQ4; and consortium of *Acinetobacter baumannii* JYQ2, *Pseudomonas nitroreducens* JYQ3, *Pseudomonas* JYQ4, respectively were added into the beakers designated as B_3, B_4, B_5 and B_6. All the beakers were incubated at 30 °C, 150 rpm in an incubator shaker for 15 days. Everyday, the medium was replaced with fresh wastewater to maintain biofilm growth and development.

The composition of synthetic dairy industry wastewater used in the present study is summarized in Table 3.2. The formulation of synthetic dairy industry wastewater given by Dawood *et al.* (2011) was used in the present study with slight modifications. The glass slides were removed at the end of day 1, 10 and 15 and stained with 0.1% crystal violet for 30 minutes and washed four times with distilled water. Then the glass slides were dried and observed under the microscope at 100X magnification to observe the biofilm formation and inhibition.

Table 3.2 Composition of synthetic dairy industry wastewater

Composition	Concentration (g/ L)
NH_4Cl	1.4
$CaCl_2$	0.038
$MgSO_4.7H_2O$	0.05
KH_2PO_4	1
$NaHCO_3$	2
Powdered milk	2.5

3.8.2 Biofilm growth inhibition studies on membrane filter

The batch scale experiments were conducted to investigate the ability of QQ bacteria to control biofilm formation on cellulose acetate membrane surfaces prior to applying QQ bacteria IMN beads in membrane bioreactors (MBR). The efficiency was monitored in terms of SEM, CLSM and membrane flux studies.

3.8.2.1 Inhibition of *Pseudomonas aeruginosa* 3541 biofilm by IMN beads

The inhibition of *Pseudomonas aeruginosa* 3541 biofilm development on the cellulose acetate membrane surface using QQ bacteria IMN beads was investigated as per the procedure suggested by Lee *et al.* (2014). A total of 98 cellulose acetate membranes of pore size 0.45 µm were fixed on the sterile glass slides and immersed in seven 100 mL sterile beakers labelled as C_1 to C_7 (Table 3.3). The experimental set up was conducted in triplicates. About 1 mL of biofilm forming bacteria *Pseudomonas aeruginosa* 3541 was mixed with 49 mL of synthetic dairy industry wastewater in each beaker. Around 10 IMN beads of *Acinetobacter baumannii* JYQ2; *Pseudomonas nitroreducens* JYQ3; *Pseudomonas* JYQ4; consortium of *Acinetobacter baumannii* JYQ2, *Pseudomonas nitroreducens* JYQ3, *Pseudomonas* JYQ4; and *Bacillus cereus* 1306, respectively were added to the beakers designated as C_3 to C_7. In the previous study, *Bacillus cereus* 1306 have been known to possess better QQ activity (Chan *et*

al., 2007). So, the IMN beads prepared with *Bacillus cereus* 1306 was used as positive control in this study.

Table 3.3 Experimental design for *Pseudomonas aeruginosa* 3541 biofilm inhibition studies

Beakers label	Immobilized magnetic nanoparticle beads	Number of membranes added		
		Flux studies	SEM	CLSM
C_1	No beads	6	4	4
C_2	Blank nanoparticle beads	6	4	4
C_3	*Acinetobacter baumannii* JYQ2	6	4	4
C_4	*Pseudomonas nitroreducens* JYQ3	6	4	4
C_5	*Pseudomonas* JYQ4	6	4	4
C_6	Consortium of JYQ2, JYQ3 and JYQ4	6	4	4
C_7	*Bacillus cereus* 1306	6	4	4

Flask C_1 (without QQ bacteria IMN beads) and C_2 (blank nanoparticle beads) were designated as control 1 and 2, respectively. All the beakers were incubated at 30 °C and 150 rpm in an incubator shaker for 30 days. The substrate in the beakers was replaced everyday with fresh synthetic dairy industry wastewater. At intervals of 5 days, one membrane was removed from each beaker and used for flux measurement studies. Likewise, two membranes were removed after every 10 days for SEM and CLSM analysis. The details of SEM and CLSM are given in sections 3.10.2 and 3.10.3, respectively. Calculations for flux studies are given in section 3.11.

3.8.2.2 Inhibition of sludge bacterial biofilm using IMN beads

In this section, the ability of QQ bacteria IMN beads to inhibit the biofilm formation by the sludge microorganisms was assessed. The activated sludge was acclimatized to the synthetic dairy industry wastewater in a sequencing batch reactor (SBR). The acclimatized sludge was used for further experiments.

3.8.2.2.1 Acclimatization and Cultivation of Activated sludge

A rectangular glass tank of dimensions 18cm X 15.5cm X 15.5cm (L X W X H) with working volume of 2L was fabricated and used as sequencing batch reactor (SBR). Figure 3.4 (a) and (b) depicts the schematic and photographic view of SBR used for the acclimatization of WAS to synthetic dairy industry wastewater, respectively. The reactor was operated in fill and draw mode consisting of four phases: fill (30 min), react (22h), settle (30 min) and decant (1h). The seed sludge collected from the Verka effluent treatment plant, Dabwali road, Bathinda was added into the reactor and aerated for 24 h. The aeration was provided through two stone diffusers connected to the air pump. The dissolved oxygen (DO) and pH of the reactor was maintained at 3-4 mg/L and 7-7.5, respectively. The sequence followed for acclimatization is summarized in Table 3.4.

After 24 h, the aeration was stopped and the sludge was allowed to settle for 30 minutes. Around 10% of supernatant was removed and replaced with 10% synthetic dairy industry wastewater. After addition of wastewater, the aeration was resumed. The process was repeated after 24 h. The MLSS of the sludge was measured once in two days to assess the growth of biomass. Gradually, the percentage of wastewater addition was increased from 20 to 30% and so on till 100% wastewater. The process was continued in 100% wastewater until MLSS concentration reached to 4000 mg/L.

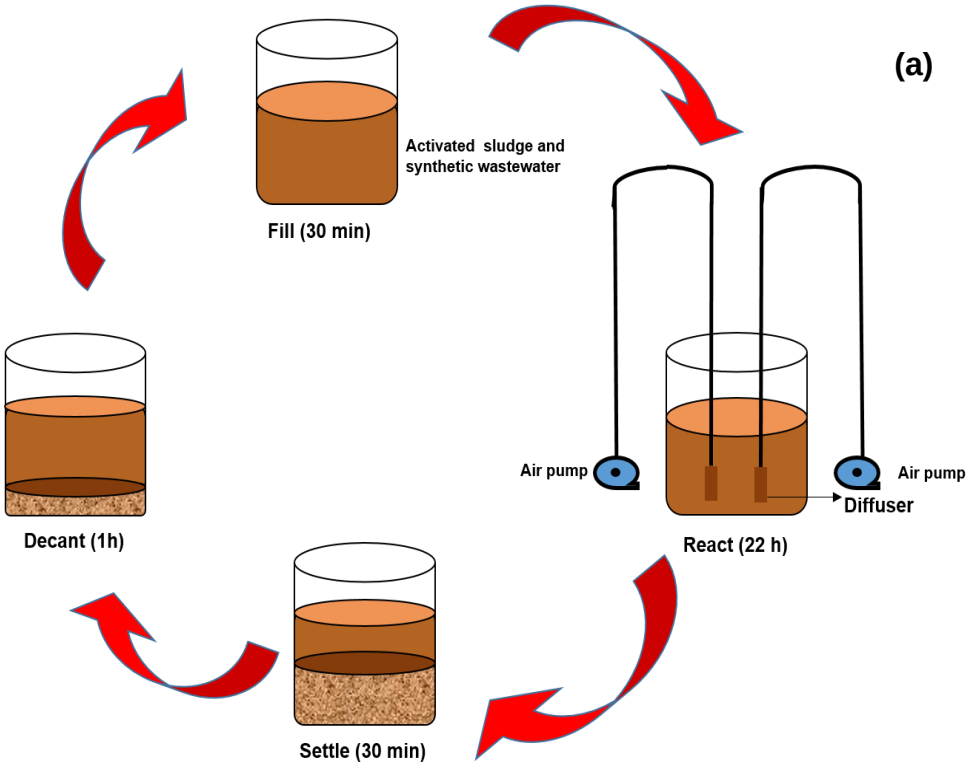

(b)

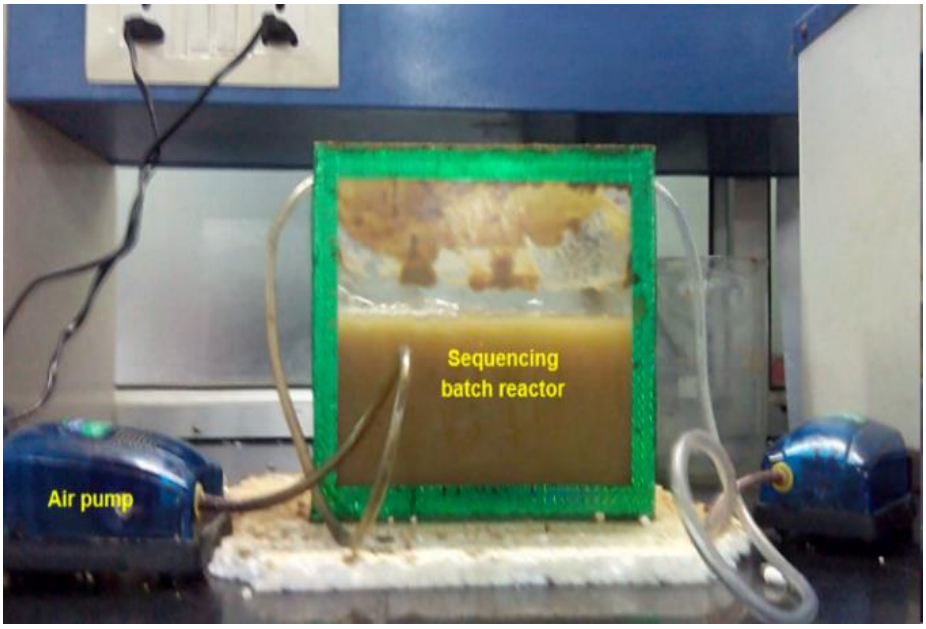

Figure 3.4 Acclimatization of sludge in SBR (a) Schematic view (b) Photograph view

Table 3.4 Acclimatization sequence

Days	Acclimatization sequence	
	Supernatant decanted (%)	**Synthetic dairy industry wastewater added (%)**
1	Aeration of activated sludge	
3	10	10
5	20	20
7	30	30
9	40	40
11	50	50
13	60	60
15	70	70
17	80	80
19	90	90
21	100	100

3.8.2.2.2 Inhibition of biofilm developed by activated sludge bacteria

The experimental set up was conducted in triplicates in the beakers labelled as D_1 to D_7. A total of 70 cellulose acetate membranes having a pore size of 0.45 µm were attached to the glass slides and suspended in the beakers labelled as D_1 to D_7. The details of the number of membranes added to each beaker are given in Table 3.5. 250 mL of synthetic dairy industry wastewater and 50 mL acclimatized sludge in the ratio of 5:1 was added to each beaker.

Around 20 IMN beads of *Acinetobacter baumannii* JYQ2; *Pseudomonas nitroreducens* JYQ3; *Pseudomonas* JYQ4; consortium of *Acinetobacter baumannii* JYQ2, *Pseudomonas nitroreducens* JYQ3, *Pseudomonas* JYQ4; and *Bacillus cereus* 1306, respectively were added to the beakers designated as D_3 to D_7. Beakers D_1 (devoid of QQ IMN beads) and D_2 (blank nanoparticle beads) were run as controls. All the beakers were incubated in an incubator shaker at 30 °C and 150 rpm for 30 days. Every day,

the synthetic wastewater was replaced with fresh wastewater to maintain biofilm growth on the membrane surfaces. Every 5th day, one membrane was withdrawn from each beaker to assess the flux of the membrane. The membrane surface was examined with CLSM analysis to visualize the biofilm architecture. To carry out the CLSM analysis, the second membrane was removed from the beaker at 10th day of incubation.

Table 3.5 Experimental design for sludge microbial biofilm inhibition

Beaker label	IMN beads	Number of membranes added	
		Flux studies	CLSM
D_1	No beads	6	4
D_2	Blank nanoparticle beads	6	4
D_3	*Acinetobacter baumannii* JYQ2	6	4
D_4	*Pseudomonas nitroreducens* JYQ3	6	4
D_5	*Pseudomonas* JYQ4	6	4
D_6	Consortium of JYQ2, JYQ3 and JYQ4	6	4
D_7	*Bacillus cereus* 1306	6	4

3.9 Membrane bioreactor studies

This section discusses the detailed methodology of MBR fabrication; operation and performance evaluation.

3.9.1 Membrane resistance studies

The resistance of the membrane module was measured by filtering pure water through the membrane at varying flux conditions. The TMP was recorded for the corresponding fluxes using a mercury manometer. A linear line was obtained by plotting the flux on x

axis and TMP on y axis. The resistance of the membrane was derived from the slope of the linear curve using equation 3.2.

$$J = \frac{\Delta P}{\mu R_t} \quad \text{.....(3.2)}$$

Where J= Permeate flux (L/m^2h)

ΔP= Transmembrane pressure (KPa)

μ= Viscosity of the permeate (Ns/m^2)

R_t= Total resistance (m^{-1})

3.9.2 Fabrication of MBR

The submerged aerobic MBR consisted of a rectangular tank of dimensions 43cm X 8cm X 35cm was made up of plexiglass (Figure 3.5 a and b). A hollow fiber membrane made of polyethersulfone (PES) with pore size and surface area of 0.4 µm and 0.4 m^2, respectively was inserted into the reactor. The feed was supplied from the feed tank through a pump fitted with water level sensor to maintain a constant supply of wastewater. The homogeneity of the feed was maintained with a stirrer fixed to the feed tank. The MBR was aerated through fine bubble aeration systems- two stone diffusers located at the side and a perforated pipe at the bottom of the reactor. The DO within the reactor was maintained at 2-4 mg/L. The permeate was collected through a permeate pipe located at the top of the reactor using a peristaltic pump. The MBR was operated at a filtration cycle of 10 min 'On' and 2 min 'cut off'. The solenoid valve fixed between the peristaltic pump and membrane was used to maintain the filtration cycle. The MBR was operated at a flux of 12.5 L/ (m^2h). The TMP was monitored using a U shaped mercury manometer.

3.9.3 MBR operation

The sludge acclimatized in the SBR (2 L) was transferred to the MBR and used as an inoculum. The MBR was filled with synthetic dairy industry wastewater having

BOD/COD ratio of 0.2 signifying poor biodegradability of dairy wastewater and operated at HRT of 8h. The detailed operating conditions for the MBR are listed in Table 3.6. The DO and pH of MBR was maintained at 2 to 4 mg/L and 7 to 7.3, respectively. The MBR was operated at sludge retention time (SRT) of 30 days at each MLSS. The MBR was kick started with the MLSS concentration of 4000 mg/L.

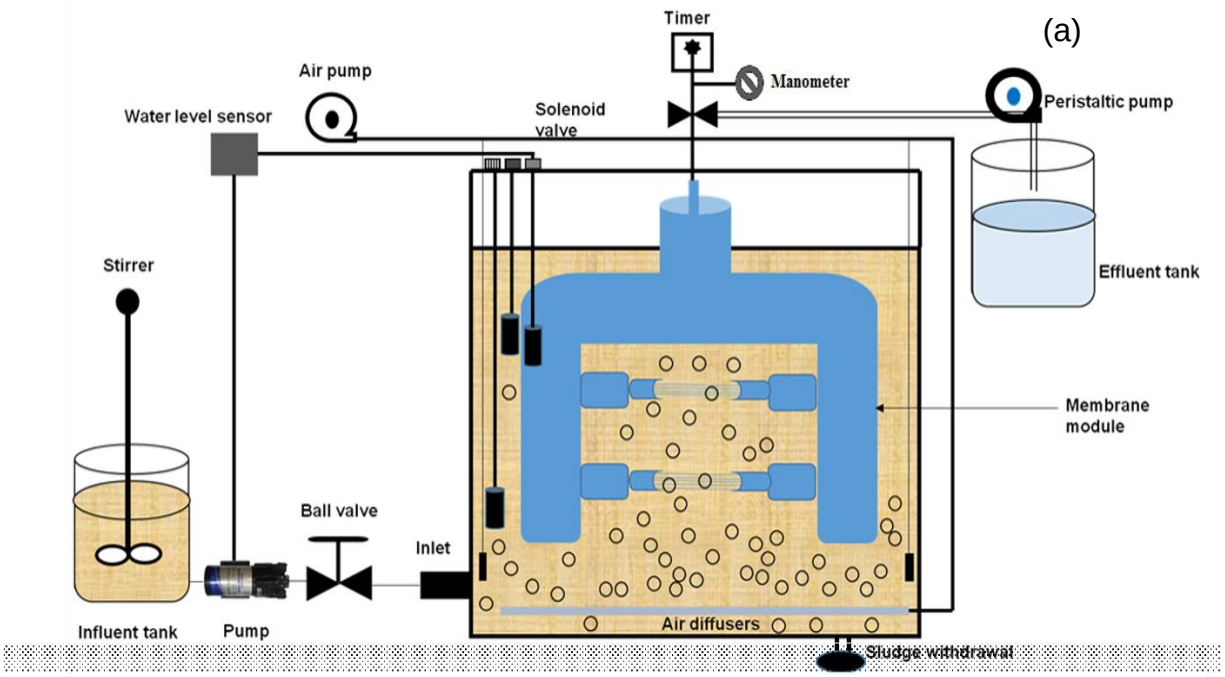

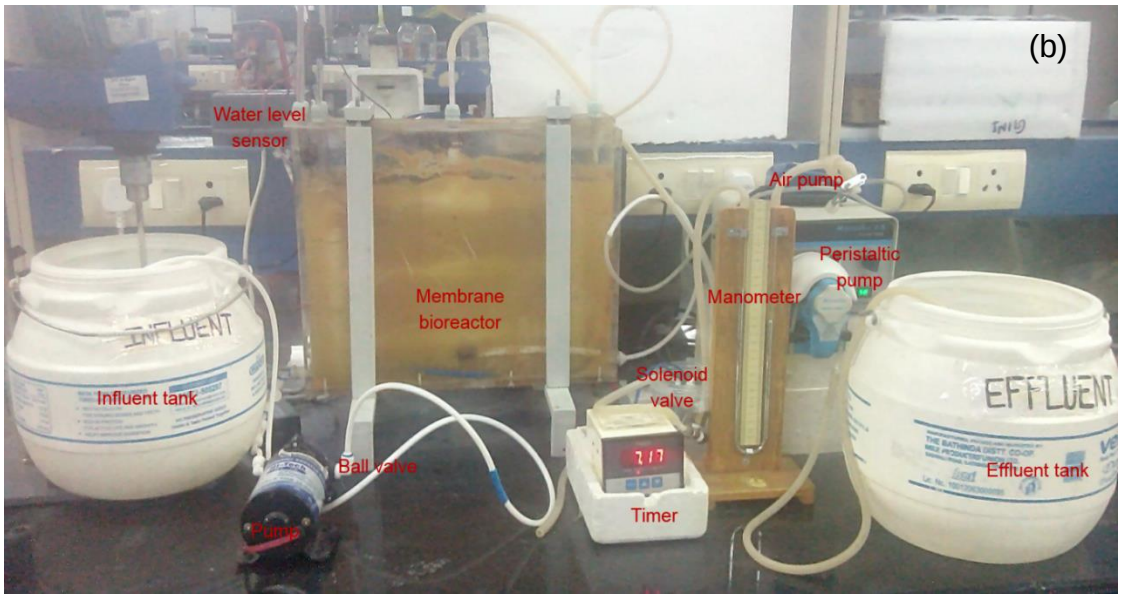

Figure 3.5 Membrane bioreactor set up (a) Schematic illustration (b) Photographic view

Table 3.6 Operational parameters for the MBR

S.No.	Operational parameters	Value
1.	Working volume	4 L
2.	Hydraulic Retention Time (HRT)	8 h
3.	Sludge Retention Time (SRT)	MLSS 4000 mg/L- 16- 18 days MLSS 7000 mg/L- 20- 22 days MLSS 10,000 mg/L- 28- 30 days
4.	Permeate flux	12.5 L/ (m^2h)
5.	Mixed Liquor Suspended Solids (MLSS)	4000 mg/L, 7000 mg/L and 10,000 mg/L
6.	Food to microorganism ratio (F/M)	0.06 to 0.1
7.	BOD	816 mg/L
8.	BOD/COD	0.2

During the operation period, the permeate was removed periodically and their effluent quality was determined to assess the performance of MBR. The effluent quality was assessed through pH, total solids (TS), total suspended solids (TSS), total dissolved solids (TDS), total volatile solids (TVS), Chemical oxygen demand (COD), Total kjeldahl nitrogen (TKN), ammonical nitrogen, nitrate, nitrite and phosphate. Likewise, the sludge quality was determined in terms of pH, MLSS, MLVSS and sludge volume index (SVI). The membrane fouling was assessed through tightly bound; and loosely bound EPS and soluble EPS. Carbohydrate and proteins fractions of EPS were also determined. Membrane flux and TMP were continuously monitored. Flux was regularly adjusted to maintain the constant flux of 12.5 L/ (m^2h). Once the reactor obtained a stable condition, the MLSS concentration of the MBR was increased to 7000 mg/L. The performance

was once again assessed through effluent quality, sludge and fouling characteristics. The procedure was repeated for MLSS 10,000 mg/L.

3.9.4 Membrane cleaning

The membrane of the reactor was subjected to cleaning when the TMP increases above 30 kPa. Figure 3.6 depicts the photograph of cleaned and fouled membrane. The membrane module was disconnected from the suction and other lines. The deposited cake layer on the membrane was removed through pressurized water flushing through spray cans.

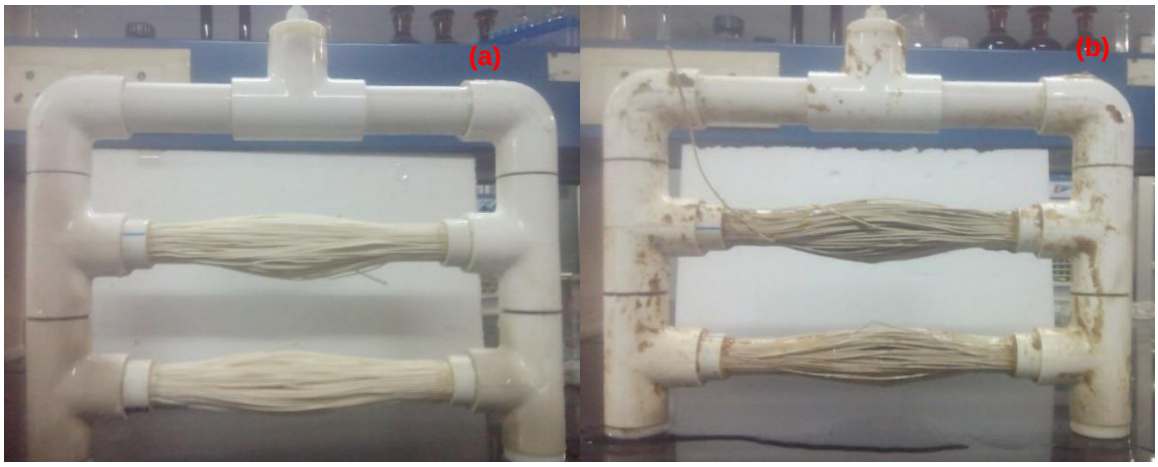

Figure 3.6 Photograph of (a) clean and (b) fouled membrane

After complete removal of cake layer, membrane module was immersed in 1000 ppm NaOCl solution for three hours. The membrane was then rinsed with distilled water till complete removal of residual chlorine. Subsequent to chemical cleaning, the resistance of the membrane was measured. On recovering the 80% of the resistance of virgin membrane, the cleaned membrane is connected to suction lines and used in filtration process.

3.9.5 MBR operation with Immobilized QQ bacteria

Once the MBR reached the stable operation, beads of *Pseudomonas nitroreducens* JYQ3 and *Pseudomonas* JYQ4 were introduced into MBR operated at MLSS of 4000 mg/L. The QQ-MBR is of completely stirred reactors (Figure 3.7). *Pseudomonas*

nitroreducens JYQ3 and *Pseudomonas* JYQ4 were selected based on their higher QQ activity and increased biofilm retardation rate. About 100 IMN beads of *Pseudomonas nitroreducens* JYQ3 (50 beads) and *Pseudomonas* JYQ4 (50 beads) were added into the reactor. The number of beads was selected on the basis of the batch experiments conducted to study biofilm growth retardation by the IMN beads. The MBR was operated at 4000 mg/L for 30 days. During this period, the MBR was continuously assessed for effluent quality, sludge and fouling characteristics mentioned in section 3.9.3. Similar to 4000 mg/L, the MBR with immobilized beads were also operated at MLSS 7000 and 10,000 mg/L. At each MLSS, the MBR performance and fouling potential was analyzed and compared to assess the efficiency of QQ bacteria in controlling biofilm formation.

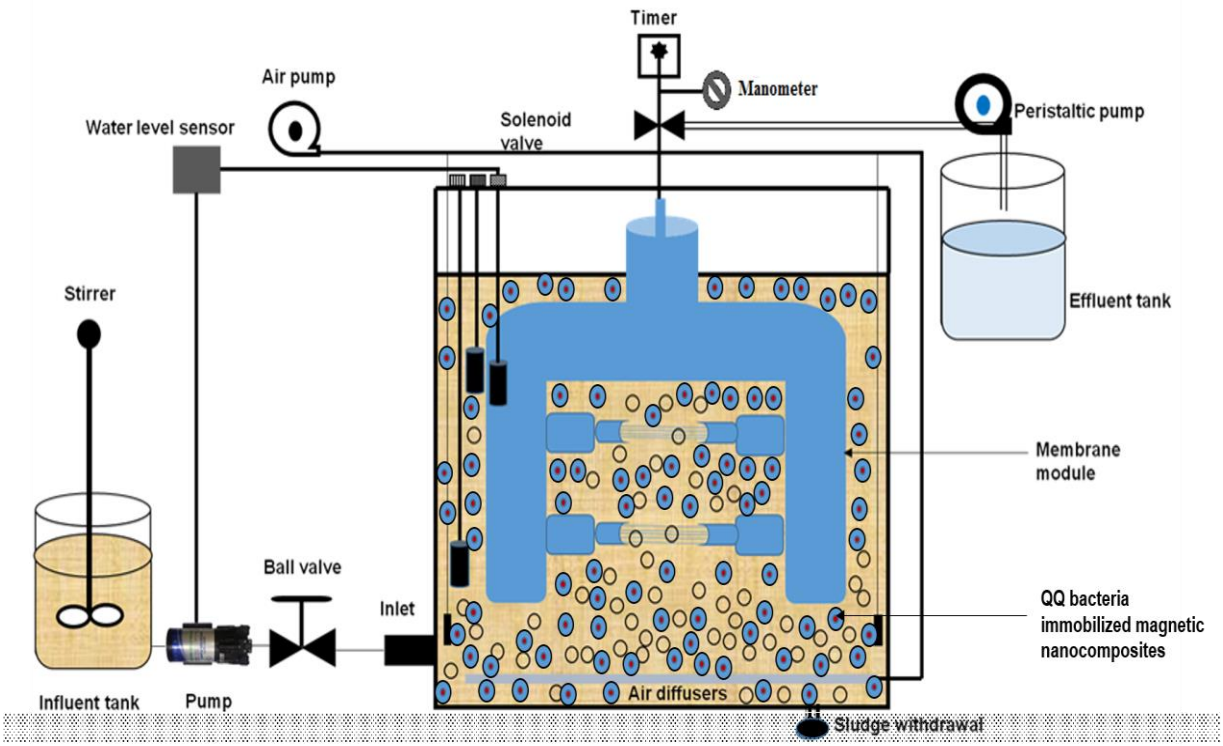

Figure 3.7 Membrane bioreactor with quorum quenching bacteria IMN beads

3.10 Analytical methods

All the analytical parameters in the influent and effluent were examined according to the Standard Methods of Water and Wastewater (APHA, 2012) and Bureau of Indian

standards (BIS, 1989). Table 3.6 summarizes the analytical methods performed during the study. MLSS and MLVSS in the sludge were done according to Standard methods for the examination of water and wastewater (APHA, 2012).

Table 3.7 Analytical parameters

S.No.	Parameters	Method used	Reference
1.	pH	Glass electrode	OAKTON RC2700
2.	Chemical oxygen demand	Open reflux method	APHA 5220 B, 5-17
3.	Phosphate	Stannous chloride method	APHA 4500-P D, 4-154
4.	Nitrite	Sulphanalamide reaction method	BIS IS:3025(Part 34) 1988, 12
5.	Nitrate	Chromotrophic acid method	BIS IS:3025(Part 34) 1988, 9
6.	Total kjeldahl nitrogen	Kjeldahl	BIS IS:3025(Part 34) 1988, 13
7.	Total ammonical nitrogen	Phenate method	APHA 4500-NH_3 F, 4-115
8.	Total solids	Gravimetric	APHA 2540 B, 2-64
9.	Total dissolved solids	Gravimetric	APHA 2540 C, 2-65
10.	Total suspended solids	Gravimetric	APHA 2540 D, 2-66
11.	Total volatile solids	Gravimetric	APHA 2540 E, 2-67

3.10.1 Extraction and characterization of EPS

Loosely and tightly bound EPS was analyzed according to method given by Zhang *et al.* (2009b). 25 mL of MBR sludge was centrifuged at 7300 rpm for 5 min. The supernatant was discarded and sludge was resuspended in 15 mL of 0.9% NaCl solution. The solution was treated by ultrasound for 2 min, shaked at 150 rpm for 10 min and again treated by ultrasound for 2 min. The solution was finally centrifuged at 8400 rpm for 10 minutes. The supernatant was kept aside as loosely bound (LB) EPS. The extraction of tightly bound (TB) EPS was done by resuspending the sludge pellet

in 25 mL of 0.9% NaCl and then treated by ultrasound for 3 min. The suspension was heated in a water bath at 80 °C for 20 min. The suspension was then centrifuged at 10,300 rpm for 20 min. The supernatant was collected as TB-EPS. Soluble EPS was extracted as per method given by Chang and Lee (1998). Briefly, 50 mL of MBR sludge was centrifuged at 3200 rpm for 30 min. The supernatant was regarded as soluble EPS. The TB-EPS, LB-EPS and soluble EPS were expressed in terms of carbohydrates and proteins.

3.10.1.1 Determination of carbohydrate

The total carbohydrate of EPS was determined by phenol-sulphuric acid method (Dubois *et al.*, 1956). To 1 mL of sample, 1 mL of 5% phenol and 5 mL of 96% sulphuric acid was added. The solution was incubated at room temperature for 20 minutes and absorbance was read at 490 nm. The concentration of total carbohydrate was determined by plotting a standard graph against different concentration of glucose.

3.10.1.2 Determination of protein

The protein in EPS was estimated by Bradford method (Bradford, 1976). 5 mL of Commassie brilliant blue solution was added to 1 mL of sample in a test tube. The solution was thoroughly mixed on a vortex mixture and allowed to stand at room temperature for 5 minutes. The absorbance was measured at 595 nm. The concentration of protein was determined by plotting a standard graph against different concentration of bovine serum albumin (BSA).

3.10.2 SEM

The growth of biofilm on the cellulose acetate membrane was examined with SEM. The sample was prepared as per the method specified by Prior and Perkins (1974). The membranes were suspended in solution of glutaraldehyde (3%), 4% sucrose (pH 7.3) and 0.05M phosphate buffer. Membranes were left overnight in the solution for fixation at 4 °C. Next day, membranes were washed with distilled water (four times). The washed membranes were then kept on the aluminium foil and dehydrated with ethanol gradients (10%, 20%, 30%, 50%, 70%, 90% and 100%). After complete dehydration,

the membranes were kept in oven for drying at 70 °C and then coated with gold for SEM analysis.

3.10.3 CLSM

The 3-dimensional structure of the *Pseudomonas aeruginosa* 3541 and sludge microbial biofilm on the membrane surface was supervised visually using CLSM. For visualizing proper growth on the membrane surface, the membranes were stained with 0.01% acridine orange. A Z section image stack viewing 3-dimensional structure was created with FV10-ASW 4.2 viewer software. The images were taken with 100X objective lens and recorded in the green channel (excitation wavelength of 488 nm and emission wavelength of 520 nm). The CLSM images were further analysed for the quantification of biofilm growth on cellulose acetate membrane using COMSTAT software.

3.11 Calculations

3.11.1 Flux measurements

The biofouling on the membrane surface was examined quantitatively through decrease in membrane flux over 30 days' time period. Briefly, 100 mL of distilled water was allowed to pass through the cellulose acetate membrane at a constant pressure of 10 kPa. The membrane flux (flow of liquid per unit area of membrane surface) is calculated as per the equation 3.3,

$$J = \frac{Q_p}{A_m} \quad \ldots\ldots\ldots\ldots\ldots\ldots\ldots\ldots\ldots\ldots \quad (3.3)$$

where J = Flux, $m^3/m^2/h$

Q_p = Filtrate flow rate through the membrane, m^3/h

A_m = Membrane surface area, m^2

3.12 Statistical Analysis

All the observations were done in triplicates. All the experiments were performed thrice except for reactor study which was performed twice during the study period for confirming reproducibility of data. Results were analyzed statistically and expressed as mean± S.E. One way Analysis Of Variance (ANOVA) was performed using software package SPSS Statistics 20 to evaluate the significant difference between antifouling potential of different QQ bacteria immobilized beads and also C6-HSL degradation at different time intervals. Differences were considered significant at $p<0.05$.

CHAPTER IV

RESULTS AND DISCUSSION

4.1 Isolation of QQ bacteria from dairy waste activated sludge (WAS)

The dairy WAS suspension inoculated in KG medium amended with C6-HSL as a sole source of nitrogen and carbon turned turbid within 48 h of incubation. The turbidity indicated the growth of QQ bacteria. However, no growth was observed in control KG medium devoid of C6-HSL. The dairy WAS consortium was enriched up to sixth enrichment cycle and plated on the LB agar. Five bacterial isolates namely JYQ1, JYQ2, JYQ3, JYQ4 and JYQ5 grew on the plates, the pure colonies of which were obtained after repeated streaking in LB agar. Table 4.1 summarizes the morphological characteristics of all the five isolates. Isolated bacteria were identified to be gram negative rods except for JYQ2 which showed coccobacilli morphology. Except JYQ2, all the four isolates appeared smooth, circular and formed creamish white colour colonies with entire margin. The isolate JYQ2 formed off white, irregular, contoured and lobate colonies.

Table 4.1 Colony Morphology of isolated QQ bacteria

S.No.	Strain	Colour	Colony surface	Colony form	Elevation	Margin
1.	JYQ1	Creamish white	Smooth	Circular	Convex	Entire
2.	JYQ2	Off white	Contoured	Irregular	Convex	Lobate
3.	JYQ3	Creamish white	Smooth	Circular	Convex	Entire
4.	JYQ4	Creamish white	Smooth	Circular	Convex	Entire
5.	JYQ5	Creamish white	Smooth	Circular	Convex	Entire

4.2 Identification of isolated QQ bacteria

QQ bacteria grown on the KG medium were identified by biochemical and molecular analysis. The results of the analysis are summarized below.

4.2.1 Biochemical analysis

Table 4.2 enlists the biochemical tests performed for the identification of QQ bacteria. A total of twenty six tests were performed for the identification of QQ bacteria which included 11 carbohydrate fermentation tests, 5 amino acid utilization tests along with 10 other biochemical tests. All the isolates showed positive results towards catalase enzyme. The oxidase tests for the isolates JYQ3 and JYQ4 were positive while the other three isolates exhibited negative oxidase activity. Among the different isolates, JYQ1 can ferment all the 11 carbohydrates mentioned in Table 4.2 and hence appeared versatile in its choice of carbohydrate. On the contrary, JYQ3 was able to ferment only glucose. When the isolates were subjected to amino acid utilization tests, the isolate JYQ1 and JYQ5 showed positive results towards o-nitrophenyl-β-D-galactoside (ONPG), lysine and urease.

On the basis of biochemical tests, the isolates were identified using Bergey's Manual of Determinative Bacteriology (Krieg and Holt, 1984). The biochemical tests of the isolates revealed that the isolated strains JYQ1 and JYQ5 belonged to genus *Klebsiella*. Likewise, the isolates JYQ3 and JYQ4 were identified to belong to the genus *Pseudomonas* and JYQ2 to genus *Acinetobacter*.

4.2.2 Molecular identification

The PCR amplification of 16S rDNA gene produced sequences of approximately 1400 bp. Figure 4.1 showed the separation of five PCR amplified products on agarose gel electrophoresis. The five sequences isolated from dairy WAS were aligned using Codon code aligner software and analyzed by BLAST search in NCBI to find their closest relatives. Table 4.3 summarizes the detailed molecular characterization of isolated QQ bacteria. The 16S rDNA of bacterial isolates JYQ1 and JYQ5 both showed 99% sequence similarity with *Klebsiella pneumoniae*.

Bacterial isolates JYQ2, JYQ3 and JYQ4 both shared 99% sequence similarity with *Acinetobacter baumannii*, *Pseudomonas nitroreducens* and *Pseudomonas*, respectively. The sequences were submitted in the GenBank under accession numbers KP189202 (JYQ1), KP340458 (JYQ2), KP340459 (JYQ3), KU555415 (JYQ4), and KP780263 (JYQ5). It could be seen that the isolates JYQ1 to JYQ5 contributed 40% relative abundance whereas JYQ2 represented only 20% of the

Table 4.2 Biochemical characterization of quorum quenching bacteria

S.No.	Biochemical characteristics	Quorum quenching isolates				
		JYQ1	**JYQ2**	**JYQ3**	**JYQ4**	**JYQ5**
I	**Amino acid utilization tests**					
1.	ONPG test	Positive	Negative	Negative	Negative	Positive
2.	Lysine utilization	Positive	Negative	Negative	Negative	Positive
3.	Ornithine utilization	Negative	Negative	Negative	Negative	Negative
4.	Urease	Positive	Negative	Negative	Negative	Positive
5.	Phenylalanine deamination	Negative	Negative	Negative	Negative	Negative
II	**Biochemical tests**					
1.	Nitrate reduction	Positive	Negative	Positive	Positive	Positive
2.	Hydrogen sulphide (H_2S) production	Negative	Negative	Negative	Negative	Negative
3.	Citrate utilization	Positive	Positive	Positive	Positive	Positive
4.	Voges Proskauer's	Positive	Negative	Negative	Negative	Positive
5.	Methyl red	Negative	Negative	Negative	Negative	Negative
6.	Indole	Negative	Negative	Negative	Negative	Negative

7.	Malonate utilization	Positive	Positive	Negative	Positive	Positive
8.	Esculin hydrolysis	Positive	Negative	Negative	Positive	Positive
9.	Oxidase	Negative	Negative	Positive	Positive	Negative
10.	Catalase	Positive	Positive	Positive	Positive	Positive
III	**Carbohydrate fermentation**					
1.	Arabinose	Positive	Negative	Negative	Positive	Positive
2.	Xylose	Positive	Positive	Negative	Positive	Positive
3.	Adonitol	Positive	Negative	Negative	Negative	Negative
4.	Rhamnose	Positive	Positive	Negative	Negative	Positive
5.	Cellobiose	Positive	Negative	Negative	Negative	Positive
6.	Melibiose	Positive	Negative	Negative	Negative	Positive
7.	Saccharose	Positive	Negative	Negative	Negative	Positive
8.	Raffinose	Positive	Negative	Negative	Negative	Positive
9.	Trehalose	Positive	Negative	Negative	Positive	Positive
10.	Glucose	Positive	Positive	Positive	Positive	Positive
11.	Lactose	Positive	Positive	Negative	Negative	Positive
Genus		*Klebsiella*	*Acinetobacter*	*Pseudomonas*	*Pseudomonas*	*Klebsiella*

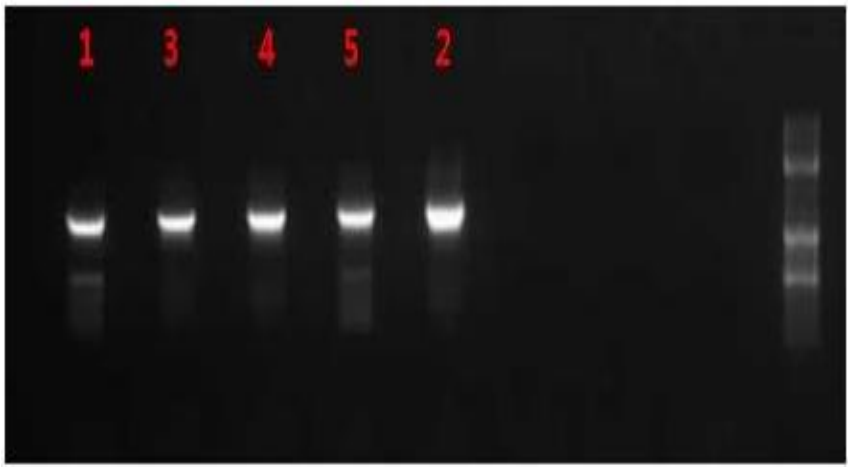

Figure 4.1 Gel electrophoresis patterns of 16SrRNA genes from dairy WAS quorum quenching bacterial isolates. Lane 1: *Klebsiella pneumoniae* JYQ1; Lane 2: *Acinetobacter baumannii* JYQ2; Lane 3: *Pseudomonas nitroreducens* JYQ3; Lane 4: *Pseudomonas* JYQ4 and Lane 5: *Klebsiella pneumoniae* JYQ5.

total isolated bacteria from the dairy WAS. All the five QQ isolates belonged to Gamma Proteobacteria and families Enterobacteriaceae (JYQ1 and JYQ5), Moraxellaceae (JYQ2) and Pseudomonadaceae (JYQ3 and JYQ4). The results of the present study corroborated with the previous study by Uroz *et al*. (2009) that reported the occurrence of QQ activity in the bacteria belonging to Proteobacteria. The evolutionary relationship among the species isolated from the dairy WAS was inferred through phylogenetic tree. Phylogenetic tree constructed by using maximum likelihood method is depicted in Figure 4.2. The results of phylogenetic analysis revealed that the sequences of isolates showed 99% sequence homology with the 16S rDNA sequences of the known genus in GenBank database, exhibiting a phylogenetic relationship with the sequences of the sewage sludge, hospital effluent, soil and rhizosphere bacteria (Wu *et al.*, 2008a; Adav *et al.*, 2010; Li *et al.*, 2013b). Furthermore, the result also reveals that the isolate JYQ3 and JYQ4 were closely related and clustered phylogenetically with the members of genus *Pseudomonas* whereas the isolates JYQ1 and JYQ5 were phylogenetically clustered with the genus *Klebsiella*. Isolate JYQ2, however was different from rest of the isolates and clustered closely with the members of *Acinetobacter* genus.

Table 4.3 Molecular identification of five bacterial isolates by 16S rDNA sequencing

S.No.	Isolates	Accession number	Closest relative	Similarity	Phylogenetic description	
					Class	Family
1.	JYQ1	KP189202	*Klebsiella pneumoniae*	99%	Gamma proteobacteria	Enterobacteriaceae
2.	JYQ2	KP340458	*Acinetobacter baumannii*	99%		Moraxellaceae
3.	JYQ3	KP340459	*Pseudomonas nitroreducens*	99%		Pseudomonadaceae
4.	JYQ4	KU555415	*Pseudomonas*	99%		
5.	JYQ5	KP780263	*Klebsiella pneumoniae*	99%		Enterobacteriaceae

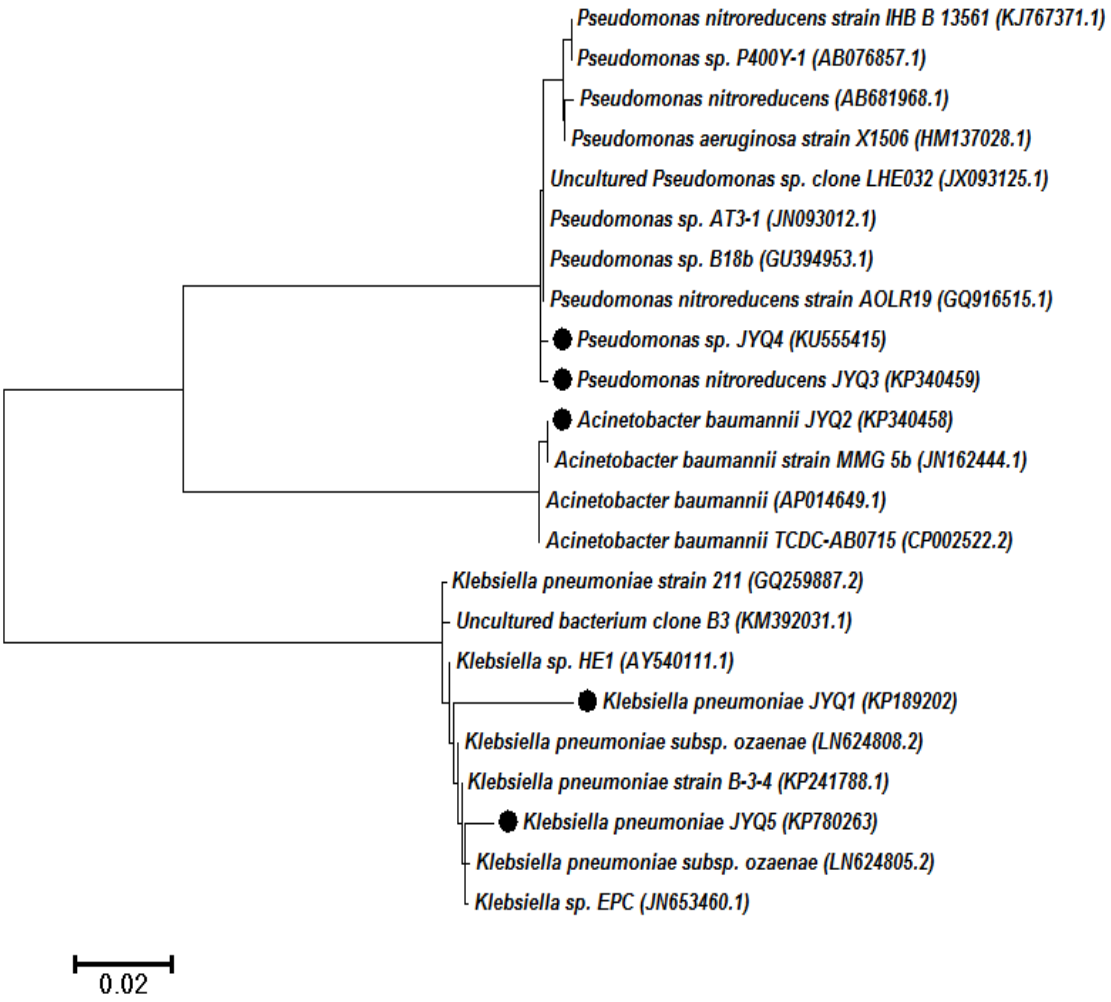

Figure 4.2 Maximum likelihood tree of dairy waste activated sludge isolated quorum quenching bacteria.

The ability of *Klebsiella*, *Acinetobacter* and *Pseudomonas* to metabolize AHL's molecules has already been reported in previous studies (Park *et al.*, 2003; Sio *et al.*, 2006; Shepherd and Lindow, 2009; Ma *et al.*, 2013; Ochiai *et al.*, 2014; Alymanesh *et al.*, 2016; Gul and Koyuncu, 2017). These bacteria are commonly present in varied habitats. Uroz *et al.* (2003) reported the presence of *Pseudomonas* genus in the tobacco rhizosphere. Gul and Koyuncu (2017) reported the occurrence of *Pseudomonas nitroreducens* in the estuary. Similarly, organisms belonging to genus *Acinetobacter* and *Klebsiella* are found to be present in cucumber rhizosphere and activated sludge of sewage treatment plant (Kang *et al.*, 2004; Chan *et al.*, 2011). So far, diverse habitats comprising, rhizosphere of tobacco, tomato, biofouled reverse osmosis membranes, soil, activated sludge has been

explored for the existence of QQ bacteria. But the dairy WAS remained unexplored for the presence of QQ bacteria to the best of author's knowledge. This is the first study which demonstrates that the bacteria present in the dairy WAS can inactivate AHL molecules.

4.3 Detection of QQ activity in bacterial isolates

The ability of QQ bacteria in degrading C6-HSL signalling molecules was evaluated both qualitatively and quantitatively via purple pigment decolourization and GC-MS analysis, respectively.

4.3.1 Qualitative determination of QQ activity

The isolates were tested for their ability to inhibit the synthesis of purple pigment violacein in biosensor strain CV026 appended with signalling molecule C6-HSL. The zone of decolourization on the CV026 lawn indicated the quenching of C6-HSL molecule by the isolates. All the five isolates revealed positive QQ activity, showing decolourization zone around the spotted lawns (Figure 4.3). The diameter of decolourization zone developed around the bacterial isolates is measured for each isolate, the results of which are summarized in Table 4.4. From the Table, it is observed that the zone of decolourization varied for each isolates. At 0^{th} h, the bacterial isolates did not show any decolourization. With increase in incubation time, the zone of decolourization showed a gradual increase.

Pseudomonas nitroreducens JYQ3 and *Pseudomonas* JYQ4 showed a zone of decolourization of 1.35± 0.05 cm and 1.84± 0.05 cm, respectively at the 6^{th} h of incubation. Further increase in incubation time to 12h resulted in complete decolourization of purple pigment by QQ bacteria *Pseudomonas* JYQ4. Hence, *Pseudomonas* JYQ4 showed maximum decolourization zone in minimum incubation time (6h) indicating better QQ ability. The isolate *Acinetobacter baumannii* JYQ2 showed 1.15± 0.05 cm diameter of decolorization in 18h as compared to 24h (1.25± 0.04 cm). The QQ bacteria *Klebsiella pneumoniae* JYQ1 and JYQ5 showed lowest decolourization diameter of 1.3± 0.1 cm and 1.1± 0.1 cm, respectively in 24h thereby showing lowest QQ ability among others. The results of the present study are consistent with the previous findings that reported loss of purple pigment after incubation with *Acinetobacter*, *Pseudomonas* and *Klebsiella* (Chan *et al.*, 2011;

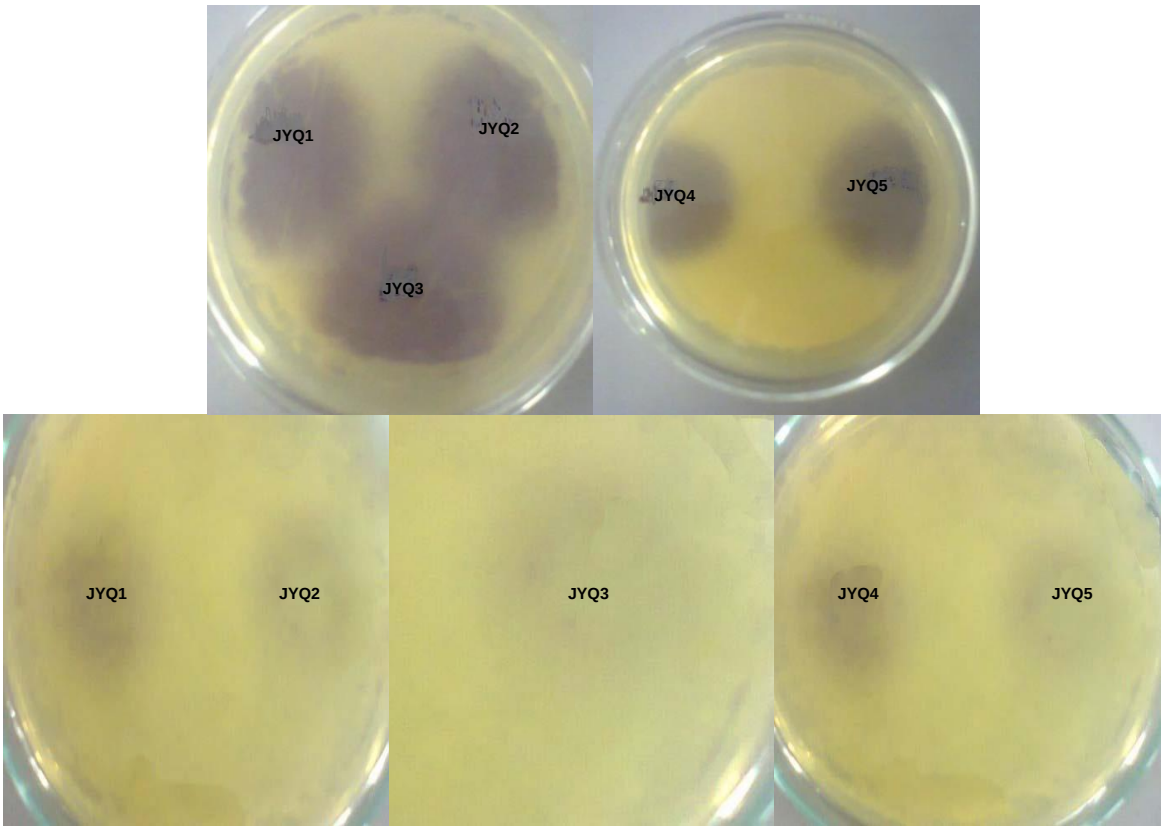

Figure 4.3 C6-HSL degradation by *Klebsiella pneumoniae* (JYQ1 and JYQ5), *Acinetobacter baumannii* JYQ2, *Pseudomonas nitroreducens* JYQ3 and *Pseudomonas* JYQ4. Each dairy WAS isolate was incubated with C6-HSL at different intervals. Pigment formation in the top row indicates presence of C6-HSL in 0h incubation with QQ bacteria whereas the bottom row indicates absence of pigment formation indicating QQ activity by *Klebsiella pneumoniae* (JYQ1 and JYQ5), *Acinetobacter baumannii* JYQ2, *Pseudomonas nitroreducens* JYQ3 and *Pseudomonas* JYQ4 in 24h, 18h, 12h and 6h, respectively.

Devaraj *et al.*, 2017). In the study by Chong *et al.* (2012), no trace of C6-HSL was detected by the biosensor CV026, indicating significant QQ activity of *Pseudomonas*. Chan *et al.* (2011) observed the absence of residual 3-oxo-C6-HSL after incubation of ginger rhizosphere associated *Acinetobacter* sp. and *Klebsiella* sp. with 3-oxo-C6-HSL for 24h. Contrary, Ochiai *et al.* (2013) reported weak degradation activity of *Acinetobacter* strain isolated from activated sludge of wastewater treatment plant against C6-HSL.

Table 4.4 Quorum quenching activity of different bacterial isolates against CV026

S.No.	Isolates	Inhibition zone diameter± S.E. (cm)				
		0 hour	6 hour	12 hour	18 hour	24 hour
1.	*Klebsiella pneumoniae* JYQ1	No decolourization	No decolourization	0.7± 0.06	0.85±0.005	1.3±0.1
2.	*Acinetobacter baumannii* JYQ2	No decolourization	No decolourization	0.81± 0.04	1.15± 0.05	1.25± 0.04
3.	*Pseudomonas nitroreducens* JYQ3	No decolourization	1.35± 0.05	1.61± 0.005	-	-
4.	*Pseudomonas* JYQ4	No decolourization	1.84± 0.05	-	-	-
5.	*Klebsiella pneumoniae* JYQ5	No decolourization	No decolourization	0.55± 0.05	0.8± 0.02	1.1± 0.1

4.3.2 Quantitative characterization of QQ activity

The degradation activities of five QQ bacteria against C6-HSL were assessed quantitatively using GC-MS analysis. The effect of five QQ bacteria (*Klebsiella pneumoniae* JYQ1 and JYQ5, *Acinetobacter baumannii* JYQ2, *Pseudomonas nitroreducens* JYQ3 and *Pseudomonas* JYQ4) on C6-HSL degradation was examined at different time intervals. Figure 4.4 depicts the residual C6-HSL after incubation with five QQ bacteria at different time intervals. It was observed that with the increase in incubation time, the bacterial isolates showed a significant ($p<0.05$) degradation of C6-HSL. The C6-HSL degradation by QQ bacteria ranged from 57.7% (*Klebsiella pneumoniae* JYQ5) to 83.8% (*Pseudomonas* JYQ4) within 6h incubation. The isolates *Klebsiella pneumoniae* JYQ1 and JYQ5 showed 59.3% and 57.7% degradation with increase in incubation time from 0h to 6h. Isolates *Acinetobacter baumannii* JYQ2, *Pseudomonas nitroreducens* JYQ3 and *Pseudomonas* JYQ4 showed degradation percentage of 62.7%, 62.5% and 83.8%, respectively at the 6h of incubation. Increase in incubation time from 6h to 12h resulted in further degradation of C6-HSL by all the five isolates. *Klebsiella pneumoniae* JYQ1 and JYQ5 showed degradation efficiency of 60.3% and 59%, respectively at 12 h. Likewise, *Acinetobacter baumannii* JYQ2 and *Pseudomonas nitroreducens* JYQ3 exhibited degradation percentage of 66% and 68.4%, respectively. The isolate *Pseudomonas* JYQ4 showed no trace of C6-HSL after 6 h indicating its better QQ activity. The results of the quantitative analysis is in complete agreement with the qualitative analysis. An increase in degradation percentage to 66.3% and 79.7% was seen at increased incubation time of 18h, when incubated with isolates *Klebsiella pneumoniae* JYQ1 and JYQ5, respectively. Compared to all other isolates, *Klebsiella pneumoniae* JYQ1 and JYQ5 showed least degradation ability.

Acinetobacter baumannii JYQ2 showed a drop in degradation ability at the 24th h of incubation (76.8%) when compared to 18th h (79.4%). The increase in C6-HSL in the medium might be due to the ability of *Acinetobacter* to produce C6-HSL (Chan *et al.*, 2014a). The result of the present study is supported by previous studies that reported AHL synthesis and degradation in genus *Acinetobacter* (Gonzalez *et al.*, 2001). The genus *Acinetobacter* was known to produce QS signalling molecules (Gonzalez *et al.*, 2001; Chan *et al.*, 2011).

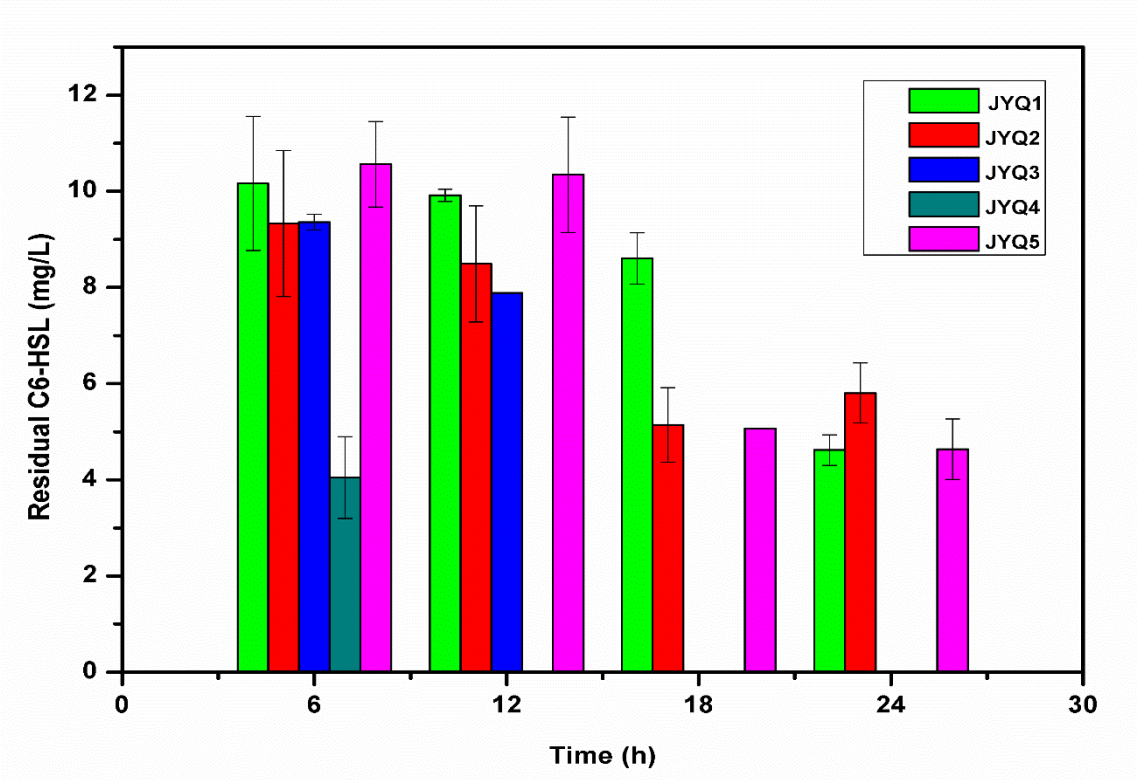

Figure 4.4 C6-HSL degradation by QQ bacteria at different time intervals

Chan *et al.* (2014a) reported the production of short chain AHL i.e. C6-HSL by *Acinetobacter baumannii* which is in concordance with the present findings. Contrary, Chan *et al.* (2011) reported the production of long chain signalling molecules such as 3-oxo-C12-HSL and 3-hydroxy-C12-HSL by *Acinetobacter* isolated from *Zingiber officinale* rhizosphere. According to their study, the rhizosphere associated *Acinetobacter* was more efficient in degrading the long chain acyl chain AHL rather than short chain AHL molecules. Unlike *Zingiber officinale* rhizosphere associated *Acinetobacter*, the *Acinetobacter baumannii* JYQ2 exhibited degradation of short chain AHL, C6-HSL. Kang *et al.* (2004) also reported the reduction of 40 ng of C6-HSL within 4 or 6h of incubation by *Acinetobacter* sp. strain C1010 isolated from cucumber rhizosphere. Chan *et al.* (2011) reported short chain AHL i.e. 3-oxo-C6-D-HSL degradation by genus *Klebsiella* too.

The AHL degradation activity by genus *Pseudomonas* has also been reported in the previous studies (Chan *et al.*, 2014b; Kim *et al.*, 2014). According to Huang *et al*. (2003), *Pseudomonas* utilized long chain signalling molecule *N*-3-oxododecanoyl-L-homoserine lactone (OC12HSL) for their growth. Sio *et al.* (2006) in his study

observed that the PA2385 protein in *P. aeruginosa* PAO1 is responsible for hydrolyzing the long chain AHL (acyl chain length ranging from 11 to 14 carbon atoms) such as 3-oxo-C12-HSL within 6 hours of incubation. However, this protein resisted the degradation of short chain AHLs (N-butanoyl homoserine lactone (BHL) and C6-HSL). But, in the present study, complete degradation of short chain AHL molecules was observed when incubated with the *Pseudomonas nitroreducens* (JYQ3) and *Pseudomonas* (JYQ4) bacteria.

The degradation products of C6-HSL were identified by GC-MS analysis. Table 4.5 enlists the metabolites of C6-HSL degradation by five different QQ bacteria. Four metabolites namely hexadecanoic acid, pentadecanoic acid, octadecanoic acid and tetradecanoic acid were identified. Figure 4.5 illustrates the degradation of C6-HSL after incubation with *Pseudomonas* JYQ4. Presence of fatty acid metabolites indicated the presence of enzyme acylase in QQ bacteria that degraded C6-HSL into corresponding fatty acid products (Chen *et al.*, 2013).

Table 4.5 Metabolites of C6-HSL degradation by different QQ bacteria

S.No.	Isolates	Degradation products
1.	*Klebsiella pneumoniae* JYQ1	Pentadecanoic acid, octadecanoic acid
2.	*Acinetobacter baumannii* JYQ2	n- hexadecanoic acid
3.	*Pseudomonas nitroreducens* JYQ3	n-hexadecanoic acid, octadecanoic acid
4.	*Pseudomonas* JYQ4	Hexadecanoic acid
5.	*Klebsiella pneumoniae* JYQ5	n-hexadecanoic acid, tetradecanoic acid, octadecanoic acid

The degradation of AHL by acylase in the QQ bacteria *Pseudomonas aeruginosa* PAO1 genome sequence and *Acinetobacter* isolated from activated sludge has already been reported by Sio *et al.* (2006) and Ochiai *et al.* (2014), respectively. According to Ochiai *et al.* (2014), the AmiE in *Acinetobacter* sp. strain Ooi24, isolated from the activated sludge functions as an AHL acylase that hydrolyzed the amide bond in AHL molecule. On the other hand, *Acinetobacter* sp. GG2 associated with the rhizosphere of *Zingiber officinale* possessed an enzyme AHL lactonase that

hydrolyzed the lactone ring forming n-acyl homoserine compound (Chan *et al.*, 2011). In addition, the previous researches also reported the lactonase activity behind the QQ activity of other two bacteria i.e. *Klebsiella* and *Pseudomonas* which is contrary to the present study (Park *et al.*, 2003; Chan *et al.*, 2011; Ma *et al.*, 2013).

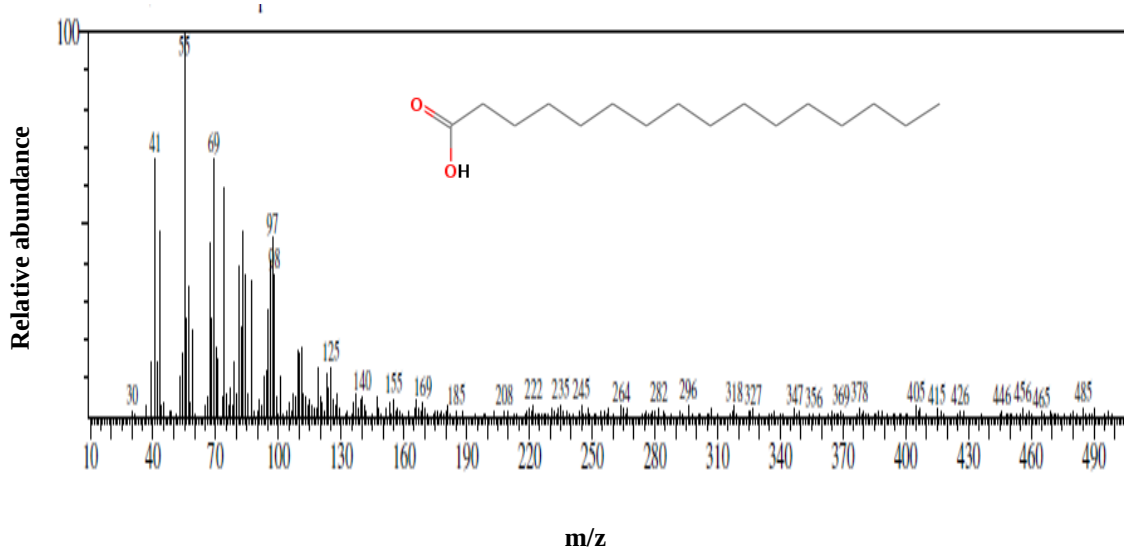

Figure 4.5 Mass spectra of n-hexadecanoic acid product generated by degradation of C6-HSL by *Pseudomonas* JYQ4.

Keeping in mind the pathogenicity of *Klebsiella pneumoniae* JYQ1 and JYQ5, these strains were exempted from being used in immobilization studies.

4.4 Evaluation of QQ activity of immobilized magnetic nanocomposite (IMN) beads

The magnetic iron nanoparticles in the IMN beads were used as a carrier to facilitate the magnetic separation of IMN beads from the sludge suspension during the reactor studies. However, the magnetic property is controlled by the physicochemical properties of the iron nanoparticles such as size, shape, functionality of the nanoparticles. In this section, the results of various physico-chemical properties of magnetic iron nanoparticles and their successful immobilization within the beads are explained. Also, the outcomes of the ability of these prepared QQ IMN beads to quench C6-HSL molecule is discussed in the following section.

4.4.1 Characterization of prepared nanoparticles

The magnetic iron nanoparticles prepared by co-precipitation of Fe^{2+} and Fe^{3+} ions were characterized for their size, morphology, elemental composition, functional groups, crystalline nature, thermal stability and magnetic property.

4.4.1.1 Morphological characterization

The surface morphology and size of magnetic iron nanoparticles were examined using SEM and TEM. Figure 4.6 depicts the SEM micrographs of magnetic iron nanoparticles. The synthesized magnetic iron nanoparticles were cubical in shape. The agglomeration observed in the micrographs might be due to precipitation of salts during preparation. The agglomeration might be due to the limited supply of OH^- ions provided by NaOH during preparation. The precipitant played an indispensable role in the formation of nanostructure of iron nanoparticles (Zheng *et al.*, 2010). It functions as a pH buffer which when reacts with water, supplies OH^- ions. The structure of nanoparticles is mainly dependent on its constant supply. Similar agglomeration was also reported by Yang *et al.* (2014) during the preparation of Fe_3O_4 nanoparticles with NaOH. Few studies reported Fe_3O_4 nanoparticles of cubical shape (Wei *et al.*, 2012; Mahdavi *et al.*, 2013) and quasi spherical shape (Hong *et al.*, 2008; Yang *et al.*, 2014; Silva *et al.*, 2016). The shape and size distribution of iron nanoparticles were also confirmed by TEM analysis. Figure 4.7 (a) and (b) shows the TEM micrographs and size distribution pattern of magnetic iron nanoparticles, respectively. The histogram of size distribution was prepared from TEM micrographs using Image J software considering 150 nanoparticles. From the histogram, it can be seen that the particles were nanosized and were in the range of 5-19 nm with an average particle size of 15 nm. The results are in accordance with the previous studies that reported the particle size distribution in the range of 5-20 nm (Hong *et al.*, 2008; Wei *et al.*, 2012; Hariani *et al.*, 2013). In another study, Peternele *et al.* (2014) synthesized iron nanoparticles with average size of around 9.82 nm. The smaller particle size of synthesized magnetic iron nanoparticles might be attributed to the pH of the solution (pH 10) during nanoparticle preparation. According to Mahdavi *et al.* (2013), at pH lower than 11, the size of magnetic iron nanoparticle decreases with the increase in solution pH.

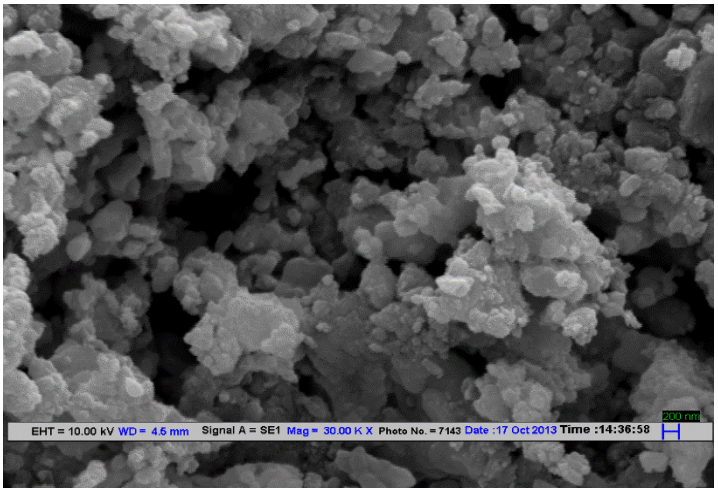

Figure 4.6 SEM micrograph of magnetic iron nanoparticles

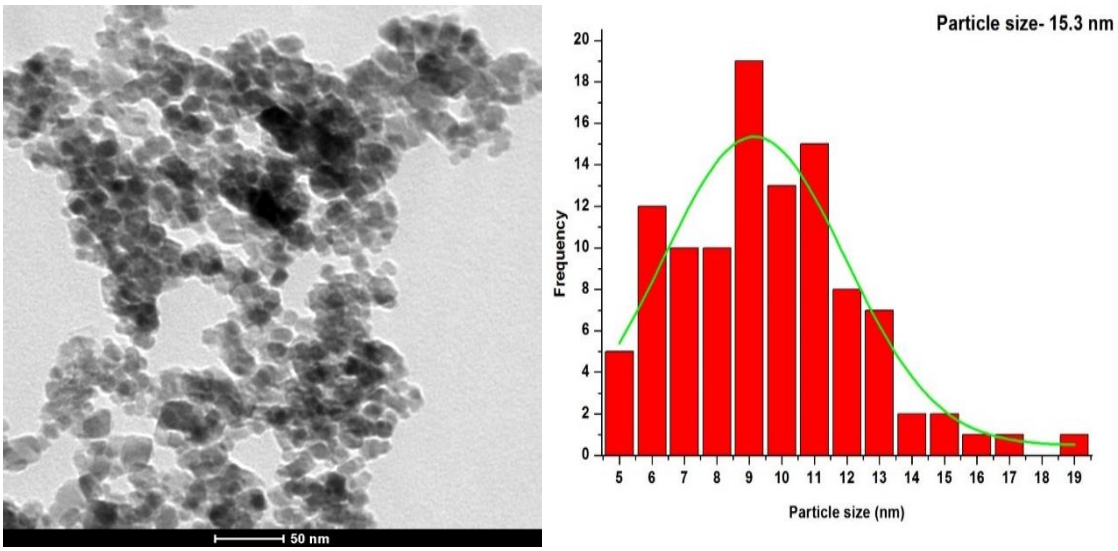

Figure 4.7 (a) TEM image of magnetic iron nanoparticles; (b) Size distribution of magnetic iron nanoparticles

4.4.1.2 Elemental composition

The structural composition and elemental distribution of magnetic iron nanoparticles was determined using SEM/ EDS analysis. Figure 4.8 and 4.9 depicts the EDS spectra and elemental maps of Fe and O, respectively. The EDS spectra revealed peaks of two major elements corresponding to Fe and O. The few extra peaks in the EDS spectra corresponds to the element Au which might have occurred due to gold coating over nanoparticles during SEM analysis. The atomic percent of Fe and O

was determined from EDS and was found to be around 64.7% and 35.2%, respectively (Table 4.6).

Table 4.6 Atomic percent of elements in magnetic iron nanoparticles

S.No.	Elements	Atomic percent (%)
1.	Fe K	64.7
2.	O K	35.2

The spectra of the synthesized nanoparticles suggested the presence of Fe and O as the main constituents in the magnetic iron nanoparticles. Shaker *et al.* (2013) also confirmed the presence of Fe and O. Hariani *et al.* (2013) reported a comparatively higher Fe and O of 73.3% and 21%, respectively in Fe_3O_4 nanoparticles.

4.4.1.3 Functional groups

The functional groups present in the magnetic iron nanoparticles was determined using FTIR analysis. Figure 4.10 depicts the FTIR spectra of magnetic iron nanoparticles recorded in the range of 500-4500 cm^{-1}. The peak at 580 cm^{-1} corresponded to Fe-O bond. The presence of Fe-O vibration indicated the magnetic property of nanoparticles (Mahdavi *et al.*, 2013).

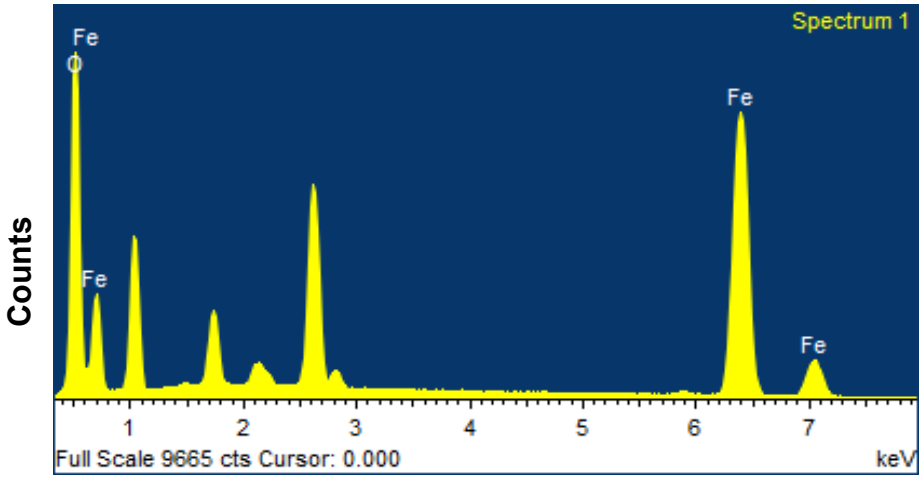

Figure 4.8 SEM/EDS spectra of magnetic iron nanoparticles

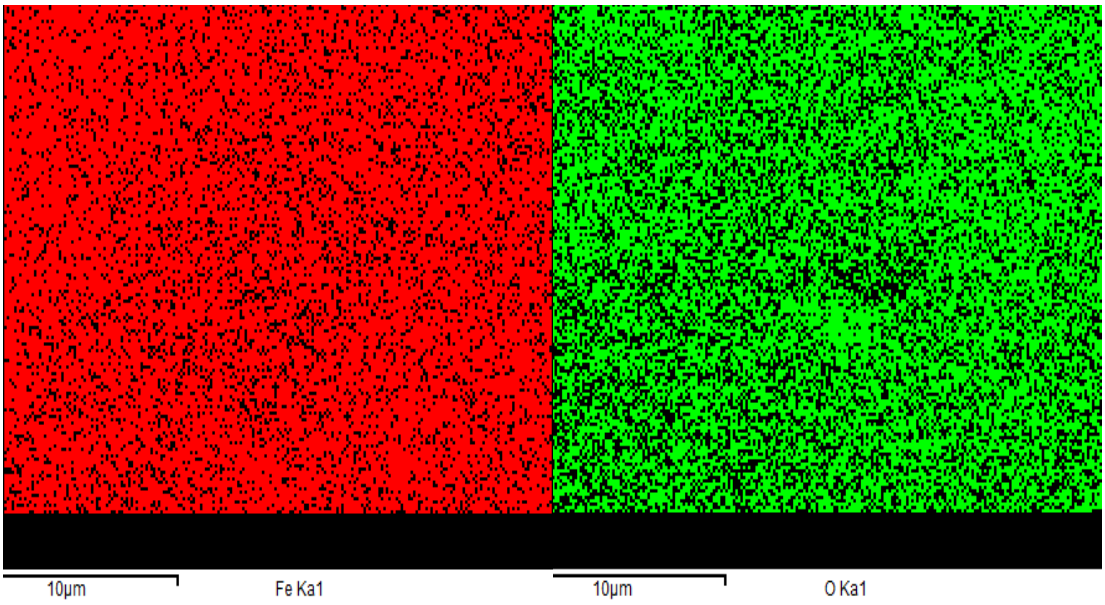

Figure 4.9 EDS mapping of magnetic iron nanoparticles

The appearance of broad band at 3200 cm^{-1} was due to the stretching vibration of hydroxyl group thereby representing the absorption of -OH by the magnetic iron nanoparticles indicating the completion of the crystallization process. The results are in agreement with the previous studies by Abdalla *et al.* (2011) and Sulistyaningsih *et al.* (2017) who also reported the presence of characteristic peaks corresponding to the Fe-O vibration and stretching vibration of -OH group in Fe_3O_4 nanoparticles.

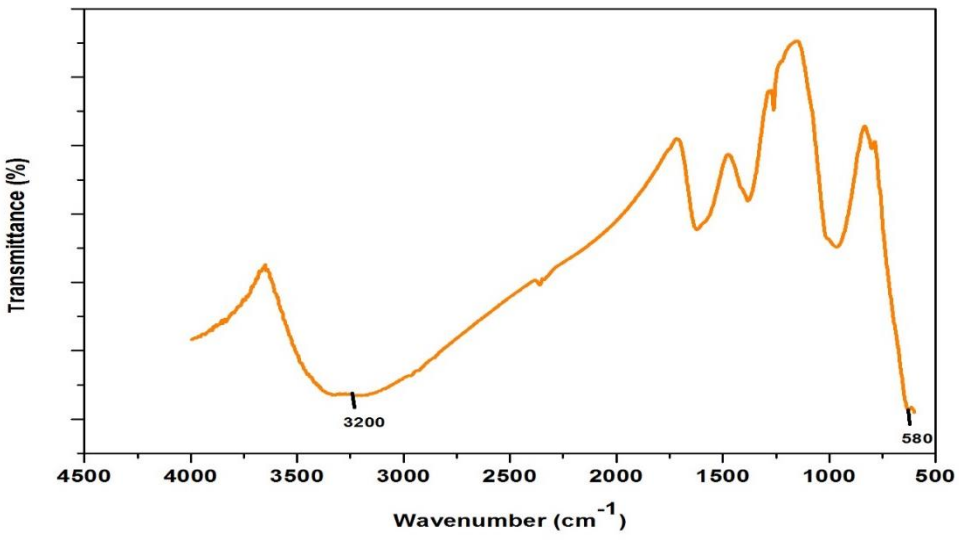

Figure 4.10 FTIR spectra of magnetic iron nanoparticles

4.4.1.4 Crystalline structure

The crystalline structure of the magnetic iron nanoparticles was obtained using Selected area electron diffraction pattern (SAED) and X-ray diffraction (XRD) analysis which is explained in the following sections**.**

4.4.1.4.1 SAED analysis

The SAED patterns of magnetic iron nanoparticles are depicted in Figure 4.11. The particles showed polycrystalline structure confirmed by the presence of white ring like structures in the SAED image. The ring patterns could be assigned to planes 220, 400, 422, 440.

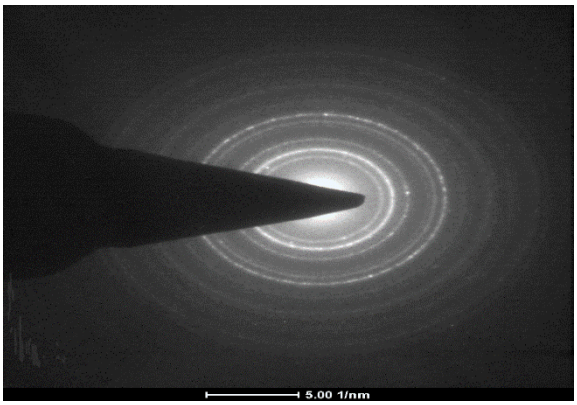

Figure 4.11 TEM SAED pattern of magnetic iron nanoparticles

The d-spacings confirmed that the synthesized nanoparticles possessed a face centered cubic structure with cell parameters a=b=c 8.4 A°. The results of SAED pattern in the present study matched with the SAED patterns reported by Shete *et al.* (2013). The SAED images obtained in their study also confirmed the presence of planes 220, 400 and 422. Moreover, they also reported the polycrystalline nature of the magnetic iron nanoparticles.

4.4.1.4.2 XRD analysis

Figure 4.12 depicts the XRD pattern of the magnetic iron nanoparticles prepared using co-precipitation method. A series of characteristic peaks appearing at 2θ range of 35.6, 57, 63.07 can be assigned to 311, 511 and 440 planes of Fe_3O_4

(JCPDS card no. 72-2303), respectively. It was seen that the position and relative intensities of peaks of nanoparticles obtained in the present study can match with the diffraction peaks of standard Fe_3O_4 samples indicating the magnetic property of synthesized iron nanoparticles (Thunemann *et al.*, 2006). The sharp peaks in the XRD indicated good crystalline structure of magnetic iron nanoparticles. Further, the presence of diffraction peak at 511 corresponded to the inverse spinel cubical Fe_3O_4 particles which is also confirmed by SAED pattern.

The crystallite size D of the synthesized nanoparticles can be calculated from Debye-Scherrer formula given in equation 4.1.

$$D_{hkl} = 0.9\ \lambda /\ \beta \cos \theta \qquad \cdots\cdots\cdots\cdots\cdots\cdots \qquad (4.1)$$

Where λ= X- ray wavelength and is equal to 0.154 nm, β= half high width of the diffraction peak of sample, θ= diffraction angle.

The calculated crystallite size of the magnetic iron nanoparticles was found to be around 6.9 nm confirming the results of TEM analysis.

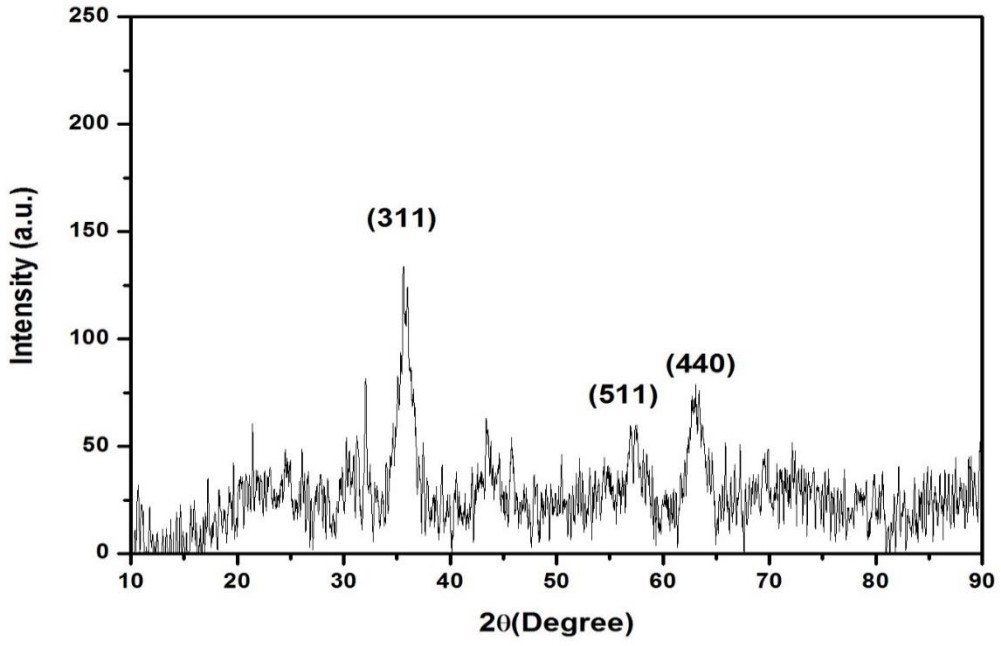

Figure 4.12 XRD diffraction pattern of magnetic iron nanoparticles

4.4.1.5 Magnetic property

The magnetic property of magnetic iron nanoparticles was analyzed using VSM. Figure 4.13 depicts the saturation magnetization of the synthesized nanoparticles. The saturation magnetization of the magnetic iron nanoparticles was 39 emu g^{-1}. The saturation magnetization obtained in the present study falls within the range of 30- 80 emu g^{-1} as given by Wu *et al.* (2008b) in his study. The saturation magnetization (M_S) obtained in the present study was smaller than those mentioned in previous studies. Liao and Chen (2001) and Yang *et al.* (2014) reported a saturation magnetization of 63 emu g^{-1} and 83.7 emu g^{-1}, respectively. The smaller M_S might be due to the smaller particle size. Smaller particle size results in surface disorder. The disordered spins at the surface prevented the aligning of core spins along the direction of magnetic field, thereby resulting in decreased M_S (Ghandoor *et al.*, 2012). The saturation magnetization obtained in the present study is sufficient to facilitate the separation of QQ bacteria IMN beads when used in bioreactors.

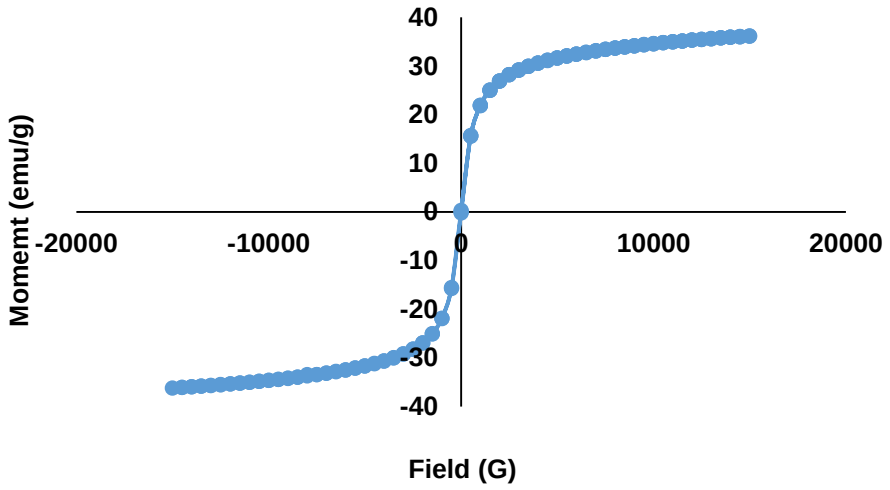

Figure 4.13 Magnetization curve of magnetic iron nanoparticles

4.4.2 Characterization of QQ bacteria immobilized magnetic nanocomposites (IMN) beads

The magnetic iron nanocomposites prepared by mixing the nanoparticles with the sodium alginate were used for QQ bacteria immobilization. The three QQ bacteria namely *Acinetobacter baumannii* JYQ2, *Pseudomonas nitroreducens* JYQ3,

Pseudomonas JYQ4 and consortium of three QQ bacteria were immobilized in IMN beads. The successful immobilization of whole QQ bacterial cells within the beads was determined using SEM analysis.

Figure 4.14 depicts the cross-sectional SEM micrographs showing the morphologies of blank and QQ bacteria IMN beads. The blank and IMN beads possessed microporous structure (Figure 4.14 a). The polysaccharide moiety within the alginate beads formed a network with large empty spaces or voids as a result of inhomogenously distributed aggregates.

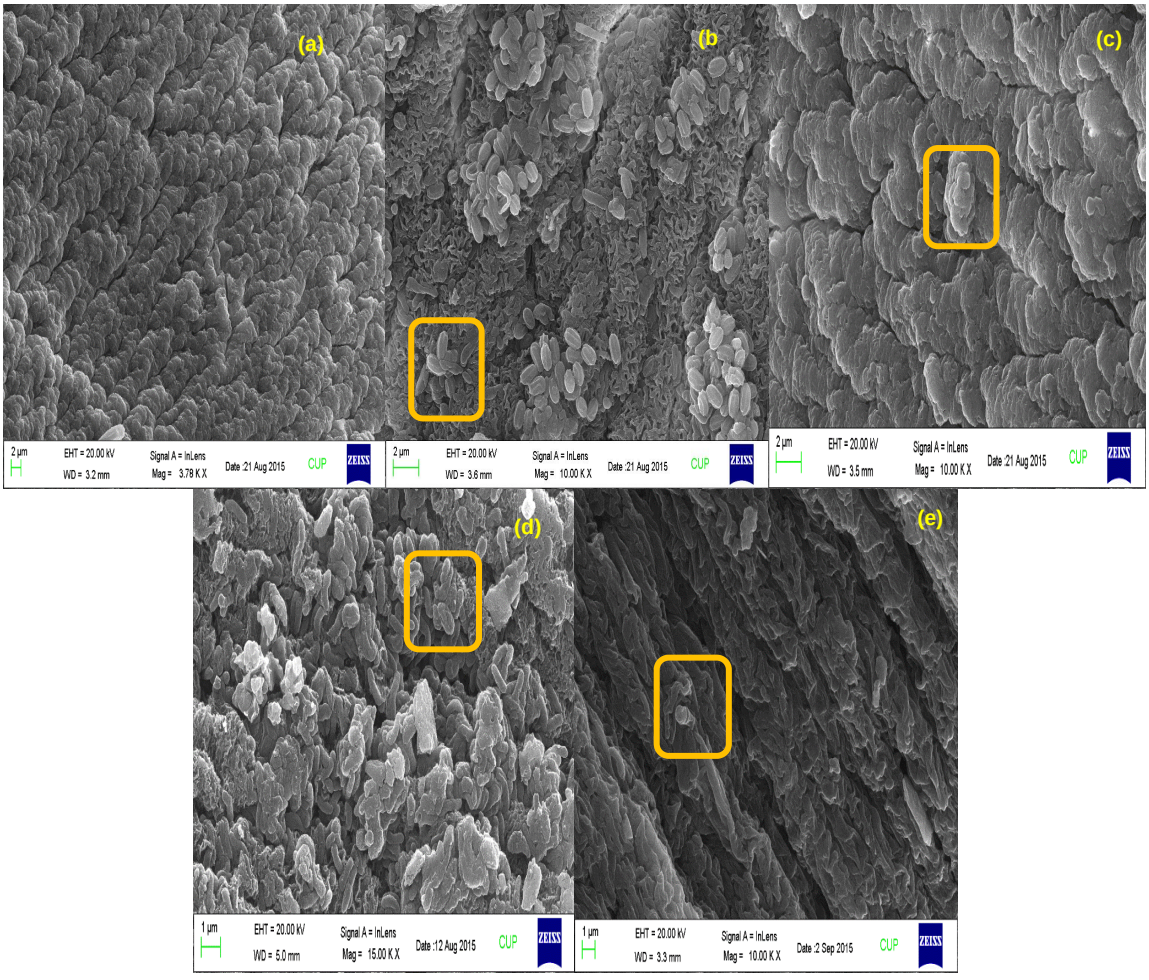

Figure 4.14 SEM images of the IMN beads: cross section of (a) Blank magnetic iron nanoparticles beads without immobilized bacteria. Scale bar = 2 µm, (b) *Acinetobacter baumannii* JYQ2 IMN beads. Scale Bar = 2 µm, (c) *Pseudomonas nitroreducens* JYQ3 IMN beads. Scale Bar = 2 µm, (d) *Pseudomonas* JYQ4 IMN beads. Scale Bar = 1 µm, (e) Consortium IMN beads. Scale Bar = 1 µm.

The presence of voids within the beads might provide sufficient space for the colonization of a high density of micro-organisms (Serp *et al.*, 2002). From the Figure 4.14 a, it is clearly evident that no bacteria was present inside the voids of blank beads, whereas the QQ bacteria successfully occupied the voids in IMN beads (Figure 4.14 b-e). The presence of almost round, rod shaped structures in Figure 4.14 (b) confirmed the entrapment of *Acinetobacter baumannii* JYQ2 within the beads. Further, the appearance of rod shaped structures indicated the entrapment of *Pseudomonas* JYQ4 within the pores of beads (Figure 4.14 d). Sodium alginate has provided internal cavities for the attachment, growth and multiplication of micro-organisms. Moreover, they do not limit the heat and mass transfer (Covarrubias *et al.*, 2012).

The entrapment of QQ bacteria was also reported in previous studies. *Rhodococcus* sp. BH4 and *Bacillus methylotrophicus* sp. WY QQ bacteria entrapment within the alginate matrix was reported by Kim *et al.* (2013) and Khan *et al.* (2016), respectively.

4.4.3 QQ activity of IMN beads

The QQ bacteria immobilized in IMN beads were inspected for their QS inhibitory activity against *CV*2656. All the QQ bacteria IMN beads revealed QS inhibitory activity which can be confirmed owing to the absence of purple colouration in the flasks incubated with *Acinetobacter baumannii* JYQ3, *Pseudomonas nitroreducens* JYQ3 and *Pseudomonas* JYQ4 IMN beads (Figure 4.15). However, the control flask incubated with the blank nanoparticle beads showed purple colouration. The absence of purple colouration clearly confirmed that the QQ bacteria IMN beads have the potential to degrade the signalling molecule C6-HSL produced by *CV*2656 within 24 h of incubation.

The C6-HSL degraded by the QQ bacteria IMN beads was evaluated quantitatively using GC-MS analysis. The QQ bacteria IMN beads showed significant degradation of C6-HSL with increase in incubation time (Figure 4.16 and Figure 4.17). Among the different QQ bacteria IMN beads, *Pseudomonas* JYQ4 IMN beads showed 90% degradation within 6h of incubation. At the end of 1st h of incubation, *Pseudomonas*

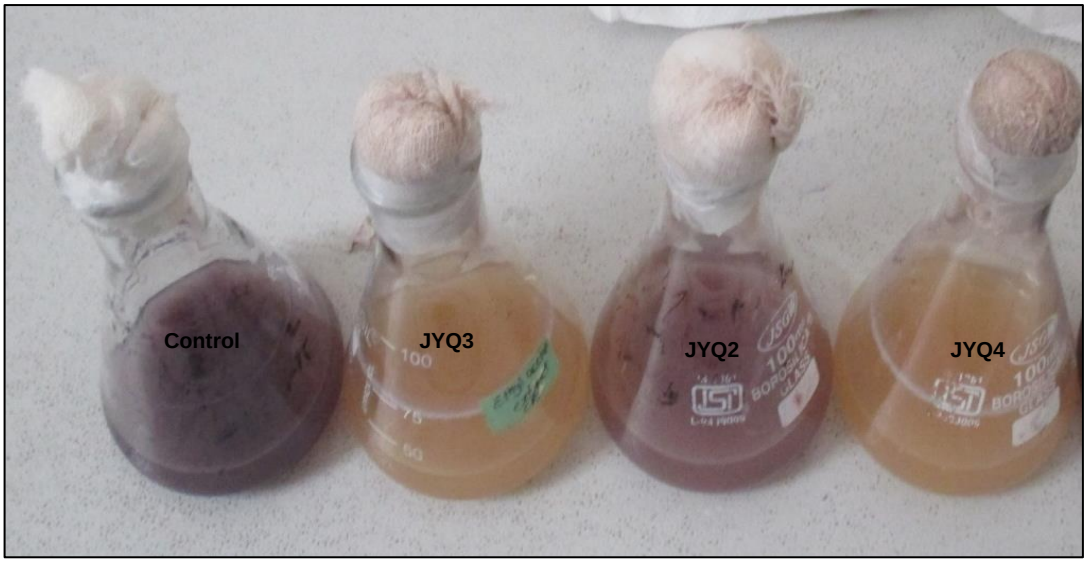

Figure 4.15 QS inhibitory activity of QQ bacteria IMN beads against CV2656

nitroreducens JYQ3 and *Pseudomonas* JYQ4 IMN beads showed residual C6-HSL of 16.3± 0.2 mg/L and 16.2± 1.3 mg/L, respectively.

An abrupt decrease in residual C6-HSL concentration was seen at 3rd h of incubation in flasks containing *Pseudomonas nitroreducens* JYQ3 and *Pseudomonas* JYQ4 IMN beads showing a residual C6-HSL of 9± 1.6 mg/L and 8.7± 1.2 mg/L, respectively. The degradation efficiency was increased with increase in incubation time. The maximum C6-HSL degradation of 90% was observed at 6th h in flasks incubated with *Pseudomonas* JYQ4 IMN beads. Likewise, the lowest degradation percentage of 73% was recorded in *Acinetobacter baumannii* JYQ2 IMN beads incubated flasks.

Acinetobacter baumannii JYQ2 IMN beads showed a different behaviour when compared to other QQ bacteria (Figure 4.16). The concentration of C6-HSL within the flasks undulated throughout the incubation period. At the 1st h of incubation, *Acinetobacter baumannii* JYQ2 IMN beads showed a degradation percentage of 49.2% which later decreased to 41.8% on the 2nd h of incubation. Likewise, C6-HSL degradation increased to 48.4% at 3h and once again showed a decrease and reached 74.4% at 6th h when compared to 5th h (75.1%). The inconsistent trend in QQ activity of *Acinetobacter baumannii* JYQ2 IMN beads might be due to the QS activity of *Acinetobacter*. Similar response was also observed in *Acinetobacter baumannii* JYQ2 free cells too.

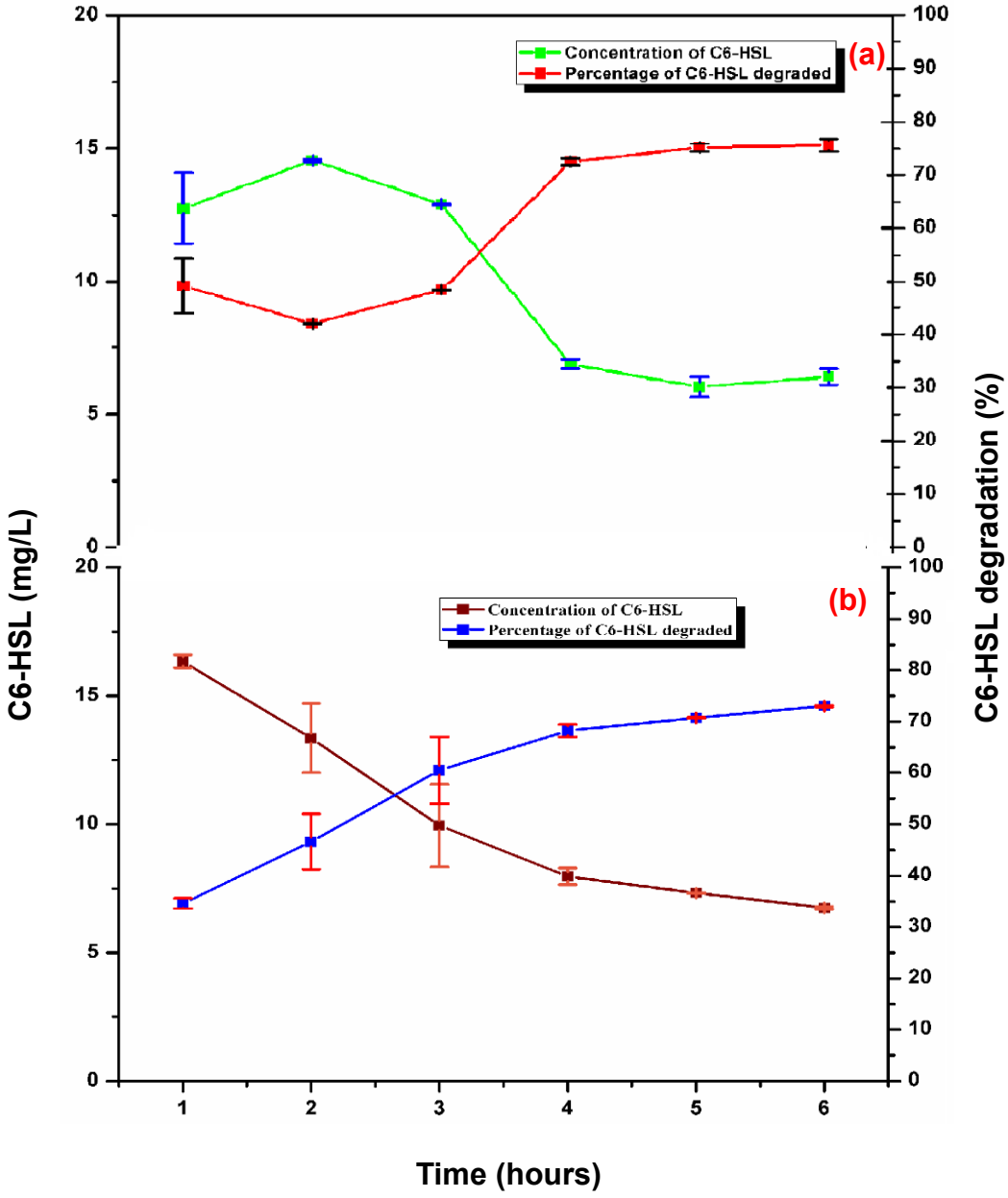

Figure 4.16 QQ activity of (a) *Acinetobacter baumannii* JYQ2 and (b) *Pseuodomonas nitroreducens* JYQ3 IMN beads

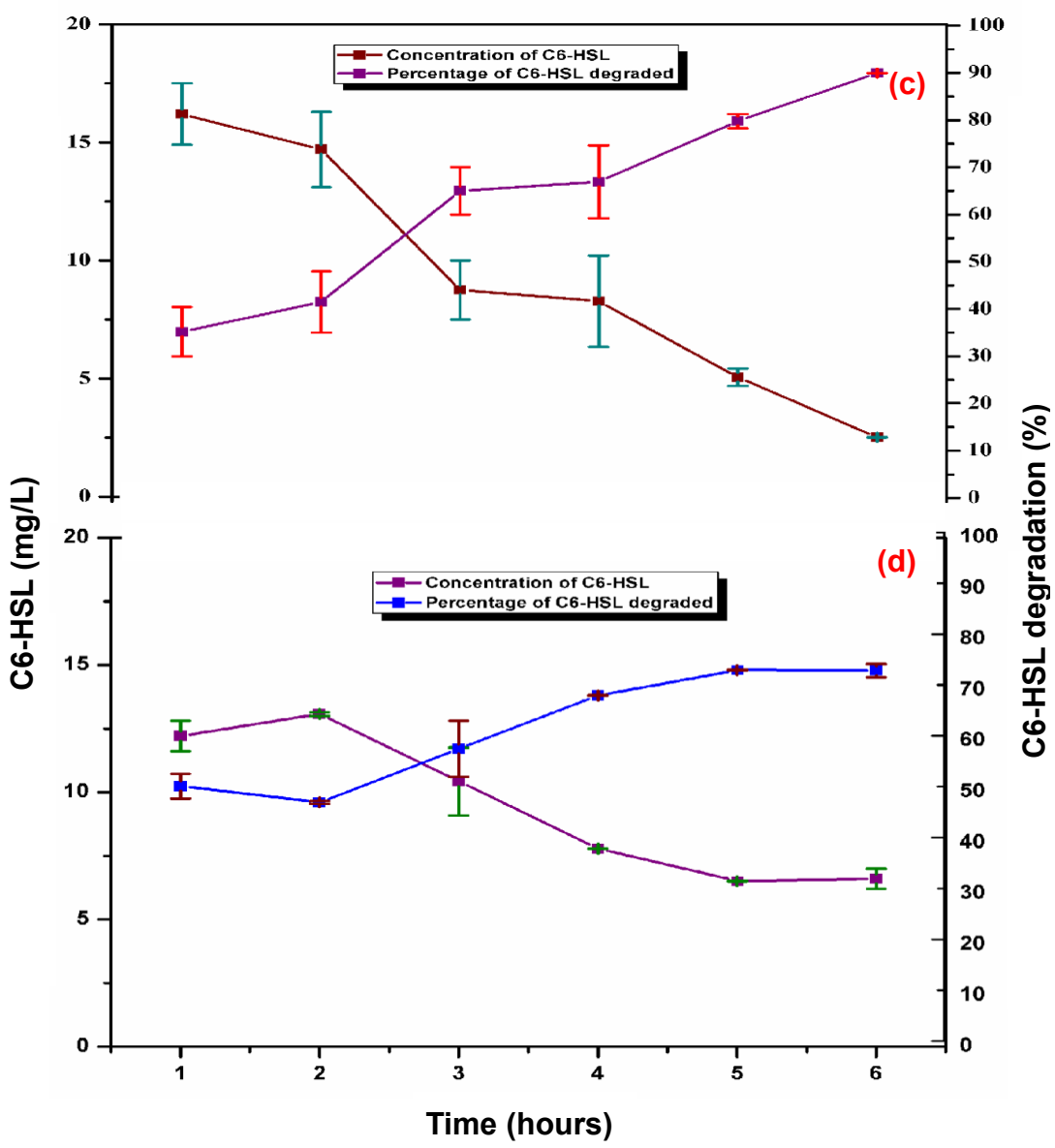

Figure 4.17 QQ activity of (c) *Pseuodomonas* JYQ4 and (d) Consortium IMN beads

The consortium also showed similar trend as that of JYQ2 as they too contained *Acinetobacter baumannii* JYQ2. The consortium showed overall C6-HSL degradation percentage in the range between 51.2% and 73.9%. At the end of 1st h, the consortium showed around 51.2% C6-HSL degradation. It further dropped to 48% at the end of 2nd h and once again increased to 58.5% at the 3rd h. After 3h, a continous increase in C6-HSL degradation percentage was seen in consortium IMN beads incubated flasks. At 6th h, a residual C6-HSL of 6.6± 0.4 mg/L was obtained.

Degradation of AHL by immobilized *Pseudomonas* has been reported previously by many researchers. Cheong *et al.* (2013) used microbial vessel made from hollow fiber microporous membrane for immobilization of *Pseudomonas* sp. 1A1 isolated from wastewater treatment plant. They observed 45% degradation of long chain signalling molecule N-(octanoyl)-DL-homoserine lactone (C8-HSL) within 90 minutes of incubation. Few studies reported the ability of consortium to quench signalling molecules. Waheed *et al.* (2017) investigated the effectiveness of QQ consortium comprising *Microbacterium* sp., *Enterobacter cloaca* and *Pseudomonas* sp. immobilized in polymer coated alginate beads against degradation of QS signalling molecules. The signalling molecules, N-butyryl-homoserine lactone (C4-HSL), N-(3-oxohexanoyl)-homoserine lactone (3OC6-HSL), N-hexanoyl-homoserine lactone (C6-HSL) and N-(3-oxotetradecanoyl)-L-homoserine lactone (3OC14-HSL) were lower than the quantification limit in QQ-MBR thereby showing the quenching effect of QQ consortium.

In order to examine the mechanism behind the C6-HSL degradation, two controls- A_1 devoid of bead and other A_2 with blank nanoparticle beads were run. Control A_1 (without beads) exhibited 4.2± 0.5% degradation with residual C6-HSL of 23.9± 0.1 mg/L. On the other hand, control A_2 flask showed C6-HSL of 23.6± 0.1 mg/L showing 5.5±0.4% degradation of C6-HSL. From the results, it is clear that C6-HSL underwent self-degradation and showed a degradation efficiency of 4.2± 0.56% whereas the nanoparticle beads degraded around 1.3±0.1% of C6-HSL. Kim *et al.* (2013) in his study reported negligible adsorption of C8-HSL onto the blank alginate beads. In another study by Mutlu *et al.* (2016), about 9.5% of C8-HSL removal through surface adsorption of CEB was observed.

The degradation mechanism exhibited by QQ bacteria IMN beads was determined through GC-MS analysis. The MS spectrum showed two peaks during degradation of C6-HSL (Figure 4.18). In the MS profile, one fragment abundant ion was observed at m/z (mass-to-charge ratio) 228 according to the retention time of 10.4 min whereas the second fragment abundant ion was seen at m/z 143 at 9.7 min of retention time. The first peak corresponded to n-hexanoic acid and the second peak was identified to be of the product n-homoserine lactone. The proposed mechanism behind the C6-HSL degradation is depicted in Figure 4.19. The fragment ion obtained at 143 m/z was most probably due to McLafferty rearrangement which can

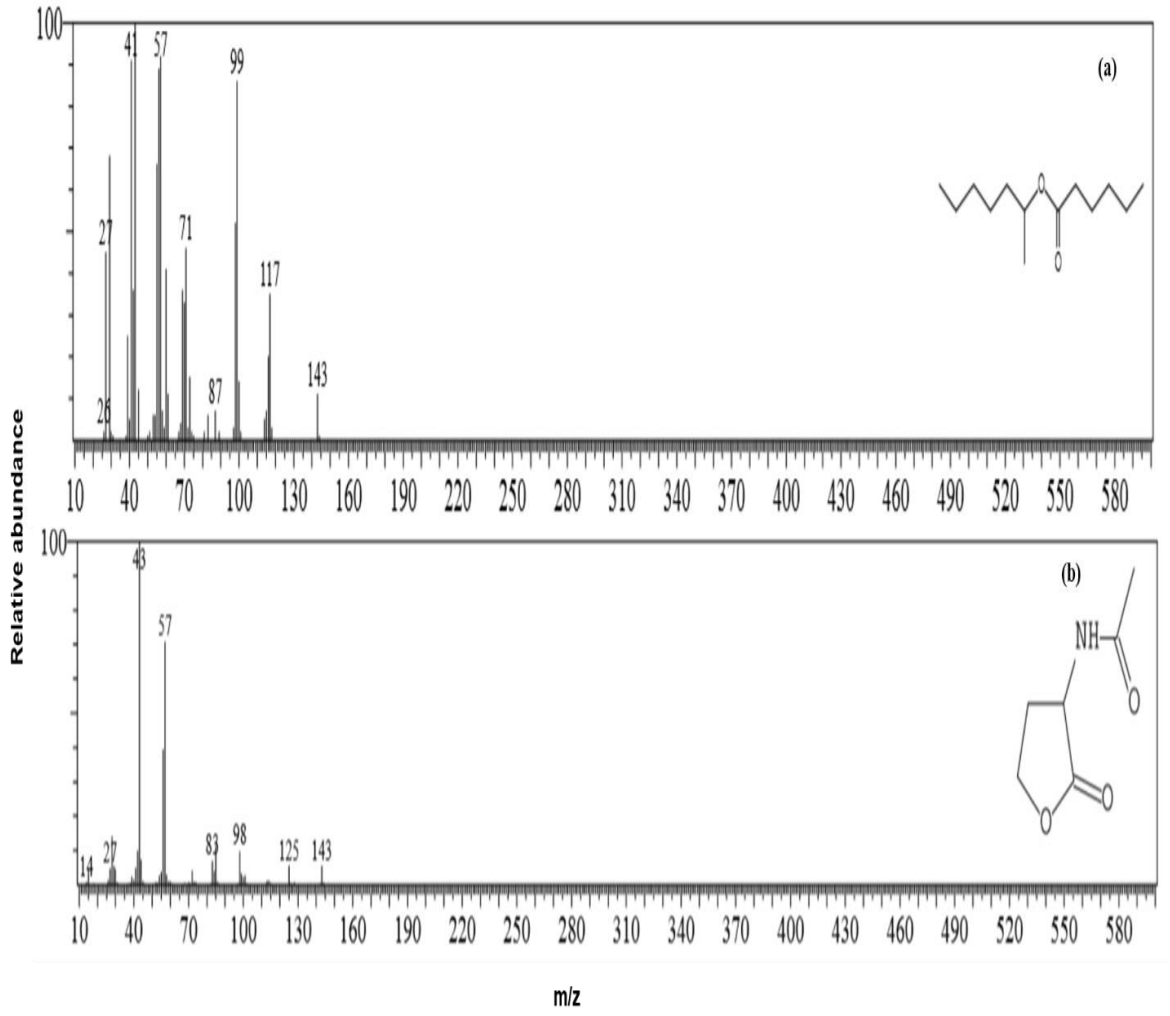

Figure 4.18 Mass spectra of (a) n-hexanoic acid and (b) L-homoserine lactone product generated during degradation of C6-HSL by *Pseudomonas* JYQ4

occur on carbonyl group with hydrogen atom on the γ-position. This breaks the molecule into two parts i.e. enolic fragment and an olefin. This might have also undergone complete degradation. The fragment ion at m/z 143 has also been reported by Cataldi *et al.* (2004).

Moreover, in the present study the presence of fatty acid degradation products both in free form and immobilized form further confirmed the acylase enzyme mode of action in degrading the C6-HSL into fatty acid products (Chen *et al.*, 2013). Hence, the principal mechanism in C6-HSL degradation is bacterial QQ activity via acylase enzyme rather than the adsorption or self-degradation.

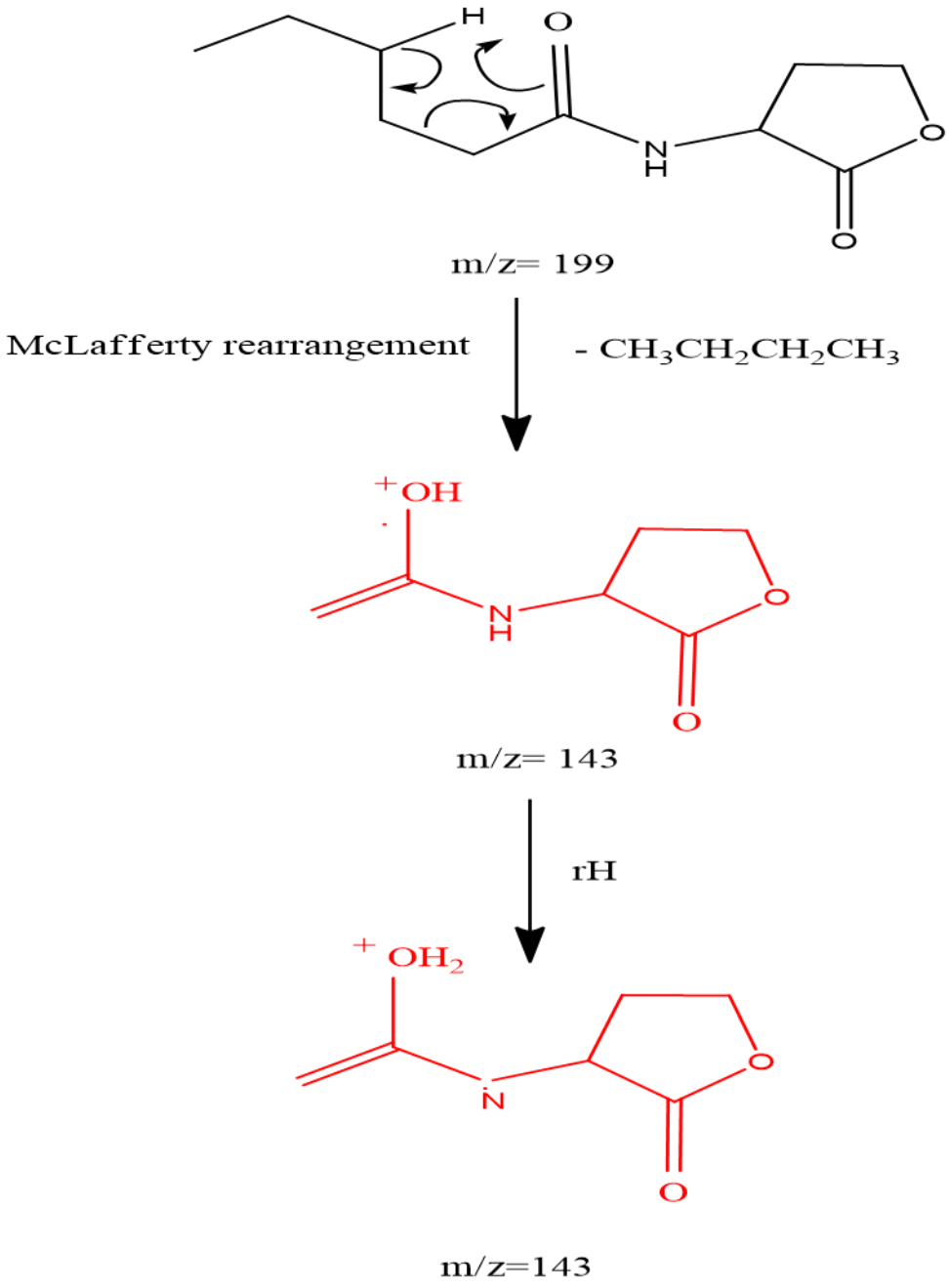

Figure 4.19 Proposed mechanism of degradation of C6-HSL by IMN beads

4.5 Effect of QQ bacteria IMN beads on biofilm growth inhibition

Biofilm formation is considered as the root cause of fouling on the membrane surfaces. In the present study, an attempt has been made to control the biofilm formation using IMN beads of different QQ bacteria. In this section, the ability of QQ bacteria IMN beads to control the biofilm developed by *Pseudomonas aeruginosa* 3541 and sludge microbes was assessed and results are summarized below.

4.5.1 Effect of QQ bacteria IMN beads on *Pseudomonas aeruginosa* 3541 biofilm

The efficiency of three QQ bacteria *Acinetobacter baumannii* JYQ2, *Pseudomonas nitroreducens* JYQ3 and *Pseudomonas* JYQ4 and the consortium of these three bacteria on the inhibition of biofilm growth was investigated using microscopic techniques such as SEM and CLSM. The 3D images acquired by CLSM was examined using COMSTAT software for studying the biofilm structures and to elucidate the effect of IMN beads on the biofilm structure. Further, the impact of QQ IMN beads on the filtration performance was evaluated by measuring the permeate flux of the membranes. The results are explained in the following sections

4.5.1.1 Effect of QQ bacteria IMN beads on inhibition of membrane biofilm

The inhibitory effects of IMN beads of QQ bacteria *Acinetobacter baumannii* JYQ2, *Pseudomonas nitroreducens* JYQ3, *Pseudomonas* JYQ4 and the consortium of three bacteria on QS mediated biofilm formed by *Pseudomonas aeruginosa* 3541 was confirmed by visualizing the cellulose acetate membrane surface using SEM. Figure 4.20 depicts the SEM micrographs of biofilm developed by *Pseudomonas aeruginosa* 3541 on the cellulose acetate membrane during 30 days growth period. It can be seen from the Figure 4.20 (a) and (b) that the cells of *P. aeruginosa* 3541 covered the entire surface of the control membrane unlike, the surfaces of the membranes incubated with QQ IMN beads which were barely covered with *P. aeruginosa* 3541 cells (Figure 4.20 c to f). This indicated that the IMN beads had a stronger tendency to control membrane biofouling. As discussed in the QQ experiments, the QQ bacteria in IMN beads secreted QQ enzyme acylase that can disrupt the communication among the *Pseudomonas aeruginosa* 3541 cells. As a result of this, the adhesive forces between the *Pseudomonas aeruginosa* 3541 cells and membrane got weakened and resulted in less attachment of microorganisms on the membranes incubated with IMN beads. Further, the IMN beads of different QQ bacteria exhibited difference in their biofilm controlling ability which is apparent from the SEM micrographs. It can be seen that the surface of membrane incubated with *Pseudomonas* JYQ4 IMN beads was covered with few bacterial cells of biofilm forming bacteria relative to the other QQ bacteria IMN beads incubated membrane surfaces indicating the better biofilm reduction potential of *Pseudomonas* JYQ4.

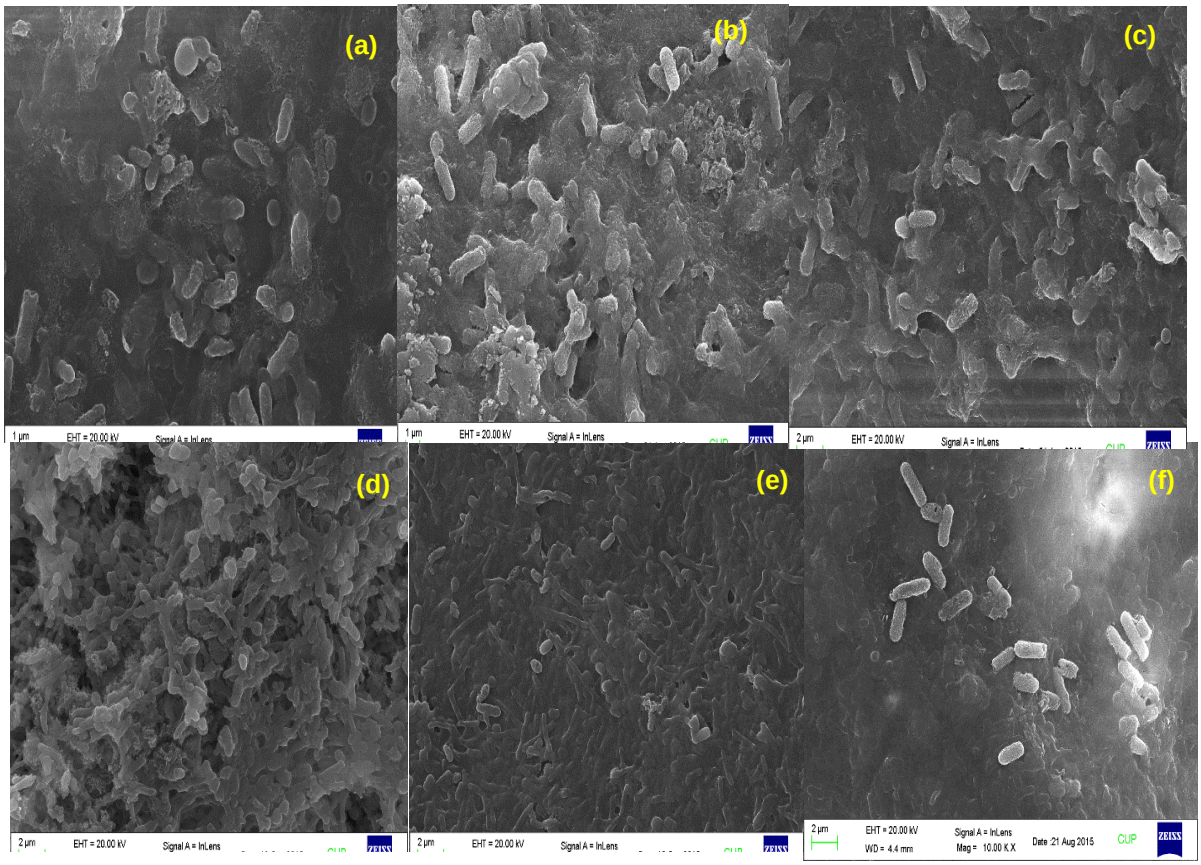

Figure 4.20 SEM images of *Pseudomonas aeruginosa* 3541 cells distribution on the membranes incubated with (a) Control 1, (b) Control 2, (c) *Acinetobacter baumannii* JYQ2 IMN beads, (d) *Pseudomonas nitroreducens* JYQ3 IMN beads, (e) *Pseudomonas* JYQ4 IMN beads, (f) Consortium IMN beads. The SEM images of the blank and QQ bacteria IMN beads were taken at the magnification of 10,000 X except for *Pseudomonas* JYQ4 (15,000X magnification).

The knowledge about the architecture of biofilm is essential in order to understand the biofilm inhibition efficiency of QQ bacteria IMN beads. A classic biofilm cycle begins with the attachment of single cells on to the membrane surface by weak van der waals interactions. The adhered bacteria then undergo cell division which results in formation of microcolonies. This step is followed by the matured biofilm formation which is induced by QS mechanism. The cycle finally completes with the biofilm expansion and detachment of cells from the matured biofilm (Kolter *et al.*, 1993; Jamal *et al.*, 2015). The effect of QQ bacteria IMN beads induced alterations on the structure of *Pseudomonas aeruginosa* 3541 biofilm was studied through CLSM (Figure 4.21). The CLSM images showed the presence of a large number of biofilm

forming bacteria *Pseudomonas aeruginosa* 3541 cells on the membrane surface of the control membranes after 24 h of operation. It can be inferred that the *Pseudomonas aeruginosa* 3541 rapidly colonized the surfaces of both the control membranes. Within 10 days, the cells of *Pseudomonas aeruginosa* 3541 formed robust biofilm. The formation of biofilm was associated with the formation of large number of colonies (Figure 4.21). On the 20th day, the colonies on the surface extended thereby forming elongated cell clusters which eventually developed into matured biofilm within 30 days of incubation.

On the other hand, the membranes incubated with IMN beads of *Acinetobacter baumannii* JYQ2, *Pseudomonas nitroreducens* JYQ3, *Pseudomonas* JYQ4 and consortium of these three isolated strains showed thinner and reduced biomass deposition. The surfaces of membranes incubated with *Pseudomonas nitroreducens* JYQ3 was covered with the thick biofilm in 20 days which eventually showed signs of maturation in 30 days. But, there was no obvious biofilm formation on the membrane incubated with *Pseudomonas* JYQ4 IMN beads in 20 days of incubation. Though in 30 days incubation, dispersed and disintegrated microcolonies appeared on the membrane surface, unlike the *Pseudomonas aeruginosa* 3541 microcolonies which were still in the process of developing matured biofilm.

The surfaces of the membrane incubated with IMN beads of *Acinetobacter baumannii* JYQ2 and consortium however showed signs of biofilm maturation in 20 days. Previous study reported an inhibition of *Pseudomonas aeruginosa* PAO1 biofilm by acylase enzyme entrapped in the magnetically separable mesoporous silica on the membrane surface (Lee *et al.*; 2014). The results of our study indicated that the *Pseudomonas* JYQ4 IMN beads were effective in preventing the transition of biofilm structure from the surface colonization stage to matured biofilm up to 30 days. Further, the CLSM images were analyzed using COMSTAT software which validated the results of CLSM images. Two parameters, biovolume and surface to biovolume ratio were selected to assess the inhibition of biofilm growth by QQ bacteria IMN beads. The biovolume represent the biomass in the biofilm and surface to biovolume ratio illustrates the fraction of biofilm exposed to the nutrient flow. High biovolume and low surface to biovolume ratio represents the growth of biofilm (Beyenal *et al.*, 2004).

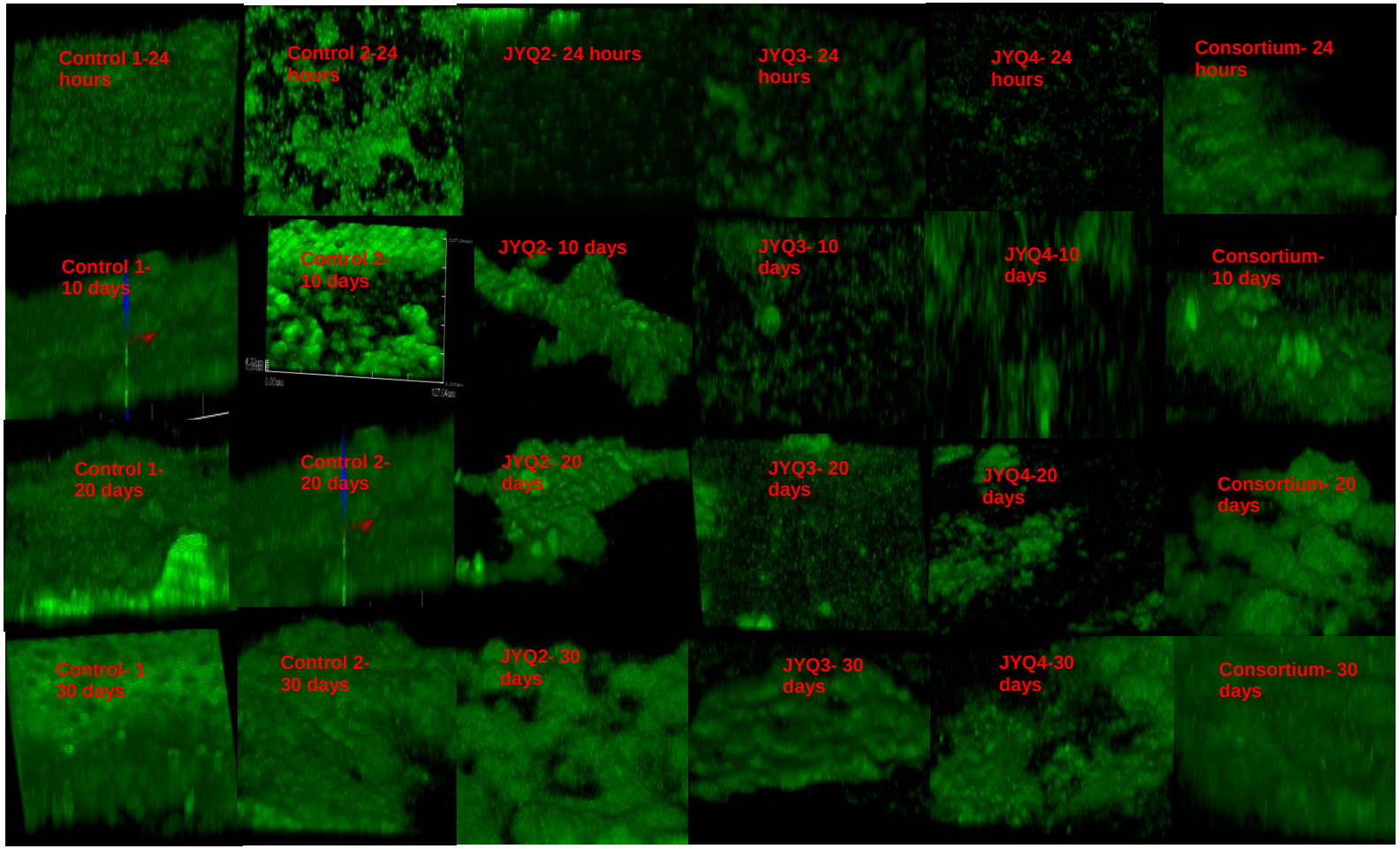

Figure 4.21 Confocal laser scanning micrographs of *Pseudomonas aeruginosa* 3541 biofilm formed with and without IMN beads at different time intervals.

The results obtained from the biofilm structural analysis by COMSTAT is summarized in Table 4.7. From the results, it is evident that at the end of the 1st day of incubation, all the membranes immobilized with QQ bacteria IMN beads showed low biovolume and high surface to biovolume ratio indicating the inhibition of biofilm initiation.

The biovolume of *Pseudomonas aeruginosa* 3541 cultivated on the control 1 and control 2 membranes was measured to be 0.037± 0.001 $\mu m^3/\mu m^2$ and 0.034± 0.05 $\mu m^3/\mu m^2$, respectively on 1st day which later increased with the incubation time. The increase in the biovolume was associated with an increase in the number of *Pseudomonas aeruginosa* 3541 attached to the membrane surface. The surface to biovolume ratio for the control 1 and control 2 membranes was about 1.24± 0.005 and 1.2± 0.01 $\mu m^2/\mu m^3$, respectively on 1st day. During the 30 days of operation, the biomass volume of *Pseudomonas aeruginosa* 3541 biofilm on the control 1 and 2 membrane surfaces increased to 0.06± 0.003 $\mu m^3/\mu m^2$ and 0.07± 0.02 $\mu m^3/\mu m^2$, respectively and the corresponding surface to biovolume ratio decreased to 0.21± 0.005 $\mu m^2/\mu m^3$ and 0.26± 0.02 $\mu m^2/\mu m^3$, respectively. The low surface to biovolume ratio and large biovolume values indicated the formation of large number of microcolonies on the membrane surface.

As mentioned previously, the biofilm developed by *Pseudomonas aeruginosa* 3541 on the membranes incubated with the QQ bacteria IMN beads was thinner relative to the control. More specifically, around 86% and 97% reduction in biomass volume was observed on the membranes incubated with *Pseudomonas nitroreducens* JYQ3 and *Pseudomonas* JYQ4 IMN beads, respectively on 1st day when compared to control membrane. Likewise, the *Acinetobacter baumannii* JYQ3 (0.02± 0.0003 $\mu m^3/\mu m^2$) and consortium (0.017± 0.0005 $\mu m^3/\mu m^2$) incubated membranes also showed reduced biovolume. During 30 days operation, the *Pseudomonas aeruginosa* 3541 biomass volume on *Pseudomonas nitroreducens* JYQ3 and *Pseudomonas* JYQ4 IMN beads incubated membranes reached to 0.02± 0.0003 $\mu m^3/\mu m^2$ and 0.015± 0.001 $\mu m^3/\mu m^2$, respectively.

The biovolume of *Pseudomonas aeruginosa* 3541 on the *Acinetobacter baumannii* JYQ3 and consortium incubated membranes also increased and reached 0.041± 0.0005 $\mu m^3/\mu m^2$ and 0.04± 0.003 $\mu m^3/\mu m^2$, respectively. However, all the

Table 4.7 Biovolume and surface to biovolume ratio of *Pseudomonas aeruginosa* 3541 biofilm

S.No.	Parameters studied	Time (days)	Control 1	Control 2	*Acinetobacter baumannii* JYQ2	*Pseudomonas nitroreducens* JYQ3	*Pseudomonas* JYQ4	Consortium
1.	Biovolume ($\mu m^3/\mu m^2$)	1	0.03± 0.001	0.034± 0.05	0.02± 0.0003	0.005± 0.0003	0.001± 0.0003	0.017± 0.0005
		10	0.05±0.0003	0.05± 0.01	0.026± 0.0003	0.01± 0.0005	0.008± 0.0003	0.02 ± 0.001
		20	0.06± 0.003	0.06± 0.05	0.031± 0.0003	0.013± 0.0005	0.012± 0.0003	0.033±0.003
		30	0.06± 0.003	0.07± 0.02	0.041± 0.0005	0.02± 0.0003	0.015± 0.001	0.04± 0.003
2.	Surface to biovolume ratio ($\mu m^2/\mu m^3$)	1	1.24± 0.005	1.2± 0.01	2.15± 0.003	2.86± 0.03	3.43± 0.03	1.98± 0.003
		10	1.02± 0.003	1.0± 0.03	1.83± 0.03	2.23± 0.03	3.16± 0.03	1.52±0.03
		20	0.83± 0.03	0.80± 0.01	1.6± 0.05	1.91± 0.008	2.42± 0.01	1.07± 0.008
		30	0.21± 0.005	0.26± 0.02	0.61± 0.02	0.88± 0.005	0.93± 0.003	0.70± 0.003

QQ bacteria IMN beads incubated membrane still exhibited less biomass volume compared to that of control membranes.

Other parameter i.e. surface to biovolume ratio was quite high during 1st day of incubation. High surface to biovolume ratio indicates the decreased tendency of sludge bacteria to form microcolonies. On 1st day, the surface to biovolume ratio was maximum for the membrane incubated with *Pseudomonas* JYQ4 IMN beads and lower for the consortium IMN beads incubated membrane among other QQ bacteria IMN beads incubated membranes. On 30th day, the *Acinetobacter baumannii* IMN beads incubated membrane showed surface to biovolume ratio of 0.61± 0.02 $\mu m^2/\mu m^3$ which was found to be least among other QQ bacteria IMN beads incubated membranes. Among the QQ IMN beads tested, it can be seen that the *Pseudomonas* JYQ4 IMN beads was more efficient and *Acinetobacter baumannii* IMN beads was least effective in controlling the biofilm formation which is clearly evident from their biovolume and surface to biovolume ratio values (Table 4.7). Ma *et al.* (2018) observed reduction in *Pseudomonas aeruginosa* PAO1 biofilm biomass by 43.9% in the presence of QQ bacteria *Staphylococcus hominis*. From the biovolume and surface to biovolume ratio of the QQ bacteria IMN beads incubated membranes, it can be concluded that the decrease in *Pseudomonas aeruginosa* 3541 biofilm on the membrane surface might be due to the interference of *Pseudomonas aeruginosa* 3541 communication channels by QQ bacteria.

4.5.1.2 Membrane flux studies

Figure 4.22 depicts the antifouling potential of QQ bacteria IMN beads in terms of membrane flux. The pure water flux for QQ bacteria IMN beads incubated cellulose acetate membranes was evaluated at the operating pressure of 10 kPa. From the Figure, it is clearly evident that the QQ-IMN beads delayed the flux drop more effectively when compared to control. It was observed that both the control membranes experienced severe biofouling as indicated by the sharp flux decline during the experimental period. Briefly, in 24th h of incubation, the membranes of control 1 and control 2 showed flux decline of 26% and 25.4%, respectively. The membrane fluxes of *Acinetobacter baumannii* JYQ2, *Pseudomonas nitroreducens* JYQ3, *Pseudomonas* JYQ4 and consortium IMN beads incubated membranes showed decline of 20.3%, 19.8%, 17.6% and 22.4%, respectively. Increase in

incubation time to 10 and 20 days resulted in drastic flux decline of both the control membranes. Control 1 membranes experienced 56.9% and 69.9% decrease in flux in 10 and 20 days incubation, respectively whereas the flux of control 2 membrane dropped further within 10 and 20 days of incubation period showing values of 56.8% and 69.2%, respectively. However, among the individual bacterial beads, the membranes incubated with *Pseudomonas* JYQ4 IMN beads exhibited 29.3% decline in permeate flux (3.99± 0.09 $m^3/m^2/h$) after 10 days of incubation. In contrast, the *Acinetobacter baumannii* JYQ2 IMN beads showed 43.5% *flux* decline within the same incubation period of 10 days which might again be due to the QS ability of *Acinetobacter baumannii* JYQ2 strain.

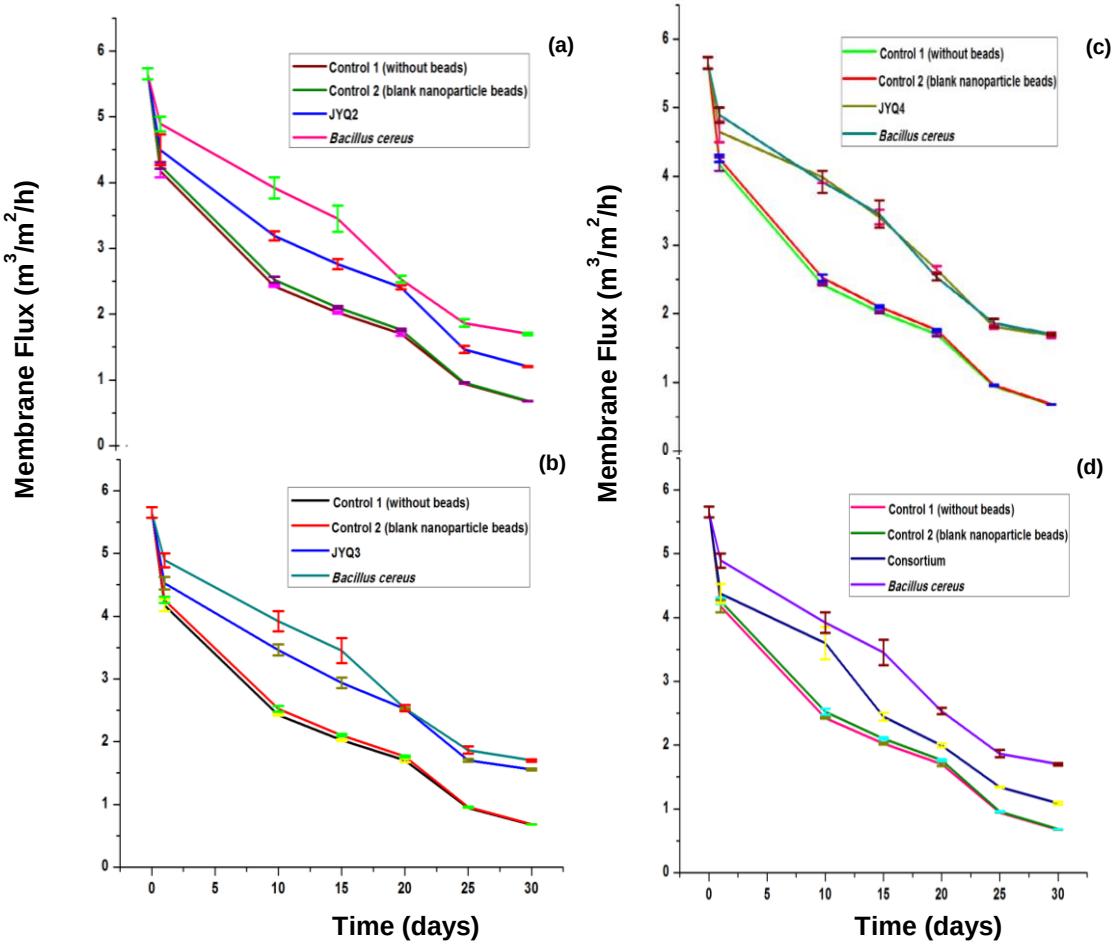

Figure 4.22 Comparison of the filtration performance of membranes after incubation with *Pseudomonas aeruginosa* 3541, IMN beads of QQ bacteria (a) *Acinetobacter baumannii* JYQ2, (b) *Pseudomonas nitroreducens* JYQ3, (c) *Pseudomonas* JYQ4 and (d) Consortium.

The 30 days incubation time resulted in the permeate flux decline to 87.9% for both the control membranes (C_1 and C_2). This might be due to the fact that biofilm formed on the surface of the membrane could have augmented the filtration resistance thereby resulting in the reduction of the water transport through the membrane pores which might have sequentially resulted in flux decline. However, membranes incubated with *Pseudomonas* JYQ4 IMN beads reached the 70% flux decrease in 30 days showing slower flux decline rate compared to control membranes. Also, the flux profile of *Pseudomonas* JYQ4 IMN beads incubated membrane is similar to that of *Bacillus cereus* IMN beads incubated membranes which is reported to be the best QQ bacteria for degrading AHL molecules in the literature (Chan *et al.*, 2007). The *Acinetobacter baumannii* JYQ2, *Pseudomonas nitroreducens* JYQ3 and consortium IMN beads however exhibited 78.7%, 72.3% and 80.7% flux drop, respectively within 30 days of incubation period.

The delay in flux decline could be attributed to the fact that the immobilized *Pseudomonas* JYQ4 might have inhibited the communication mechanism among the biofilm forming bacteria *Pseudomonas aeruginosa* 3541 thereby hindering the biofilm formation onto the membrane surface. It is worthy to note that QQ IMN beads incubated membranes exhibited better flux than that reported by Lee *et al.* (2014) that observed no rapid flux drop up to 14 days.

4.5.2 Inhibition of biofilm formed by sludge bacteria

QS is a principal mechanism used by the microorganisms in the activated sludge to form biofilm over the cellulose acetate membrane surface. So, the IMN beads of QQ bacteria *Acinetobacter baumannii* JYQ2, *Pseuodomonas nitroreducens* JYQ3 and *Pseudomonas* JYQ4 were tested for biofilm control over the cellulose acetate membrane surface. The consortium of these three bacteria was also tested and compared with the individual bacteria for their biofilm controlling ability. The sludge was acclimatized to the synthetic dairy industry wastewater. This section will discuss about the characterization of the synthetic dairy industry wastewater, biofilm inhibition studies on the glass slide and membrane surface, and flux studies of QQ bacteria IMN beads incubated membranes.

4.5.2.1 Characterization of synthetic wastewater

The physico-chemical characterization of synthetic dairy industry wastewater is summarized in Table 4.8. The synthetic dairy industry wastewater showed a pH of around 7.2. The COD of the wastewater was around 4800± 40 mg/L depicting the characteristics of high strength wastewater.

Table 4.8 Characterization of synthetic dairy industry wastewater

S.No.	Parameters	Value
1.	pH	7.2± 0.1
2.	COD (mg/L)	4800± 40
3.	TS (mg/L)	4445± 30
4.	TDS (mg/L)	1610± 15
5.	TSS (mg/L)	489± 10
6.	TVS (mg/L)	1865± 10
7.	TKN (mg/L)	145.6± 2.8
8.	Total ammonical nitrogen (mg/L)	65.4± 0.05
9.	Nitrite (mg/L)	0.1± 0.01
10.	Nitrate (mg/L)	0.3± 0.01
11.	Phosphate (mg/L)	19.1± 0.01

The wastewater contained TS of 4445± 30 mg/L, out of which 41.9% was VS and 36.2% was TDS. TSS constituted about 11% of TS. The ammonical nitrogen, TKN, nitrite and nitrate were around 65.4± 0.05 mg/L, 145.6± 2.8 mg/L, 0.1± 0.01 and 0.3± 0.01, respectively. The dairy wastewater characteristics obtained in the present study are in line with the previous study. Arumugam and Sabarethinam (2008) and Dawood *et al.* (2011) reported pH of 7-8 and 7, respectively in dairy wastewater. The COD in the dairy wastewater was reported to be in the range of 921-9004 mg/L by Farizoglu and Uzuner (2011). They also reported SS concentration of 398.3 mg/L in their study. The previous findings by Tikariha and Sahu (2014) reported phosphate and nitrite nitrogen in the range between 18- 26.4 mg/L and 0.037- 0.7 mg/L, respectively in dairy wastewater.

4.5.2.2 Cultivation and Acclimatization of waste activated sludge (WAS)

The waste activated sludge was acclimatized to the synthetic dairy industry wastewater for 21 days under fill and draw mode using SBR. The development of MLSS and MLVSS along with the MLVSS/MLSS ratio was monitored during the process and is depicted in Figure 4.23. During the start-up of the experiment, the MLSS and MLVSS concentrations of the activated sludge was 1000 and 780 mg/L, respectively.

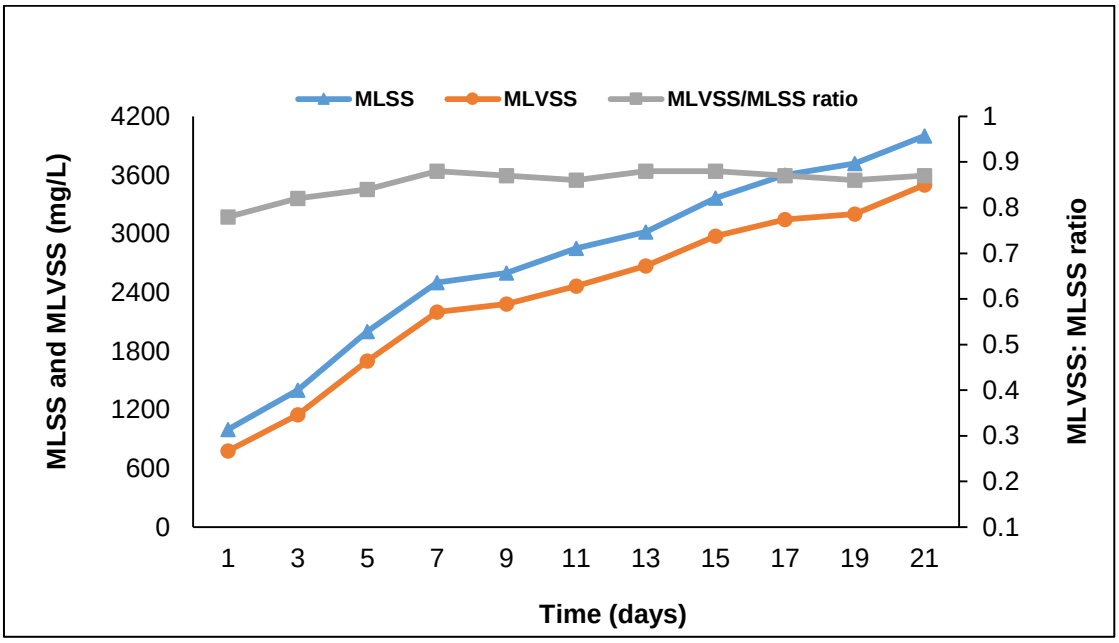

Figure 4.23 Development of MLSS and MLVSS during the acclimatization of activated sludge

With time, a steady and gradual increase in MLSS was observed. After 21 days of acclimatization, the MLSS and MLVSS concentrations stabilized at around 4000 and 3500 mg/L, respectively. The sludge quality during the acclimatization was determined by MLVSS to MLSS ratio. The ratio of MLVSS to MLSS indicates the amount of active micro-organisms in the organic matter of the sludge. In the present study, the MLVSS to MLSS ratio was in the range 0.75-0.9.

4.5.2.3 Effect of QQ bacteria IMN beads on biofilm developed by sludge bacteria

The reduction of biofilm formation on the glass slides and membrane surface by the QQ bacteria IMN beads was evaluated. Figure 4.24 shows the light microscopy

analysis of sludge bacteria biofilm formed on the surface of the glass slides. The IMN beads of three QQ bacteria viz., *Acinetobacter baumannii* JYQ2, *Pseudomonas nitroreducens* JYQ3, *Pseudomonas* JYQ4 and consortium of three QQ bacteria efficiently prevented the biofilm formation on the glass slide surface when compared to control as evidenced from the Figure 4.24. Light microscopy analysis of the glass slides revealed the attachment of large number of microbial cells on the surface of both the control slides, forming dense biofilm on the slide surface. Unlike control, the glass slides incubated with QQ bacteria IMN beads showed presence of few microbial flocs on the surface. Among the different IMN beads incubated glass slides, the *Pseudomonas* JYQ4 incubated slides exhibited better suppression of biofilm. On the contrary, the QQ bacteria *Acinetobacter baumannii* JYQ2 IMN beads showed biofilm formation which is evident from the dense coverage of sludge bacteria on the glass slide hence showing less efficiency in controlling membrane biofilm formation (Figure 4.24 c). This clearly indicated the decreased efficiency of *Acinetobacter baumannii* JYQ2 IMN beads in controlling membrane biofilm formation which is due to its QS ability.

The results of the present study were comparable with the previous study of Kim *et al.* (2014) that reported delay in *Aeromonas* sp. T3-4 biofilm initiation and maturation after incubation with QQ bacteria *Pseudomonas*. The reduction in biofilm by the QQ bacteria suggest that disruption of signalling molecules in the biofilm predominated in the presence of QQ bacteria. The biofilm forming ability of *Acinetobacter baumannii* was supported by Tomaras *et al.* (2003). The production of signalling molecule such as C6-HSL might be attributed to the decreased biofilm controlling ability of *Acinetobacter baumannii* JYQ2.

4.5.2.4 CLSM studies of membrane surface

The potential of IMN beads in biofilm inhibition was also evaluated on the cellulose acetate membrane surface. The CLSM images of the cellulose acetate membrane exploring the different stages of biofilm development is presented in Figure 4.25. The biofilm forming bacteria present in the sludge communicate with each other through secretion of AHL which resulted in colonization of more bacteria that ultimately lead to the formation of biofilm. As evident from Figure 4.25, the biofilm forming bacteria cover the entire surface of both control membranes within 24 h of

incubation. With increase in incubation time to 10 days, the sludge bacterial cells formed patchy structures or microcolonies thereby, indicating signs of biofilm development. The membrane porosity of control membrane disappeared completely within 30 days indicating serious biofouling.

The biofilm structure developed by the sludge bacteria on the membrane incubated with *Acinetobacter baumannii* JYQ2, *Pseudomonas nitroreducens* JYQ3 and *Pseudomonas* JYQ4 IMN beads showed a clear difference from the control IMN beads incubated membranes. After 10 days of incubation, *Pseudomonas nitroreducens* JYQ3 and *Pseudomonas* JYQ4 IMN beads incubated membranes exhibited few sludge bacterial cells on the membrane surface. Signs of biofilm maturation was observed on membranes incubated with *Pseudomonas nitroreducens* JYQ3 IMN beads with increase incubation time to 20 days. On the other hand, *Pseudomonas* JYQ4 IMN beads delayed the maturation of biofilm up to 30 days. This indicated that the *Pseudomonas* JYQ4 IMN beads incubated membrane controlled the sludge bacterial biofilm in the planktonic phase through disruption of AHL molecules resulting in decreased production of extracellular polysaccharides (EPS). The membranes incubated with *Acinetobacter baumannii* JYQ2 and consortium IMN beads showed complete maturation of biofilm in 20 days of incubation. The QS ability of bacteria might be the reason behind the early biofilm maturation on the surface of *Acinetobacter baumannii* JYQ2 and consortium IMN beads incubated membranes (Weerasekara *et al.*, 2016). The results of the present study were comparable with the previous findings in which the QQ bacteria were reported to prevent the formation of thick biofilm (Oh *et al.*, 2012; Kim *et al.*, 2013; Khan *et al.*, 2016). Cheong *et al.* (2014) in his study observed retardation in biocake development on the surface of membrane incubated with QQ bacteria *Pseudomonas* sp. 1A1 during 30 days of experiment. In another study, Khan *et al.* (2016) witnessed fewer biomass deposition on the membrane surface after 72h incubation with the QQ bacteria *Bacillus methylotrophicus* strain WY.

The quantitative analysis of the effect of QQ bacteria IMN beads on structure of sludge bacterial biofilm was done by COMSTAT software. Two variables such as biovolume and surface to biovolume ratio of the biofilm structure were chosen for the quantitative characterization of three- dimensional biofilm images, the results of which is summarized in Table 4.9.

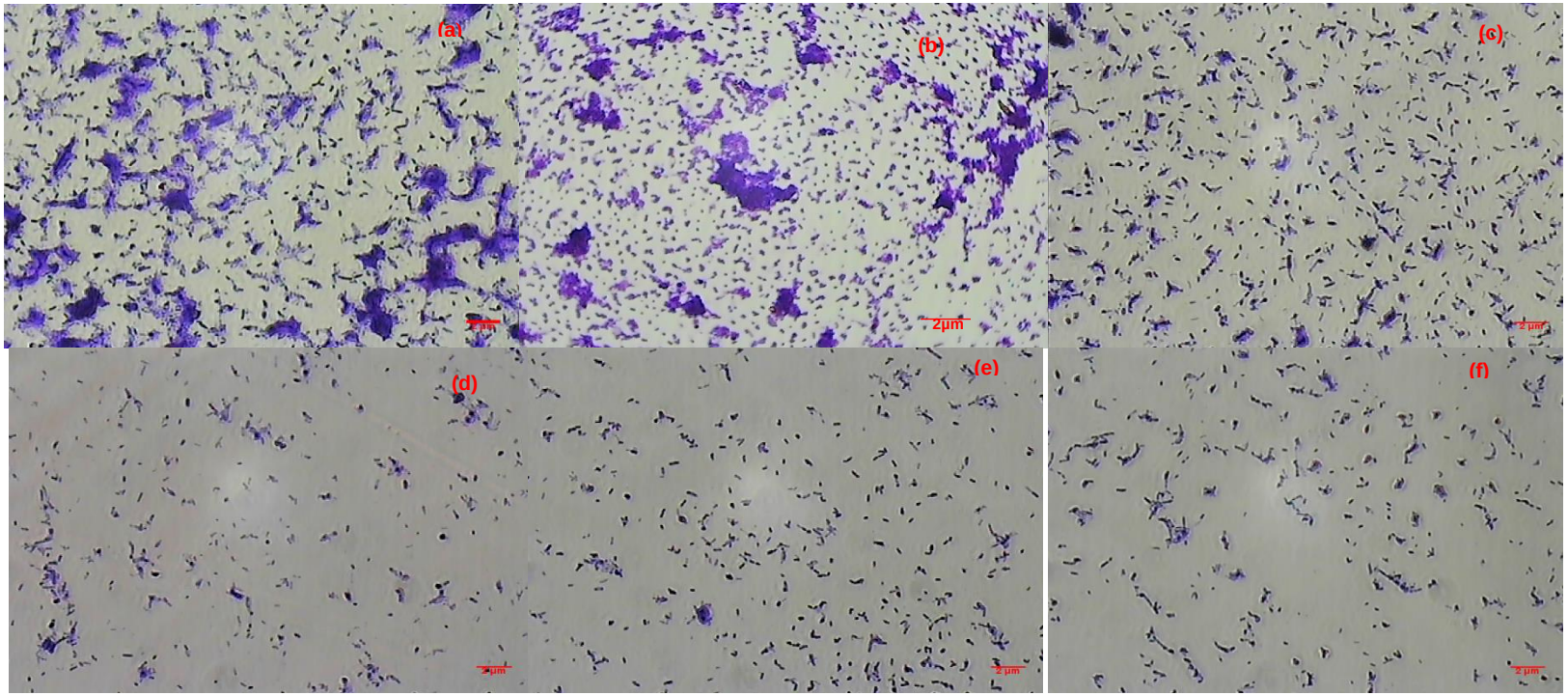

Figure 4.24 Inhibition of biofilm development on glass slides by QQ bacteria IMN beads within 15 days incubation. Light microscopy analysis (Scale bar= 2 μm) of glass slide incubated with (a) Control 1 without IMN beads. (b) Control 2 with blank nanoparticle beads. (c) *Acinetobacter baumannii* JYQ2 IMN beads. (d) *Pseudomonas nitroreducens* JYQ3 IMN beads. (e) *Pseudomonas* JYQ4 IMN beads. (f) Consortium IMN beads.

Furthermore, the outcomes of COMSTAT software analysis authenticated the CLSM micrographs results representing the notable structural differences in the sludge bacterial biofilm architecture after incubation with QQ bacteria IMN beads.

After the first day of incubation, around 0.039± 0.03 $\mu m^3/\mu m^2$ and 0.033± 0.05 $\mu m^3/\mu m^2$ of biovolume was detected on the surfaces of control 1 and control 2 membranes, respectively. By the 10^{th} and 20^{th} day incubation, an increase in biomass volume was observed. Towards the end of the study i.e. on 30^{th} day, the biovolume on control 1 and 2 membranes reached 0.065± 0.06 $\mu m^3/\mu m^2$ and 0.06± 0.02 $\mu m^3/\mu m^2$, respectively. The surface to biovolume ratio of sludge bacteria biofilm on the surfaces of control 1 (1.42± 0.49 $\mu m^2/\mu m^3$) and control 2 (1.48± 0.51 $\mu m^2/\mu m^3$) membrane was high after the 1^{st} day of incubation. The high surface to biovolume ratio corresponds to the attachment of single cells or cell clusters on the membrane surface. Both the control membranes exhibited decreased surface to biovolume ratio at 10^{th} and 20th day. On 30^{th} day, the surface to biovolume ratio for control 1 and 2 membrane further decreased and reached 0.18± 0.14 $\mu m^2/\mu m^3$ and 0.16± 0.38 $\mu m^2/\mu m^3$, respectively. This indicated that the single cells might undergo division and form large microcolonies which is also reflected in large biomass volume at 30^{th} day.

On the other hand, the QQ IMN beads showed good control over the biofilm architecture. It is evident from the Table 4.9 that at the end of the 1^{st} day of incubation, all the membranes immobilized with QQ bacteria IMN beads showed low biovolume and high surface to biovolume ratio compared to control membranes indicating the inhibition of biofilm initiation. After 1^{st} day, *Pseudomonas nitroreducens* JYQ3 and *Pseudomonas* JYQ4 IMN beads incubated membranes showed lesser biomass volume in the range 78.7 to 82% and 84.5 to 87%, respectively when compared with both the control membranes. The surface to biovolume ratio was about 1.77± 0.50 $\mu m^2/\mu m^3$ and 3.87± 0.06 $\mu m^2/\mu m^3$ for the *Pseudomonas nitroreducens* JYQ3 and *Pseudomonas* JYQ4 IMN beads incubated membranes. Likewise, around 61 to 67% and 30.3 to 41% reduced biomass volume of sludge bacteria was developed on the membranes incubated with *Acinetobacter baumannii* and consortium IMN beads, respectively. The surface to biovolume ratio was around 1.64± 0.71 $\mu m^2/\mu m^3$ and 1.57± 0.51 $\mu m^2/\mu m^3$ for the *Acinetobacter baumannii* and consortium IMN beads incubated membranes, respectively.

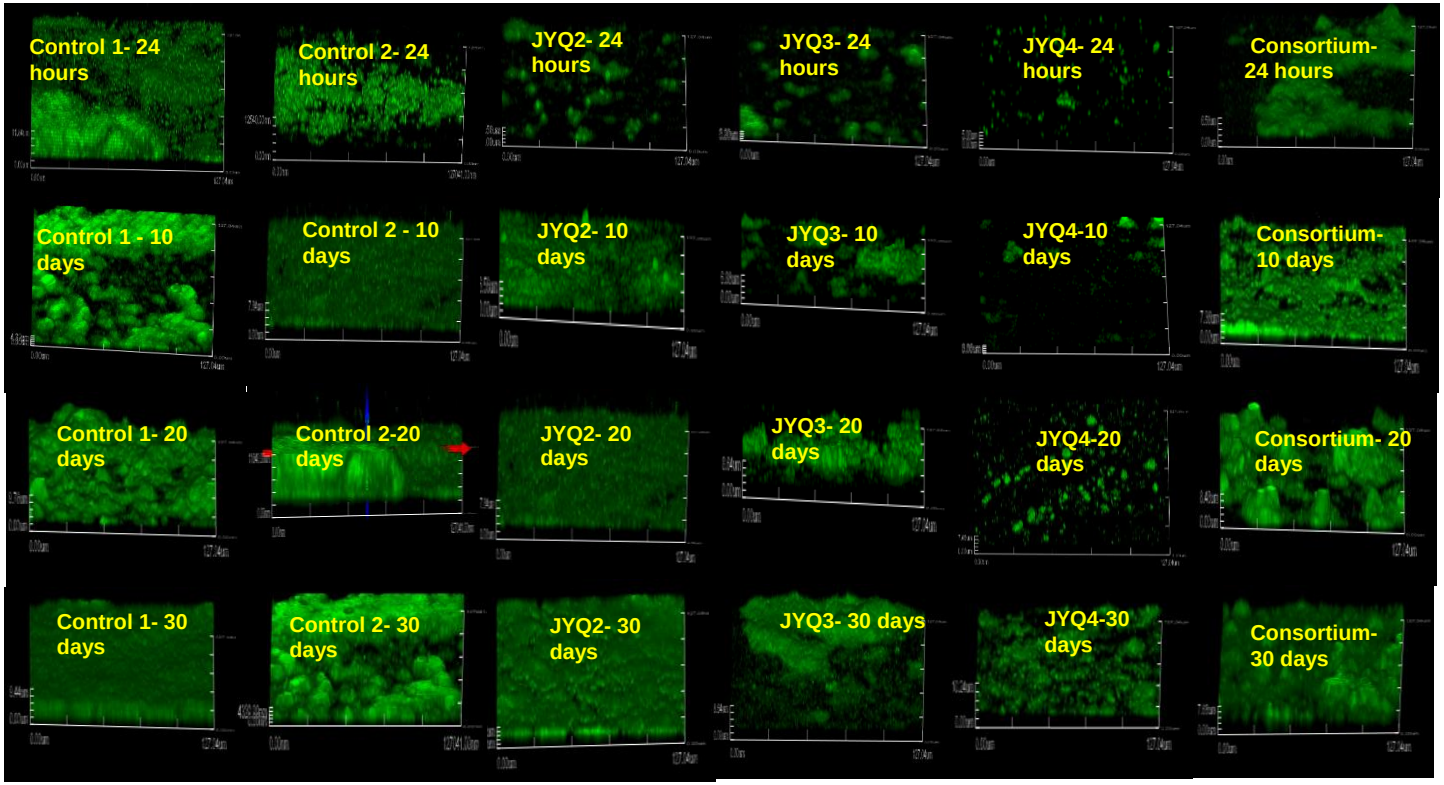

Figure 4.25 Confocal images of biofilm developed by sludge bacteria on cellulose acetate membranes at different time intervals. Scale bar= 127.04 µm

Table 4.9 Biovolume and surface to biovolume ratio of sludge bacterial biofilm

S.No.	Parameters studied	Time (days)	Control 1	Control 2	*Acinetobacter baumannii* JYQ2	*Pseudomonas nitroreducens* JYQ3	*Pseudomonas* JYQ4	Consortium
1.	Biovolume ($\mu m^3/\mu m^2$)	1	0.039±0.035	0.033±0.05	0.013± 0.009	0.007± 0.004	0.005± 0.001	0.023± 0.02
		10	0.040±0.03	0.037±0.02	0.018± 0.014	0.009± 0.006	0.005± 0.001	0.029± 0.02
		20	0.046±0.042	0.043±0.01	0.022± 0.01	0.012± 0.009	0.010± 0.006	0.030± 0.02
		30	0.065± 0.061	0.06± 0.02	0.035± 0.031	0.032± 0.027	0.019± 0.015	0.036± 0.032
2.	Surface to biovolume ratio ($\mu m^2/\mu m^3$)	1	1.42± 0.49	1.48± 0.51	1.64± 0.71	1.77± 0.50	3.87± 0.06	1.57± 0.51
		10	1.29± 0.38	1.27± 0.52	1.49± 0.61	1.73± 0.57	2.05± 0.68	1.49± 0.59
		20	0.79± 0.60	0.78± 0.45	1.59± 0.55	1.66± 0.67	1.67± 0.52	1.47± 0.55
		30	0.18± 0.14	0.16± 0.38	0.65± 0.53	0.75± 0.56	0.85± 0.65	0.57± 0.45

The difference in biomass volume and surface to biovolume ratio among the different QQ bacteria IMN beads is because of the difference in QQ potential of different bacteria. Among them, *Pseudomonas* JYQ4 IMN beads was more effective in preventing attachment of sludge bacterial cells which is evident from its low biovolume of 0.005± 0.001 $\mu m^3/\mu m^2$ and high surface to biovolume ratio of 3.87± 0.06 $\mu m^2/\mu m^3$ compared to other QQ bacteria IMN beads incubated membranes. The biomass volume increased and correspondingly surface to biovolume ratio decreased with the increase in incubation time. On 30th day, the 0.019± 0.015 $\mu m^3/\mu m^2$ biovolume and 0.85± 0.65 $\mu m^2/\mu m^3$ surface to biovolume ratio was observed for the *Pseudomonas* JYQ4 incubated membrane. Likewise, the *Acinetobacter baumannii* JYQ2, *Pseudomonas nitroreducens* JYQ3 and consortium IMN beads incubated membranes exhibited biovolume of 0.035± 0.031 $\mu m^3/\mu m^2$, 0.032± 0.027 $\mu m^3/\mu m^2$ and 0.036± 0.032 $\mu m^3/\mu m^2$, respectively on the 30th day. The surface to biovolume ratio also increased for all the QQ bacteria IMN beads incubated membranes. Nahm *et al.* (2017b) in his study reported 90% decrease in microbial biovolume after incubation with *Undibacterium* sp. DM1 entrapping beads.

4.5.2.5 Flux studies

The potential of QQ bacteria IMN beads in mitigating membrane biofouling in membrane filtration system was evaluated through flux studies. The membranes from the beakers were removed and membrane fluxes were measured at pressure of 10kPa. The decline in the permeate flux is linked to the factors such as biofilm thickness and hydraulic resistance of biofilm (Dreszer *et al.*, 2013). During the initial periods of growth, the biofilm has thin porous structure that offers low hydraulic resistance, hence causing slower flux decline. With time, the biofilm thicken that leads to the membrane pores blockage. This results in high hydraulic resistance and increase in flux decline rates. The changes in flux rate of membranes incubated with sludge and different QQ bacteria IMN beads are depicted in Figure 4.26. The flux of membranes incubated with *Pseudomonas nitroreducens* JYQ3 and *Pseudomonas* JYQ4 IMN beads showed a decline of 9.4% and 3.3%, respectively within 24h of incubation. After 10 days of incubation, the flux of *Pseudomonas nitroreducens* JYQ3 and *Pseudomonas* JYQ4

IMN beads incubated membranes were around 3.45± 0.01 $m^3m^{-2}\,h^{-1}$ and 4.32± 0.05 $m^3m^{-2}\,h^{-1}$, respectively showing flux decline of 39% and 23%, respectively. Further, increase in incubation time to 20 days and 30 days resulted in 52% and 70% drop in flux, respectively in membranes incubated with *Pseudomonas nitroreducens* JYQ3 IMN

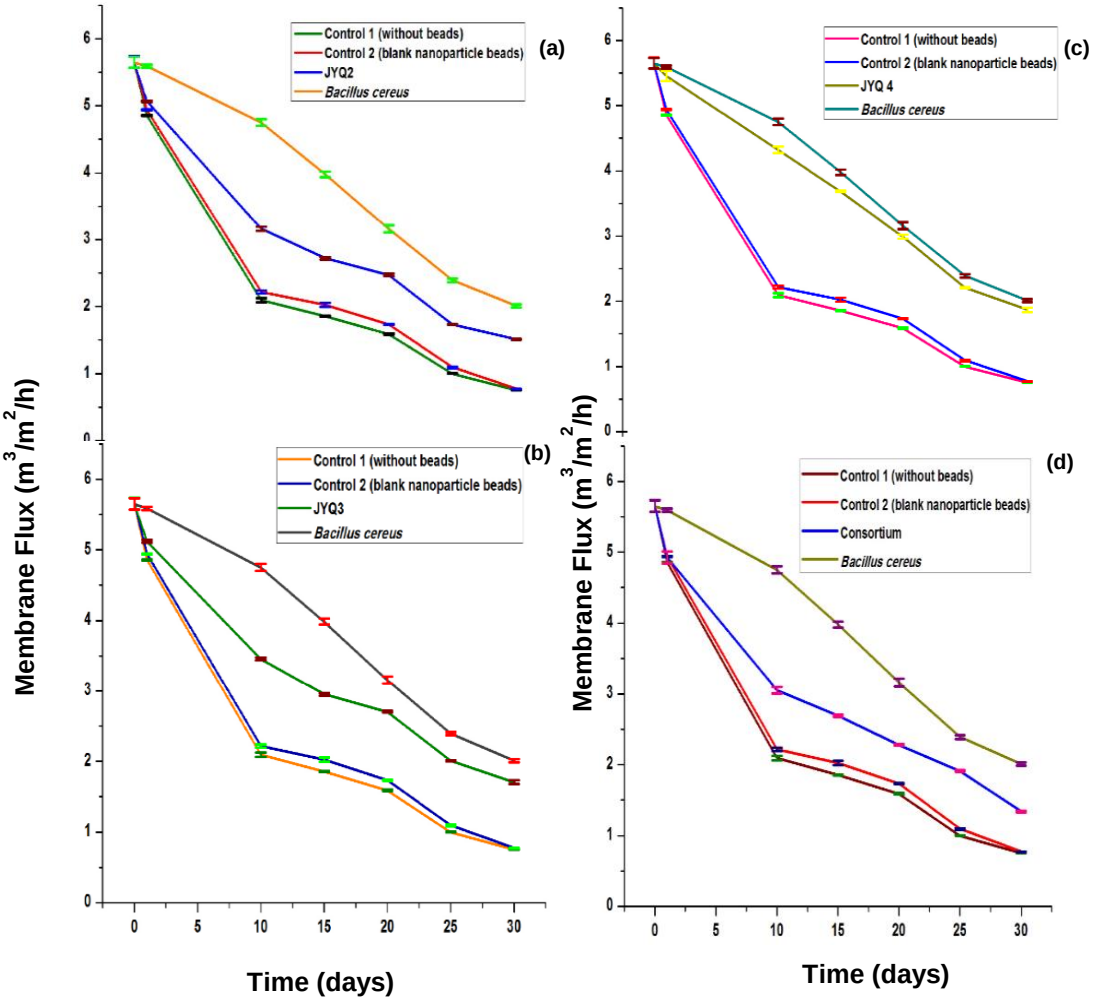

Figure 4.26 Comparison of the filtration performance of membranes after incubation with mixed species micro-organisms of sludge, and IMN beads of QQ bacteria (a) *Acinetobacter baumannii* JYQ2, (b) *Pseudomonas nitroreducens* JYQ3, (c) *Pseudomonas* JYQ4 and (d) Consortium.

beads. The *Pseduomonas* JYQ4 IMN beads incubated membrane however, showed 47% and 67% flux decline after 20 and 30 days, respectively. The formation of

microcolonies and biofilm development might be the reason behind the increased flux decline in 30 days incubated membranes. The matured biofilm blocked the membrane pores as a result of which the increase in hydraulic resistance was observed. This leads to the reduction in water flow per unit area of membrane which consecutively decreased the membrane flux.

The *Pseudomonas* JYQ4 IMN beads maintained the membrane flux up to 30 days, hence showing slow drop in flux rate when compared with previous study by Khan *et al.* (2016) in which rapid flux decline was noticed after 17 days of incubation with QQ bacteria *Bacillus methylotrophicus* sp. WY. The degradation of AHL molecule with extracellular enzyme acylase secreted by *Pseudomonas* might be the reason for the reduction in EPS production by the sludge bacteria and delayed biofilm formation (Cheong *et al.*, 2013; Kim *et al.*, 2013). Flux studies with *Acinetobacter baumannii* JYQ2 and consortium IMN beads showed flux decline of 10% and 13%, respectively within 24h incubation period. In membranes incubated for 10 and 20 days, the flux values were recorded as 3.16± 0.03 m^3m^{-2} h^{-1} and 2.47± 0.01 $m^3m^{-2}h^{-1}$, respectively for *Acinetobacter baumannii* JYQ2 IMN beads incubated membrane and 3.05± 0.04 $m^3m^{-2}h^{-1}$ and 2.28± 0.01 $m^3m^{-2}h^{-1}$, respectively for consortium IMN beads incubated membrane. With increase in incubation to 30 days, the *Acinetobacter baumannii* JYQ2 and consortium IMN beads incubated membranes showed 73% and 76% flux decline, respectively. As mentioned earlier, the QS ability of *Acinetobacter baumannii* JYQ2 strain might be the reason for higher flux drop.

The flux of both the control membranes showed significant ($p<0.05$) drop with increase in incubation time. Flux of control 1 (without beads) membrane showed significant decrease of 14%, 63%, 72% and 87%, respectively at 24h, 10 days, 20 days and 30 days, respectively. Flux of control 2 (blank nanoparticle beads) membranes showed decrease of 12.5%, 61%, 69% and 86%, within 24h, 10 days, 20 days and 30 days incubation, respectively. The results of the present study clearly indicated the QQ ability of QQ bacteria IMN beads. In addition, the QQ potential of QQ bacteria IMN beads was also compared with biofouling controlling bacteria *Bacillus cereus* 1306. It was found that *Pseudomonas* JYQ4 IMN beads showed the antifouling potential nearly similar to

that of *Bacillus cereus* 1306 IMN beads. Hence, it was clearly seen that *Pseudomonas* JYQ4 IMN beads was more efficient in controlling flux decline (Figure 4.26).

4.6 MBR studies

The application of MBR in treating dairy industry wastewater was investigated. The MBR was operated at three MLSS viz. 4000, 7000 and 10,000 mg/L at constant flux of 12.5 L/ (m^2h). The performance of MBR was evaluated on the basis of organic removal, nutrient and solid removal; sludge characteristics and membrane biofouling characteristics. The results of the experiment are summarized in the following section.

4.6.1 Effluent quality

4.6.1.1 pH

The pH of influent and effluent samples measured during MBR operation at MLSS of 4000, 7000 and 10,000 mg/L is depicted in Figure 4.27. The pH of the influent and effluent ranged between 7- 7.3 and 8.3- 8.8, respectively.

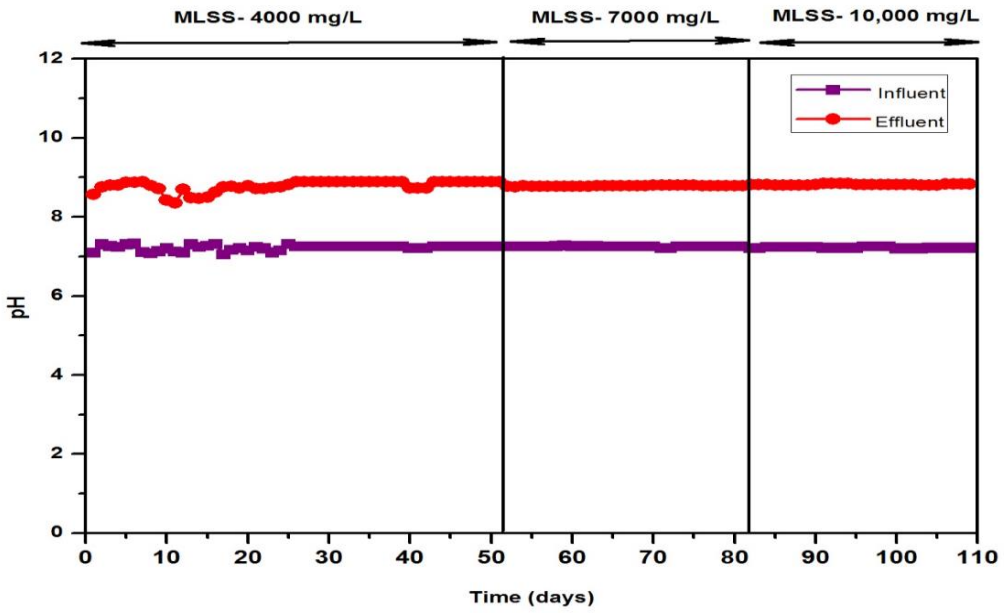

Figure 4.27 Variation of pH in the control MBR operated at operated at different MLSS

The pH within the MBR ranged between 6.6- 7.4. The results are in agreement with the previous study by Arumugam and Sabarethinam (2008) who reported dairy influent pH in the range 7- 8. The pH of the treated dairy effluent was comparable to the pH of the previous study by Chandrasekhar *et al.* (2017) who reported pH of 8.1. Benefield and Randall (1981) reported near neutral pH in the MBR which is considered to be optimum for biological performance of MBR.

4.6.1.2 COD removal

Figure 4.28 depicts the COD removal profile of the control MBR operated at three different MLSS. The results indicated that the control MBR achieved excellent COD removal efficiency when operated under MLSS 4000, 7000 and 10,000 mg/L. The influent COD varied from 4600 to 4800 mg/L with average COD concentration of 4717± 13.9 mg/L. At MLSS of 4000 mg/L, the COD removal efficiency varied in the range of 160- 200 mg/L. The maximum COD removal efficiency of 96.6± 0.5% was observed at MLSS of 4000 mg/L. After that, the MLSS was increased from 4000 mg/L to 7000 mg/L. The maximum COD removal of 97.5± 0.01% was achieved at 7000 mg/L showing effluent COD of 120 mg/L. Further increase in MLSS to 10,000 mg/L resulted in effluent COD of 40 to 80 mg/L with maximum removal efficiency of 99.2± 0.2%. The results of the present study is comparable to the results of Farizoglu *et al.* (2004) that reported COD removal efficiency in the range between 90- 94% during the treatment of whey. However, Hirooka *et al.* (2009) in his study reported COD removal efficiency of 88- 89% while treating dairy effluent. Few studies also reported the effect of MLSS on COD removal efficiency. Damayanti *et al.* (2011) in his study observed an increase in COD removal efficiency from 98.7% to 99.2% with increase in MLSS from 5000 to 20,000 mg/L, respectively in an MBR treating palm oil mill effluent. Similar increase in COD removal efficiency was also achieved in the present study at high MLSS of 10,000 mg/L. The increase in COD removal efficiency with increasing MLSS might be due to increasing biomass within the MBR. High biomass concentration may degrade more organic matter resulting in high COD removal (Alaboud, 2009). In addition, the effectual retention of suspended solids by the membrane might be the other reason behind efficient COD removal efficiency (Dong and Jiang, 2009).

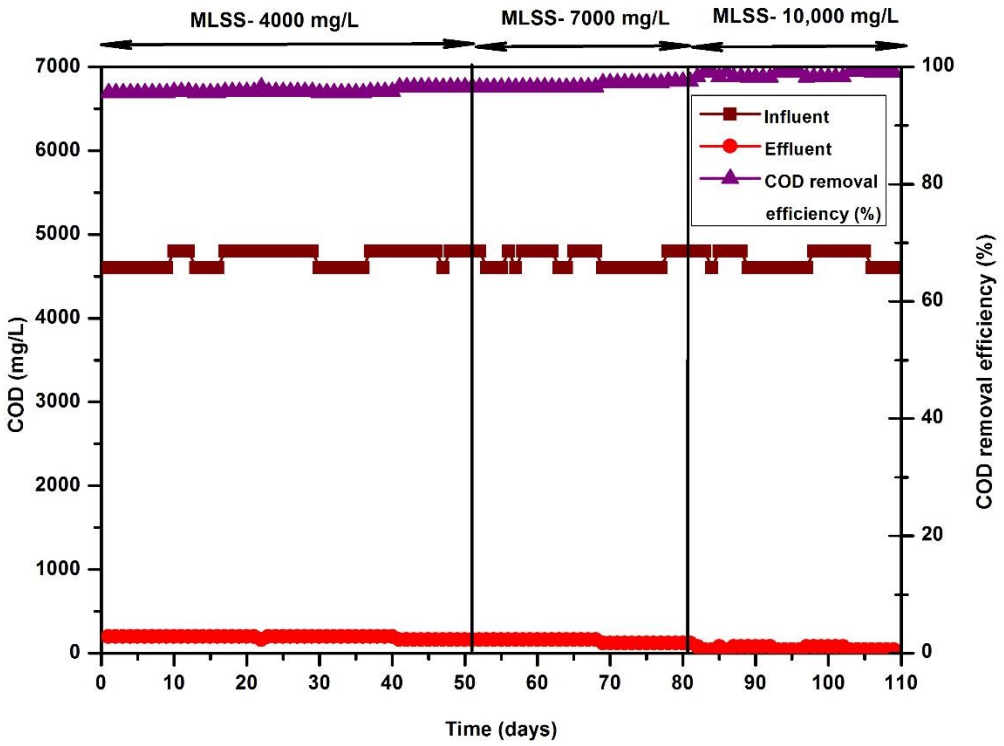

Figure 4.28 Variation of COD in the control MBR operated at different MLSS

4.6.1.3 Solids removal

Figure 4.29 and 4.30 depicts the influent and effluent TS and TDS of control MBR operated under different MLSS. The TS and TDS of the influent were in the range of 4405- 4435 mg/L and 1600- 1650 mg/L, respectively. TS and TDS also followed similar trend of COD and was observed to increase with increase in MLSS. The maximum TS and TDS removal efficiencies of 21.9±0.02% and 5.8±0.8%, respectively were achieved at MLSS of 4000mg/L. The effluent TS and TDS ranged between 3400 to 3500 mg/L and 1506 to 1525 mg/L, respectively. When the MLSS in the MBR was increased from 4000 to 7000 mg/L, a decrease in the effluent TS and TDS was observed and was around 3050 to 3081 mg/L and 1480 to 1490 mg/L, respectively. The effluent TS and TDS further decreased and was found to be in the range of 2780- 2790 mg/L and 1318 to 1345 mg/L, respectively at the MLSS of 10,000 mg/L. Maximum TS and TDS removal efficiency of 37% and 18.6%, respectively was achieved at MLSS 10,000 mg/L. The TDS removal efficiency in the present study was lower than the previous study of

Chandrasekhar *et al.* (2017) that reported TDS removal efficiency of 62.3% while treating dairy wastewater with ultrafiltration membrane.

Figure 4.31 and 4.32 depicts the variation of effluent TSS and VS in MBR operated at different MLSS. The TSS and VS of influent was in the range of 472 to 489 mg/L and 1850 to 1892 mg/L, respectively. At MLSS 4000 mg/L, the maximum TSS and VS removal was observed to be around 57.6± 0.5% and 71.2± 0.01%, respectively. The effluent TSS and VS ranged between 200 to 214 mg/L and 530 to 551 mg/L, respectively. The TSS and VS removal efficiencies further increased when the MLSS in MBR was increased to 7000 mg/L and was around 77± 0.04% and 81.2± 0.4%, respectively. The effluent TSS and VS were in the range of 110 to 113 mg/L and 350 to 356 mg/L, respectively. A maximum TSS and VS removal of 88.4± 0.8% and 90.8± 0.09%, respectively was observed when the MLSS inside the MBR increased to 10,000 mg/L. The effluent TSS and VS ranged from 55 to 62 mg/L and 170 to 180 mg/L, respectively. Previous studies reported more than 90% of TSS removal in MBR operated with various substrates which is higher than the results of present study (Katayon *et al.*, 2004; Hosseinzadeh *et al.*, 2014). Katayon *et al.* (2004) achieved 99%

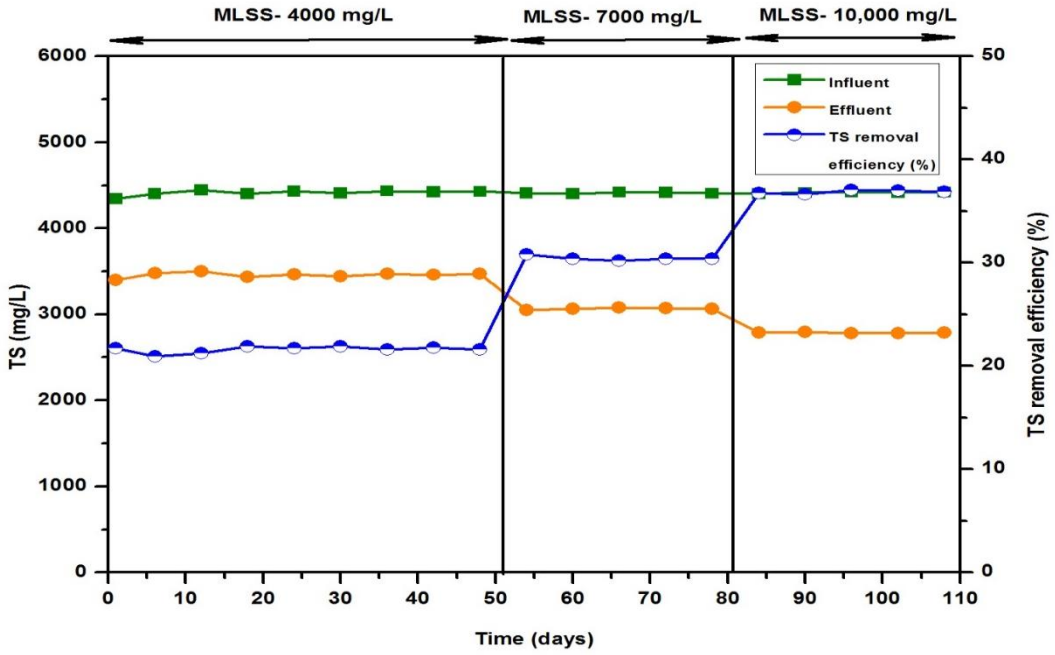

Figure 4.29 Variation of TS in the control MBR operated at operated at different MLSS

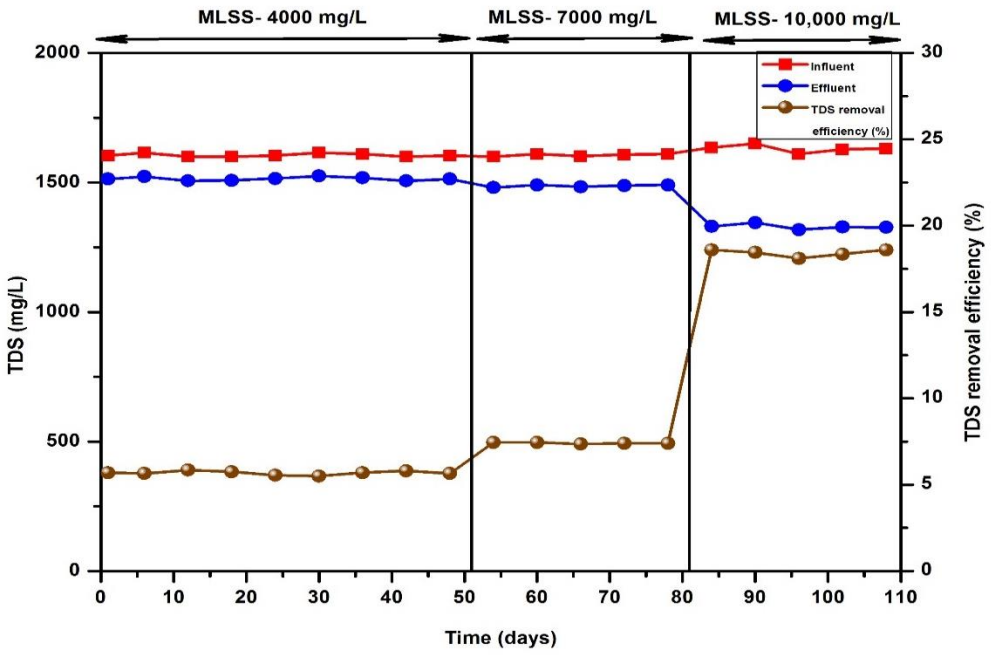

Figure 4.30 Variation of TDS in the control MBR operated at different MLSS

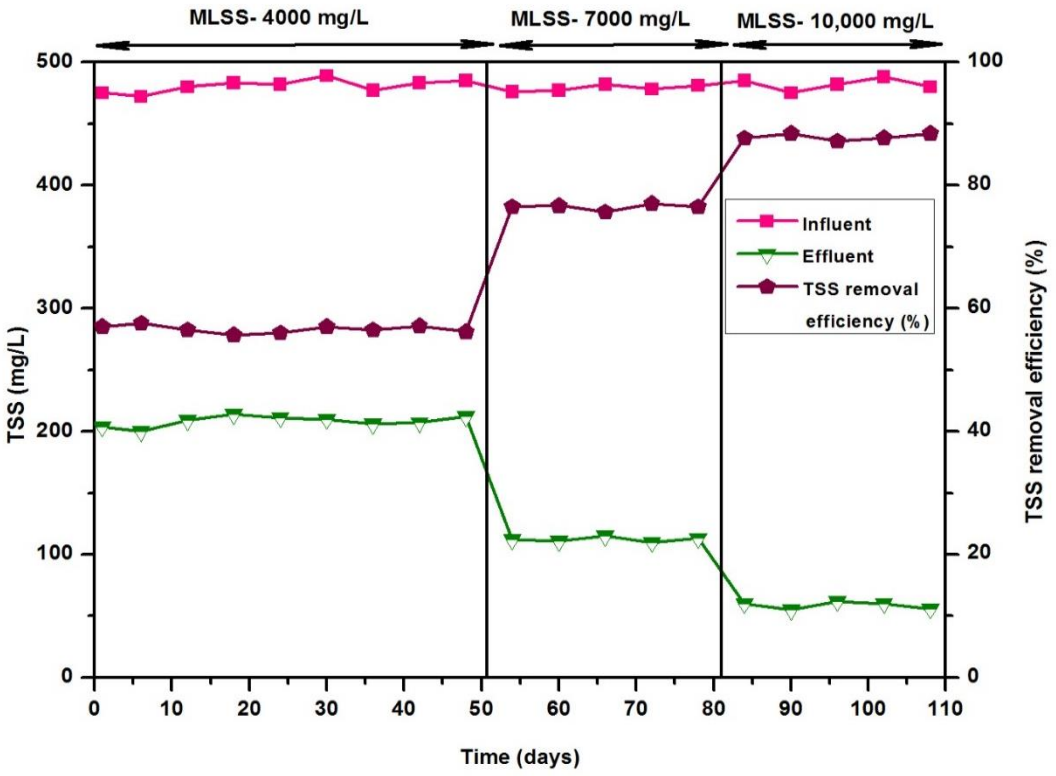

Figure 4.31 Variation of TSS in the control MBR operated at different MLSS

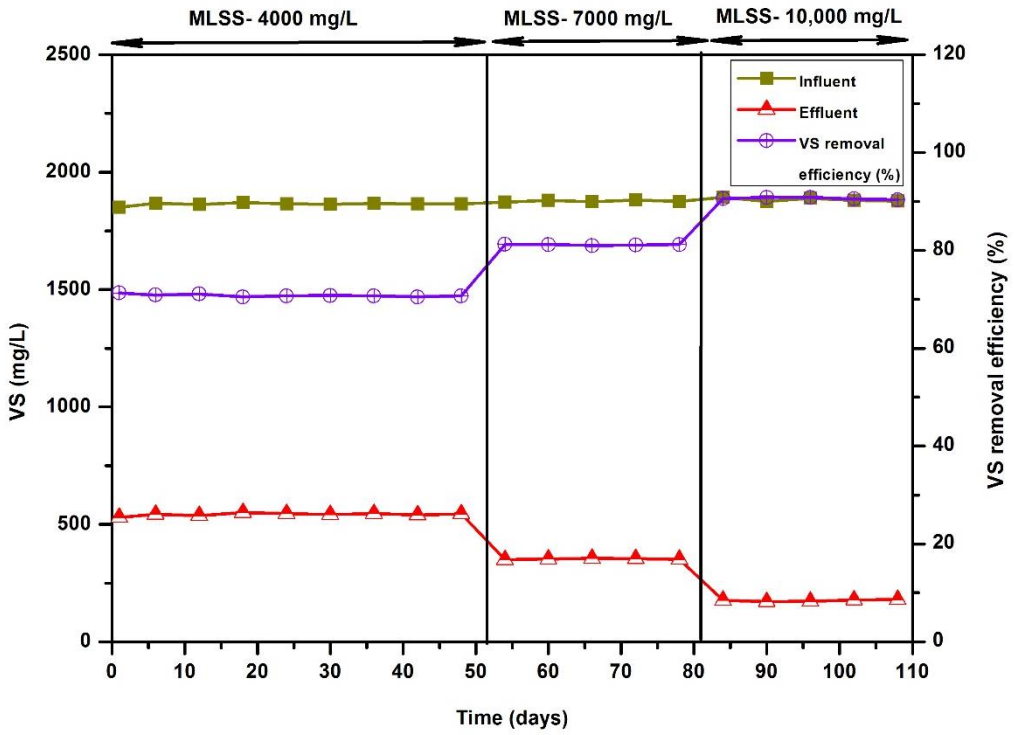

Figure 4.32 Variation of VS in the control MBR operated at different MLSS

TSS removal in MBR operated with food industry wastewater. Andrade *et al.* (2013) evaluated the use of microfiltration membrane for the treatment of dairy wastewater and obtained VS removal efficiency of 94%. The solids removal by the MBR might be related to the retention of inorganic particulate material by the membrane that is mainly dependent on the pore size and integrity of membranes (Hosseinzadeh *et al.*, 2014). The use of microfiltration membrane of pore size 0.4 µm and high solids in simulated dairy wastewater might be the reason behind the decreased solid removal efficiency in the MBR (Andrade *et al.*, 2013).

4.6.1.4 Nitrogen removal

Figure 4.33 depicts the TKN removal efficiency of control MBR. The TKN in the influent ranged between 141.4- 142.6 mg/L. About 88± 0.08% to 90.3± 0.1% of TKN removal efficiency was recorded when the MBR was operated at the MLSS of 4000 mg/L which further increased to 93.2± 0.5% at MLSS 7000 mg/L. The effluent TKN ranged between 9.8 to 11.2 mg/L at MLSS 7000 mg/L. The TKN removal efficiency as high as 95± 0.5% was recorded at MLSS of 10,000 mg/L. The corresponding effluent TKN varied between

7 to 9.8 mg/L. The TKN removal efficiency in the present study was quite high when compared to the previous studies. Mutlu *et al.* (2016) reported TKN removal efficiency of 45% in MBR operated with synthetic wastewater at MLSS of 12,000 to 13,000 mg/L.

The varying ammonical nitrogen (NH_3-N), nitrite nitrogen (NO_2-N) and nitrate nitrogen (NO_3-N) within the MBR at different MLSS is depicted in Figures 4.34 to 4.36. The overall NH_3-N removal efficiency was high and was above 93± 0.08%. The influent showed NH_3-N in the range of 65.2 to 65.8 mg/L. At MLSS of 4000 mg/L, the NH_3-N removal efficiency was maximum and showed an efficiency of 93.9± 0.5%. The effluent NH_3-N ranged from 3.9 to 4.1 mg/L. Similar to COD, a slight increase in NH_3-N removal efficiency was observed when the MLSS was increased to 7000 mg/L. No change in NH_3-N removal efficiency was observed when MLSS was increased to 10,000 mg/L. The maximum removal efficiency of 94.6± 0.5% was observed at MLSS of 7000 and 10,000 mg/L.

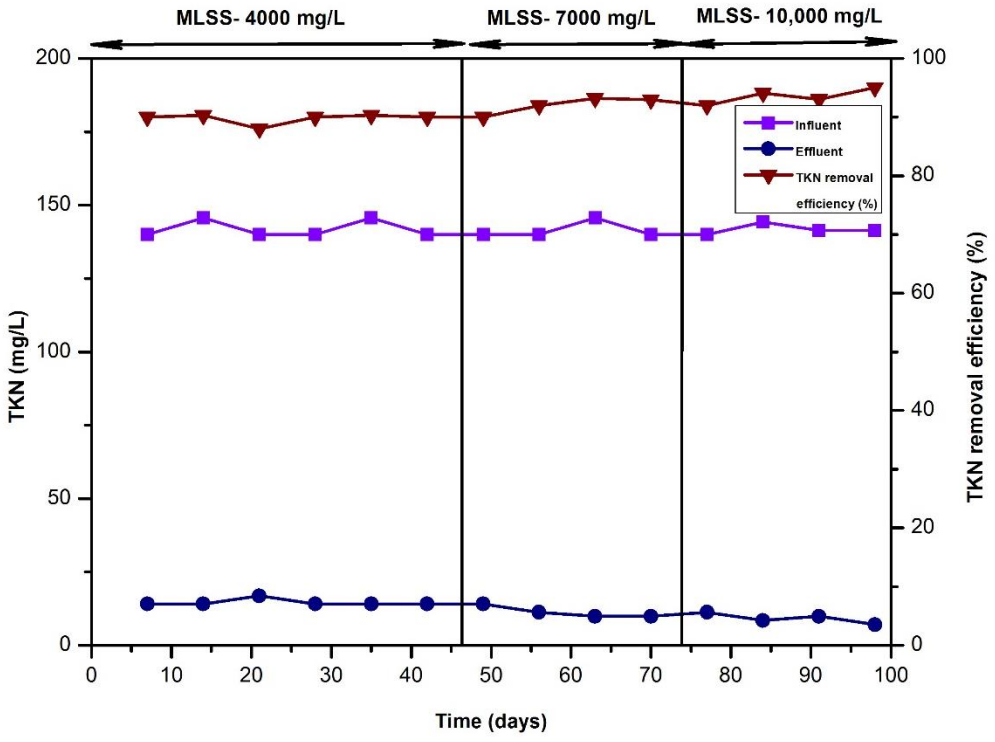

Figure 4.33 Variation of TKN in the control MBR operated at different MLSS

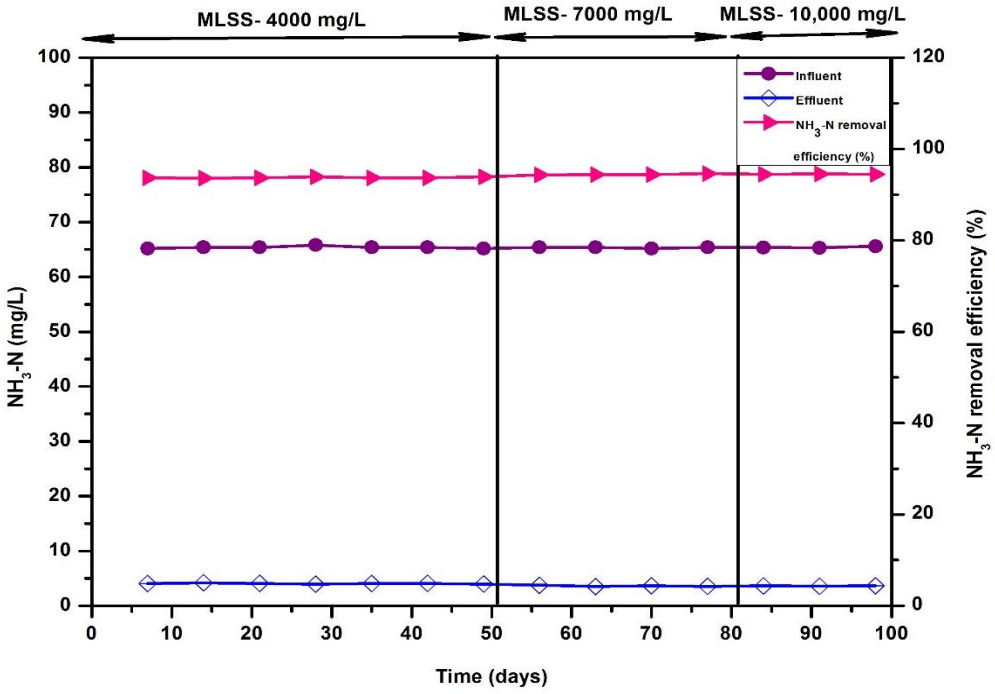

Figure 4.34 Variation of ammonical nitrogen in the control MBR operated at different MLSS

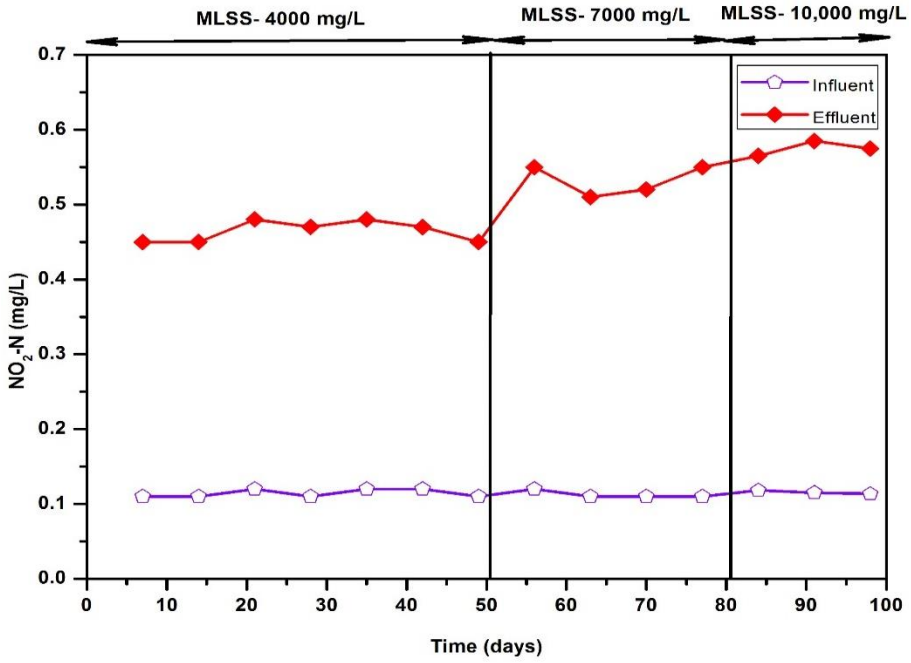

Figure 4.35 Variation of nitrite nitrogen in the control MBR operated at different MLSS

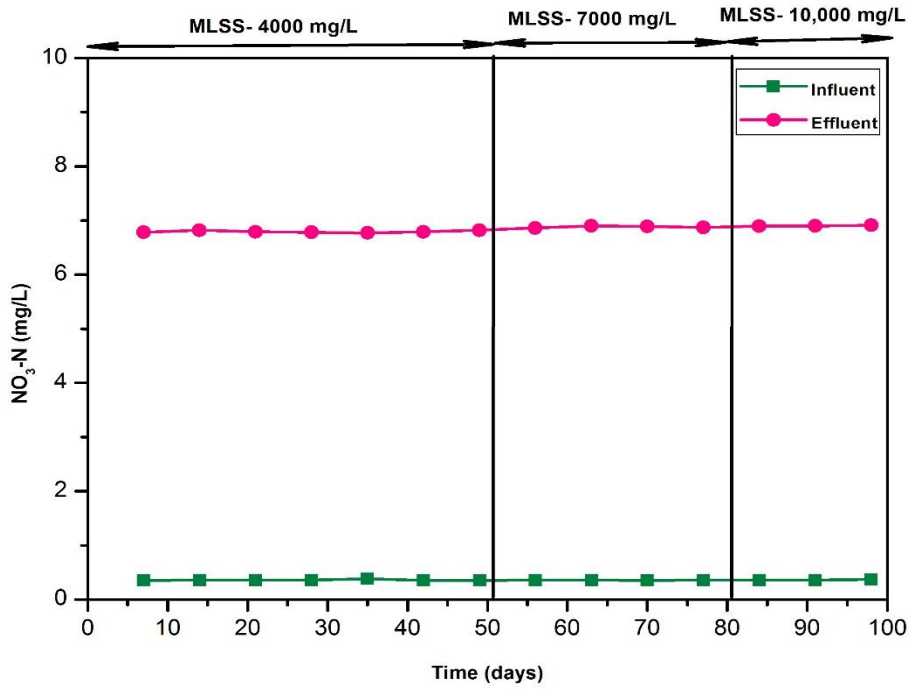

Figure 4.36 Variation of nitrate nitrogen in the control MBR operated at different MLSS

The average nitrate in the effluent was 6.7± 0.007 mg/L, 6.8± 0.009 mg/L and 6.9± 0.004 mg/L at 4000 mg/L, 7000 mg/L and 10,000 mg/L MLSS, respectively. Likewise, the nitrite concentration was 0.46± 0.005 mg/L, 0.53± 0.01 mg/L and 0.57± 0.005 mg/L at MLSS of 4000, 7000 and 10,000 mg/L, respectively. The NH_3-N in effluent decreased with subsequent increase in effluent nitrate indicated the occurrence of nitrification within the reactor (Wen *et al.*, 2015). The nitrogen removal by micro-organism can be achieved either by microbial cell assimilation or by nitrification process (Tan and Ng, 2008).

Nitrogen removal by cell assimilation is accomplished by sludge wasting from the reactor. The most common method of nitrogen removal is nitrification. The rate of nitrification is affected by the fraction of slow growing nitrifying organisms in the mixed liquor. The high removal efficiency in the MBR in the present study is ascribed to the complete retention of nitrifying micro-organisms by the membrane filtration without sludge wasting (Cote *et al.*, 1997).

Similar to COD, with increase in MLSS, an increase in nitrogen removal efficiency was observed which is comparable to the study of Damayanti *et al.* (2011) that reported NH_3-N removal between 97.6% and 98.7% when MLSS in the MBR was increased from 5000 to 20,000 mg/L. Andrade *et al.* (2013) too reported NH_3-N removal efficiency of 96% in his study. Deng (2015) reported lesser NH_3-N removal of 86.4% when compared to the present study.

4.6.1.5 Phosphate removal

The removal of phosphate by the control MBR operated under different MLSS is depicted in Figure 4.37. The influent phosphate was around 19.1 mg/L. At MLSS of 4000 mg/L, the phosphate in the effluent was around 14.1 mg/L showing removal efficiencies between 25.5± 0.6 to 26.7± 0.05%. The increase in MLSS to 7000 mg/L improved the removal efficiency resulting in maximum removal of 31.2± 0.2%. The effluent phosphate varied between 9.8 to 11.2 mg/L during this stage. A slight increase in phosphate removal efficiency was noted during operation of MBR at 10,000 mg/L MLSS when compared to other two MLSS. The maximum phosphate removal of 33.2± 0.5% was achieved at MLSS 10,000 mg/L. The phosphate removal efficiency observed in MBR operated at different MLSS in the present study was in the range of 25.5% to 33.2%. Previous studies however showed variation in phosphate removal efficiency in MBR. Johir (2015) observed around 43.7% of phosphate removal efficiency by submerged MBR. Yun (2016) examined the performance of MBR treating synthetic wastewater and reported a phosphate removal efficiency of around 42%. The maximum phosphate removal of 68.7% was reported by Deng (2015) at MLSS of 6980 mg/L. The phosphate removal can occur by luxury uptake. Merely a slight amount of phosphorus is consumed by micro-organisms during growth of new cells (Radjenovic *et al.*, 2008). The luxury uptake of phosphorus required the anaerobic compartment along with the aerobic compartment. The assimilation of required phosphate by the biomass and washing out of the remaining phosphate in the effluent might be the reason behind the less phosphate removal efficiency obtained in the present study (Yogalakshmi, 2008).

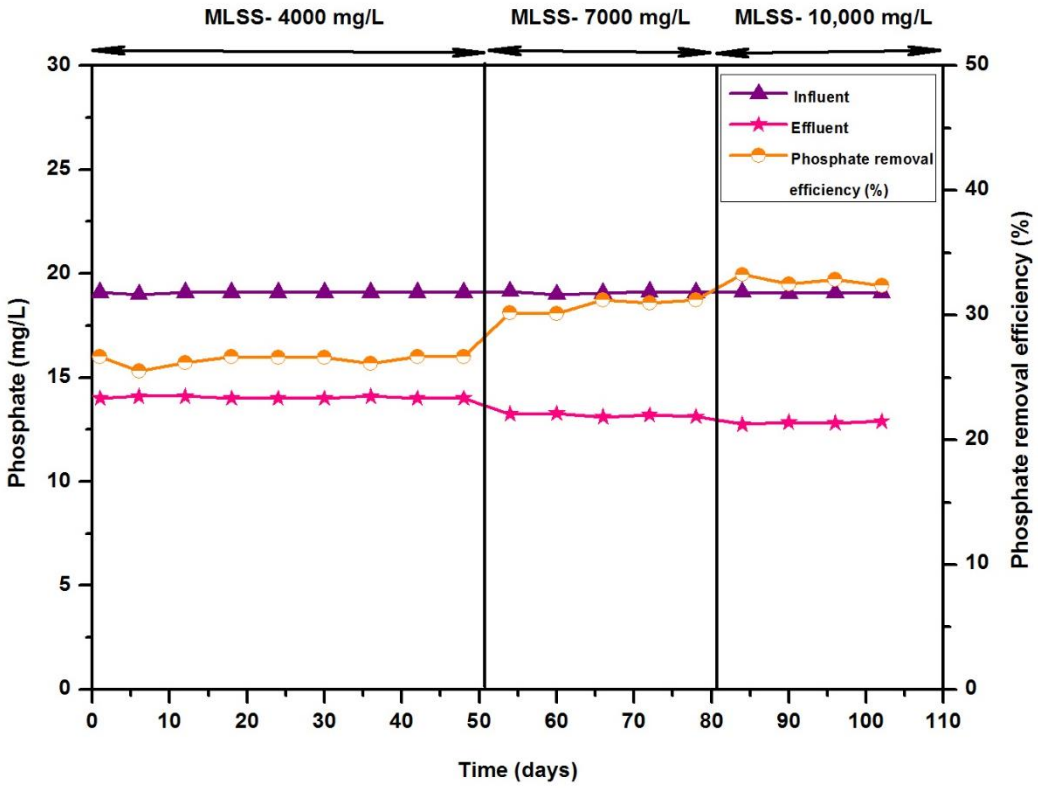

Figure 4.37 Variation of phosphate in the control MBR operated at different MLSS

4.6.1.6 Overall MBR treatment performance

The percent removal of COD, TS, TDS, TSS, VS, TKN, NH_3-N and phosphate by the MBR operated under different MLSS of 4000, 7000 and 10,000 mg/L is depicted in Figure 4.38. The control MBR showed good control over organic, nutrients and solids removal. Among all the three MLSS, the highest removal efficiency was observed at 10,000 mg/L. At MLSS 10,000 mg/L, the MBR showed 98.7± 0.08% COD removal, 36.8± 0.07% TS removal, 18.4± 0.09% TDS removal, 87.8± 0.2% TSS removal and 90.6± 0.09% VS removal. The TKN (94± 0.5%), NH_3-N (94.4± 0.03%) and phosphate removal (32.7± 0.2%) was also high at MLSS of 10,000 mg/L.

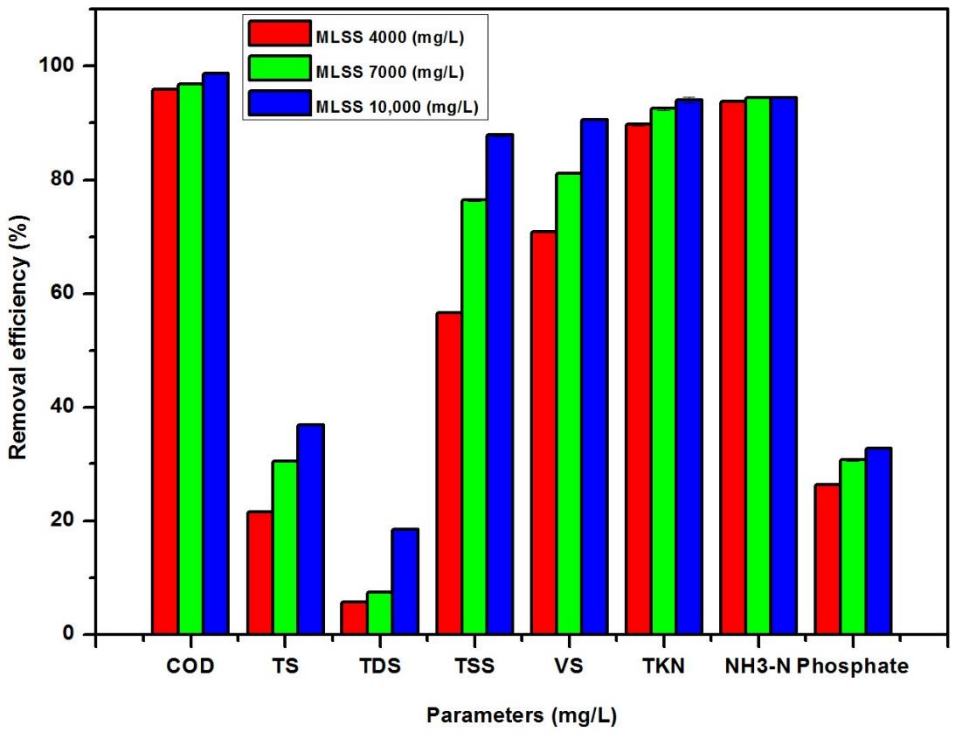

Figure 4.38 Overall MBR performance (effluent quality) at different MLSS

4.6.2 Sludge characteristics

4.6.2.1 MLSS and MLVSS

Figure 4.39 shows the variation of MLSS in the MBR during the experimental period. The MBR operation started with an initial MLSS and MLVSS of around 3968 mg/L and 3200 mg/L, respectively. With time, the MLSS gradually increased to 4000 mg/L. The MBR was maintained at MLSS 4000 mg/L for 51 days to analyze its performance. After 51 days, the biomass in the reactor was allowed to increase gradually to 7000 mg/L and maintained at this MLSS for almost 30 days. Subsequently, the MLSS in MBR was further increased to 10,000 mg/L and maintained for another 30 days. During the operation period, the excess sludge was withdrawn intermittently to control the MLSS within the reactor. The sludge activity was assessed through MLVSS to MLSS ratio. It was observed that the MLVSS/ MLSS ratio varied between 0.85- 0.9. This indicates a good biological condition within the MBR. At the start of experiment, the MLVSS/ MLSS ratio was around 0.8 which increased to 0.9 with the increase in MLSS and MLVSS. Tadkaew (2010) in his study also reported MLVSS/ MLSS ratio of 0.9, irrespective of

the increase in MLSS. In another study by Deng (2015), MLVSS/ MLSS ratio of 0.82 was reported which is comparatively lesser than that reported in the present study. The high MLVSS/ MLSS ratio in the MBR might be attributed to the higher growth of micro-organisms (Aim and Semmens, 2003).

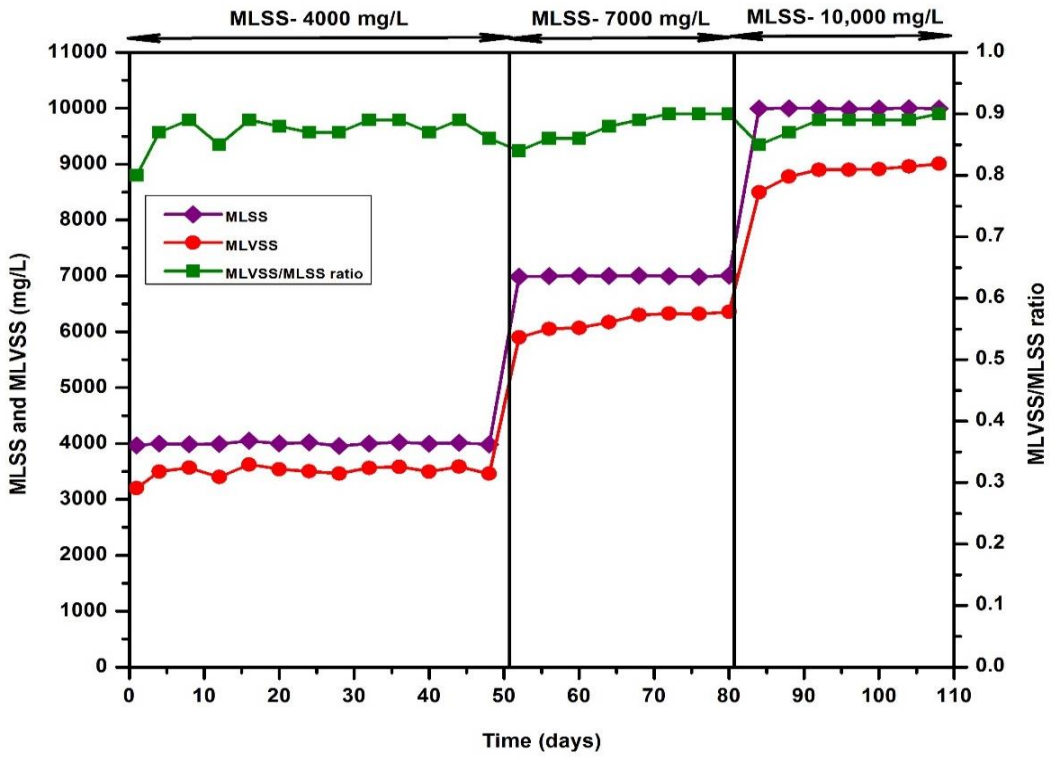

Figure 4.39 MLSS in the MBR

4.6.2.2 Sludge volume index (SVI)

SVI is an important process control parameter employed for assessing the quality of sludge (Adyasari, 2014). The settleability of sludge is determined through the SVI (Martins *et al.*, 2003). The MBR sludge showed a SVI of 90 mL/g at MLSS 4000 mg/L, thereby indicating the good settleability of the sludge. At 7000 mg/L, slightly higher SVI of 98 mL/g was observed. With increase in MLSS to 10,000 mg/L, negligible change in SVI (100 mL/g) was seen. Adyasari (2014) reported SVI between 170 to 250 mL/g in the MBR treating municipal wastewater which indicate poor settleability and bulking sludge condition due to the presence of large quantity of filamentous bacteria.

4.6.3 Membrane fouling characteristics

The membrane fouling characteristics were evaluated through changes in transmembrane pressure (TMP) and extracellular polymeric substances (tightly bound, loosely bound and soluble).

4.6.3.1 Transmembrane pressure in control MBR

The TMP profile gives an indication of membrane filterability and is directly related to membrane fouling i.e. an increase in TMP corresponds to the increase in membrane fouling. The TMP profile of the MBR operated at different MLSS is depicted in Figure 4.40. During the initial 8 days when the MBR is operated at 4000 mg/L, the TMP was slightly impacted, leading to a slight increase in TMP. More specifically, the TMP increased from 0.5 kPa (1st day) to 0.62 kPa (8th day). After 8 days, a moderate TMP increase from 1 to 13.5 kPa was observed at the end of 51 days. The TMP continued to increase gradually with time. During the operation at 7000 mg/L, comparatively high rate of TMP development was observed.

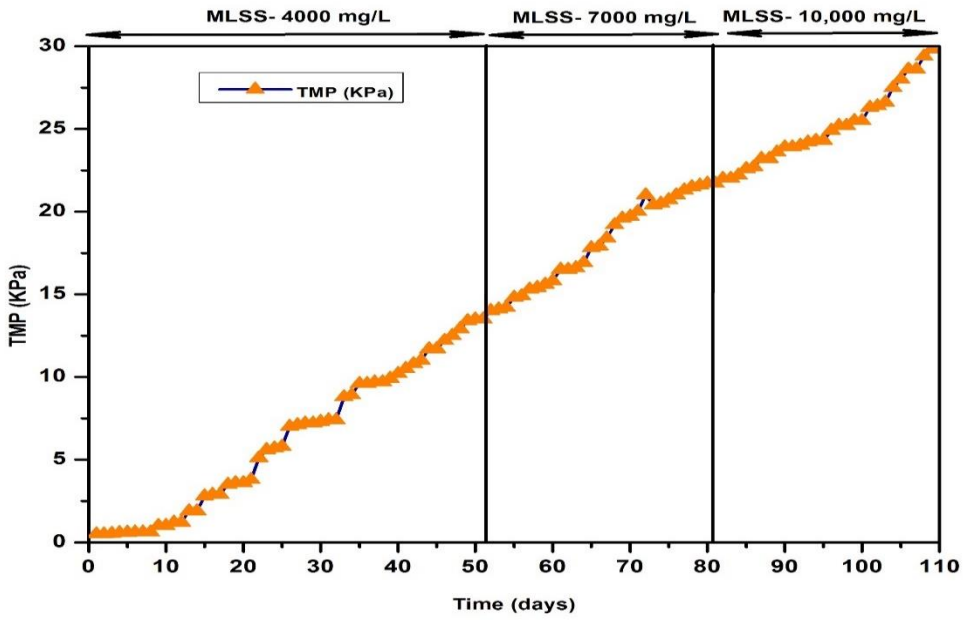

Figure 4.40 TMP profile of MBR operated at different MLSS

At 7000 mg/L, the TMP increased from 14 to 21.7 kPa. Likewise, during the operation of MBR at 10,000 mg/L MLSS, it increased to 29.8 kPa. Nahm *et al.* (2017b) reported

rise in TMP to 20 kPa in just 8.5 days in MBR operated at 4500- 5000 mg/L MLSS.As already mentioned with increase in MLSS, an increase in the EPS concentrations of the mixed liquor occurs which thereby leads to increased TMP (Wang *et al.*, 2009b). The EPS get deposited faster on the membrane surface thereby producing biocake. This results in reduction of filtration period and decline in filterability resulting in augmentation of membrane fouling.

4.6.3.2 Extracellular polymeric substances (EPS)

Extracellular polymeric substances (EPS) are high molecular weight natural polymers secreted by bacteria. They are one of the main causative agent of membrane biofouling. They play a central role in maintaining the structural and functional integrity of biofilms. EPS is responsible for aggregation of biofilm cells and also affects the density, porosity, binding of water molecules, sorption of organic and inorganic ions and compounds and mechanical stability of biofilm (Flemming and Wingender, 2010; Zeng *et al.*, 2016). The EPS is fractionized into tightly bound EPS, loosely bound EPS and soluble EPS on the basis of their distribution position on the bacterial cell (Murthy and Novak, 1998). The polysaccharides and proteins are the major components of EPS and play a key role in membrane biofouling. Hence, EPS and their composition is quantified and presented in the following section.

4.6.3.2.1 Loosely bound EPS (LB-EPS)

Figure 4.41 depicts the variation of LB- EPS in terms of polysaccharides and proteins in control MBR at different MLSS. Both the polysaccharides and proteins were measured for the LB- EPS. The protein in the LB-EPS increased continuously during the operation of MBR at different MLSS concentrations. Similar trend was also followed by the polysaccharide. At MLSS of 4000 mg/L, polysaccharide in LB-EPS was around 11.7± 0.8 mg/L at the start of operation which continued to rise slowly and reached 17.7± 0.3 mg/L on 49th day of operation i.e. at the end of the cycle of MLSS 4000 mg/L. Likewise, the protein in LB-EPS was around 38.5± 0.4 mg/L on the 7th day of operation with MLSS 4000 mg/L which gradually increased and reached 56.1± 0.1 mg/L on 49th day. At MLSS 7000 mg/L, the polysaccharide and protein of the LB-EPS increased from 25.5± 0.1 mg/L and 81.1± 0.02 mg/L to 36.2± 0.01 mg/L and 115.9± 0.1 mg/L at the

end of the cycle. The protein of LB-EPS showed a drastic increase at MLSS 7000 mg/L and continued to increase at MLSS 10,000 mg/L reaching a protein of 186.5± 0.3 mg/L at the end of MLSS 10,000 mg/L operation. The polysaccharide also showed an increase and attained a concentration of 58.5± 0.5 mg/L at the end of MLSS 10,000 mg/L cycle. The ratio of LB-EPS protein to polysaccharide (PN/ PS) was also investigated to gain insight into the extent of fouling. The PN/ PS of LB-EPS was around 3.1 at all the MLSS tested showing no change in PN/PS with the increase in MLSS. From the results, it is clear that in LB-EPS, the proteins are present in significantly higher amount compared to polysaccharides. The excretion of large quantities of exoenzymes by bacteria in the floc might be the reason behind predominance of proteins in the mixed liquor (Sponza, 2003).

The results of the present study is in accordance with the previous studies of Higgins and Novak (1997), Jorand *et al.* (1998) and Zhang *et al.* (2009b). Waheed *et al.* (2017) in his study reported higher LB-EPS protein fraction in the range of 70 to 150 mg/m^2 than the polysaccharide (40 to 70 mg/m^2) in MBR operated at MLSS of 8000 mg/L. High SRT of more than 100 days might be the reason behind the decreased production of polysaccharides. Lee *et al.* (2003) also reported decrease in polysaccharide when the SRT was increased from 20 to 40 days, thereby indicating decline in polysaccharide in mixed liquor with increase in SRT. The protein obtained in the present study was found to be 3.2 times more than that of polysaccharides.

The large amount of EPS increased the floc strength through polymer entanglement thereby facilitating the agglomeration of sludge flocs which results in the fouling of membrane (Mikkelsen and Keiding, 2002). It has been reported that the bound EPS particularly LB-EPS possess a major role in membrane fouling. They are particularly known to facilitate floc formation. Among the protein and polysaccharide fraction of bound EPS, the protein fraction play a key role in bioflocculation process which is attributed to high content of amino acids (Laspidou and Rittmann, 2002). Due to high amino acid content, proteins form electrostatic bonds with multivalent ions thereby leading to flocculation. According to Lee *et al.* (2003), PN/ PS ratio is an important parameter which control the membrane hydrophobicity and sludge flocs' surface

charge (Lee *et al.*, 2003). The higher value of PN/ PS ratio in the bound EPS is positively correlated to the hydrophobicity of sludge.

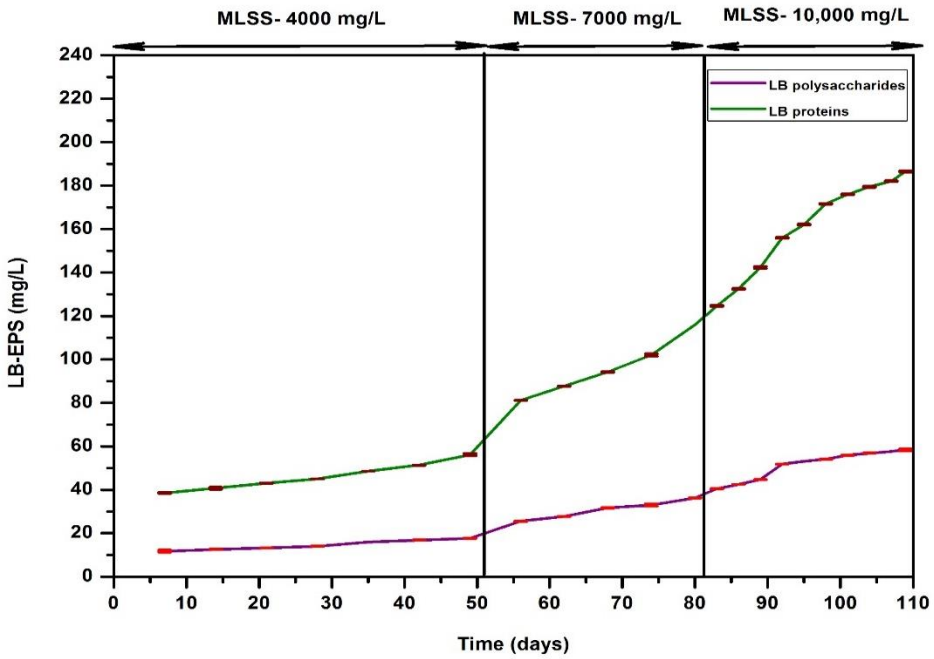

Figure 4.41 Loosely bound polysaccharides and proteins profile in the MBR operated at different MLSS

4.6.3.2.2 Tightly bound EPS (TB-EPS)

Figure 4.42 depicts the variation of TB polysaccharides and proteins in the control MBR operated at MLSS of 4000, 7000 and 10,000 mg/L. At MLSS of 4000 mg/L, the TB polysaccharides and proteins in the control MBR were in the range of 32-42.6 mg/L and 34.2- 50.7 mg/L, respectively with the PN/PS ratio of around 1.1. At MLSS of 7000 mg/L, the TB polysaccharides and proteins increased further and exhibited a range of 59.9- 71.3 mg/L and 61.6- 80.3 mg/L, respectively. Similarly, TB polysaccharides and proteins at MLSS 10,000 mg/L were in the range of 76.6- 92.6 mg/L and 85.9- 115.9 mg/L, respectively. The PN/PS ratio remains the same at MLSS 7000 mg/L and increased to 1.2 at 10,000 mg/L.

The TB-EPS was higher than the LB-EPS and are in concordance with the results of Zhang *et al.* (2009b). Jiang *et al.* (2013) reported protein and polysaccharide of ~48

and ~162 mg/L, respectively in the TB-EPS. Conversely, the LB-EPS was reported to contain protein and polysaccharide of ~ 38 mg/L.

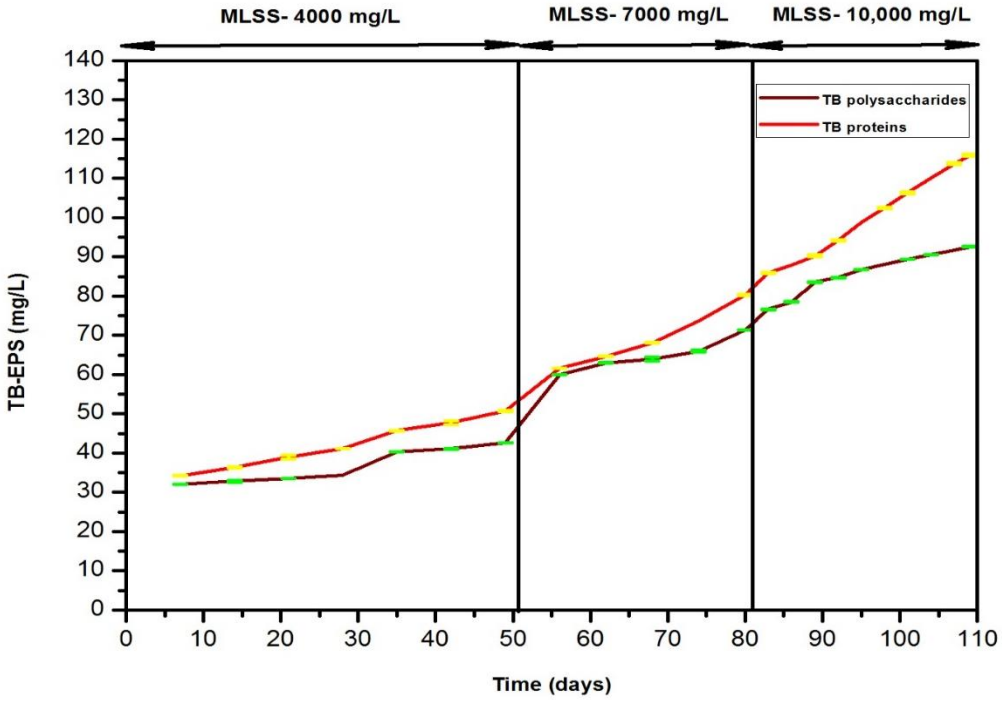

Figure 4.42 Tightly bound polysaccharides and proteins profile in the MBR operated at different MLSS

4.6.3.2.3 Soluble EPS

The variation of soluble polysaccharides and proteins in the control MBR operated at different MLSS is displayed in Figure 4.43. The soluble polysaccharides at MLSS of 4000, 7000 and 10,000 mg/L were in the range of 23.4 to 31.8 mg/L, 40.2 to 53.2 mg/L and 22.2 to 72.3 mg/L, respectively. Likewise, the soluble proteins were in the range of 30.3 to 48.1 mg/L, 56.3 to 75 mg/L and 25.2 to 101.1 mg/L at MLSS of 4000, 7000 and 10,000 mg/L, respectively. The PN/PS ratio in the supernatant which was related to the filtration resistance was observed to be in the range of 1.32 to 1.4 in the MBR operated at different MLSS. As apparent in the present study, the quantity of soluble EPS increases with increase in MLSS. Increase in MLSS under longer SRT induced a decrease in F/M ratio. As a result of this, the substrate in the MBR become limited due to which more lysis of cell and cell hydrolysis took place, thereby releasing more soluble EPS in the mixed liquor (Yigit *et al.*, 2008). Hence, the control MBR exhibited increase

in soluble EPS with increase in MLSS. The increase in soluble EPS with the increased MLSS is also reported by Hejzlar and Chudoba (1986). Previous study by Maqbool *et al.* (2015) reported the soluble polysaccharide and protein in the range of 45 to 75 mg/L and 35 to 42 mg/L, respectively in the MBR operated at MLSS of 10-11 mg/L.

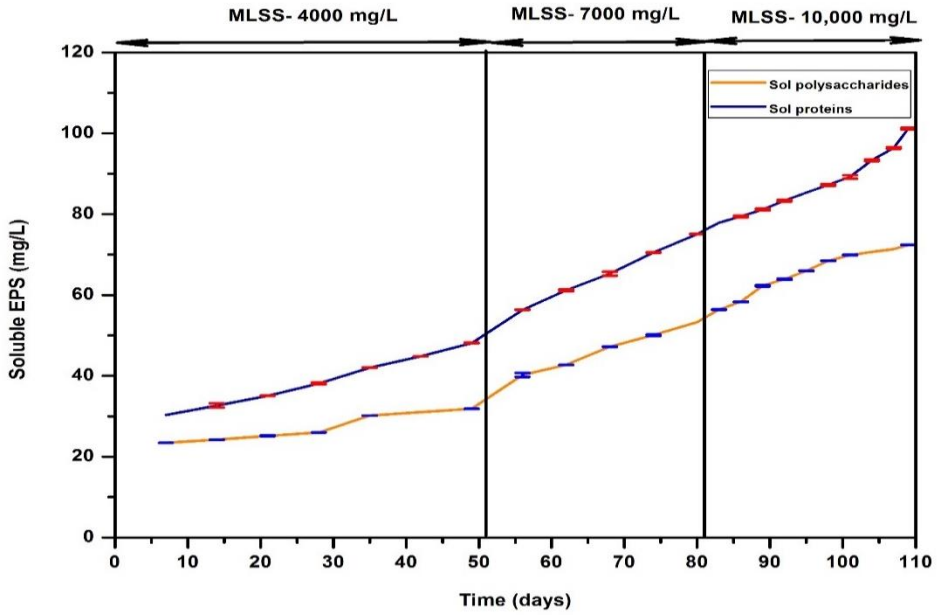

Figure 4.43 Soluble polysaccharides and proteins profile in the MBR operated at different MLSS

The soluble EPS is known to affect the filtration flux of the membrane. An inverse relation exist between the soluble EPS and the filtration flux. Higher the suspended EPS, lesser will be the filtration flux of the membrane (Lin *et al.*, 2014). According to Rosenberger and Kraume (2002), increase in soluble EPS from 15 to 90 mg/L resulted in decrease in filtration index by 80% which is evident from the TMP profile of control MBR which exhibited rapid increase.

4.6.3.2.4 Overall EPS profile of mixed liquor in MBR

Figure 4.44 depicts the composition of LB-EPS, TB-EPS and soluble EPS in the mixed liquor of MBR operated at varying MLSS. A consistently increasing trend in the carbohydrate and protein of different EPS (TB-EPS, LB-EPS and soluble EPS) was

observed with increase in MLSS from 4000 to 10,000 mg/L. At 10,000 mg/L, the average concentration of protein and carbohydrates of all EPS was maximum.

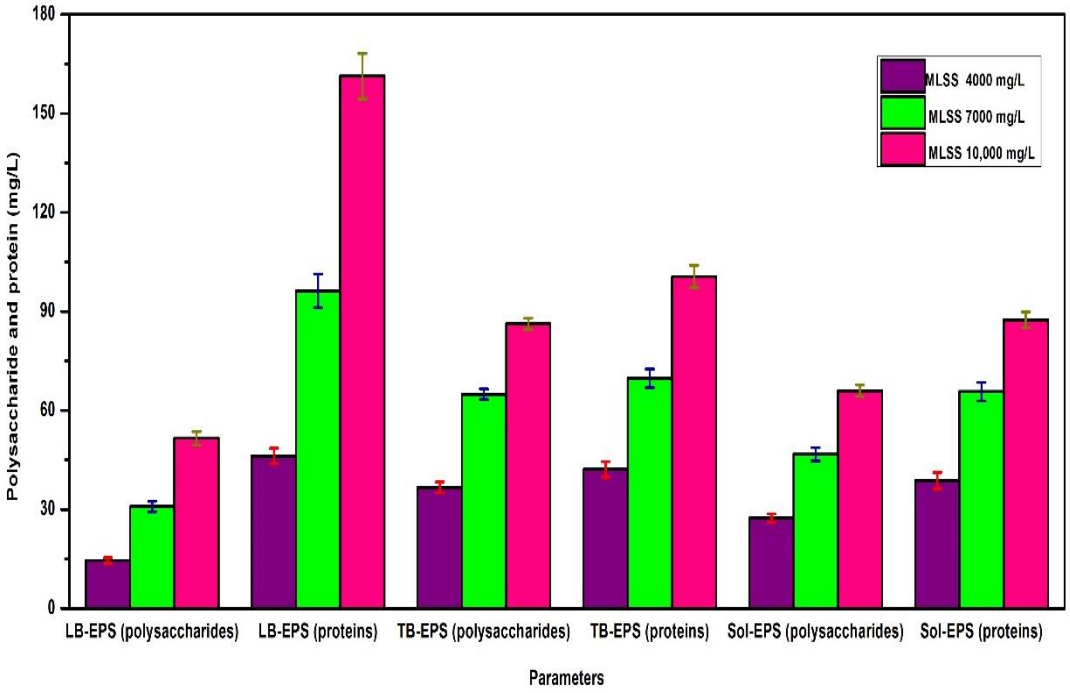

Figure 4.44 Composition of bound EPS (LB and TB) and soluble EPS profile in the control MBR operated at different MLSS

Further, among the different EPS, the highest carbohydrate was observed for the TB-EPS showing value of 86.2± 1.7 mg/L followed by soluble EPS (65.9± 1.7 mg/L) and LB-EPS (51.5± 2 mg/L), respectively. The highest protein of 161.2± 6.8 mg/L was observed for LB-EPS which was followed by TB-EPS (100.5± 3.4 mg/L) and soluble EPS (87.4± 2.4 mg/L), respectively.

4.7 QQ-MBR operation

The influence of QQ bacteria IMN beads in the MBR performance was assessed based on the effluent quality and fouling potential. Fouling control was monitored regularly at MLSS of 4000, 7000 and 10,000 mg/L, the results of which are discussed in detail in the following sections.

4.7.1 Effluent quality

The quality of the effluent was monitored through organic removal, nutrient removal and solid removal.

4.7.1.1 pH

Figure 4.45 depicts the variation of pH in the QQ-MBR operated at different MLSS. The influent had pH in the range of 7.21 to 7.26. The pH of the treated effluent varied in the range between 8.70- 8.83. The changes in the effluent was negligible during the operational period at three different MLSS.

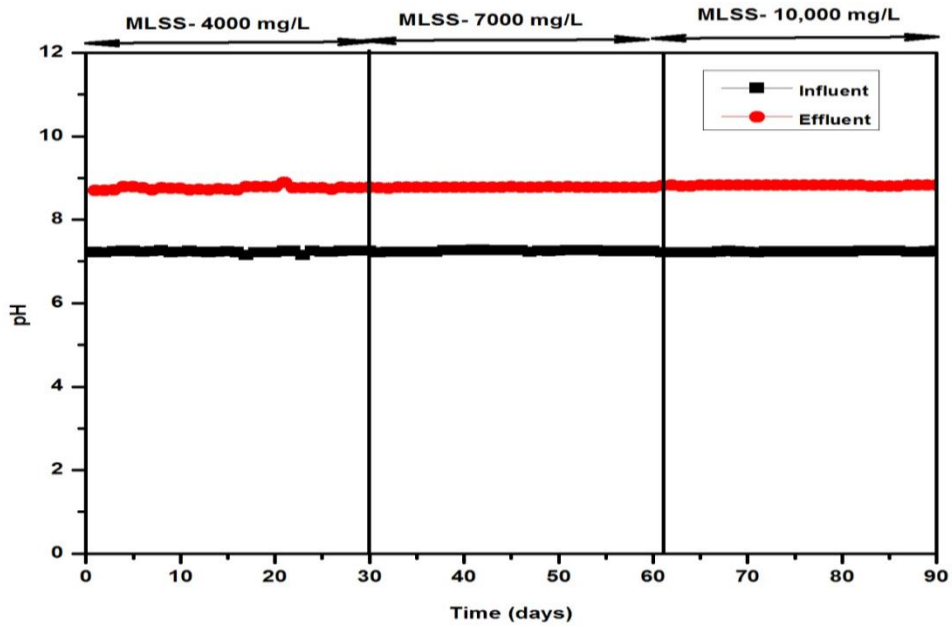

Figure 4.45 Variation of pH in the QQ-MBR operated at different MLSS

4.7.1.2 COD removal

Figure 4.46 represents the COD removal efficiency of the QQ-MBR operated at different MLSS. Initially, at MLSS of 4000 mg/L, the maximum COD removal of 96.6± 0.85% was achieved with the effluent COD varying in the range of 160 to 200 mg/L. Likewise, the COD removal efficiencies evaluated at MLSS 7000 and 10,000 mg/L showed a maximum COD removal rate of 97.5± 0.85% and 99.1± 0.5%, respectively. The effluent COD varied in the range of 120 to 160 mg/L and 40 to 80 mg/L at 7000

and 10,000 mg/L, respectively. It was observed that the performance of QQ-MBR in terms of COD removal had a marginal difference of 0.2% when compared to the control MBR. Previous studies also reported removal efficiency in the range of 93 to 98% after addition of QQ bacteria in the MBR (Oh *et al.*, 2012; Jiang *et al.*, 2013; Cheong *et al.*, 2014). Kim *et al.* (2013) and Kim *et al.* (2015) using *Rhodococcus* sp. BH4 entrapping beads and *Rhodococcus* sp. BH4 macrocapsules reported more than 93% COD removal efficiency.

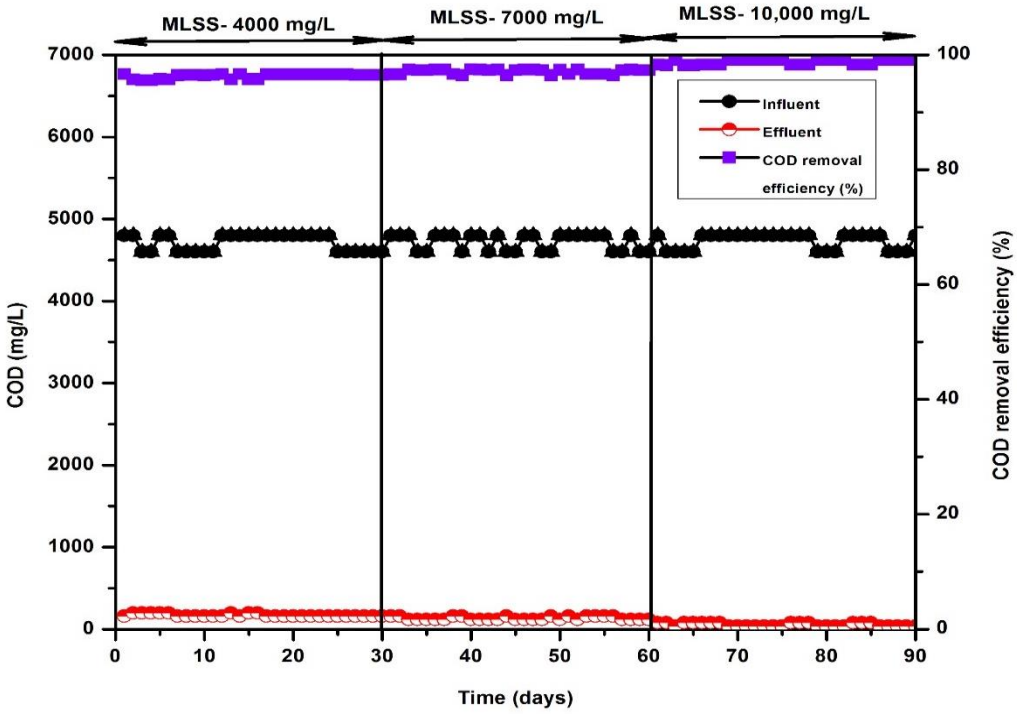

Figure 4.46 Variation of COD in the QQ-MBR operated at different MLSS

4.7.1.3 Solids removal

Figure 4.47 and 4.48 depicts the effect of MLSS on the TS and TDS removal in QQ-MBR. From the Figure, it is clearly evident that effluent TS and TDS increases with increase in MLSS. Maximum TS removal efficiency of 22.8± 0.4% was observed at MLSS 4000 mg/L which was 3.1% higher than that of the control MBR. However, the TDS removal efficiency of QQ-MBR was similar to that of control MBR showing a maximum removal efficiency of 5.9± 0.4%. With increase in MLSS up to 7000 mg/L, the maximum TS and TDS removal efficiencies reached to 30.9± 0.2% and 9.1± 0.1%,

respectively. The QQ-MBR showed 1.3% and 17.5% higher TS and TDS removal, respectively than control MBR. At MLSS 10,000 mg/L, both TS and TDS removal efficiencies increased and reached maximum value of 39.7± 0.5% and 19.4± 0.2%, respectively. The maximum effluent TS and TDS was around 2700 mg/L and 1330 mg/L, respectively at MLSS of 10,000 mg/L. The operation of QQ-MBR at 10,000 mg/L exhibited 7% and 3.9% higher TS and TDS removal efficiency, respectively compared to control MBR.

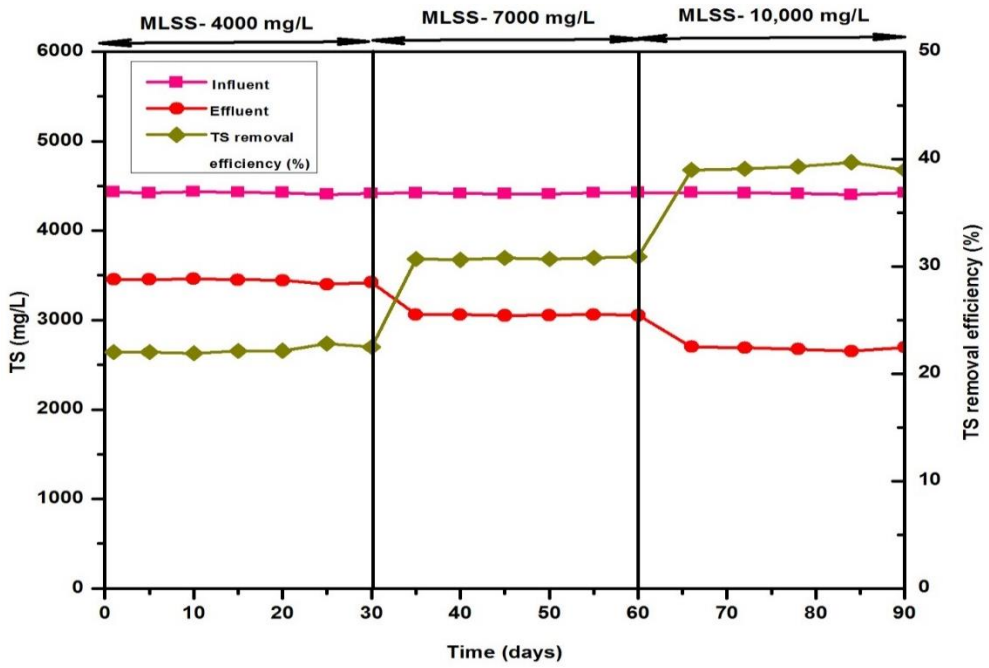

Figure 4.47 Variation of TS in the QQ-MBR operated at different MLSS

The behavior of QQ-MBR operated at different MLSS concentration in terms of TSS and VS removal is depicted in Figures 4.49 and 4.50. The influent showed a TSS and VS in the range of 474- 494 mg/L and 1875- 1894 mg/L, respectively. During the operation period of QQ-MBR, the TSS removal was increased by 2.3% compared to the control MBR at MLSS of 4000 mg/L. On the other hand, the VS removal efficiency was comparable between QQ-MBR and control MBR showing a maximum removal rate of 71.1± 0.5%. The removal efficiencies of TSS and VS improved further when the QQ-MBR was operated at 7000 mg/L. The maximum removal rates of TSS and VS of 79.2± 0.05% and 82.1± 0.2%, respectively was achieved in the QQ-MBR.

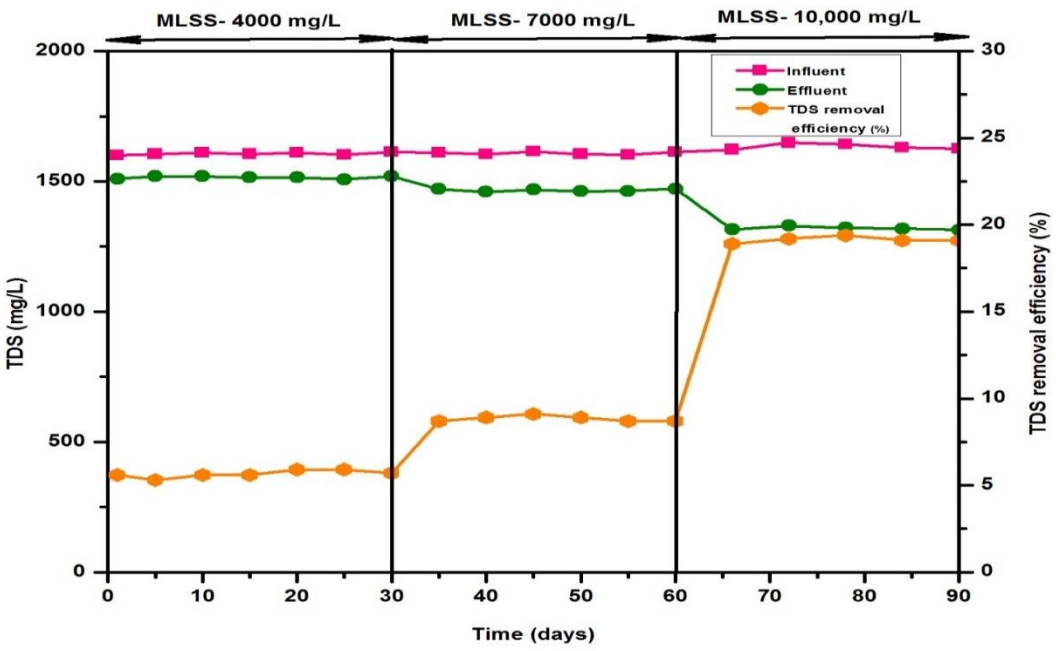

Figure 4.48 Variation of TDS in the QQ-MBR operated at different MLSS

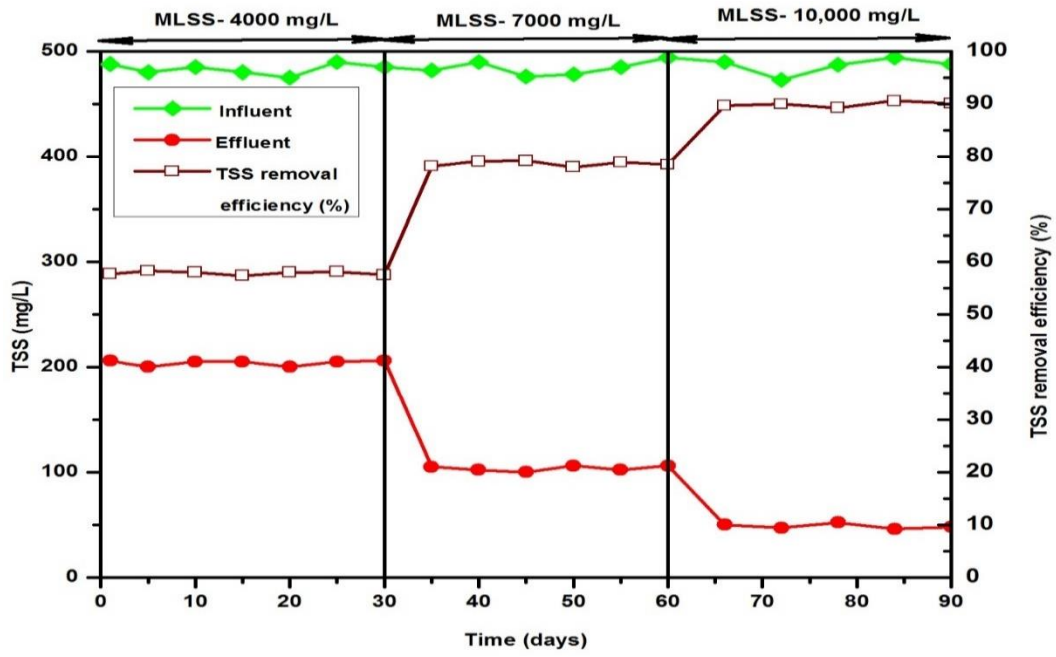

Figure 4.49 Variation of TSS in the QQ-MBR operated at different MLSS

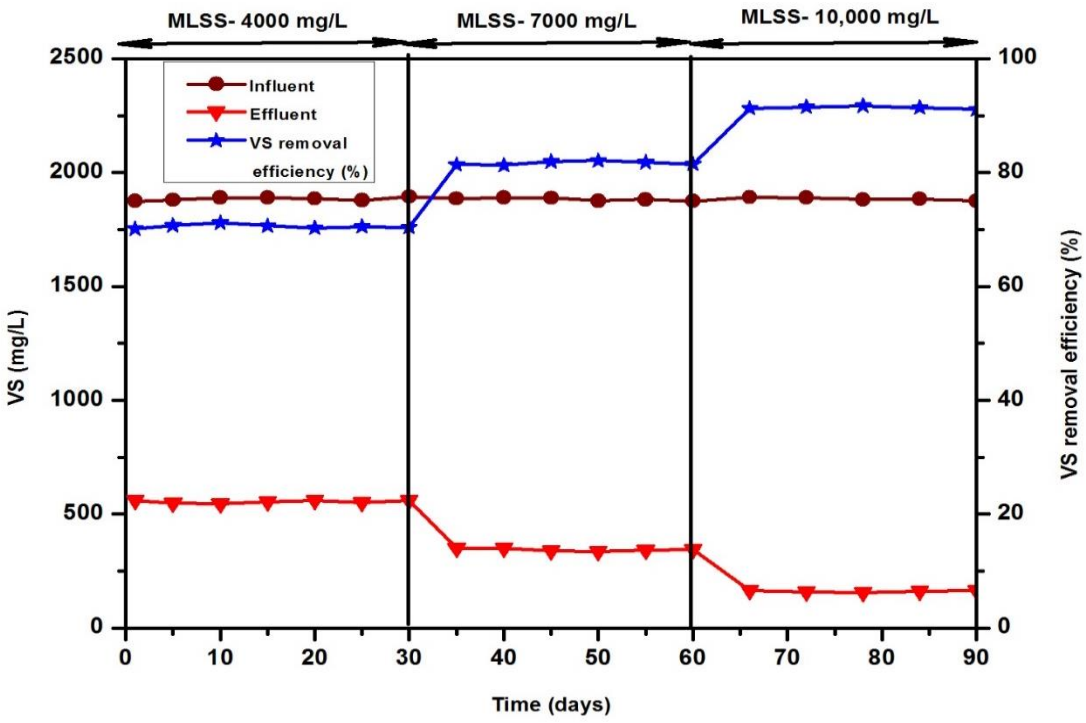

Figure 4.50 Variation of VS in the QQ-MBR operated at different MLSS

When compared to control, it was found that the TSS (2.2% higher) and VS (0.9% higher) removal efficiencies were higher in QQ-MBR. An increase in MLSS to 10,000 mg/L in the reactor induced an increase of the TSS and VS removal rates of 90.6± 0.1% and 91.7± 0.6%, respectively. The TSS and VS removal efficiency were observed to be around 2.7% and 0.8%, respectively higher as compared to control MBR which proved that the QQ-IMN beads addition could induce the solids removal efficiency.

4.7.1.4 Nitrogen removal

Figure 4.51 depicts the TKN removal in the MBR operated with QQ bacteria at different MLSS. The QQ-MBR exhibited effluent TKN of 140- 144.2 mg/L similar to that of control reactor showing a maximum removal efficiency of 90.1± 0.1% at MLSS of 4000 mg/L. However, at MLSS of 7000 and 10,000 mg/L, the maximum TKN removal of 93.2± 0.5% and 95.1± 0.3%, respectively was observed. When compared to the control MBR, a marginal difference of 0.2% and 0.9% was observed in TKN removal at MLSS of 7000

and 10,000 mg/L, respectively. Few studies reported similar TKN removal efficiency in control and QQ-MBR. Mutlu *et al.* (2016) observed TKN removal efficiency of 48% using *Rhodococcus* immobilized cell entrapping beads. In another study, an improved rate of TKN removal efficiency was observed in the MBR operated with QQ bacteria. Johir (2015) reported TKN removal efficiency of 36.8% after incorporating GAC in the MBR which was more than the MBR without GAC addition (29.8%).

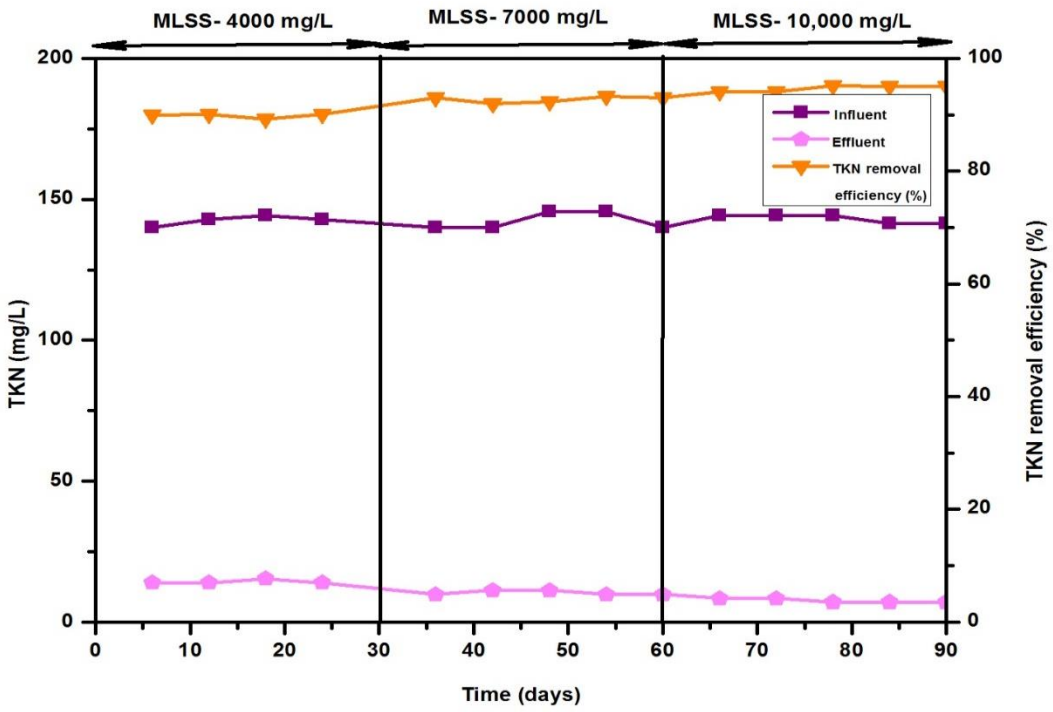

Figure 4.51 Variation of TKN in the QQ-MBR operated at different MLSS

Figure 4.52, 4.53 and 4.54 depicts the variation of NH_3-N, NO_2-N and NO_3-N in the effluent obtained from QQ-MBR operated at different MLSS. At MLSS of 4000 mg/L, the maximum NH_3-N removal efficiency was recorded to be 93.7± 0.04% which further increased to 94.6± 0.1% at MLSS of 7000 mg/L. When the QQ-MBR was operated at MLSS of 10,000 mg/L, no change in removal efficiency (94.6± 0.5%) was seen. The removal efficiency exhibited by the QQ-MBR was comparable to that obtained in control MBR. The effluent NO_2-N and NO_3-N of QQ-MBR at MLSS of 4000, 7000 and 10,000

mg/L was similar to that of the control MBR. With the MLSS of 4000 mg/L, the average values of effluent NO_2-N and NO_3-N was 0.46± 0.002 mg/L and 6.7± 0.01 mg/L, respectively. The NO_2-N in the effluent was increased to 0.52± 0.007 mg/L and 0.57± 0.004 mg/L at MLSS of 7000 and 10,000 mg/L, respectively. The average NO_3-N at MLSS 7000 and 10,000 mg/L was found to be 6.8± 0.02 mg/L and 6.9± 0.004 mg/L, respectively. Overall, the NH_3-N removal efficiency was found to be more or less similar to that of control indicating no significant impact of QQ mechanism on the NH_3-N removal of MBR.

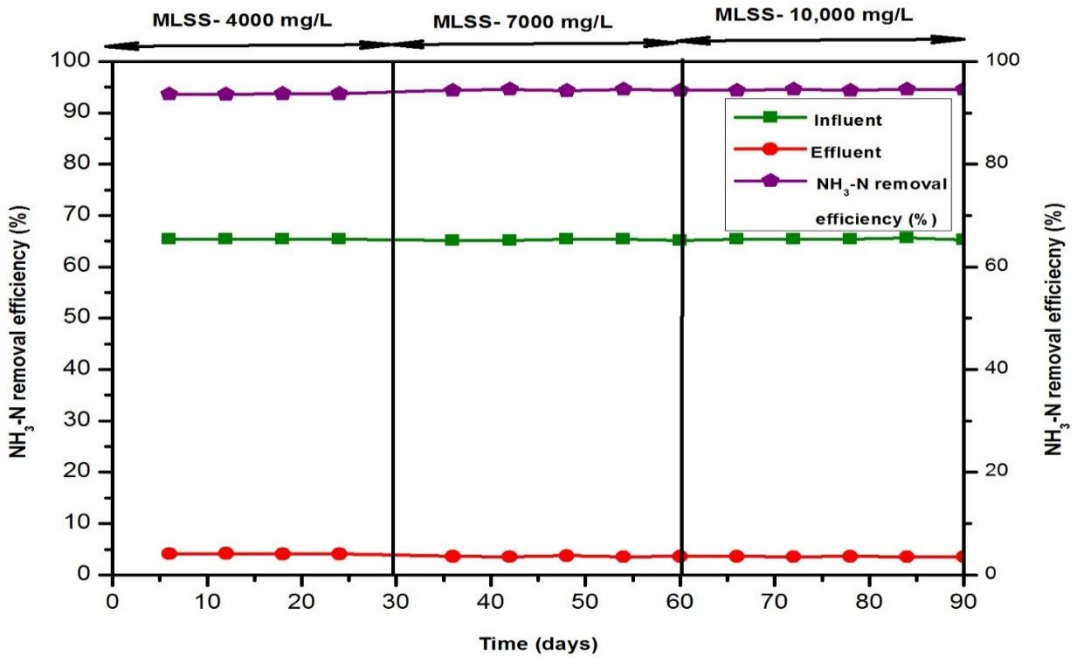

Figure 4.52 Variation of ammonical nitrogen in the QQ-MBR operated at different MLSS

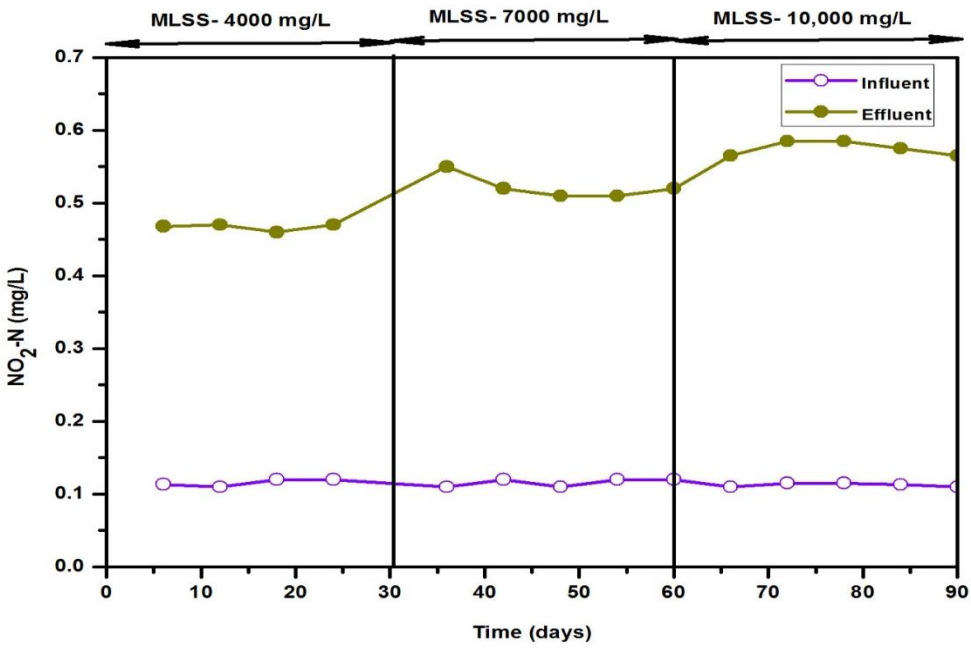

Figure 4.53 Variation of nitrite nitrogen in the QQ-MBR operated at different MLSS

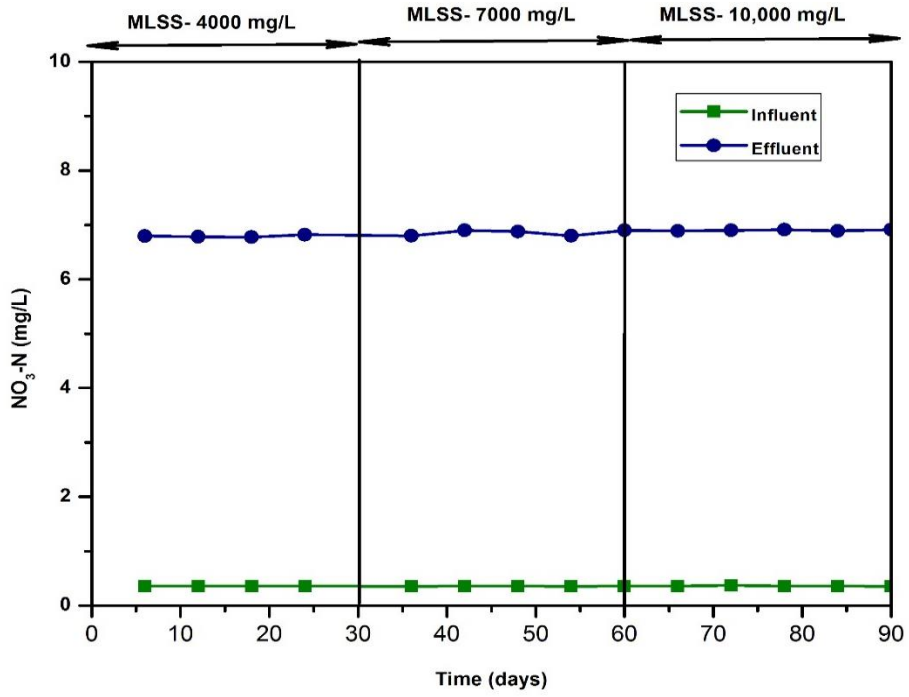

Figure 4.54 Variation of nitrate nitrogen in the QQ-MBR operated at different MLSS

Similar findings was also reported in the previous studies. Jiang *et al.* (2013) while investigating the effect of immobilized acylase on the reactor performance observed above 95% NH_3-N removal efficiency which is similar to that of control MBR. Certain studies reported less NH_3-N removal efficiency than the present study. Maqbool *et al.* (2015) while using *Rhodococcus sp.* entrapped sodium alginate beads reported 55.4% NH_3-N removal efficiency which is lower than the value obtained in the present study.

4.7.1.5 Phosphate removal

The phosphate removal in the QQ-MBR operated at different MLSS is depicted in Figure 4.55. At MLSS 4000 mg/L, the phosphate removal efficiency of 27± 0.2% was observed. Compared to the control MBR, the removal efficiency was enhanced by 0.7%. Further, the phosphate removal increased to 31.3± 0.2% and 33.6± 0.5%, respectively at 7000 and 10,000 mg/L.

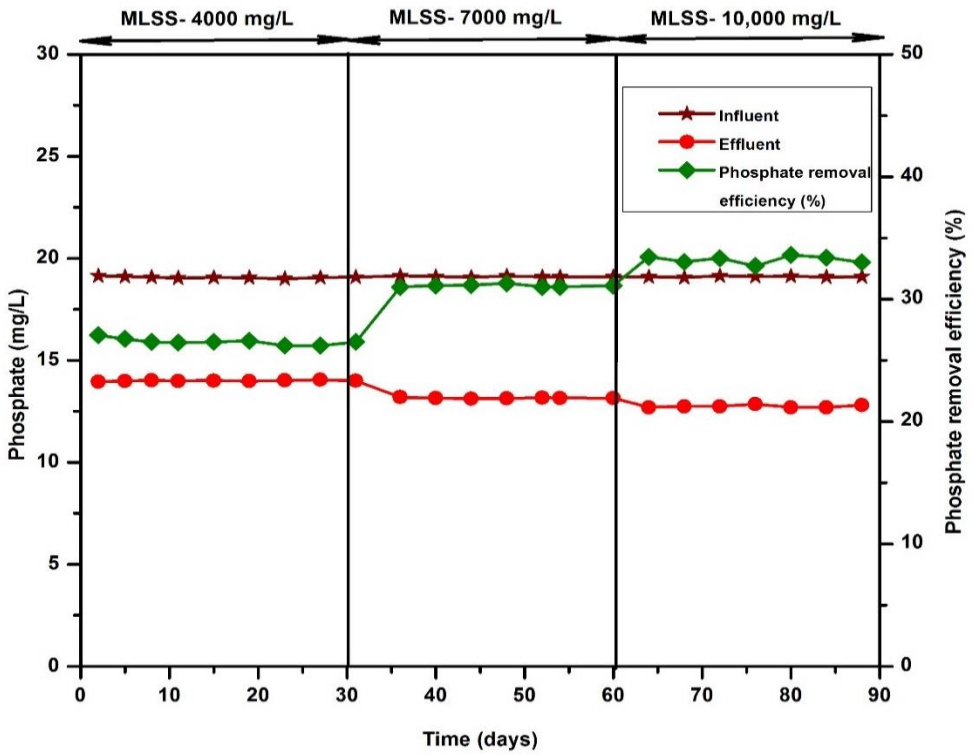

Figure 4.55 Variation of phosphate in the QQ-MBR operated at different MLSS

In comparison to control, the phosphate removal rates in the QQ-MBR was improved by 1% and 0.2% at MLSS of 7000 and 10,000 mg/L, respectively. Hence, a negligible difference in phosphate removal rate was observed between control and QQ-MBR.

The results were in accordance with the previous study by Waheed *et al.* (2017) that reported consistency in phosphate removal efficiency of MBR with antifouling consortium and control MBR. However, Guo *et al.* (2008) observed higher performance of sponge submerged MBR for removing phosphate compared to conventional MBR.

4.7.1.6 Overall QQ-MBR performance

The overall performance of MBR operated with QQ bacteria beads at three MLSS of 4000, 7000 and 10,000 mg/L is depicted in Figure 4.56. From the Figure, it is clearly evident that the QQ-MBR showed COD, NH_3-N and TKN removal in the range of 96.1 to 98.5%, 93.6 to 94.6% and 89.8 to 94.9%, respectively when operated at MLSS of 4000, 7000 and 10,000 mg/L.

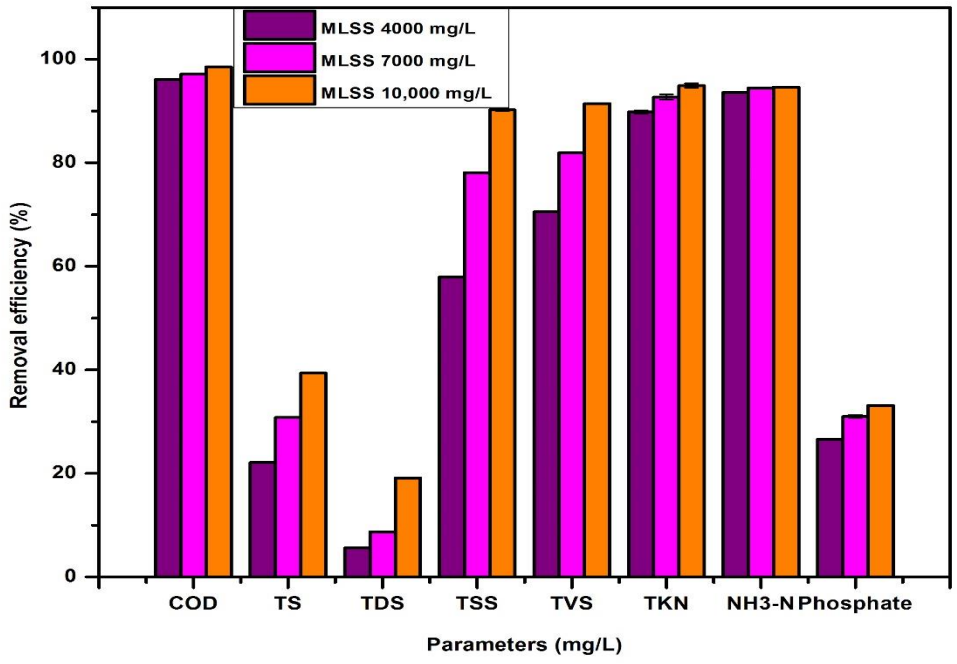

Figure 4.56 Overall QQ-MBR performance at different MLSS

At all the tested MLSS, very slight change in COD, NH_3-N and TKN removal by the QQ-MBR was observed. However, significant differences in the removal efficiencies of TS, TDS, TSS and TVS were observed at different MLSS. The maximum solids removal rate was recorded at MLSS of 10,000 mg/L. More specifically, the QQ-MBR achieved 39.4± 0.01% TS, 19.1± 0.05% TDS, 90.2± 0.2% TSS and 91.4± 0.08% TVS removal at MLSS of 10,000 mg/L. The phosphate removal efficiency varied in the range of 26.4% to 32.7% when the MLSS concentration in the reactor was changed from 4000 to 10,000 mg/L, respectively. It was found that the QQ-MBR performed well on TS and TDS removal relative to control MBR. While QQ-MBR exhibited only marginal differences in the removal efficiencies in terms of TSS, TVS, COD, NH_3-N and TKN, phosphate when compared to control MBR.

4.7.2 Sludge characteristics

4.7.2.1 MLSS and MLVSS

Figure 4.57 depicts the variation of MLSS in the QQ-MBR. The MLSS and MLVSS in the QQ-MBR was comparable with the control MBR. The initial MLSS was 3892 mg/L with corresponding MLVSS of 3050 mg/L. Without any sludge withdrawal, the MBR reached the required MLSS of 4000 mg/L in 4 days. The MBR was operated at this concentration for 30 days. Then MLSS was allowed to increase gradually till it attained the concentration of 7000 mg/L. The MBR was operated at this concentration for next 30 days. During this phase, slight fluctuation in MLSS in the range between 6999 to 7062 mg/L was observed. After 30 days, the MLSS was again increased to 10,000 mg/L. The MLSS fluctuated between 9982 to 10,006 mg/L during this phase. The MLVSS/ MLSS ratio ranged from 0.8 to 0.92 during the entire operation. At start, the MLVSS/ MLSS ratio was 0.78 which eventually increased to 0.9 with increase in MLSS and MLVSS, indicating rich biomass content in sludge.

4.7.2.2 SVI

The addition of QQ-IMN beads into the MBR did not show any significant change in the SVI. The SVI in the range of 85 to 95 mL/g was observed in the QQ-MBR. In a study by Waheed *et al.* (2017), SVI value of >90 and <140 mL/g was observed in QQ-MBR.

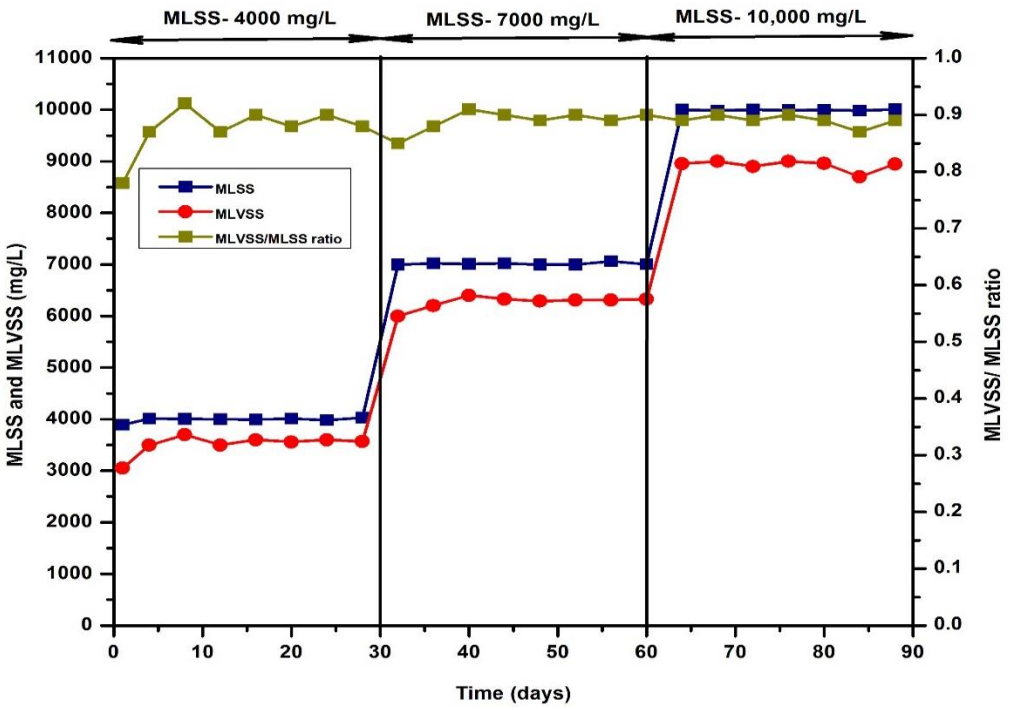

Figure 4.57 MLSS in the QQ-MBR

4.7.3 Membrane fouling characteristics

4.7.3.1 TMP profile in QQ-MBR

The TMP profile showing fouling propensity for QQ-MBR is portrayed in Figure 4.58. During the operation of QQ-MBR at 4000 mg/L, a slow increase in TMP was seen showing TMP values in the range between 0.4 to 2.1 kPa. The TMP of QQ-MBR showed 6.4 times reduced TMP when compared to control MBR. The TMP profile followed a similar trend in 7000 and 10,000 mg/L MLSS too. The TMP development at 7000 mg/L was in the range of 2.1 to 10.5 kPa which was 2 times lesser than control MBR. The TMP showed a drastic TMP rise to 27 kPa at 10,000 mg/L MLSS. A slight difference was observed in QQ-MBR when compared to control MBR. From this, it is clearly evident that QQ bacteria were effective in delaying membrane fouling. Previous studies also reported a slow rate of TMP development in the reactor using QQ bacteria compared to that of control MBR. Maqbool *et al.* (2015) while using *Rhodococcus* sp. BH4 reported around seven times less biofouling compared to control MBR. In a study by Waheed *et al.* (2018), *Rhodococcus* sp. BH4 was effective in delaying membrane

fouling in MBR after 24 days of operation. The results of present study suggested a significant reduction in membrane fouling and hence improvement in filterability in the QQ-MBR which was due to the inhibition of biofilm formation by the QQ bacteria IMN beads. The QQ bacteria present in the IMN beads might have resulted in the degradation of signalling molecule. As a result of this, the adhesive forces between the sludge bacteria might have weakened resulting in reduction of biofilm formation.

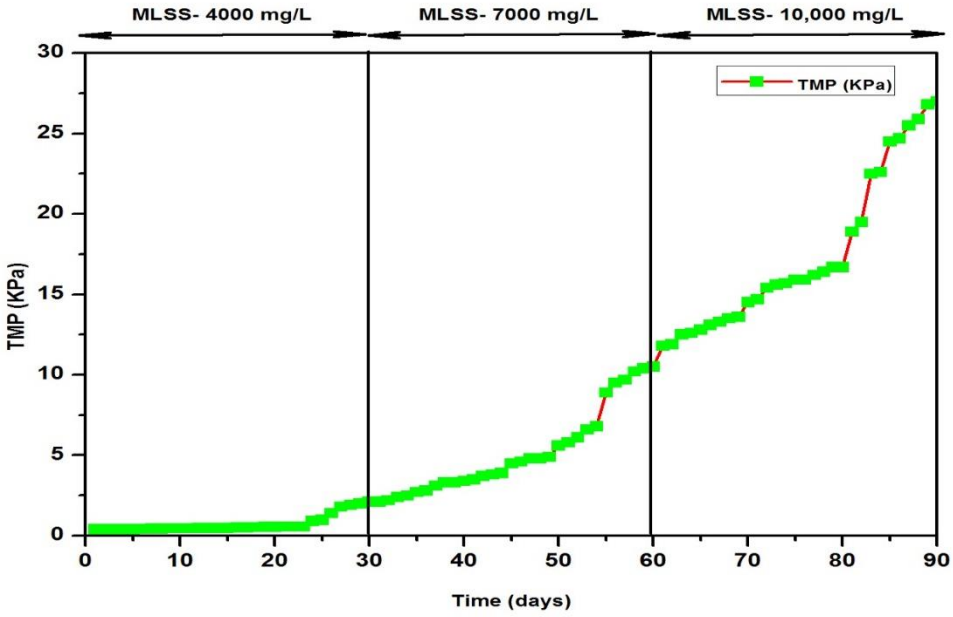

Figure 4.58 TMP profile of QQ-MBR operated at different MLSS

4.7.3.2 EPS

4.7.3.2.1 Loosely bound EPS

The variation of LB polysaccharides and proteins in the QQ-MBR responding to different MLSS concentration is displayed in Figure 4.59. At MLSS 4000 mg/L, the LB polysaccharides and proteins in the QQ-MBR were in the range of 4 to 6.6 mg/L and 13.7 to 22 mg/L, respectively. But the polysaccharides (8.6 to 14.9 mg/L) and proteins (23.7 to 45.5 mg/L) of LB-EPS varied remarkably at MLSS of 7000 mg/L. A further increase in MLSS to 10,000 mg/L resulted in polysaccharides and proteins levels of LB-EPS in the range of 22 to 28 mg/L and 55 to 80.7 mg/L, respectively. A decrease in PN/PS ratio was seen with the increasing MLSS. The PN/PS ratio at MLSS 4000 mg/L

was around 3.3 which decreased to 3.1 at 7000 mg/L. At 10,000 mg/L, the PN/PS ratio further decreased and reached 2.6. The PN/ PS ratio in QQ-MBR was higher at MLSS 4000 mg/L when compared to control MBR. The higher PN/ PS ratio indicated higher relative hydrophobicity (RH) of the activated sludge. Higher RH leads to decrease in interaction between the hydrophobic flocs and the hydrophilic PES membrane which ultimately improves the membrane performance (Lee *et al.*, 2003).

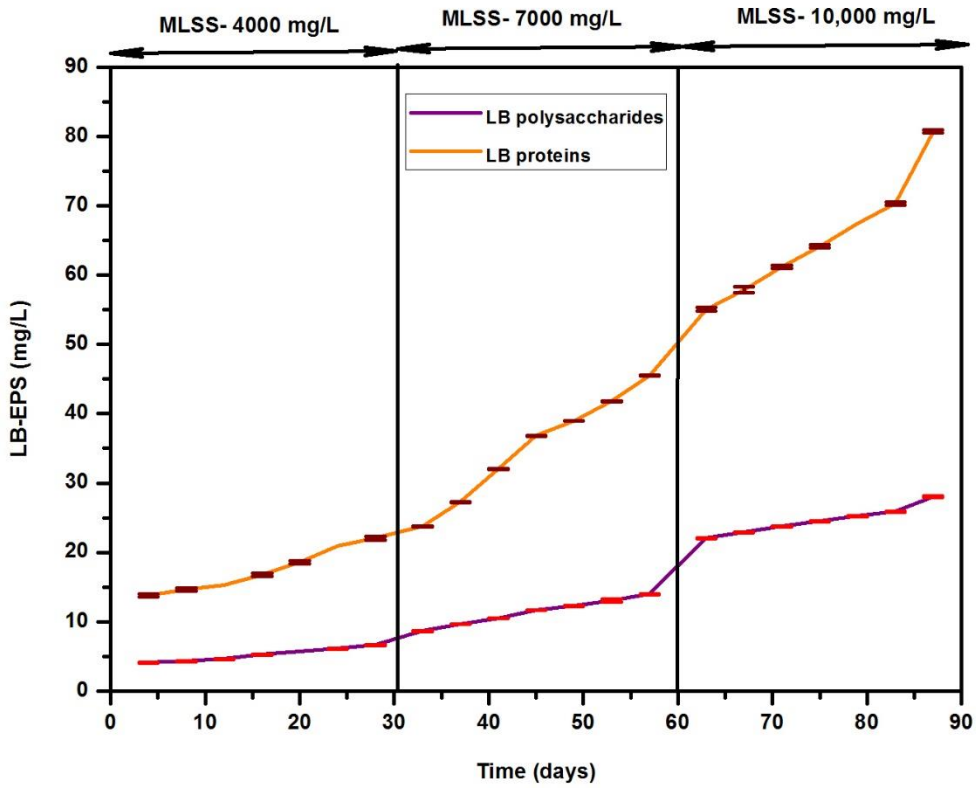

Figure 4.59 Loosely bound polysaccharides and proteins profile in the QQ-MBR operated at different MLSS

Although, the QQ-MBR possessed considerably higher LB-EPS polysaccharides and proteins at MLSS of 10,000 mg/L, it is comparatively lesser than that of control MBR. The QQ-MBR showed 64%, 63.1% and 52.2% lower LB-EPS polysaccharides and 62.2%, 63.4% and 59.5% lower LB-EPS proteins at MLSS 4000 mg/L, 7000 mg/L and 10,000 which could be due to the addition of QQ-IMN beads in QQ-MBR.

4.7.3.2.2 Tightly bound EPS

Figure 4.60 depicts the variation of TB polysaccharides and proteins in the QQ-MBR operated at different MLSS. The TB polysaccharides and proteins in the QQ-MBR varied in the range of 8 to 10.3 mg/L and 11.6 to 20.3 mg/L, respectively at MLSS 4000 mg/L. When compared with the control MBR, the QQ-MBR exhibited 75.3% and 63.2% lower TB polysaccharides and protein, respectively at MLSS 4000 mg/L. Further increase in MLSS resulted in the increase in the polysaccharides and proteins i.e. at MLSS of 7000 mg/L, the TB polysaccharides and proteins were recorded in the range of 16 to 22.9 mg/L and 8.6 to 13.9 mg/L, respectively. At this stage, around 69.7% and 57.3% lower TB polysaccharides and proteins was observed compared to the control MBR operated at MLSS of 7000 mg/L.

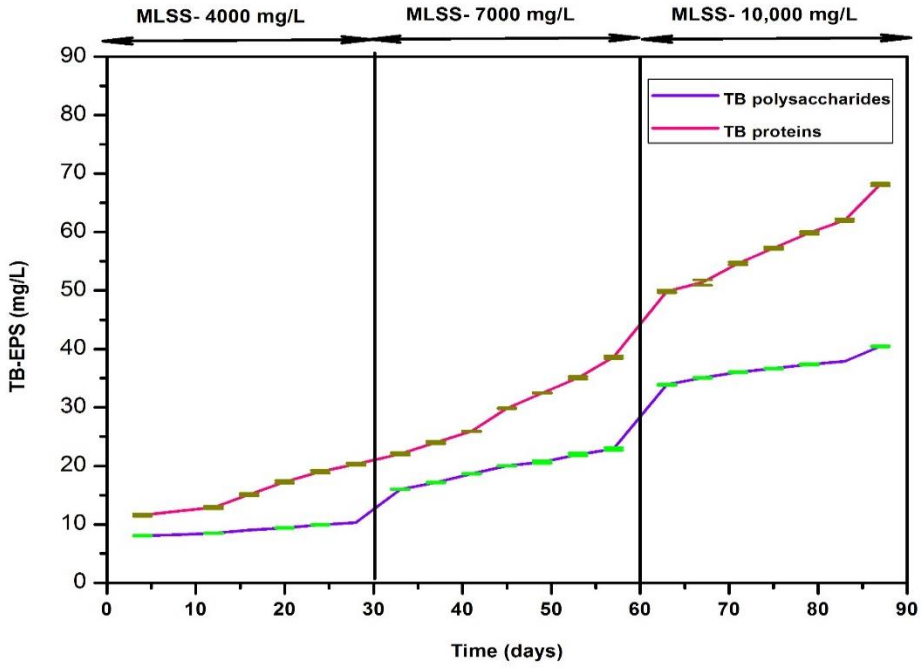

Figure 4.60 Tightly bound polysaccharides and proteins profile in the QQ-MBR operated at different MLSS

Further, the trend of TB polysaccharides and proteins was evaluated at MLSS of 10,000 mg/L and compared with the TB polysaccharides and proteins of the control MBR operated at the same MLSS. Around 57.3% and 42.7% decreased TB polysaccharides and proteins were observed in the QQ-MBR relative to control MBR. The ratio of PN/

PS of the TB in the QQ-MBR was about 1.7 at MLSS of 4000 mg/L which decreased to 1.5 at MLSS of 7000 mg/L. However, at 10,000 mg/L, no change in PN/ PS ratio was observed showing a value of around 1.5. The reduction in TB polysaccharides and protein fraction of TB-EPS were reported previously (Zhang *et al.*, 2009b). Nahm *et al.* (2017a) reported around 38% and 72% lower polysaccharide and protein concentration of TB-EPS in the QQ sheet MBR was seen compared to control MBR operated at MLSS of 4500 to 5000 mg/L. The reduced production of TB- EPS might be due to the QQ activity of the entrapped QQ bacteria.

4.7.3.1.3 Soluble EPS

The variation of soluble polysaccharides and proteins in QQ-MBR operated at different MLSS is depicted in Figure 4.61. It was found that the soluble polysaccharides at MLSS 4000 and 7000 mg/L decreased by 77% and 72.3%, respectively in the QQ-MBR compared to control MBR. Likewise, the soluble proteins decreased by 68.7% and 61.7%, respectively at MLSS 4000 and 7000 mg/L. The soluble polysaccharides and proteins at MLSS of 4000 mg/L were varied in the range of 5.3 to 7.5 mg/L and 8.1 to 16.6 mg/L, respectively. Continuous increase in soluble polysaccharides and proteins was observed with increase in MLSS. At 7000 and 10,000 mg/L, soluble polysaccharides were in the range of 9.9 to 15.5 mg/L and 23.4 to 29.5 mg/L, respectively. The soluble proteins showed a tremendous increase exhibiting a range of 18.5 to 32.9 mg/L and 42 to 63.3 mg/L at MLSS of 7000 and 10,000 mg/L, respectively. The soluble polysaccharides and proteins were however, comparatively lesser than control MBR operated at MLSS of 10,000 mg/L. At this MLSS, the soluble polysaccharides and proteins decreased by 60.7% and 40.3%, respectively compared to control MBR. The PN/PS ratio varied in the range between 1.92 to 2.01 at all the MLSS tested.

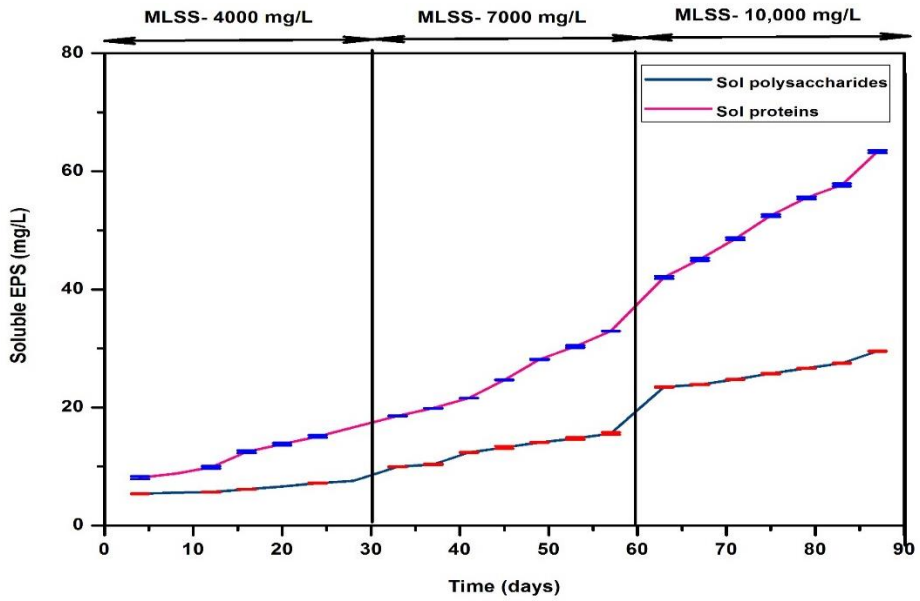

Figure 4.61 Soluble polysaccharides and proteins profile in the QQ-MBR operated at different MLSS

The results are in accordance with the previous study by Maqbool *et al.* (2015) and Lee *et al.* (2016b) who also reported reduction in soluble polysaccharides and proteins concentrations when compared to control MBR. Lee *et al.* (2016b) demonstrated the remarkable decrease of around 60% in the soluble EPS when *Rhodococcus* sp. BH4 immobilized beads was added into the MBR**.** According to Le-Clech *et al.* (2006), lesser the protein content in the soluble EPS, less is the hydrophobicity of the sludge flocs which causes decreased attachment of microbial flocs. So, the decrease in the soluble proteins compared to control specified less hydrophobicity of the sludge flocs thus indicating the inhibition of biofilm formation by QQ bacteria.

4.7.3.2.4 Overall EPS profile of mixed liquor in QQ- MBR

Figure 4.62 depicts the EPS profile of the QQ-MBR operated at different MLSS of 4000, 7000 and 10,000 mg/L. It can be seen from the Figure 4.62 that the amount of polysaccharides and proteins of all the three EPS were higher when MBR was operated at MLSS of 10,000 mg/L. The TB-EPS showed higher polysaccharides of around 36.1± 0.8 mg/L.

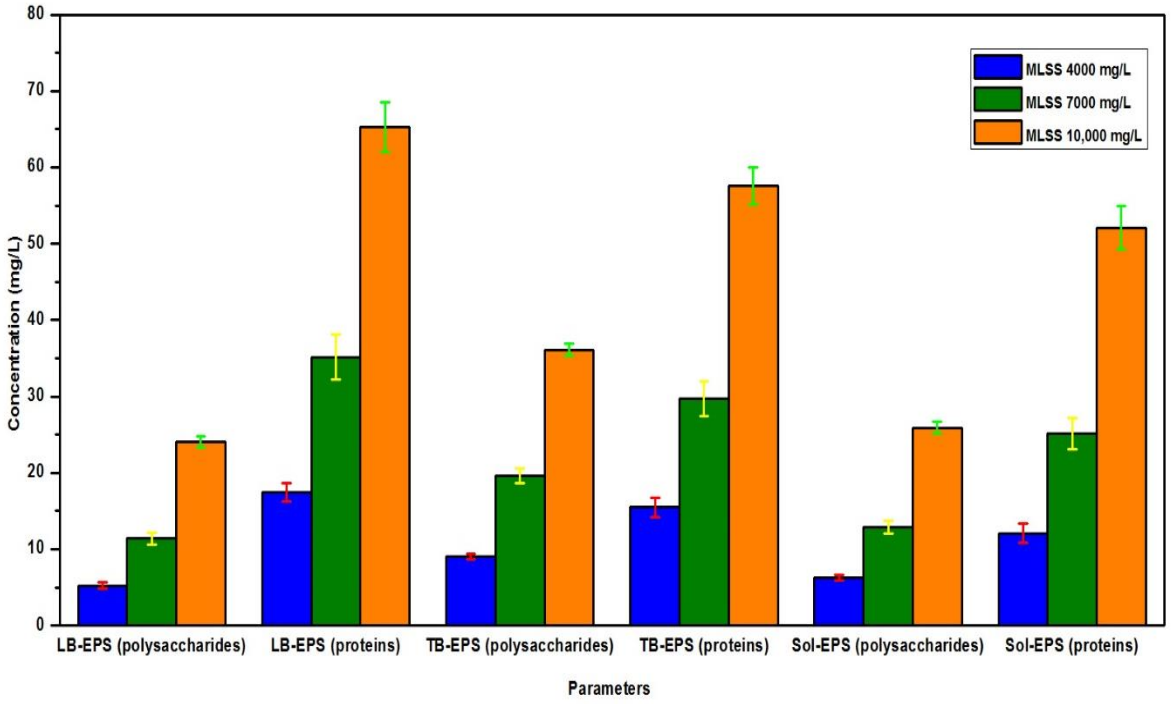

Figure 4.62 Composition of bound EPS (LB and TB) and soluble EPS profile in the QQ-MBR at different MLSS

The LB-EPS and soluble EPS however, exhibited polysaccharides concentration of around 24± 0.7 and 25.9± 0.8 mg/L, respectively. No significant difference was observed between LB-EPS and soluble EPS polysaccharides. The amount of proteins were higher in the LB-EPS (65.2± 3.2 mg/L) followed by TB-EPS (57.5± 2.4 mg/L) and soluble EPS (52± 2.8 mg/L), respectively.

CHAPTER V

SUMMARY AND CONCLUSIONS

5.1 Summary

Membrane bioreactors (MBR) that combines suspended growth reactors with the membrane processes is widely applied for the treatment of municipal and industrial wastewater. Compared to other existing wastewater treatment technologies such as activated sludge process, MBR produces high effluent quality that meet the stringent water quality requirements. Other advantages such as compact footprint and complete solid - liquid separation has led to its growth in the market. Membrane fouling hinders the extensive application of MBR in wastewater treatment. Fouling occurs as a result of the interaction between the membrane material and components of mixed liquor (colloids, soluble compounds along with the biological flocs formed by the micro-organisms). TMP increase, membrane flux decline, reduction in permeate yield and increased operational cost are some of the consequences of membrane fouling. Among the different types of fouling, viz. particulate, biofouling, organic and inorganic fouling, biofouling is acknowledged as a major contributor to the membrane fouling process.

Biofilm formation is an outcome of cross communication through the exchange of signal molecules by a phenomenon termed as quorum sensing (QS). Acyl homoserine lactone (AHL) is the main signalling molecule involved in biofilm formation. Though, an array of conventional methods such as physical and chemical cleaning, modification of sludge characteristics, membrane surface modification, and optimization of operating conditions are developed to mitigate the membrane fouling, they do not prove to be an effective measure to control biofouling contributed through biofilm formation. Recently, a new biological method was developed to quench these AHL and other signal molecules using a special group of bacteria termed the quorum quenching (QQ) bacteria and the process termed as quorum quenching. QQ is done using enzymes (acylase and lactonase) or QQ bacteria.

In the present study, the efficiency of QQ bacteria isolated from dairy waste activated sludge (WAS) was evaluated for its potential in controlling biofouling in MBR. The dairy WAS collected from effluent treatment plant of Verka milk industry,

Bathinda, Punjab was screened for the indigenous QQ bacteria. About five QQ bacteria were isolated after enrichment in n-hexanoyl homoserine lactone (C6-HSL) containing KG medium and were identified as *Klebsiella pneumoniae* JYQ1 and JYQ5 (KP189202 and KP780263, respectively), *Acinetobacter baumannii* JYQ2 (KP340458), *Pseudomonas nitroreducens* JYQ3 (KP340459); and *Pseudomonas* JYQ4 (KU555415) through biochemical and molecular identification. The ability of isolates to degrade AHL molecule C6-HSL was confirmed through AHL inactivation assay. All the five isolates degraded the C6-HSL which was confirmed qualitatively through appearance of colourless zone around the *Chromobacterium violaceum* CV026 spotted lawns. The C6-HSL degradation determined quantitatively with GC-MS analysis showed that *Pseudomonas* JYQ4 possessed highest degradation percentage of 83.8% within 6 h of incubation. The other isolates showed maximum degradation of 81.5% (*Klebsiella pneumoniae* JYQ1), 76.8% (*Acinetobacter baumannii* JYQ2) and 81.4% (*Klebsiella pneumoniae* JYQ5) at 24 h and; 68.4% (*Pseudomonas nitroreducens* JYQ3) at 12 h of incubation time.

Three among five QQ bacteria namely *Acinetobacter baumannii* JYQ2, *Pseudomonas nitroreducens* JYQ3 and *Pseudomonas* JYQ4 were selected and immobilized onto the magnetic iron nanocomposite beads which was prepared by encapsulating QQ bacteria in the mixture of magnetic iron nanoparticles and sodium alginate. The magnetic iron nanoparticles so prepared by co-precipitation of ferrous and ferric chloride were cubical in shape with the size ranging from 5-19 nm. The XRD analysis confirmed the magnetite phase of magnetic iron nanoparticles. The magnetic iron nanoparticles possessed saturation magnetization of 39 emu g^{-1} which was sufficient enough to facilitate separation of the IMN beads from the MBR. The SEM analysis of QQ bacteria IMN beads showed the appearance of almost round to rod shaped bacteria within the individual beads indicating their successful immobilization within the IMN beads.

The ability of QQ bacteria IMN beads in C6-HSL degradation was evaluated through disappearance of purple pigment in flasks inoculated with the biosensor strain *Chromobacterium violaceum* CV2656. All the three tested QQ bacteria, *Acinetobacter baumannii* JYQ2, *Pseudomonas nitroreducens* JYQ3 and *Pseudomonas* JYQ4 IMN beads and consortium of three bacterial isolates did not show any purple colouration when compared to control. Quantitative estimation of

C6-HSL degradation by QQ bacteria IMN beads evaluated through GC-MS analysis showed that *Pseudomonas* JYQ4 IMN beads showed maximum degradation percentage of 90% in 6 h. Other isolates i.e., *Acinetobacter baumannii* JYQ2, *Pseudomonas nitroreducens* JYQ3 and consortium showed a C6-HSL degradation of 75.6%, 73% and 73.9%, respectively. However, *Acinetobacter baumannii* JYQ2 exhibited fluctuations in degradation efficiency in free and immobilized form due to its ability to possess QS and QQ activity.

The efficiency of QQ bacteria IMN beads in controlling the biofilm formation on cellulose acetate membranes formed by *Pseudomonas aeruginosa* 3541 was evaluated. The experimental set up was designated as C_1 (control 1 without IMN beads), C_2 (control 2 blank nanoparticle beads), C_3 (*Acinetobacter baumannii* JYQ2 IMN beads), C_4 (*Pseudomonas nitroreducens* JYQ3 IMN beads), C_5 (*Pseudomonas* JYQ4 IMN beads), C_6 (consortium of JYQ2, JYQ3 and JYQ4 IMN beads) and C_7 (*Bacillus cereus* 1306 IMN beads). The SEM analysis of membranes revealed that less number of bacterial cells were attached to the membrane incubated with QQ bacteria IMN beads when compared to control. However, among the different QQ IMN beads, the *Pseudomonas* JYQ4 IMN beads exhibited better biofilm controlling ability. The biofilm growth evaluated by CLSM analysis showed that *Pseudomonas* JYQ4 IMN beads delayed the biofilm maturation till 30 days when compared to control that showed *Pseudomonas aeruginosa* 3541 biofilm maturation within 10 days of incubation. Isolate *Pseudomonas nitroreducens* JYQ3 incubated membrane showed biofilm maturation in 30 days whereas on *Acinetobacter baumannii* JYQ2 and consortium incubated membranes, signs of biofilm maturation appeared within 20 days of incubation. COMSTAT analysis of biofilm structure too confirmed the biofilm controlling ability of *Pseudomonas* JYQ4 IMN beads showing a biomass volume of 0.015± 0.001 $\mu m^3/\mu^2$ and surface to biovolume ratio of 0.93± 0.003 $\mu m^2/\mu^3$ when compared to control membrane which showed more biomass volume (0.06± 0.003 $\mu m^3/\mu^2$) and less surface to biovolume ratio (0.21± 0.005 $\mu m^2/\mu^3$). Higher surface to biovolume ratio and less biomass volume indicates the formation of single cells and small cell clusters. Other isolates *Acinetobacter baumannii* JYQ2, *Pseudomonas nitroreducens* JYQ3 and consortium incubated membranes showed biomass volume of 0.041± 0.0005 $\mu m^3/\mu^2$, 0.02± 0.0003 $\mu m^3/\mu^2$ and 0.04± 0.003 $\mu m^3/\mu^2$, respectively and surface to biovolume ratio of 0.61± 0.02 $\mu m^2/\mu^3$, 0.88±

0.005 $\mu m^2/\mu^3$ and 0.70± 0.003 $\mu m^2/\mu^3$, respectively. The delay in membrane fouling was also confirmed through flux studies. The flux of the IMN beads incubated membranes showed higher flux than control membrane. *Pseudomonas* JYQ4 IMN beads incubated membrane showed around 20.3% higher flux followed by *Pseudomonas nitroreducens* JYQ3 (17.7% higher flux), *Acinetobacter baumannii* JYQ2 (10.4% higher flux) and consortium (8.1% higher flux) when compared to control membrane.

The inhibition of biofilm developed by the sludge bacteria on the glass slides and membrane surface was also studied. The results were comparable to *Pseudomonas aeruginosa* 3541 biofilm studies. The light microscopy analysis of the QQ bacteria IMN beads incubated glass slides reveled few bacterial cells on the surface when compared to control. Among the different QQ bacteria IMN beads, *Pseudomonas* JYQ4 IMN beads showed efficient biofilm reduction ability. The detailed analysis of biofilm developed on the membranes incubated with QQ IMN beads further revealed delay in biofilm maturation. The control membrane showed biofilm maturation in 10 days. On the other hand, QQ IMN beads incubated membrane showed delay in biofilm maturation. *Pseudomonas* JYQ4 IMN beads was more effective among the other three QQ IMN beads which is evident from its ability to prevent biofilm maturation till 30 days. The membranes incubated with *Pseudomonas nitroreducens* JYQ3 IMN beads showed maturated sludge bacteria biofilm in 30 days. On the contrary, the membranes incubated with IMN beads of other isolates (i.e.) *Acinetobacter baumannii* JYQ2 and consortium showed matured biofilm within 20 days. COMSTAT analysis also supported the biofilm controlling potential of QQ IMN beads. The biomass volume and surface to biovolume ratio of sludge bacteria developed on the *Pseudomonas* JYQ4 IMN beads was 0.019± 0.015 $\mu m^3/\mu^2$ and 0.85± 0.65 $\mu m^2/\mu^3$, respectively. Nevertheless, control 1 (without IMN beads) incubated membranes, showed sludge bacteria biomass volume and surface to biovolume ratio of 0.065± 0.061 $\mu m^3/\mu^2$ and 0.18± 0.14 $\mu m^2/\mu^3$, respectively whereas control 2 (blank nanoparticle beads) incubated membranes showed biomass volume of 0.06± 0.02 $\mu m^3/\mu^2$ and surface to biovolume ratio of 0.16± 0.38 $\mu m^2/\mu^3$. Other isolates *Acinetobacter baumannii* JYQ2, *Pseudomonas nitroreducens* JYQ3 and consortium incubated membranes showed surface to biovolume ratio of 0.65± 0.53 $\mu m^2/\mu^3$, 0.75± 0.56 $\mu m^2/\mu^3$ and 0.57± 0.45 $\mu m^2/\mu^3$, respectively and biomass

volume of 0.035± 0.031 $\mu m^3/\mu^2$, 0.032± 0.027 $\mu m^3/\mu^2$ and 0.036± 0.032 $\mu m^3/\mu^2$, respectively. The flux studies showed that *Pseudomonas* JYQ4 IMN beads incubated membranes showed 22% higher flux when compared to control. *Pseudomonas nitroreducens* JYQ3, *Acinetobacter baumannii* JYQ2 and consortium also exhibited 19%, 16% and 12.6%, respectively higher flux compared to control membrane within 30 days incubation. The flux profile of *Bacillus cereus* incubated membrane was similar to that of *Pseudomonas* JYQ4 incubated membranes.

The biofouling controlling potential of QQ bacteria IMN beads was examined in MBR. A submerged MBR with polyethersulfone hollow fiber membrane module (pore size 0.4 µm) was operated at three different MLSS (4000, 7000 and 10,000 mg/L). The MBR was run at filtration mode of 10 min 'On' and 2 min 'cut off' and HRT of 8 h. The MBR was fed with synthetic dairy industry wastewater of pH 7.2± 0.1 and COD of 4800± 40 mg/L. The performance of control and QQ-MBR at different MLSS is summarized in Table 5.1. The MBR showed high removal efficiency when operated at MLSS of 10,000 mg/L compared to its operation at 4000 and 7000 mg/L. The maximum COD and TSS removal efficiency of 99.2% and 88.4%, respectively was attained during operation of QQ-MBR at 10,000 mg/L. The effluent quality of control and QQ-MBR are comparable and is almost similar.

The membrane fouling in MBR was assessed through EPS- tightly bound (TB) polysaccharides and proteins; loosely bound (LB) polysaccharides and proteins; and soluble polysaccharides and proteins. The TMP increased from 0.5 to 13.5 KPa at MLSS of 4000 mg/L and to 21.7 kPa and 29.8 kPa at 7000 and 10,000 mg/L MLSS, respectively. The rapid increase of TMP in control MBR was due to membrane biofouling. The LB-EPS, TB-EPS and soluble EPS polysaccharides were in the range of 11.7- 17.7 mg/L, 32- 42.6 mg/L and 23.4- 31.8 mg/L, respectively at MLSS 4000 mg/L; 25.5- 36.2 mg/L, 59.9- 71.3 mg/L and 40.2- 53.2 mg/L, respectively at 7000 mg/L MLSS; and 40.4- 58.5 mg/L, 76.6- 92.6 mg/L and 56.4- 72.3 mg/L, respectively at MLSS 10,000 mg/L. Likewise, the LB-EPS, TB- EPS and soluble EPS proteins were 38.5- 56.1 mg/L, 34.2- 50.7 mg/L and 30.3- 48.1 mg/L, respectively at 4000 mg/L MLSS; 81.1- 115.9 mg/L, 61.6- 80.3 mg/ and 56.3- 75 mg/L, respectively at MLSS of 7000 mg/L; and 124.6- 186.5 mg/L, 85.9- 115.9 mg/L and 77.9- 101.1 mg/L, respectively at 10,000 mg/L MLSS.

Table 5.1 Performance of control and QQ-MBR operated at different MLSS

Operation of MBR		Control			QQ-MBR		
MLSS		4000 mg/L	7000 mg/L	10,000 mg/L	4000 mg/L	7000 mg/L	10,000 mg/L
Effluent quality parameters Removal efficiency (%)	COD	95.6-96.6	96.5- 97.5	98.2- 99.2	95.6- 96.6	96.4- 97.4	98.2- 99.1
	TS	20.9- 21.9	30.2- 30.8	36.6- 37	21.9- 22.8	30.6- 30.9	39.1- 39.7
	TDS	5.5- 5.85	7.3- 7.45	18.1- 18.6	5.3- 5.9	8.7- 9.1	18.9- 19.4
	TSS	55.7-57.6	75.6-77	87.1- 88.4	57.3- 58.3	78- 79.2	89.3- 90.6
	VS	70.5-71.3	81-81.25	90.3-90.8	70.1- 71.1	81.3- 82.1	91.1- 91.7
	TKN	88- 90.3	92- 93.2	93- 95	89.2- 90.1	92- 93.2	94.1- 95.1
	NH_3-N	93.6-93.9	94.3- 94.6	94.4-94.5	93.6- 93.7	94.3- 94.6	94.4- 94.6
	Phosphate	25.5-26.7	30.1- 31.2	32.3- 33.2	26.2- 27	31- 31.3	33- 33.6

Sludge characteristics	MLSS (mg/L)	3960- 4050	6986- 7008	9986- 10003	3892- 4032	6998- 7062	9982- 10006
	MLVSS (mg/L)	3200- 3626	5899- 6356	8500- 9006	3050- 3701	6000- 6400	8900- 9000
	SVI (mL/g)	90	98	100	85	92	95
Membrane fouling	TB polysaccharides (mg/L)	32- 42.6	59.9- 71.3	76.6- 92.6	8- 10.3	16- 22.9	33.8- 40.4
	TB proteins (mg/L)	34.2- 50.7	61.6- 80.3	85.9- 115.9	11.6- 20.3	22- 38.5	49.8- 68.1
	LB polysaccharides (mg/L)	11.7- 17.7	25.5- 36.2	40.4- 58.5	4- 6.6	8.6- 13.9	22- 28
	LB proteins (mg/L)	38.5- 56.1	81.1- 115.9	124.6- 186.5	13.7- 22	23.7- 45.5	55- 80.7
	Soluble polysaccharides (mg/L)	23.4-31.8	40.2- 53.2	56.4- 72.3	5.3- 7.5	9.9- 15.5	23.4- 29.5
	Soluble proteins (mg/L)	30.3- 48.1	56.3- 75	77.9- 101.1	8.1- 16.6	18.5- 32.9	42- 63.3
	TMP (KPa)	0.5- 13.5	14- 21.7	22- 29.8	0.4- 2.1	2.1- 10.5	11.8- 27

The protein component was high in all type of EPS (i.e.) TB-EPS, LB-EPS and soluble EPS. Higher the protein concentration, faster is the rate of fouling.

Among the three QQ bacteria IMN beads, the *Pseudomonas nitroreducens* JYQ3 and *Pseudomonas* JYQ4 IMN beads were selected to investigate their ability in mitigating membrane biofouling in MBR treating dairy wastewater. The QQ-MBR loaded with QQ bacteria IMN beads showed almost similar effluent quality at the MLSS of 4000, 7000 and 10,000 mg/L. The SVI of the QQ-MBR sludge varied between 85- 95 mL/g. The QQ IMN beads showed no influence on effluent quality and sludge characteristics. However, the fouling behavior in QQ-MBR varied from control MBR. At MLSS 4000 mg/L, the TMP increase was delayed by 60 days indicating the extension of biofouling control potential of QQ bacteria. The TB-EPS polysaccharides and proteins decreased by 75.3% and 63.2% in QQ-MBR when compared to control. Similarly, 64% and 62.2%; and 77% and 68.7% reduction in LB-EPS polysaccharides and proteins; and soluble EPS polysaccharides and proteins, respectively was observed. At 7000 mg/L MLSS, the LB-EPS polysaccharides and proteins reduced by 63.1% and 63.4%, respectively and TB-EPS polysaccharides and proteins reduced by 69.7% and 57.3%, respectively. Similarly the soluble EPS polysaccharides and proteins showed a reduction of 72.3% and 61.7%, respectively compared to control MBR. With increase in MLSS to 10,000 mg/L, around 52.2% and 59.5% decrease in LB-EPS polysaccharides and proteins, respectively; and 57.3% and 42.7% in TB-EPS polysaccharides and proteins fractions, respectively was seen. The soluble EPS polysaccharides and proteins decreased by 60.7% and 40.3%, respectively compared to control MBR.

In conclusion, the *Pseudomonas* JYQ4 showed good degradation of C6-HSL in both free and immobilized state. Further, *Pseudomonas* JYQ4 IMN beads prevented the formation of matured biofilm developed by *Pseudomonas aeruginosa* 3541 and sludge bacteria. In QQ-MBR, *Pseudomonas* JYQ4 IMN beads successfully delayed the membrane biofouling.

5.2 Conclusions

The present study has revealed that the dairy waste activated sludge harbors quorum quenching bacteria that has the potential to degrade signaling molecules. In MBR, the effectiveness of QQ bacteria for membrane biofouling mitigation was further appraised through EPS reduction (both polysaccharides and proteins) which is evidenced in delay in TMP rise. In details, the major conclusions of the study includes:

- *Klebsiella pneumoniae* (JYQ1 and JYQ5), *Acinetobacter baumannii* JYQ2, *Pseudomonas nitroreducens* JYQ3 and *Pseudomonas* JYQ4 were the QQ bacteria isolated from dairy WAS. All isolates possessed an inherent ability to degrade C6-HSL.
- The strain *Pseudomonas* JYQ4 exhibited highest QQ activity of 84±3.3% within 6th h of incubation compared to all other isolated QQ bacteria.
- The magnetic iron nanoparticle prepared by co-precipitation were cubical in shape with the size ranging between 5-19 nm. The magnetic strength of the magnetic iron nanoparticles was 39 emu g^{-1} that is adequate to enable easy separation of QQ bacteria IMN beads from the bioreactors.
- *Pseudomonas* JYQ4 when immobilized in IMN beads again found to be more efficient in degrading C6-HSL which is evident from its highest QQ activity of 90±0.02% within 6 h of incubation when compared to other isolates.
- The strain *Acinetobacter baumannii* JYQ2 acted as both QS and QQ bacteria as evidenced by decrease in QQ percentage from 79±3.1% to 76.8±2.5% thus limiting its C6-HSL degrading ability.
- QQ activity studies of IMN beads conducted in batch experiments demonstrated that *Pseudomonas* JYQ4 IMN beads were effective in delaying *Pseudomonas aeruginosa* 3541 and sludge bacteria biofilm maturation till 30 days compared to control membranes which exhibited signs of biofilm maturation in 10 days.
- Other isolates such as *Acinetobacter baumannii* JYQ2 and consortium IMN beads incubated membranes showed onset of maturation of *Pseudomonas aeruginosa* 3541 and sludge bacteria biofilm in 20 days. Contrary, the biofilm of *Pseudomonas*

aeruginosa 3541 and sludge bacteria showed signs of delayed maturation (i.e.) in 30 days when incubated with *Pseudomonas nitroreducens* JYQ3 IMN beads.

- The incubation of membranes with biofilm forming bacteria *Pseudomonas aeruginosa* 3541 and IMN beads of *Pseudomonas* JYQ4 showed 70% flux decline, followed by *Acinetobacter baumannii* JYQ2 (78.7%), *Pseudomonas nitroreducens* JYQ3 (72.3%) and consortium (80.7%) IMN beads incubated membranes as compared to control membranes that showed flux decline of 87.9%.
- The flux studies of sludge bacteria and *Pseudomonas* JYQ4 IMN beads incubated membranes showed 22% higher flux compared to control in 30 days incubation. Other isolates *Acinetobacter baumannii* JYQ2, *Pseudomonas nitroreducens* JYQ3 and consortium IMN beads incubated membranes exhibited 16%, 19% and 12.6% higher flux, respectively compared to control membranes.
- The QQ bacteria IMN beads was equally effective in controlling both *Pseudomonas aeruginosa* 3541 and sludge bacteria biofilm.
- In MBR studies, the QQ-MBR with QQ bacteria (*Pseudomonas nitroreducens* JYQ3 and *Pseudomonas* JYQ4) IMN beads did not show any negative effect on effluent quality and showed nearly similar effluent quality and sludge characteristics as that of control MBR (99.2% COD removal, 95% TKN removal and 88.4% TSS removal).
- In membrane fouling investigations, the severe fouling was observed in control MBR operated at MLSS of 10,000 mg/L showing TB-EPS, LB-EPS and soluble EPS polysaccharides of 92.6 mg/L, 58.5 mg/L and 72.3 mg/L, respectively. Likewise, the protein fraction of the TB-EPS, LB-EPS and soluble EPS was found to be around 115.9 mg/L, 186.5 and 101.1 mg/L, respectively. Moreover, EPS protein fraction was higher than polysaccharide fraction indicating the faster rate of fouling.
- Compared to control, in QQ-MBR, membrane fouling behaviour was different at all the MLSS studied (4000, 7000 and 10,000 mg/L). The polysaccharide of TB-EPS, LB-EPS and soluble EPS reduced by 75.3%, 64% and 77%, respectively at 4000 mg/L MLSS when compared to control MBR. The proteins too decreased by 63.2%, 62.2% and 68.7% in TB-EPS, LB-EPS and soluble EPS, respectively.

- At 7000 mg/L, polysaccharides and protein reduction of around 69.7%, 63.1% and 72.3%; and 57.3%, 63.4% and 61.7%, respectively was observed in TB-EPS, LB-EPS and soluble EPS, respectively. QQ-MBR when operated at MLSS 10,000 mg/L however showed lesser reduction in polysaccharide (57.3%, 52.2% and 60.7%) and protein (42.7%, 59.5% and 40.3%) fraction of TB-EPS, LB-EPS and soluble EPS when compared to MLSS of 4000 and 7000 mg/L.
- QQ-MBR also delayed the TMP rise by 60 days when operated at MLSS 4000 mg/L and by 30 days at 7000 and 10,000 mg/L MLSS as compared to control, thereby, indicating better fouling control efficiency.

5.3 Future perspectives:

1) The identification of QQ bacterial community in the MBR sludge can be studied using high end sequencing.
2) A detailed, continuous and long term evaluation of QQ bacteria IMN beads in controlling MBR fouling performance is required.
3) Immobilization of QQ bacteria on the membrane surface and its efficiency in fouling control can be investigated.
4) More detailed study evaluating the stability of IMN beads is required.

REFERENCES

Abdalla, M.A., Jaafar, M.H., Al-Othman, Z.A., Alfadul, S.M. and Khan, M.A. (2011). New route for preparation and characterization of magnetite nanoparticles. *Arabian Journal of Chemistry* **4**(2): 235-237.

Abdessemed, D., Adin, A. and Aim, R.B. (1998). Coupling flocculation with micro-ultrafiltration for waste water treatment and reuse. *Desalination* **118**(1): 323-323.

Adav, S.S., Lee, D.J. and Lai, J.Y. (2010). Potential cause of aerobic granular sludge breakdown at high organic loading rates. *Applied Microbiology and Biotechnology* **85**(5): 1601-1610.

Adham, S., Gagliardo, P., Boulos, L., Oppenheimer, J. and Trussell, R. (2001). Feasibility of the membrane bioreactor process for water reclamation. *Water Science & Technology* **43**(10): 203-209.

Adyasari, D. (2014). Municipal wastewater treatment using salsnes filter and hollow fiber membrane bioreactor (HMFB). Master's thesis, University of Stavanger, Norway.

Ahmed, Z., Cho, J., Lim, B.R., Song, K.G. and Ahn, K.H. (2007). Effects of sludge retention time on membrane fouling and microbial community structure in a membrane bioreactor. *Journal of Membrane Science* **287**(2): 211-218.

Ahn, K.H., Song, J.H. and Cha, H.Y. (1998). Application of tubular ceramic membranes for reuse of wastewater from buildings. *Water Science & Technology* **38**(4-5): 373-382.

Aim, R.B. and Semmens, M.J. (2003). Membrane bioreactors for wastewater treatment and reuse: a success story. *Water Science and Technology* **47**(1): 1-5.

Alaboud, T.M. (2009). Membrane bioreactor for wastewater reclamation-pilot plant study in Jeddah, Saudi Arabia. *Research Journal of Environmental Sci*ences **3**(2): 267-277.

Al-Hussaini, R. and Mahasneh, A.M. (2009). Microbial growth and quorum sensing antagonist activities of herbal plant extracts. *Molecules* **14**(9): 3425-3435.

Alnaizy, R., Aidan, A. and Luo, H. (2011). Performance assessment of a pilot-size vacuum rotation membrane bioreactor treating urban wastewater. *Applied Water Science* **1**(3-4): 103-110.

Alymanesh, M.R., Taheri, P. and Tarighi, S. (2016). *Pseudomonas* as a frequent and important quorum quenching bacterium with biocontrol capability against many phytopathogens. *Biocontrol Science and Technology* **26**(12): 1719-1735.

Amoudi, A.A. and Lovitt, R.W. (2007). Fouling strategies and the cleaning system of NF membranes and factors affecting cleaning efficiency. *Journal of Membrane Science* **303**(1-2): 4-28.

Andrade, L.H., Motta, G.E. and Amaral, M.C.S. (2013). Treatment of dairy wastewater with a membrane bioreactor. *Brazilian Journal of Chemical Engineering* **30**(4): 759-770.

Anitha, K. and Mahalakshmi, T. (2012). Screening of south Indian herbs for quorum quenching property. *International Journal of Pharma and Bio Sciences* **3**(4): 974-979.

APHA (2012). Standard method for the examination of water and wastewater. 22nd Edition American Public Health Association, AWWA, Washington DC, USA.

Arumugam, A. and Sabarethinam, P.L. (2008). Performance of a three-phase fluidized bed reactor with different support particles in treatment of dairy wastewater. *ARPN Journal of Engineering and Applied Sciences* **3:** 42-44.

Asatekin, A., Kang, S., Elimelech, M. and Mayes, A.M. (2007). Anti-fouling ultrafiltration membranes containing polyacrylonitrile-graft-poly(ethylene oxide) comb copolymer additives. *Journal of Membrane Science* **298**(1-2): 136-146.

Aydin, B. and Civelekoglu, G. (2010). Effects of ultrasonic treatment on the waste activated sludge. *Journal of Engineering Science and Design* **1**(1): 28-32.

Bae, T.H. and Tak, T.M. (2005a). Effect of TiO_2 nanoparticles on fouling mitigation of ultrafiltration membranes for activated sludge filtration. *Journal of Membrane Science* **249**(1-2): 1-8.

Bae, T.H. and Tak, T.M. (2005b). Preparation of TiO_2 self-assembled polymeric nanocomposite membranes and examination of their fouling mitigation effects in a membrane bioreactor system. *Journal of Membrane Science* **266**(1-2): 1-5.

Balakumar, S., Mahalakshmi, T. and Jeyanthi, A. (2010). Inhibition of N-acyl homoserine lactone mediated quorum sensing in *Pseudomonas aeruginosa* by *Phyllanthus emblica* and *Quercus infectoria*. *Journal of Pharmaceutical Sciences and Research* **2**(8): 521-526.

Barker, D.J. and Stuckey, D.C. (1999). A review of soluble microbial products (SMP) in wastewater treatment systems. *Water Research* **33**(14): 3063-3082.

Basri, H., Ismail, A.F., Aziz, M., Nagai, K., Matsuura, T., Abdullah, M.S. and Ng, B.C. (2010). Silver-filled polyethersulfone membranes for antibacterial applications- Effect of PVP and TAP addition on silver dispersion. *Desalination* **261**(3): 264-271.

Benefield, L.D. and Randall, C.W. (1981). Biological process design for wastewater treatment. Prentice Hall, Englewood Cliffs.

Beyenal, H., Donovan, C., Lewandowski, Z. and Harkin, G. (2004). Three-dimensional biofilm structure quantification. *Journal of Microbiological Methods* **59**(3): 395-413.

Bhattacharya, A. and Misra, B.N. (2004). Grafting: a versatile means to modify polymers techniques, factors and applications. *Progress in Polymer Science* **29**(8): 767-814.

Bin, Z., Baosheng, S., Min, J., Taishi, G. and Zhenghong, G. (2008). Extraction and analysis of extracellular polymeric substances in membrane fouling in submerged MBR. *Desalination* **227**(1-3): 286-294.

Bitton, G. (2005). *Wastewater Microbiology*, pp. 225. John Wiley & Sons, Hoboken, New Jersey.

Boonyungyuen, W. and Wichitsathian, B. (2014). Effect of activated carbon addition with enhance performance on a membrane bioreactor (MBR). *Journal of Clean Energy Technologies* **2**(2): 122-125.

Boributh, S., Chanachai, A. and Jiraratananon, R. (2009). Modification of PVDF membrane by chitosan solution for reducing protein fouling. *Journal of Membrane Science* **342**(1-2): 97-104.

Bougrier, C., Albasi, C., Delgenes, J.P. and Carrere (2006). Effect of ultrasonic, thermal and ozone pre-treatments on waste activated sludge solubilisation and anaerobic biodegradability. *Chemical Engineering and Processing: Process Intensification* **45**(8): 711-718.

Bouhabila, E.H., Aim, R.B. and Buisson, H. (1998). Microfiltration of activated sludge using submerged membrane with air bubbling (application to wastewater treatment). *Desalination* **118**(1-3): 315-322.

Bouhabila, E.H., Aim, R.B. and Buisson, H. (2001). Fouling characterisation in membrane bioreactors. *Separation and Purification Technology* **22-23:** 123-132.

Braak, E., Alliet, M., Schetrite, S. and Albasi, C. (2011). Aeration and hydrodynamics in submerged membrane bioreactors. *Journal of Membrane Science* **379**(1-2): 1-18.

Bradford, M.M. (1976). A rapid and sensitive method for the quantitation of microgram quantities of protein utilizing the principle of protein-dye binding. *Analytical Biochemistry* **72**(1-2): 248-254.

Braguglia, C.M., Gianico, A. and Mininni, G. (2012). Comparison between ozone and ultrasound disintegration on sludge anaerobic digestion. *Journal of Environmental Management* **95:** S139-S143.

Brooun, A., Liu, S. and Lewis, K. (2000). A dose-response study of antibiotic resistance in *Pseudomonas aeruginosa* biofilms. *Antimicrobial Agents and Chemotherapy* **44**(3): 640-646.

Bryjak, M., Gancarz, I., Pozniak, G. and Tylus, W. (2002). Modification of polysulfone membranes 4. Ammonia plasma treatment. *European Polymer Journal* **38**(4): 717-726.

Burdman, S., Jurkevitch, E., Soria-Díaz, M.E., Serrano, A.M.G. and Okon, Y. (2000). Extracellular polysaccharide composition of *Azospirillum brasilense* and its relation with cell aggregation. *FEMS Microbiology Letters* **189**(2): 259-264.

Bureau of Indian Standards (1989). Method of sampling and test (physical and chemical) for water and wastewater. IS: 3025 (Part 34).

Campbell, P., Srinivasan, R., Knoell, T., Phipps, D., Ishida, K., Safarik, J., Cormack, T. and Ridgway, H. (1999). Quantitative Structure-Activity Relationship (QSAR) analysis of surfactants influencing attachment of a *Mycobacterium* sp. to cellulose acetate and aromatic polyamide reverse osmosis membranes. *Biotechnology and Bioengineering* **64**(5): 527-544.

Carp, O., Huisman, C.L. and Reller, A. (2004). Photoinduced reactivity of titanium dioxide. *Progress in Solid State Chemistry* **32**(1-2): 33-177.

Cataldi, T.R.I., Bianco, G., Frommberger, M. and Schmitt-Kopplin, P. (2004). Direct analysis of selected N-acyl-L-homoserine lactones by gas chromatography/mass spectrometry. *Rapid Communications in Mass Spectrometry* **18**(12): 1341-1344.

Cescutti, P., Toffanin, R., Pollesello, P. and Sutherland, I.W. (1999). Structural determination of the acidic exopolysaccharide produced by a *Pseudomonas* sp. strain 1.15. *Carbohydrate Research* **315**(1-2): 159-168.

Chan, K.G., Atkinson, S., Mathee, K., Sam, C.K., Chhabra, S.R., Camara, M., Koh, C.L. and Williams, P. (2011). Characterization of n-acyl homoserine lactone-degrading bacteria associated with the *Zingiber officinale* (ginger) rhizosphere: Co-existence of quorum quenching and quorum sensing in *Acinetobacter* and *Burkholderia*. *BMC Microbiology* **11**(51): 1-13.

Chan, K.G., Cheng, H.J., Chen, J.W., Ying, W.F. and Ngeow, Y.F. (2014a). Tandem mass spectrometry detection of quorum sensing activity in multidrug resistant

clinical isolate *Acinetobacter baumannii*. *The Scientific World Journal* **2014:**1-6.

Chan, K.G., Tuez, S.Z. and Ng, C.C. (2007). Rapid isolation method of soil bacilli and screening of their quorum quenching activity. *Asia Pacific Journal of Molecular Biology and Biotechnology* **15**(3): 153-156.

Chan, K.G., Wong, C.S., Yin, W.F. and Chan, X.Y. (2014b). Draft genome sequence of quorum-sensing and quorum-quenching *Pseudomonas aeruginosa* strain MW3a. *Genome Announcements* **2**(2): 1-2.

Chan, K.G., Yin, W.F., Sam, C.K. and Koh, C.L. (2009). A novel medium for the isolation of N-acyl homoserine lactone-degrading bacteria. *Journal of Industrial Microbiology and Biotechnology* **36**(2): 247-251.

Chan, R. and Chen, V. (2004). Characterization of protein fouling on membranes: opportunities and challenges. *Journal of Membrane Science* **242**(1-2): 169-188.

Chandrasekhar, S.S., Srinath, D., Sahu, N. and Sridhar, S. (2017). Treatment of Dairy Industry Effluent using Membrane Bioreactor. *International Journal of Pure and Applied Bioscience* **5**(6): 71-79.

Chang, I.S. and Kim, S.N. (2005). Wastewater treatment using membrane filtration-effect of biosolids concentration on cake resistance. *Process Biochemistry* **40**(3-4): 1307-1314.

Chang, I.S. and Lee C.H. (1998). Membrane filtration characteristics ion membrane coupled activated sludge system- the effect of physiological states of activated sludge on membrane fouling. *Desalination* **120**(3): 221–233.

Chang, I.S., Le-Clech, P., Jefferson, B. and Judd, S. (2002). Membrane fouling in membrane bioreactors for wastewater treatment. *Journal of Environmental Engineering* **128**(11): 1018-1029.

Chang, S., Fane, T.G. and Waite, T.D (2005). Effect of coagulation within the cake layer on fouling transitions with dead-end hollow fiber membranes. Proceedings of the International Congress on Membranes and Membrane Processes (ICOM), Pp. 21-26, Seoul, Korea.

Chen, F., Gao, Y., Chen, X., Yu, Z. and Li, X. (2013). Quorum quenching enzymes and their application in degrading signal molecules to block quorum sensing-dependent infection. *International Journal of Molecular Sciences* **14**(9): 17477–17500.

Chen, H. and Belfort, G. (1999). Surface modification of poly(ether sulfone) ultrafiltration membranes by low temperature plasma-induced graft polymerization. *Journal of Applied Polymer Science* **72**(13): 1699-1711.

Chen, J.P., Yang, C.Z., Zhou, J.H. and Wang, X.Y. (2007). Study of the influence of the electric field on membrane flux of a new type of membrane bioreactor. *Chemical Engineering Journal* **128**(2-3): 177-180.

Chen, R., Nie, Y., Hu, Y., Miao, R., Utashiro, T., Li, Q., Xu, M. and Li, Y.Y. (2017). Fouling behaviour of soluble microbial products and extracellular polymeric substances in a submerged anaerobic membrane bioreactor treating low-strength wastewater at room temperature. *Journal of Membrane Science* **531:** 1-9.

Chen, X., Schauder, S., Potier, N., Van Dorsselaer, A., Pelczer, I., Bassler, B.L. and Hughson, F.M. (2002). Structural identification of a bacterial quorum-sensing signal containing boron. *Nature* **415**(6871): 545-549.

Chen, X.H., Wang, X.T., Lou, W.Y., Li, Y., Wu, H., Zong, M.H., Smith, T.J. and Chen, X.D. (2012). Immobilization of *Acetobacter* sp. CCTC M209061 or efficient asymmetric reduction of ketones and biocatalyst recycling. *Microbial Cell Factories* **11:** 1-13.

Cheong, W.S., Kim, S.R., Oh, H.S., Lee, S.H., Yeon, K.M., Lee, C.H. and Lee, J.K. (2014). Design of quorum quenching microbial vessel to enhance cell viability for biofouling control in membrane bioreactor. *Journal of Microbiology and Biotechnology* **24**(1): 97-105.

Cheong, W.S., Lee, C.H., Moon, Y.H., Oh, H.S., Kim, S.R., Lee, S.H., Lee, C.H. and Lee, J.K. (2013). Isolation and identification of indigenous quorum quenching bacteria, *Pseudomonas* sp. 1A1, for biofouling control in MBR. *Industrial & Engineering Chemistry Research* **52**(31): 10554-10560.

Cheryan, M. (1st ed.) (1998). *Ultrafiltration and Microfiltration Handbook.* Technomic Publishing Co. Inc. Lancaster, PA, USA.

Cho, B.D. and Fane, A.G. (2002). Fouling transients in nominally sub-critical flux operation of a membrane bioreactor. *Journal of Membrane Science* **209**(2): 391-403.

Choi, H., Zhang, K., Dionysiou, D.D., Oerther, D.B. and Sorial, G.A. (2005). Effect of permeate flux and tangential flow on membrane fouling for wastewater treatment. *Separation and Purification Technology* **45**(1): 68-78.

Choi, J.G., Bae, T.H., Kim, J.H., Tak, T.M. and Randall, A.A. (2002). The behaviour of membrane fouling initiation on the crossflow membrane bioreactor system. *Journal of Membrane Science* **203**(1-2): 103–113.

Choi, O., Deng, K.K., Kim, N.J., Ross, L., Surampalli, R.Y. and Hu, Z.Q. (2008). The inhibitory effects of silver nanoparticles, silver ions and silver chloride colloids on microbial growth. *Water Research* **42**(12): 3066-3074.

Chong, T.M., Koh, C.L., Sam, C.K., Choo, Y.M., Yin, W.F. and Chan, K.G. (2012). Characterization of quorum sensing and quorum quenching soil bacteria isolated from Malaysian Tropical Montane Forest. *Sensors* **12**(4): 4846-4859.

Choo, J.H., Rukayadi, Y. and Hwang, J.K. (2006). Inhibition of bacterial quorum sensing by vanilla extract. *Letters in Applied Microbiology* **42**(6): 637-641.

Choudhary, S. and Schmidt-Dannert, C. (2010). Applications of quorum sensing in biotechnology. *Applied Microbiology and Biotechnology* **86**(5): 1267-1279.

Christiaen, S.E., Brackman, G., Nelis, H.J. and Coenye, T. (2011). Isolation and identification of quorum quenching bacteria from environmental samples. *Journal of Microbiological Methods* **87**(2): 213-219.

Christianto, B. and Yogiara (2011). Screening of quorum quenching activity of bacteria isolated from Ant Lion. *Microbiology Indonesia* **5**(1): 46-49.

Chu, W., Zhou, S., Jiang, Y., Zhu, W., Zhuang, X. and Fu, J. (2013). Effect of traditional Chinese herbal medicine with antiquorum sensing activity on

Pseudomonas aeruginosa. *Evidence-Based Complementary and Alternative Medicine* **2013:** 1-7.

Chua, H.C., Arnot, T.C. and Howell, J.A. (2002). Controlling fouling in membrane bioreactors operated with a variable throughput. *Desalination* **149**(1-3): 225-229.

Cicek, N. (2003). A review of membrane bioreactors and their potential application in the treatment of agricultural wastewater. *Canadian Biosystems Engineering* **45:** 37-49.

Cote, P., Buisson, H., Pound, C. and Arakaki, G. (1997). Immersed membrane activated sludge for the reuse of municipal wastewater. *Desalination* **113:** 189-196.

Covarrubias, S.A., de-Bashan, L.E., Moreno, M. and Bashan, Y. (2012). Alginate beads provide a beneficial physical carrier against native micro-organisms in wastewater treated with immobilized bacteria and microalgae. *Applied Microbiology and Biotechnology* **93**(6): 2669-2680.

Damayanti, A., Ujang, Z., Salim, M.R. and Olsson, G. (2011). The effect of mixed liquor suspended solids (MLSS) on the biofouling in a hybrid membrane bioreactor for the treatment of high concentration organic wastewater. *Water Science & Technology* **63:** 1701-1706.

Davies, D.G., Parsek, M.R., Pearson, J.P., Iglewski, B.H., Costerton, J.W. and Greenberg, E.P. (1998). The involvement of cell-to-cell signals in the development of a bacterial biofilm. *Science* **280**(5361): 295-298.

Dawood, A.T., Kumar, A. and Sambi, S.S. (2011). Study on anaerobic treatment of synthetic milk wastewater under variable experimental conditions. *International Journal of Environmental Science and Development* **2**(1): 17-23.

Deng, L. (2015). Development of specific membrane bioreactors for membrane fouling control during wastewater treatment for reuse. Ph.D. thesis, University of Technology, Sydney.

Deng, L., Guo, W., Ngo, H.H., Zhang, J., Liang, S., Xia, S., Zhang, Z. and Li, J. (2014). A comparison study on membrane fouling in a sponge-submerged membrane bioreactor and a conventional membrane bioreactor. *Bioresource Technology* **165:** 69-74.

Devaraj, K., Tan, G.Y.A. and Chan, K.G. (2017). Quorum quenching properties of *Acinetobacter* isolated from Malaysian tropical soils. *Archives of Microbiology* **199**(6): 897-906.

Diebold, U. (2003). The surface science of titanium dioxide. *Surface Science Reports* **48**(5-8): 53-229.

Diggle, S.P., Crusz, S.A. and Camara, M. (2007). Quorum sensing. *Current Biology* **17**(21): R907-R910.

Dignac, M.F., Urbain, V., Rybacki, D., Bruchet, A., Snidaro, D. and Scribe, P. (1998). Chemical description of extracellular polymers: implication on activated sludge floc structure. *Water Science and Technology* **38**(8-9): 45-53.

Dong, B. and Jiang, S. (2009). Characteristics and behaviors of soluble microbial products in sequencing batch membrane bioreactors at various sludge retention times. *Desalination* **243:** 240-250.

Dong, Y.H., Gusti, A.R., Zhang, Q., Xu, J.L. and Zhang, L.H. (2002). Identification of Quorum-Quenching *N*-Acyl Homoserine Lactonases from *Bacillus* Species. *Applied and Environmental Microbiology* **68**(4): 1754-1759.

Donlan, R.M. (2002). Biofilms: Microbial life on surfaces. *Emerging Infectious Diseases* **8**(9): 881-890.

Dreszer, C., Vrouwenvelder, J.S., Paulitsch-Fuchs, A.H., Zwijnenburg, A., Kruithof, J.C. and Flemming, H.C. (2013). Hydraulic resistance of biofilms. *Journal of Membrane Science* **429:** 436-447.

Drews A. (2010). Membrane fouling in membrane bioreactors- Characterisation, contradictions, cause and cures. *Journal of Membrane Science* **363**(1-2): 1-28.

Drews, A., Mante, J., Iversen, V., Vocks, M., Lesjean, B. and Kraume, M. (2007). Impact of ambient conditions on SMP elimination and rejection in MBRs. *Water Research* **41**(17): 3850-3858.

Drews, A., Vocks, M., Iversen, V., Lesjean, B. and Kraume, M. (2006). Influence of unsteady membrane bioreactor operation on EPS formation and filtration resistance. *Desalination* **192**(1-3): 1–9.

Dubois, M., Gilles, K.A., Hamilton, J.K., Rebers, P.A. and Smith, F. (1956). Colorimetric method for determination of sugars and related substances. *Analytical Chemistry* **28**(3): 350-356.

Dulebohn, J., Ahmadiannamini, P., Wang, T., Kim, S.S., Pinnavaia, T.J. and Tarabara, V.V. (2014). Polymer mesocomposites: Ultrafiltration membrane materials with enhanced permeability, selectivity and fouling resistance. *Journal of Membrane Science* **453:** 478-488.

Dvorak, L., Gomez, M., Dvorakova, M., Ruzickova, I. and Wanner, J. (2011). The impact of different operating conditions on membrane fouling and EPS production. *Bioresource Technology* **102**(13): 6870-6875.

Erden, G., Demir, O. and Filibeli, A. (2010). Disintegration of biological sludge: Effect of ozone oxidation and ultrasonic treatment on aerobic digestibility. *Bioresource Technology* **101**(21): 8093-8098.

Erkan, H.S., Gunalp, G. and Engin, G.O. (2018). Application of submerged membrane bioreactor technology for the treatment of high strength dairy wastewater. *Brazilian Journal of Chemical Engineering* **35**(1): 91-100.

Fallah, N., Bonakdarpour, B., Nasernejad, B. and Alavimoghaddam, M.R. (2010). The use of a submerged membrane bioreactor for the treatment of a styrene containing synthetic wastewater. *Iranian Journal of Environmental Health Science and Engineering* **7**(2): 115-122.

Faller, K.A., Murray, P. and Livingston, A. (1999). *Manual of water supply practices. M46 Reverse osmosis and nanofiltration.* American Water Works Association, Denver.

Fan, J.H., Yu, S.L., Zhang, P.S., Lan, Y.Q., Liu, R. and Chen, L.J. (2013). Mechanism of membrane fouling and filtration characteristics in a membrane bioreactor for industrial wastewater treatment. *Huan Jing Ke Xue* **34**(3): 950-954.

Fane, A.G. (2007). Sustainability and membrane processing of wastewater for reuse. *Desalination* **202**(1-3): 53-58.

Fane, A.G., Fell, C.J.D. and Nor, M.T. (1980). Ultrafiltration/ Activated sludge system- Development of a predictive model. *Polymer Science and Technology* **13:** 631-658.

Farizoglu, B. and Uzuner, S. (2011). The investigation of dairy industry wastewater treatment in a biological high performance membrane system. *Biochemical Engineering Journal* **57:** 46-54.

Flemming, H.C. and Wingender, J. (2001). Relevance of microbial extracellular polymeric substances (EPSs)-Part I: Structural and ecological aspects. *Water science and technology* **43**(6): 1-8.

Flemming, H.C. and Wingender, J. (2010). The biofilm matrix. *Nature Reviews Microbiology* **8:** 623-633.

Flemming, H.C., Neu, T.R. and Wozniak, D.J. (2007). The EPS matrix: the “house of biofilm cells”. *Journal of Bacteriology* **189**(22): 7945-7947.

Frank, B.P. and Belfort, G. (2003). Polysaccharides and sticky membrane surfaces: critical ionic effects. *Journal of Membrane Science* **212**(1-2): 205-212.

Fuqua, C. and Greenberg, E.P. (2002). Signalling: Listening in on bacteria: acyl-homoserine lactone signalling. *Nature Reviews Molecular Cell Biology* **3**(9): 685-695.

Gander, M., Jefferson, B. and Judd, S. (2000). Aerobic MBRs for Domestic Wastewater Treatment: A Review with cost considerations. *Separation and Purification Technology* **18**(2): 119-130.

Gao, W.J., Han, M.N., Qu, X., Xu, C. and Liao, B.Q. (2013). Characteristics of wastewater and mixed liquor and their role in membrane fouling. *Bioresource Technology* **128**: 207-214.

Geng, Z. and Hall, E.R. (2007). A comparative study of fouling-related properties of sludge from conventional and membrane enhanced biological phosphorus removal processes. *Water Research* **41**(19): 4329-4338.

Ghandoor, H.E., Zidan, H.M., Khalil, M.M.H. and Ismail, M.I.M (2012). Synthesis and some physical properties of magnetite (Fe_3O_4) nanoparticles. *International Journal of Electrochemical Science* **7**(6): 5734-5745.

Ghani, N.A., Sulaiman, J., Ismail, Z., Chan, X.Y., Yin, W.F. and Chan, K.G. (2014). *Rhodotorula mucilaginosa*, a quorum quenching yeast exhibiting lactonase activity isolated from a tropical shoreline. *Sensors* **14**(4): 6463-6473.

Gkotsis, P.K., Banti, D. Ch., Peleka, E.N., Zouboulis, A.I. and Samaras, P.E., (2014). Fouling issues in Membrane Bioreactors (MBRs) for wastewater treatment: Major mechanisms, prevention and control strategies. *Processes* **2**(4): 795-866.

Gonzalez, R.H., Nusblat, A. and Nudel, B.C. (2001). Detection and characterization of quorum sensing signal molecules in *Acinetobacter* strains. *Microbiological Research* **155**(4): 271-277.

Grelier, P., Rosenberger, S. and Tazi-Pain, A. (2006). Influence of sludge retention time on membrane bioreactor hydraulic performance. *Desalination* **192**(1-3): 10-17.

Gu, Q., Fu, L., Wang, Y. and Lin, J. (2013). Identification and characterization of extracellular cyclic dipeptides as quorum-sensing signal molecules from *Shewanella baltica*, the specific spoilage organism of *Pseudosciaena crocea* during 4°C storage. *Journal of Agricultural and Food Chemistry* **61**(47): 11645-11652.

Guan, K. (2005). Relationship between photoctalytic activity, hydrophilicity and self-cleaning effect of TiO_2/ SiO_2 films. *Surface and Coatings Technology* **191**(2-3): 155-160.

Gul, B.Y. and Koyuncu, I. (2017). Assessment of new environmental quorum quenching bacteria as a solution for membrane biofouling. *Process Biochemistry* **61:** 137-146.

Guo, W., Ngo, H.H. and Li, J. (2012). A mini review on membrane fouling. *Bioresource Technology* **122**: 27-34.

Guo, W., Ngo, H.H., Vigneswaran, S., Xing, W. and Goteti, P. (2008). A Novel Sponge-Submerged Membrane Bioreactor (SSMBR) for Wastewater Treatment and Reuse. *Separation Science and Technology* **43**(2): 273-285.

Gupta, N., Jana, N. and Majumder, C.B. (2008). Submerged membrane bioreactor system for municipal wastewater treatment process: An overview. *Indian Journal of Chemical Technology* **15:** 604-612.

Hammer, B.K. and Bassler, B.L. (2003). Quorum sensing controls biofilm formation in *Vibrio cholerae*. *Molecular microbiology* **50**(1): 101-104.

Han, S.S., Bae, T.H., Jang, G.G. and Tak, T.M. (2005). Influence of sludge retention time on membrane fouling and bioactivities in membrane bioreactor system. *Process Biochemistry* **40**(7): 2393-2400.

Hanft, S. (2011). Membrane Bioreactors: Global Markets. Business Communication Company Inc. Report MST047C.

Hao, L., Liss, S.N. and Liao, B.Q. (2017). Effect of solids retention time on membrane fouling in membrane bioreactors at a constant mixed liquor suspended solids concentration. *Membrane Water Treatment* **8**(4): 337-353.

Hariani, P.L., Faizal, M., Ridwan, Marsi and Setiabudidaya, D. (2013). Synthesis and properties of Fe_3O_4 nanoparticles by co-precipitation method to remove procion dye. *International Journal of Environmental Science and Development* **4**(3): 336-340.

Hasani Zonoozi, M., Moghaddam, M.R.A. and Maknoon, R. (2017). Investigation of HRT effects on membrane fouling in sequencing batch membrane bioreactor with respect to batch filtration mode. *Environmental Progress and Sustainable Energy* **36**(6): 1785-1793.

Hasnain, G., Khan, S.J., Arshad, M.Z. and Abdullah, H.Y. (2017). Combined Impact of Quorum Quenching and Backwashing on Biofouling Control in a Semi-Pilot Scale MBR Treating Real Wastewater. *Journal- Chemical Society of Pakistan* **39**(02): 215-223.

Hejzlar, J. and Chudoba, J. (1986). Microbial polymers in the aquatic environment-I: Production by activated sludge microorganisms under different conditions. *Water Research* **20**(10): 1209-1216.

Heldman, D.R. and Moraru, C.I. (2014). *Encyclopedia of Agricultural, Food, and Biological Engineering, -2 Volume Set*. CRC Press, USA.

Hermanowicz, S.W. (2004). Membrane filtration of biological solids: A unified framework and its applications to membrane bioreactors. In: Proceedings of the water environment-membrane technology conference, Seoul, Korea.

Hirooka, K., Asano, R., Yokoyama, A., Okazaki, M., Sakamoto, A. and Nakai, Y. (2009). Reduction in excess sludge production in a dairy wastewater treatment plant via nozzle-cavitation treatment: Case study of an on-farm wastewater treatment plant. *Bioresource Technology* **100**(12): 3161-3166.

Hofs, B., Ogier, J., Vries, D., Beerendonk, E.F. and Cornelissen, E.R. (2011). Comparison of ceramic and polymeric membrane permeability and fouling using surface water. *Separation and Purification Technology* **79**(3): 365-374.

Holman, S. and Ohlinger, K. (2007). An Evaluation of Fouling Potential and Methods to Control Fouling in Microfiltration Membranes for Secondary Wastewater Effluent. In *Proceedings of the 80th Annual Water Environment Federation Technical Exhibition and Conference*, 6417-6444. San Diego: Water Environment Federation.

Homayoonfal, M., Mehrnia, M.R., Rahmani, S. and Mojtahedi, Y.M. (2015). Fabrication of alumina/polysulfone nanocomposite membranes with biofouling mitigation approach in membrane bioreactors. *Journal of Industrial and Engineering Chemistry* **22:** 357-367.

Hong, R.Y., Feng, B., Chen, L.L., Liu, G.H., Li, H.Z., Zheng, Y. and Wei, D.G. (2008). Synthesis, characterization and MRI application of dextran-coated Fe_3O_4 magnetic nanoparticles. *Biochemical Engineering Journal* **42**(3): 290-300.

Hong, S. and Elimelech, M. (1997). Chemical and physical aspects of natural organic matter (NOM) fouling of nanofiltration membranes. *Journal of Membrane Science* **132**(2): 159-181.

Hong, S.P., Bae, T.H., Tak, T.M., Hong, S. and Randall, A. (2002). Fouling control in activated sludge submerged hollow fiber membrane bioreactors. *Desalination* **143**(3): 219-228.

Hosseinzadeh, M., Nabi Bidhendi, G., Torabian, A. and Mehrdadi, N. (2014). A Study on Membrane Bioreactor for Water Reuse from the Effluent of Industrial Town Wastewater Treatment Plant. *Iranian Journal of Toxicology* **8**(24): 983-990.

Hu, J., Ren, H., Xu, K., Geng, J., Ding, L., Yan, X. and Li, K. (2012). Effect of carriers on sludge characteristics and mitigation of membrane fouling in attached-growth membrane bioreactor. *Bioresource Technology* **122**: 35-41.

Huang, J., Wang, H. and Zhang, K. (2014). Modification of PES membrane with Ag–SiO_2: Reduction of biofouling and improvement of filtration performance. *Desalination* **336:** 8-17.

Huang, J.J., Han, J.I., Zhang, L.H. and Leadbetter, J.R. (2003). Utilization of acyl-homoserine lactone quorum signals for growth by a soil pseudomonad and *Pseudomonas aeruginosa* PAO1. *Applied and Environmental Microbiology* **69**(10): 5941-5949.

Huang, L.N., Wever, H.D. and Diels, L. (2008a). Diverse and distinct bacterial communities induced biofilm fouling in membrane bioreactors operated under different conditions. *Environmental Science and Technology* **42**(22): 8360-8366.

Huang, X., Gui, P. and Qian, Y. (2001). Effect of sludge retention time on microbial behaviour in a submerged membrane bioreactor. *Process Biochemistry* **36**(10): 1001-1006.

Huang, X., Wei, C.H. and Yu, K.C. (2008b). Mechanism of membrane fouling control by suspended carriers in a submerged membrane bioreactor. *Journal of Membrane Science* **309**(1-2): 7-16.

Huang, X. and Wu, J. (2008). Improvement of membrane filterability of the mixed liquor in a membrane bioreactor by ozonation. *Journal of Membrane Science* **318**(1-2): 210–216.

Huang, Z., Ong, S.L. and Ng, H.Y. (2011). Submerged anaerobic membrane bioreactor for low-strength wastewater treatment: effect of HRT and SRT on treatment performance and membrane fouling. *Water Research* **45**(2): 705-713.

Huisman, I.H., Pradanos, P. and Hernandez, A. (2000). The effect of protein-protein and protein-membrane interactions on membrane fouling in ultrafiltration. *Journal of Membrane Science* **179**(1-2): 79-90.

Hwang, B.K., Kim, J.H., Ahn, C.H., Lee, C.H., Song, J.Y. and Ra, Y.H. (2010). Effect of disintegrated sludge recycling on membrane permeability in a membrane bioreactor combined with a turbulent jet flow ozone contactor. *Water Research* **44**(6): 1833-1840.

Iorhemen, O.T., Hamza, R.A. and Tay, J.H. (2016). Membrane bioreactor (MBR) technology for wastewater treatment and reclamation: membrane fouling. *Membranes* **6**(2): 1-29.

Isma, M.A., Idris, A., Omar, R. and Razreena, A.P. (2014). Effects of SRT and HRT on treatment performance of MBR and membrane fouling. *International Journal ofEnvironmental and Ecological Eng*ineering **8:** 488-492.

Itonaga, T., Kimura, K. and Watanabe, Y. (2004). Influence of suspension viscosity and colloidal particles on permeability of membrane used in membrane bioreactor (MBR). *Water Science & Technology* **50**(12): 301-309.

Ivanova, V., Petrova, P. and Hristov, J. (2011). Application in the ethanol fermentation of immobilized yeast cells in matrix of alginate/magnetic nanoparticles, on chitosan-magnetite microparticles and cellulose coated

magnetic nanoparticles. *International Review of Chemical Engineering* **3**(2): 289-299.

Ivanovic, I. and Leiknes, T. (2011). Effect of addition of different additives on overall performance of biofilm-MBR (BF-MBR). *Desalination and Water Treatment* **34**(1-3): 129-135.

Jagannadh, S.N. and Muralidhara, H.S. (1996). Electrokinetics methods to control membrane fouling. *Industrial & Engineering Chemistry Research* **35**(4): 1133-1140.

Jahangir, D., Oh, H.S., Kim, S.R., Park, P.K., Lee, C.H. and Lee, J.K. (2012). Specific location of encapsulated quorum quenching bacteria for biofouling control in an external submerged membrane bioreactor. *Journal of Membrane Science* **411-412:** 130-136.

Jamal, M., Tasneem, U., Hussain, T. and Andleeb, S. (2015). Bacterial biofilm: Its composition, formation and role in human infections. *Research & Reviews: Journal of Microbiology and Biotechnology* **4**(3): 1-14.

Jarusutthirak, C. and Amy, G. (2006). Role of soluble microbial products (SMP) in membrane fouling and flux decline. *Environmental Science & Technology* **40**(3): 969-974.

Jiang, T., Kennedy, M.D., Guinzbourg, B.F., Vanrolleghem, P.A. and Schippers, J.C. (2005). Optimising the operation of a MBR pilot plant by quantitative analysis of the membrane fouling mechanism. *Water Science & Technology* **51**(6-7): 19-25.

Jiang, W., Xia, S.Q., Liang, J., Zhang, Z.Q. and Hermanowicz, S.W. (2013). Effect of quorum quenching on the reactor performance, biofouling and biomass characteristics in membrane bioreactors. *Water Research* **47:** 187-196.

Jiao, Y., Cody, G.D., Harding, A.K., Wilmes, P., Schrenk, M., Wheeler, K.E., Banfield, J.F. and Thelen, M.P. (2010). Characterization of extracellular polymeric substances from acidophilic microbial biofilms. *Applied and Environmental Microbiology* **76**(9): 2916-2922.

Jin, L., Ong, S.L. and Ng, H.Y. (2010). Comparison of fouling characteristics in different pore-sized submerged ceramic membrane bioreactors. *Water Research* **44**(20): 5907-5918.

Johir, M.A.H. (2015). Membrane bio-reactor (MBR): effect of operating parameters and nutrients removal. Ph.D. thesis, University of Technology, Sydney.

Jorand, F., Boue-Bigne, F., Block, J.C. and Urbain, V. (1998). Hydrophobic/ hydrophilic properties of activated sludge exopolymeric substances. *Water Science and Technology* **37**(4-5): 307-315.

Judd, S. (2006). The MBR Book: Principles and Applications of Membrane Bioreactors for Water and Wastewater Treatment. Elsevier, Oxford, UK.

Judd, S.J. and Judd, C. (2010). Principles and application of membrane bioreactors in water and wastewater treatment, second edition. Elsevier, London, UK.

Kang, B.R., Lee, J.H., Ko, S.J., Lee, Y.H., Cha, J.S., Cho, B.H. and Kim, Y.C. (2004). Degradation of acyl-homoserine lactone molecules by *Acinetobacter* sp. strain C1010. *Canadian Journal of Microbiology* **50**(11): 935-941.

Karr, P.R. and Keinath, T.M. (1978). Influence of Particle Size on Sludge Dewaterability. *Journal (Water Pollution Control Federation)* **50**(8): 1911-1930.

Katayon, S., Mohd. Noor, M.J.M., Ahmad, J., Ghani, L.A.A., Nagaoka, H. and Aya, H. (2004). Effects of mixed liquor suspended solid concentrations on membrane bioreactor efficiency for treatment of food industry wastewater. *Desalination* **167:** 153-158.

Khan, R., Shen, F., Khan, K., Liu, L.X., Wu, H.H., Luo, J.Q. and Wan, Y.H. (2016). Biofouling control in a membrane filtration system by a newly isolated novel quorum quenching bacterium, *Bacillus methylotrophicus* sp. WY. *RSC Advances* **6**(34): 28895-28903.

Khan, S.J., Visvanathan, C. and Jegatheesan, V. (2012). Effect of powdered activated carbon (PAC) and cationic polymer on biofouling mitigation in hybrid MBRs. *Bioresource Technology* **113:** 165-168.

Kim, A.L., Park, S.Y., Lee, C.H., Lee, C.H. and Lee, J.K. (2014). Quorum quenching bacteria isolated from the sludge of a wastewater treatment plant and their application for controlling biofilm formation. *Journal of Microbiology and Biotechnology* **24**(11): 1574-1582.

Kim, J. and Bruggen, B.V.D. (2010). The use of nanoparticles in polymeric and ceramic membrane structures: Review of manufacturing procedures and performance improvement for water treatment. *Environment Pollution* **158**(7): 2335-2349.

Kim, J.H., Choi, D.C., Yeon, K.M., Kim, S.R. and Lee, C.H. (2011). Enzyme immobilized nanofiltration membrane to mitigate biofouling based on quorum quenching. *Environmental Science & Technology* **45**(4): 1601-1607.

Kim, J.Y., Lee, C., Cho, M. and Yoon, J. (2008). Enhanced inactivation of *E. coli* and MS-2 phage by silver ions combined with UV-A and visible light irradiation. *Water Research* **42**(1-2): 356-362.

Kim, S.R., Lee, K.B., Kim, J.E., Won, Y.J., Yeon, K.M., Lee, C.H. and Lim, D.J. (2015). Macroencapsulation of quorum quenching bacteria by polymeric membrane layer and its application to MBR for biofouling control. *Journal of Membrane Science* **473:** 109-117.

Kim, S.R., Oh, H.S., Jo, S.J., Yeon, K.M., Lee, C.H., Lim, D.J., Lee, C.H. and Lee, J.K. (2013). Biofouling control with bead-entrapped quorum quenching bacteria in membrane bioreactors: physical and biological effects. *Environmental Science & Technology* **47**(2): 836-842.

Kimura, K., Yamato, N., Yamamura, H. and Watanabe, Y. (2005). Membrane fouling in pilot-scale membrane bioreactors (MBRs) treating municipal wastewater. *Environmental Science & Technology* **39**(16): 6293-6299.

Kjelleberg, S. and Molin, S. (2002). Is there a role for quorum sensing signals in bacterial biofilms?. *Current Opinion in Microbiology* **5**(3): 254-258.

Kochkodan, V., Johnson, D.J. and Hilal, N. (2014). Polymeric membranes: Surface modification for minimizing (bio)colloidal fouling. *Advances in Colloid and Interface Science* **206:** 116-140.

Kokare, C.R., Chakraborty, S., Khopade, A.N. and Mahadik, K.R. (2009). Biofilm: importance and applications. *Indian Journal of Biotechnology* **8:** 159-168.

Kolter, R., Siegele, D.A. and Tormo, A. (1993). The stationary phase of the bacterial life cycle. *Annual Review of Microbiology* **47:** 855-874.

Komlenic, R. (2010). Rethinking the causes of membrane biofouling. *Filtration & Separation* **47**(5): 26-28.

Koo, H., Hayacibara, M.F., Schobel, B.D., Cury, J.A., Rosalen, P.L., Park, Y.K., Vacca- Smith, A.M. and Bowen, W.H. (2003). Inhibition of *Streptococcus mutans* biofilm accumulation and polysaccharide production by apigenin and tt-farnesol. *Journal of Antimicrobial Chemotherapy* **52**(5): 782-789.

Kouassi, G.K., Irudayaraj, J. and McCarty, G. (2005). Activity of glucose oxidase functionalized onto magnetic nanoparticles. *Biomagnetic Research and Technology* **3**(1): 1-10.

Kovalova, L., Siegrist, H., Singer, H., Wittmer, A. and McArdell, C.S. (2012). Hospital wastewater treatment by membrane bioreactor: performance and efficiency for organic micropollutant elimination. *Environmental Science and Technology* **46**(3): 1536-1545.

Krieg, N.R. and Holt, J.C. (1984). *Bergey's Manual of Systematic Bacteriology*. William and Wilkins Publishers, Baltimore, MD.

Lade, H., Paul, D. and Kweon, J.H. (2015). Combined effects of curcumin and (–)-epigallocatechin gallate on inhibition of N-acylhomoserine lactone-mediated biofilm formation in wastewater bacteria from membrane bioreactor. *Journal of Microbiology and Biotechnology* **25**(11): 1908-1919.

Lade, H., Song, W.J., Yu, Y.J., Ryu, J.H., Arthanareeswaran, G. and Kweon, J.H. (2017). Exploring the potential of curcumin for control of N-acyl homoserine

lactone-mediated biofouling in membrane bioreactors for wastewater treatment. *RSC Advances* **7**(27): 16392-16400.

Laitinen, N., Luonsi, A., Levanen, E. and Nystrom, M. (2001). Effect of backflushing conditions on ultrafiltration of board industry wastewater with ceramic membranes. *Separation and Purification Technology* **25**(1-3): 323-331.

Lal, A. (2009). Quorum sensing. *Resonance* **14**(9): 866-871.

Lamminen, M.O., Walker, H.W. and Weavers, L.K. (2004). Mechanisms and factors influencing the ultrasonic cleaning of particle-fouled ceramic membranes. *Journal of Membrane Science* **237**(1–2): 213–223.

Langlet, M., Permpoon, S., Riassetto, D., Berthome, G., Pernot, E. and Joud, J.C. (2006). Photocatalytic activity and photo-induced superhydrophilicity of sol-gel derived TiO_2 films. *Journal of Photochemistry and Photobiology A: Chemistry* **181**(2-3): 203-214.

Laspidou, C.S. and Rittmann, B.E. (2002). A unified theory for extracellular polymeric substances, soluble microbial products, and active and inert biomass. *Water research* **36**(11): 2711-2720.

Leadbetter, J.R. and Greenberg, E.P. (2000). Metabolism of acyl-homoserine lactone quorum sensing signals by *Varivorax paradoxus. Journal of Bacteriology* **182**(24): 6921-6926.

Le-Clech, P. (2010). Membrane bioreactors and their uses in wastewater treatments. *Applied Microbiology and Biotechnology* **88**(6): 1253-1260.

Le-Clech, P., Chen, V. and Fane, T.A. (2006). Fouling in membrane bioreactors used in wastewater treatment. *Journal of Membrane Science* **284**(1-2): 17-53.

Lee, B., Yeon, K.M., Shim, J., Kim, S.R., Lee, C.H., Lee, J. and Kim, J. (2014). Effective antifouling using quorum-quenching acylase stabilized in magnetically separable mesoporous silica. *Biomacromolecules* **15**(4): 1153-1159.

Lee, J.S. and Chang, I.S. (2014). Membrane fouling control and sludge solubilization using high voltage impulse (HVI) electric fields. *Process Biochemistry* **49**(5): 858-862.

Lee, K., Lee, S., Lee, S.H., Kim, S.R., Oh, H.S., Park, P.K., Choo, K.H., Kim, Y.W., Lee, J.K. and Lee, C.H. (2016a). Fungal Quorum Quenching: A paradigm shift for energy savings in membrane bioreactor (MBR) for wastewater treatment. *Environmental Science and Technology* **50**(20): 10914-10922.

Lee, N., Amy, G., Croue, J.P. and Buisson, H. (2004). Identification and understanding of fouling in low-pressure membrane (MF/UF) filtration by natural organic matter (NOM).*Water Research* **38**(20): 4511-4523.

Lee, S.H., Lee, S., Lee, K., Nahm, C.H., Kwon, H., Oh, H.S., Won, Y.J., Choo, K.H., Lee, C.H. and Par, P.K. (2016b). More efficient media design for enhanced biofouling control in a membrane bioreactor: quorum quenching bacteria entrapping hollow cylinder. *Environmental Science and Technology* **50**(16): 8596-8604.

Lee, W., Kang, S. and Shin, H. (2003). Sludge characteristics and their contribution to microfiltration in submerged membrane bioreactors. *Journal of Membrane Science* **216**(1-2): 217-227.

Li, J.F., Xu, Z.L., Yang, H., Yu, L.Y. and Liu, M. (2009a). Effect of TiO_2 nanoparticles on the surface morphology and performance of microporous PES membrane. *Applied Surface Science* **255**(9): 4725–4732.

Li, J.H., Xu, Y.Y., Zhu, L.P., Wang, J.H. and Du, C.H. (2009b). Fabrication and characterization of a novel TiO_2 nanoparticle self-assembly membrane with improved fouling resistance. *Journal of Membrane Science* **326**(2): 659-666.

Li, M., Wang, Y. and Gong, C. (2013a). Effect of on-line ultrasound on the properties of activated sludge mixed liquor and the controlling of membrane fouling in SMBR. *Desalination and Water Treatment* **51**(19-21): 3938-3947.

Li, M.Y., Zhang, J., Lu, P, Xu, J.L. and Li, S.P. (2009c). Evaluation of biological characteristics of bacteria contributing to biofilm formation. *Pedosphere* **19**(5): 554-561.

Li, Q. and Elimelech, M. (2004). Organic fouling and chemical cleaning of nanofiltration membranes: Measurements and Mechanisms. *Environmental Science and Technology* **38**(17): 4683-4693.

Li, Q., Wang, M., Feng, J., Zhang, W., Wang, Y., Gu, Y., Song, C. and Wang, S. (2013b). Treatment of high-salinity chemical wastewater by indigenous bacteria-bioaugmented contact oxidation. *Bioresource Technology* **144:** 380-386.

Li, Y.Z., He, Y.L., Liu, Y.H., Yang, S.C. and Zhang, G.J. (2005). Comparison of the filtration characteristics between biological powdered activated carbon sludge and activated sludge in submerged membrane bioreactors. *Desalination* **174**(3): 305-314.

Liang, S., Liu, C. and Song, L. (2007). Soluble microbial products in membrane bioreactor operation: Behaviors, characteristics and fouling potential. *Water Research* **41**(1): 95-101.

Liao, B.Q., Bagley, D.M., Kraemer, H.E., Leppard, G.G. and Liss, S.N. (2004). A review of biofouling and its control in membrane separation bioreactors. *Water Environment Research* **76**(5): 425-436.

Liao, M.H. and Chen, D.H. (2001). Immobilization of yeast alcohol dehydrogenase on magnetic nanoparticles for improving its stability. *Biotechnology Letters* **23**(20): 1723-1727.

Lim, A.L. and Bai, R. (2003). Membrane fouling and cleaning in microfiltration of activated sludge wastewater. *Journal of Membrane Science* **216**(1-2): 279-290.

Lin, C.F. and Shien, Y. (2001). Sludge dewatering using centrifuge with thermal/ polymer conditioning. *Water Science & Technology* **44**(10): 321-325.

Lin, H., Wang, F., Ding, L., Hong, H., Chen, J. and Lu, X. (2011). Enhanced performance of a submerged membrane bioreactor with powdered activated carbon addition for municipal secondary effluent treatment. *Journal of Hazardous Materials* **192**: 1509-1514.

Lin, H., Zhang, M., Wang, F., Meng, F., Liao, B.Q., Hong, H., Chen, J. and Gao, W. (2014). A critical review of extracellular polymeric substances (EPSs) in membrane bioreactors: characteristics, roles in membrane fouling and control strategies. *Journal of Membrane Science* **460:** 110-125.

Liu, L., Liu, J., Gao, B., Yang, F. and Chellam, S. (2012). Fouling reductions in a membrane bioreactor using an intermittent electric field and cathodic membrane modified by vapor phase polymerized pyrrole. *Journal of Membrane Science* **394-395:** 202-208.

Liu, L., Shao, B. and Yang, F. (2013). Polydopamine coating-Surface modification of polyester filter and fouling reduction. *Separation and Purification Technology* **118:** 226-233.

Luo, M., Wen, W., Liu. J., Liu, L. and Jia, Z. (2011). Fabrication of SPES/Nano-TiO_2 composite ultrafiltration membrane and its anti-fouling mechanism. *Chinese Journal of Chemical Engineering* **19**(1): 45-51.

Luo, M.J., Zhao, J.Q., Tang, W. and Pu, C.S. (2005). Hydrophilic modification of poly(ether sulfone) ultrafiltration membrane surface by self-assembly of TiO_2 nanoparticles. *Applied Surface Science* **249**(1-4): 76–84.

Luther, S., Mettin, R., Koch, P. and Lauterborn, W. (2001). Observation of acoustic cavitation bubbles at 2250 frames per second. *Ultrasonics Sonochemistry* **8**(3): 159-162.

Lyko, S., Wintgens, T., Al-Halbouni, D., Baumgarten, S., Tacke, D., Drensla, K., Janot, A., Dott, W., Pinnekamp, J. and Melin, T. (2008). Long-term monitoring of a full-scale municipal membrane bioreactor- characterisation of foulants and operational performance. *Journal of Membrane Science* **317**(1-2): 78-87.

Ma, A., Lv, D., Zhuang, X. and Zhuang G. (2013). Quorum quenching in culturable phyllosphere bacteria from Tobacco. *International Journal of Molecular Sciences* **14**(7): 14607-14619.

Ma, L., Li, X., Du, G., Chen, J. and Shen, Z. (2005). Influence of the filtration modes on colloid adsorption on the membrane in submerged membrane bioreactor. *Colloids and Surfaces: A Physicochemical and Engineering Aspects* **264:** 120-125.

Ma, Z., Song, Y., Cai, Z., Lin, Z., Lin, G., Wang, Y. and Zhou, J. (2018). Anti-quorum Sensing Activities of Selected Coral Symbiotic Bacterial Extracts from the South China Sea. *Frontiers in Cellular and Infection Microbiology* **8:** 1-13.

Madaeni, S.S., Ghaemi, N., Alizadeh, A. and Joshaghani, M. (2011). Influence of photo-induced super hydrophilicity of titanium dioxide nanoparticles on the anti-fouling performance of ultrafiltration membranes. *Applied Surface Science* **257**(14): 6175-6180.

Magara, Y. and Itoh, M. (1991). The effect of operational factors on solid/liquid separation by ultra-membrane filtration in a biological denitrification system for collected human excreta treatment plants. *Water Science and Technology* **23**(7-9): 1583-1590.

Mahdavi, M., Ahmad, M.B., Haron, M.J., Namvar, F., Nadi, B., Rahman, M.Z.A. and Amin, J. (2013). Synthesis, surface modification and characterisation of biocompatible magnetic iron oxide nanoparticles for biomedical applications. *Molecules* **18**(7): 7533-7548.

Mahendran, B., Lin, H., Liao, B. and Liss, S.N. (2010). Surface properties of biofouled membranes from a submerged anaerobic membrane bioreactor after cleaning. *Journal of Environmental Engineering* **137**(6): 504-513.

Mahmoudi, E. and Ahmadi, A. (2012).The effect of quorum sensing inhibitor bacteria on pathogenicity of *Pectobacterium atrosepticum* Causal Agent of Potato Blackleg. *Journal of Research in Agricultural Science* **8**(2): 171-181.

Malaeb, L., Le-Clech, P., Vrouwenvelder, J.S., Ayoub, G.M. and Saikaly, P.E. (2013). Do biological-based strategies hold promise to biofouling control in MBRs?. *Water research* **47**(15): 5447-5463.

Malamis, S. and Andreadakis, A. (2009). Fractionation of proteins and carbohydrates of extracellular polymeric substances in a membrane bioreactor system. *Bioresource Technology* **100**(13): 3350-3357.

Mani, A., Hameed, S.S., Ramalingam, S. and Narayanan, M. (2012). Assessment of quorum quenching activity of *Bacillus* species against *Pseudomonas aeruginosa* MTCC2297. *Global Journal of Pharmacology* **6:** 118-125.

Maqbool, T., Khan, S.J., Waheed, H., Lee, C.H., Hashmi, I. and Iqbal, H. (2015). Membrane biofouling retardation and improved sludge characteristics using quorum quenching bacteria in submerged membrane bioreactor. *Journal of Membrane Science* **483:** 75-83.

Marius, S., Lucian, H., Marius, M., Daniela, P., Irina, G., Romeolulian, O., Simona, D. and Viorel, M. (2011). Enhanced antibacterial effect of silver nanoparticles obtained by electrochemical synthesis in poly(amide hydroxyurethane) media. *Journal of Materials Science- Materials in Medicine* **22**(4): 789-796.

Marrot, B., Barrios-Martinez, A., Moulin, P. and Roche, N. (2004). Industrial wastewater treatment in a membrane bioreactor: a review. *Environmental Progress & Sustainable Energy* **23**(1): 59-68.

Matosic, M., Crnek, V., Jakopovic, H.K. and Mijatovic, I. (2009). Municipal wastewater treatment in a membrane bioreactor. *Fresenius environmental bulletin* **18**(12): 2275-2281.

Matsumura, Y., Yoshikata, K., Kunisaki, S. and Tsuchido, T. (2003). Mode of bactericidal action of silver zeolite and its comparison with that of silver nitrate. *Applied and Environmental Microbiology* **69**(7): 4278-4281.

Maximous, N., Nakhla, G., Wan, W. and Wong, K. (2009). Preparation, characterization and performance of Al_2O_3/PES membrane for wastewater filtration. *Journal of Membrane Science* **341**(1-2): 67-75.

Meabe, E., Deleris, S., Soroa, S. and Sancho, L. (2013). Performance of anaerobic membrane bioreactor for sewage sludge treatment: Mesophilic and thermophilic processes. *Journal of Membrane Science* **446:** 26-33.

Meng, F., Chae, S.R., Drews, A., Kraume, M., Shin, H.S. and Yang, F. (2009). Recent advances in membrane bioreactors (MBRs): Membrane fouling and membrane material. *Water Research* **43**(6): 1489-1512.

Meng F., Shi, B., Yang, F. and Zhang, H. (2007a). New insights into membrane fouling in submerged membrane bioreactor based on rheology and hydrodynamics concepts. *Journal of Membrane Science* **302**(1-2): 87–94.

Meng, F., Shi, B, Yang, F. and Zhang, H. (2007b). Effect of hydraulic retention time on membrane fouling and biomass characteristics in submerged membrane bioreactors. *Bioprocess and Biosystems Engineering* **30**(5): 359-367.

Meng, F., Zhang, H., Yang, F., Zhang, S., Li, Y. and Zhang, X. (2006). Identification of activated sludge properties affecting membrane fouling in submerged membrane bioreactors. *Separation and Purification Technology* **51**(1): 95-103.

Metzger, U., Le-Clech, P., Stuetz, R.M., Frimmel, F.H. and Chen, V. (2007). Characterisation of polymeric fouling in membrane bioreactors and the effect of different filtration modes. *Journal of Membrane Science* **301**(1-2): 180-189.

Mikkelsen, L.H. and Keiding, K. (2002). Physico-chemical characteristics of full scale sewage sludges with implications to dewatering. *Water Research* **36**(10): 2451-2462.

Miller, D.J., Paul, D.R. and Freeman, B.D. (2014). An improved method for surface modification of porous water purification membranes. *Polymer* **55**(6): 1375-1383.

Miller, M.B. and Bassler, B.L. (2001). Quorum sensing in bacteria. *Annual Review of Microbiology* **55**:165-199.

Mills, A. and Hunte, S.L. (1997). An overview of semiconductor photocatalysis. *Journal of Photochemistry and Photobiology A: Chemistry* **108**(1): 1-35.

Mukai, T., Takimoto, K.; Kohno, T. and Okada, M. (1999). Ultrafiltration Behaviour of Extracellular and Metabolic Products in Activated Sludge System with UF Separation Process*. Water Research* **34**(3): 902-908.

Murthy, S. and Novak, J.T. (1998). Effects of potassium ion on sludge settling, dewatering and effluent properties. *Water Science and Technology* **37:** 317-324.

Muthukumaran, S., Kentish, S.E., Ashokkumar, M. and Stevens, G.W. (2005). Mechanisms for the ultrasonic enhancement of dairy whey ultrafiltration. *Journal of Membrane Science* **258**(1-2): 106-114.

Mutlu, B.K., Can, T.E., Koyuncu, I. and Lee, C.H. (2016). Quorum quenching MBR operations for biofouling control under different operation conditions and using different immobilization media. *Desalination and Water Treatment* **57**(38): 17696-17706.

Nagaoka, H., Ueda, S. and Miya, A. (1996). Influence of bacterial extracellular polymers on the membrane separation activated sludge process. *Water Science and Technology* **34**(9): 165-172.

Nagaoka, H., Yamanishi, S. and Miya, A. (1998). Modeling of biofouling by extracellular polymers in a membrane separation activated sludge system. *Water Science and Technology* **38**(4-5): 497-504.

Naghizadeh, A., Mahvi, A.H., Vaezi, F. and Naddafi, K. (2008). Evaluation of hollow fiber membrane bioreactor efficiency for municipal wastewater treatment. *Iranian Journal of Environmental Health, Science and Engineering* **5**(4): 257-268.

Nahm, C.H., Choi, D.C., Kwon, H., Lee, S., Lee, S.H., Lee, K., Choo, K.H., Lee, J.K., Lee, C.H. and Park, P.K. (2017a). Application of quorum quenching bacteria entrapping sheets to enhance biofouling control in a membrane bioreactor with a hollow fiber module. *Journal of Membrane Science* **526:** 264-271.

Nahm, C.H., Lee, S., Lee, S.H., Lee, K., Lee, J., Kwon, H., Choo, K.H., Lee, J.K., Jang, J.Y., Lee, C.H. and Park, P.K. (2017b). Mitigation of Membrane

Biofouling in MBR Using a Cellulolytic Bacterium, *Undibacterium* sp. DM-1, Isolated from Activated Sludge. *Journal of Microbiology and Biotechnology* **27**(3): 573-583.

Nair, R. and Chanda, S. (2008). Antimicrobial activity of *Terminalia catappa*, *Manilkara zapota*, and *Piper betle* leaf. *Indian Journal of Pharmaceutical Science* **70**(3): 390-393.

Neis, U., Nickel, K. and Tiehm, A. (2000). Enhancement of anaerobic sludge digestion by ultrasonic disintegration. *Water Science & Technology* **42**(9): 73-80.

Ng, L.Y., Mohammad, A.W., Leo, C.P. and Hilal, N. (2013). Polymeric membranes incorporated with metal/ metal oxide nanoparticles: A comprehensive review. *Desalination* **308**(2): 15-33.

Ngo, H.H., Guo, W. and Xing, W. (2008). Evaluation of a novel sponge-submerged membrane bioreactor (SSMBR) for sustainable water reclamation. *Bioresource Technology* **99**(7): 2429-2435.

Nuengjamnong, C., Kweon, J.H., Cho, J., Ahn, K.H. and Polprasert, C. (2005). Influence of extracellular polymeric substances on membrane fouling and cleaning in a submerged membrane bioreactor. *Colloidal Journal* **67**(3): 351–356.

Nywening, J.P., Zhou, H. and Husain, H. (2005). Influence of operating conditions on fouling behaviour in wastewater membrane bioreactor processes. Proceeding of the Water Environment Federation. Pp. 4791- 4808. Water Environment Federation, Alexandria.

Ochiai, S., Morohoshi, T., Kurabeishi, A., Shinozaki, M., Fujita, H., Sawada, I. and Ikeda, T. (2013). Production and degradation of n-acyl homoserine lactone quorum sensing signal molecules in bacteria isolated from activated sludge. *Bioscience, Biotechnology and Biochemistry* **77**(12): 2436-2440.

Ochiai, S., Yasumoto, S., Morohoshi, T. and Ikeda, T. (2014). AmiE, a novel N-acylhomoserine lactone acylase belonging to the amidase family, from the

activated sludge isolate *Acinetobacter* sp. strain Ooi24. *Applied and Environmental Microbiology* **80**(22): 6919-6925.

Ognier, S., Wisniewski, C. and Grasmick, A. (2002a). Influence of macromolecule adsorption during filtration of a membrane bioreactor mixed liquor suspension. *Journal of Membrane Science* **209**(1): 27-37.

Ognier, S., Wisniewski, C. and Grasmick, A. (2002b). Membrane fouling during constant flux filtration in membrane bioreactors. *Membrane Technology* **7**(1): 6–10.

Oh, H.S., Yeon, K.M., Yang, C.S., Kim, S.R., Lee, C.H., Park, S.Y., Han, J.Y. and Lee, J.K. (2012). Control of membrane biofouling in MBR for wastewater treatment by quorum quenching bacteria encapsulated in microporous membrane. *Environmental Science & Technology* **46**(9): 4877-4884.

Oh, Y.K., Lee, K.R., Ko, K.B. and Yeom, I.T. (2007). Effects of chemical sludge disintegration on the performance of wastewater treatment by membrane bioreactor. *Water Research* **41**(12): 2665–2671.

Park, J.Y., Acar, M.H., Akthakul, A., Kuhlman, W. and Mayes, A.M. (2006). Polysulfone-graft-poly(ethylene glycol) graft copolymers for surface modification of polysulfone membranes. *Biomaterials* **27**(6): 856-965.

Park, S.Y., Kang, H.O., Jang, H.S., Lee, J.K., Koo, B.T. and Yum, D.Y. (2005). Identification of extracellular N-acylhomoserine lactone acylase from a *Streptomyces* sp. and its application to quorum quenching. *Applied and Environmental Microbiology* **71**(5): 2632-2641.

Park, S.Y., Lee, S.J., Oh, T.K., Oh, J.W., Koo, B.T., Yum, D.Y. and Lee, J.K. (2003). AhID, an acylhomoserine lactonase in *Arthrobacter* sp., and predicted homologues in other bacteria. *Microbiology* **149**(6): 1541-1550.

Parsek, M.R., Val, D.L., Hanzelka, B.L., Cronan, J.E. and Greenberg, E.P. (1999). Acyl homoserine-lactone quorum-sensing signal generation. *Proceedings of the National Academy of Sciences* **96**(8): 4360-4365.

Paul, D. and Abanmy, A.R.M. (1990). Reverse osmosis membrane fouling- The final frontier. *UltraPureWater* **7**(3): 25-36.

Pervov, A.G. (1991). Scale formation prognosis and cleaning procedure schedules in reverse osmosis systems operation. *Desalination* **83**(1-3): 77-118.

Peternele, W.S., Fuentes, V.M., Fascineli, M.L., da Silva, J.R.., Silva, R.C., Lucci, C.M. and de Azevedo, R.B. (2014). Experimental investigation of the coprecipitation method: An approach to obtain magnetite and maghemite nanoparticles with improved properties. *Journal of Nanomaterials* **2014:** 1-10.

Pham, T.T.H., Brar, S.K., Tyagi, R.D. and Surampalli, R.Y. (2010). Influence of ultrasonication and Fenton oxidation pre-treatment on rheological characteristics of wastewater sludge. *Ultrasonics Sonochemistry* **17**(1): 38-45.

Praneeth, K., Moulik, S., Vadthya, P., Bhargava, S.K., Tardio, J. and Sridhar, S. (2014). Performance assessment and hydrodynamic analysis of a submerged membrane bioreactor for treating dairy industrial effluent. *Journal of Hazardous Materials* **274:** 300-313.

Prior, R.B. and Perkins, R.L. (1974). Artifacts induced by preparation for scanning electron microscopy in *Proteus mirabilis* exposed to carbenicillin. *Canadian Journal of Microbiology* **20**(5): 794-795.

Psoch, C. and Schiewer, S. (2005). Critical flux aspect of air sparging and backflushing on membrane bioreactors. *Desalination* **175**(1): 61-71.

Psoch, C. and Schiewer, S. (2006). Resistance analysis for enhanced wastewater membrane filtration. *Journal of Membrane Science* **280**(1-2): 284-297.

Radjenovic, J., Matosic, M., Mijatovic, I., Petrovic, M. and Barcelo, D. (2008). Membrane bioreactor (MBR) as an advanced wastewater treatment technology. In: Barcelo D. and Petrovic M. (Eds.) Emerging Contaminants from Industrial and Municipal Waste, pp. 37-101. Springer- Verlag, Berlin, Heidelberg.

Radjenovic, J., Petrovic, M. and Barcelo, D. (2007). Analysis of pharmaceuticals in wastewater and removal using a membrane bioreactor. *Analytical and Bioanalytical Chemistry* **387**(4): 1365-1377.

Rajesh, P.S. and Rai, V.R. (2014). Quorum quenching activity in cell-free lysate of endophytic bacteria isolated from *Pterocarpus santalinus* Linn. and its effect on quorum sensing regulated biofilm in *Pseudomonas aeruginosa* PAO1. *Microbiological Research* **169**(7-8): 561-569.

Ramesh, A., Lee, D.J. and Lai, J.Y. (2007). Membrane biofouling by extracellular polymeric substances or soluble microbial products from membrane bioreactor sludge. *Applied Microbiology and Biotechnology* **74**(3): 699-707.

Rani, S., Kumar, A., Malik, A.K. and Schmitt-Kopplin, P. (2011). Occurrence of N-Acyl homoserine lactones in extracts of bacterial strain of Pseudomonas aeruginosa and in sputum sample evaluated by gas chromatography–mass spectrometry. *American Journal of Analytical Chemistry* **2**(2): 294.

Rehman, Z.U. and Leiknes, T. (2018). Quorum Quenching Bacteria Isolated from Red Sea Sediments Reduces Biofilm Formation by *Pseudomonas aeruginosa*. *Frontiers in Microbiology* **9:** 1-13.

Rojas, M.H., Van Kaam, R., Schetrite, S. and Albasi, C. (2005). Role and variations of supernatant compounds in submerged membrane bioreactor fouling. *Desalination* **179**(1-3): 95-107.

Rosenberger, S., Evenblij, H., Te Poele, S., Wintgens, T. and Laabs, C. (2005). The importance of liquid phase analyses to understand fouling in membrane assisted activated sludge processes-six case studies of different European research groups. *Journal of Membrane Science* **263**(1-2): 113-126.

Rosenberger S., Kubin, K. and Kraume, M. (2002a). Rheology of activated sludge in membrane bioreactors. *Engineering in Life Sciences* **2**(9): 269–275.

Rosenberger, S. and Kraume, M. (2002). Filterability of activated sludge in membrane bioreactors. *Desalination* **146**(1-3): 373-379.

Rosenberger, S., Kruger, U., Witzig, R., Manz, W., Szewzyk, U. and Kraume, M. (2002b). Performance of a bioreactor with submerged membranes for aerobic treatment of municipal waste water. *Water Research* **36**(2): 413-420.

Ross, W.R., Barnard, J.P., Le-Roux, J., de Villiers, H.A. (1990). Application of ultrafiltration membranes for solid-liquid separation in anerobic digestion systems: The AUDF Process". *Water SA* **16:** 85-91.

Ross, W.R., Barnard, J.P., Strohwald, N.K.H., Grobler, C.J. and Sanetra, J. (1992). Practical application of the ADUF process to the full-scale treatment of a maize-processing effluent. *Water Science and Technology* **25**(10): 27-39.

Sato, T. and Ishii, Y. (1991). Effects of activated sludge properties on water flux of ultrafiltration membrane used for human excrement treatment. *Water Science and Technology* **23**(7-9): 1601-1608.

Sawada, I., Fachrul, R., Ito, T., Ohmukai, Y., Maruyama, T. and Matsuyama, H. (2012). Development of a hydrophilic polymer membrane containing silver nanoparticles with both organic antifouling and antibacterial properties. *Journal of Membrane Science* **387-388:** 1-6.

Schafer, A.I., Fane, A.G. and Waite, T.D. (2005). Nanofiltration- Principle and Applications. Elsevier Advanced Technology, U.K.

Seidel, A. and Elimelech, M. (2002). Coupling between chemical and physical interactions in natural organic matter (NOM) fouling of nanofiltration membranes: implications for fouling control. *Journal of Membrane Science* **203**(1-2): 245-255.

Serp, D., Mueller, M., Von Stockar, U. and Marison, I.W. (2002). Low-Temperature electron microscopy for the study of polysaccharide ultrastructures in hydrogels. II. Effect of temperature on the structure of Ca^{2+}- Alginate beads. *Biotechnology and Bioengineering* **79**(3): 253-259.

Shaker, S., Zafarian, S., Chakra, C.H.S. and Rao, K.V. (2013). Characterization of magnetite nanoparticles by sol-gel method for water treatment. *International Journal of Innovative Research in Science, Engineering and Technology* **2**(7): 2969-2973.

Shariati, S.R.P., Bonakdarpour, B., Zare, N. and Ashtiani, F.Z. (2011). The effect of hydraulic retention time on the performance and fouling characteristics of membrane sequencing batch reactors used for the treatment of synthetic petroleum refinery wastewater. *Bioresource Technology* **102**(17): 7692-7699.

Sheng, G.P., Yu, H.Q. and Li, X.Y. (2010). Extracellular polymeric substances (EPS) of microbial aggregates in biological wastewater treatment systems: a review. *Biotechnology Advances* **28**(6): 882-894.

Shepherd, R.W. and Lindow, S.E. (2009). Two dissimilar N-acyl homoserine lactone acylases of *Pseudomonas syringae* influence colony and biofilm morphology. *Applied and Environmental Microbiology* **75**(1): 45-53.

Shete, P.B., Patil, R.M., Ningthoujam, R.S., Ghosh, S.J. and Pawar, S.H. (2013). Magnetic core–shell structures for magnetic fluid hyperthermia therapy application. *New Journal of Chemistry* **37**(11): 3784-3792.

Shin, H.S. and Kang, S.T. (2003). Characteristics and fates of soluble microbial products in ceramic membrane bioreactor at various sludge retention times. *Water Research* **37**(1): 121-127.

Siddiqui, M.F., Sakinah, M.., Ismail, A.F., Matsuura, T. and Zularisam, A.W. (2012a). The anti-biofouling effect of Piper betle extract against *Pseudomonas aeruginosa* and bacterial consortium. *Desalination* **288:** 24-30.

Siddiqui, M.F., Sakinah, M., Singh, L. and Zularisam, A.W. (2012b). Targeting N-acyl-homoserine-lactones to mitigate membrane biofouling based on quorum sensing using a biofouling reducer. *Journal of Biotechnology* **161**(3): 190-197.

Silva, P.D., Moraes, C.D. and Samios, D. (2016). Iron oxide nanoparticles coated with polymer derived from epoxidized oleic acid and cis-1,2-cyclohexanedicarboxylic anhydride: synthesis and characterization. *Journal of Material Science and Engineering* **5:** 1-7.

Sio, C.F., Otten, L.G., Cool, R.H., Diggle, S.P., Braun, P.G., Bos, R., Daykin, M., Camara, M., Williams, P. and Quax, W.J. (2006). Quorum quenching by an N-acyl-homoserine lactone acylase from *Pseudomonas aeruginosa* PAO1. *Infection and Immunity* **74**(3): 1673-1682.

Skouteris, G., Saroj, D., Melidis, P., Hai, F.I. and Ouki, S. (2015). The effect of activated carbon addition on membrane bioreactor processes for wastewater treatment and reclamation–a critical review. *Bioresource Technology* **185:** 399-410.

Son, W.K., Youk, J.H., Lee, T.S. and Park, W.H. (2004). Preparation of antimicrobial ultrafine cellulose acetate fibers with silver nanoparticles. *Macromolecular Rapid Communications* **25**(18): 1632–1637.

Song, C., Ma, H., Zhao, Q., Song, S. and Jia, Z. (2012). Inhibition of quorum sensing activity by ethanol extract of *Scutellaria baicalensis* Georgi. *Journal of Plant Pathology & Microbiology* **S7:** 001- 004.

Sozanski, M.M., Kempa, E.S., Grocholski, K. and Bien, J. (1997). The rheological experiment in sludge properties research. *Water Science and Technology* **36**(11): 69-78.

Sponza, D.T. (2003). Investigation of extracellular polymer substances (EPS) and physicochemical properties of different activated sludge flocs under steady-state conditions. *Enzyme and Microbial Technology* **32**(3-4): 375-385.

Steen, M.L., Hymas, L., Havey, E.D., Capps, N.E., Castner, D.G. and Fisher, E.R. (2001). Low temperature plasma treatment of asymmetric polysulfone membranes for permanent hydrophilic surface modification. *Journal of Membrane Science* **188**(1): 97-114.

Strohwald, N.K.H. and Ross, W.R. (1992). Application of the ADUFR process to brewery effluent on a laboratory scale. *Water Science & Technology* **25**(10): 95-105.

Stypka, T., Plaza, E., Stypka, A., Trela, J. and Hultman, B. (2002). Regional planning and product recovery as tools for sustainable sludge management. *Water Science & Technology* **46**(4-5): 389-396.

Su, X., Tian, Y., Sun, Z., Lu, Y. and Li, Z. (2013). Performance of a combined system of microbial fuel cell and membrane bioreactor: wastewater treatment, sludge reduction, energy recovery and membrane fouling. *Biosensors and Bioelectronics* **49:** 92-98.

Sui, P.Z., Wen, X. and Huang, X. (2008). Feasibility of employing ultrasound for on-line membrane fouling control in an anaerobic membrane bioreactor. *Desalination* **219**(1-3): 203-213.

Sui, P.Z., Wen, X. and Huang, X. (2007). Membrane fouling control by ultrasound in an anaerobic membrane bioreactor. *Frontiers of Environmental Science and Engineering in China* **1**(3): 362-367.

Sulistyaningsih, T., Santosa, S.J., Siswanta, D. and Rusdiarso, B. (2017). Synthesis and characterization of magnetites obtained from mechanically and sonochemically assisted co-precipitation and reverse co-precipitation methods. *International Journal of Materials and Manufacturing* **5**(1): 16-19.

Sun, F.Y., Wang, X.M. and Li, X.Y. (2008). Visualisation and characterisation of biopolymer clusters in a submerged membrane bioreactor. *Journal of Membrane Science* **325**(2): 691–697.

Sun, W., Liu, J., Chu, H. and Dong, B. (2013). Pretreatment and membrane hydrophilic modification to reduce membrane fouling. *Membranes* **3**(3): 226-241.

Susanto, H., Arafat, H., Janssen, E.M.L. and Ulbricht, M. (2008). Ultrafiltration of polysaccharide-protein mixtures: Elucidation of fouling mechanisms and fouling control by membrane surface modification. *Separation and Purification Technology* **63**(3): 558-565.

Swift, S., Downie, J.A., Whitehead, N.A., Barnard, A.M., Salmond, G.P. and Williams, P. (2001). Quorum sensing as a population-density-dependent determinant of bacterial physiology. *Advances in Microbial Physiology* **45:** 199-270.

Tadkaew, N. (2010). Removal of trace organic contaminants by membrane bioreactors (MBRs). Ph.D. thesis, University of Wollongong, New South Wales, Australia.

Tan, L.Y., Yin, W.F. and Chan, K.G. (2013). *Piper nigrum*, *Piper betle* and *Gnetum gnemon* natural food sources with anti-quorum sensing properties. *Sensors* **13**(3): 3975-3985.

Tan, T.W. and Ng, H.Y. (2008). Influence of mixed liquor recycle ratio and dissolved oxygen on performance of pre-denitrification submerged membrane bioreactors. *Water research* **42**(4-5): 1122-1132.

Tang, C.Y., Chong, T.H. and Fane, A.G. (2011). Colloidal interactions and fouling of NF and RO membranes: A review. *Advances in Colloid and Interface Science* **164**(1-2): 126-143.

Taniguchi, M., Kilduff, J.E. and Belfort, G. (2003). Modes of natural organic matter fouling during filtration. *Environmental Science and Technology* **37**(8): 1676-1683.

Tay, J.H., Ivanov, V., Pan, S. and Tay, S.T. (2002). Specific layers in aerobically grown microbial granules. *Letters in Applied Microbiology* **34**(4): 254-257.

te Poele, S. and van der Graaf, J. (2005). Enzymatic cleaning in ultrafiltration of wastewater treatment plant effluent. *Desalination* **179**(1-3): 73-81.

Teychene, B., Guigui, C., Cabassud, C. and Amy, G. (2008). Toward a better identification of foulant species in MBR processes. *Desalination* **231**(1-3): 27-34.

Thunemann, A.F., Schutt, D., Kaufner, L., Pison, U. and Mohwald, H. (2006). Maghemite nanoparticles protectively coated with poly (ethylene imine) and poly (ethylene oxide)-b lock-poly (glutamic acid). *Langmuir* **22**(5): 2351-2357.

Tikariha, A. and Sahu, O. (2014). Study of characteristics and treatments of dairy industry waste water. *Journal of Applied and Environmental Microbiology* **2:** 16-22.

[TMS] The MBR Site. (2016). Oct., 10. homepage. <http://www.thembrsite.com>. Accessed 2016 Oct 10.

Tolwinska, H.M., Wencel, A. and Figaszewski, Z. (1998). The effect of hydrophilization of polypropylene membranes with alcohols on their transport properties. *Journal of Macromolecular Science* **35**(5): 857-865.

Tomaras, A.P., Dorsey, C.W., Edelmann, R.E. and Actis, L.A. (2003). Attachment to and biofilm formation on abiotic surfaces by *Acinetobacter baumannii*:

involvement of a novel chaperone- usher pili assembly system. *Microbiology* **149:** 3473-3484.

Torretta, V., Urbini, G., Raboni, M., Copelli, S., Viotti, P., Luciano, A. and Mancini, G. (2013). Effect of powdered activated carbon to reduce fouling in Membrane Bioreactors: A Sustainable Solution. Case Study. *Sustainability* **5:** 1510-1509.

Tran, T.D., Mori, S. and Suzuki, M. (2007). Plasma modification of polyacrylonitrile ultrafiltration membrane. *Thin Solid Films* **515**(9): 4148-4152.

Tu, X., Zhang, S., Xu, L., Zhang, M. and Zhu, J. (2010). Performance and fouling characteristics in a membrane sequence batch reactor (MSBR) system coupled with aerobic granular sludge. *Desalination* **261**(1-2): 191-196.

Unnanuntana, A., Bonsignore, L., Shirtliff, M.E. and Greenfield, E.M. (2009). The effects of farnesol on *Staphylococcus aureus* biofilms and osteoblasts: An in vitro study. *The Journal of Bone and Joint Surgery* **91**(11): 2683- 2692.

Urbain, V., Block, J.C. and Manem, J. (1993). Bioflocculation in Activated Sludge: An Analytic Approach. *Water Research* **27**(5): 829-838.

Uroz, S., Dessaux, Y. and Oger, P. (2009). Quorum sensing and quorum quenching: The Yin and Yang of bacterial communication. *ChemBioChem* **10**(2): 205-216.

Uroz, S., D'Angelo-Picard, C., Carlier, A., Elasri, M., Sicot, C., Petit, A., Oger, P., Faure, D. and Dessaux, Y. (2003). Novel bacteria degrading N-acylhomoserine lactones and their use as quenchers of quorum-sensing regulated functions of plant pathogenic bacteria. *Microbiology* **149**(8): 1981-1989.

Vidaurre, E.F.C., Achete, C.A., Gallo, F., Garcia, D., Simao, R. and Habert, A.C. (2002). Surface modification of polymeric materials by plasma treatment. *Materials Research* **5**(1): 37-41.

Visvanathan, C., Aim, R.B. and Parameshwaran, K. (2000). Membrane separation bioreactors for wastewater treatment. *Critical reviews in Environmental Science and Technology* **30**(1): 1-48.

Vrouwenvelder, H., Kruithof, J., Loosdrecht, M.V. (2010). Biofouling of membrane systems: a manageable problem? *Water* **53:** 49-50.

Waheed, H. and Hashmi, I. (2017). Combine effect of physical and biological based antifouling strategies in lab scale membrane bioreactor treating synthetic wastewater. *International Journal of Advances in Science Engineering and Technology* **5**(1): 76-79.

Waheed, H., Pervez, S., Hashmi, I., Khan, S.J. and Kim, S.R. (2018). High-performing antifouling bacterial consortium for submerged membrane bioreactor treating synthetic wastewater. *International Journal of Environmental Science and Technology* **15**(2): 395-404.

Waheed, H., Xiao, Y., Hashmi, I., Stuckey, D. and Zhou, Y. (2017). Insights into quorum quenching mechanisms to control membrane biofouling under changing organic loading rates. *Chemosphere* **182:** 40-47.

Wang, F., Lu, S. and Ji, M. (2006). Components of released liquid from ultrasonic waste activated sludge disintegration. *Ultrasonics Sonochemistry* **13**(4): 334-338.

Wang, H., Qiao, X., Chen, J., Wang, X. and Ding, S. (2005). Mechanisms of PVP in the preparation of silver nanoparticles (Review). *Materials Chemistry and Physics* **94**(2): 449-453.

Wang, Q., Wang, Z., Wu, Z., Ma, J. and Jiang, Z. (2012). Insights into membrane fouling of submerged membrane bioreactors by characterizing different fouling layers formed on membrane surfaces. *Chemical Engineering Journal* **179:** 169-177.

Wang, W., Yang, Q., Zheng, S. and Wu, D. (2013). Anaerobic membrane bioreactor (AnMBR) for bamboo industry wastewater treatment. *Bioresource Technology* **149:** 292-300.

Wang, X.M. and Li, X.Y. (2008). Accumulation of biopolymer clusters in a submerged membrane bioreactor and its effect on membrane fouling. *Water Research* **42**(4-5): 855-862.

Wang, X.M., Li, X.Y. and Huang, X. (2007). Membrane fouling in a submerged membrane bioreactor (SMBR): Characterisation of the sludge cake and its high filtration resistance. *Separation and Purification Technology* **52**(3): 439–445.

Wang, X.M., Sun, F.Y. and Li, X.Y. (2011a). Investigation of the role of biopolymer clusters in MBR membrane fouling using flash freezing and environmental scanning electron microscopy. *Chemosphere* **85**(7): 1154-1159.

Wang, Y.K., Sheng, G.P., Li, W.W., Huang, Y.X., Yu, Y.Y., Zeng, R.J. and Yu, H.Q. (2011b). Development of a novel bioelectrochemical membrane reactor for wastewater treatment. *Environmental Science & Technology* **45**(21): 9256-9261.

Wang, Z., Chu, J., Song, Y., Cui, Y., Zhang, H., Zhao, X., Li, Z. and Yao, J. (2009a). Influence of operating conditions on the efficiency of domestic wastewater treatment in membrane bioreactors. *Desalination* **245**(1-3): 73-81.

Wang, Z., Wu, Z. and Tang, S. (2009b). Extracellular polymeric substances (EPS) properties and their effects on membrane fouling in a submerged membrane bioreactor. *Water Research* **43**(9): 2504-2512.

Wang, Z., Wu, Z., Yin, X. and Tian, L. (2008). Membrane fouling in a submerged membrane bioreactor (MBR) under sub-critical flux operation: Membrane foulant and gel layer characterization. *Journal of Membrane Science* **325:** 238-244.

Wavhal, D.S. and Fisher, E.R. (2002). Hydrophilic modification of polyethersulfone membranes by low temperature plasma-induced graft polymerization. *Journal of Membrane Science* **209**(1): 255-269.

Weerasekara, N.A., Choo, K.H. and Lee, C.H. (2016). Biofouling control: bacterial quorum quenching versus chlorination in membrane bioreactors. *Water Research* **103:** 293-301.

Wei, C.H., Huang, X., Wang, C.W. and Wen, X.H. (2006). Effect of suspended carrier on membrane fouling in a submerged membrane bioreactor. *Water Science and Technology* **53**(6): 211-220.

Wei, Y., Han, B., Hu, X., Lin, Y., Wang, X. and Deng, X. (2012). Synthesis of Fe_3O_4 nanoparticles and their magnetic properties. *Procedia Engineering* **27:** 632-637.

Wen, J., Liu, Y., Tu, Y. and LeChevallier, M.W. (2015). Energy and chemical efficient nitrogen removal at a full-scale MBR water reuse facility. *AIMS Environmental Science* **2:** 42-55.

Wen, X., Ding, H., Huang, X. and Liu, R. (2004). Treatment of hospital wastewater using a submerged membrane bioreactor. *Process Biochemistry* **39**(11): 1427-1431.

Wen, X., Sui, P. and Huang, X. (2008). Exerting ultrasound to control the membrane fouling in filtration of anaerobic activated sludge-mechanism and membrane damage. *Water Science & Technology* **57**(5): 773-779.

Wenten, I.G. (2009). Performance of newly configured submerged membrane bioreactor for aerobic industrial wastewater treatment. *Reaktor* **12**(3): 137-145.

Widjaja, T., Altway, A. and Soeprijanto. (2010). Performance of submerged membrane bioreactor combined with powdered activated carbon addition for the treatment of an industrial wastewater. *IPTEK, The Journal for Technology and Science* **21**(1): 18-22.

Wilen, B.M., Keiding, K. and Nielsen, P.H. (2000). Anaerobic deflocculation and aerobic reflocculation of activated sludge. *Water Research* **34**(16): 3933-3942.

Williams, P., Winzer, K., Chan, W.C. and Camara, M. (2007). Look who's talking: communication and quorum sensing in the bacterial world. *Philosiophical Transcations of the Royal Series B: Biological Sciences* **362**(1483): 1119-1134.

Wisniewski, C. and Grasmick, A. (1998). Floc size distribution in a membrane bioreactor and consequences for membrane fouling. *Colloids and Surfaces A: Physicochemical and Engineering Aspects* **138**(2-3): 403-411.

Wiszniowski, J., Ziembinska, A. and Ciesielski, S. (2009). Membrane biological reactor (MBR) for treatment of wastewater contaminated by petroleum organic compounds. Proceedings of a Polish-Swedish–Ukrainian seminar. Pp. 27-33. KTH Royal Institute of Technology, Stockholm, Swedan.

Wong, C.S., Koh, C.L., Sam, C.K., Chen, J.W., Chong, Y.M., Yin, W.F. and Chan, K.G. (2013). Degradation of bacterial quorum sensing signalling molecules by the microscopic yeast *Trichosporon loubieri* isolated from tropical wetland waters. *Sensors* **13**(10): 12943-12957.

Woo, Y.C., Lee, J.J., Oh, J.S., Jang, H.J. and Kim, H.S. (2013). Effect of chemical cleaning conditions on the flux recovery of fouled membrane. *Desalination and Water Treatment* **51**(25-27): 5268-5274.

Woo, Y.C., Lee, J.K. and Kim, H.S. (2014). Fouling characteristics of microfiltration membranes by organic and inorganic matter and evaluation of flux recovery by chemical cleaning. *Desalination and Water Treatment* **52**(37-39): 6920-6929.

Wu, J. and Huang, X. (2010). Use of ozonation to mitigate fouling in a long-term membrane bioreactor. *Bioresource Technology* **101**(15): 6019-6027.

Wu, J., Chen, F. Huang, X., Geng, W. and Wen, X. (2006). Using inorganic coagulant to control membrane fouling in a submerged membrane bioreactor. *Desalination* **197**(1-3): 124-136.

Wu, K.J., Saratale, G.D., Lo, Y.C., Chen, W.M., Tseng, Z.J., Chang, M.C., Tsai, B.C., Su, A. and Chang, J.S. (2008a). Simultaneous production of 2,3-butanediol, ethanol and hydrogen with a *Klebsiella* sp. strain isolated from sewage sludge. *Bioresource Technology* **99**(17): 7966-7970.

Wu, W., He, Q. and Jiang, C. (2008b). Magnetic iron oxide nanoparticles: Synthesis and surface functionalization strategies. *Nanoscale Research Letters* **3**(11): 397-415.

Wu, Z., Wang, X., Wang, Z. and Du, X. (2009). Identification of sustainable flux in the process of using flat-sheet membrane simultaneous thickening and digestion of waste activated sludge. *Journal of Hazardous Materials* **162**(2-3): 1397–1403.

Xi, Z.Y., Xu, Y.Y., Zhu, L.P., Wang, Y. and Zhu, B.K. (2009). A facile method of surface modification for hydrophobic polymer membranes based on the adhesive behavior of poly(DOPA) and poly(dopamine). *Journal of Membrane Science* **327**(1-2): 244-253.

Xia, S., Guo, J. and Wang, R. (2008). Performance of a pilot scale submerged membrane bioreactor (MBR) in treating bathing wastewater. *Bioresource Technology* **99**(15): 6834-6843.

Xia, T., Gao, X., Wang, C., Xu, X. and Zhu, L. (2016). An enhanced anaerobic membrane bioreactor treating bamboo industry wastewater by bamboo charcoal addition: performance and microbial community analysis. *Bioresource Technology* **220:** 26-33.

Xiao, B., Yang, F. and Liu, J. (2011). Enhancing simultaneous electricity production and reduction of sewage sludge in two-chamber MFC by aerobic sludge digestion and sludge pretreatments. *Journal of Hazardous Materials* **189**(1-2): 444-449.

Xiong, Y. and Liu, Y. (2010). Biological control of microbial attachment: a promising alternative for mitigating membrane biofouling. *Applied Microbiology and Biotechnology* **86**(3): 825-837.

Xu, G., Chen, S., Shi, J., Wang, S. and Zhu, G. (2010a). Combination treatment of ultrasound and ozone for improving solubilization and anaerobic biodegradability of waste activated sludge. *Journal of Hazardous Materials* **180**(1-3): 340-346.

Xu, H. and Liu, Y. (2011). Control and cleaning of membrane biofouling by energy uncoupling and cellular communication. *Environmental Science & Technology* **45**(2): 595-601.

Xu, M., Wen, X., Huang, X. and Li, Y. (2010b). Membrane fouling control in an anaerobic membrane bioreactor coupled with online ultrasound equipment for digestion of waste activated sludge. *Separation Science and Technology* **45**(7): 941-947.

Xuan, W., Bin, Z., Zhiqiang, S., Zhigang, Q., Zhaoli, C., Min, J., Junwen, L. and Jingfeng, W. (2010). The EPS characteristics of sludge in an aerobic granule membrane bioreactor. *Bioresource Technology* **101**(21): 8046-8050.

Yan, L., Li, Y.S. and Xiang, C.B. (2005). Preparation of poly(vinylidene fluoride) ultrafiltration membrane modified by nano-sized alumina and its antifouling research. *Polymer* **46**(18): 7701-7706.

Yang, Q., Chen, J. and Zhang, F. (2006). Membrane fouling control in a submerged membrane bioreactor with porous, flexible suspended carriers. *Desalination* **189**(1-3): 292-302.

Yang, X.C., Shang, Y.L., Li, Y.H., Zhai, J., Foster, N.R., Li, Y.X., Zou, D. and Pu, Y. (2014). Synthesis of monodisperse Iron oxide nanoparticles without surfactants. *Journal of Nanomaterials* **2014:** 1-5

Yang, X.L., Song, H.L., Chen, M. and Cheng, B. (2011). Characterizing membrane foulants in MBR with addition of polyferric chloride to enhance phosphorus removal. *Bioresource Technology* **102**(20): 9490-9496.

Ye, Y., Le-Clech, P., Chen, V. and Fane, A.G. (2005). Evolution of fouling during crossflow filtration of model EPS solutions. *Journal of Membrane Science* **264**(1-2): 190–199.

Yeon, K.M., Cheong, W.S., Oh, H.S., Lee, W.N., Hwang, B.K., Lee, C.H., Beyenal, H. and Lewandowski, Z. (2009a). Quorum Sensing: A New Biofouling Control Paradigm in a Membrane Bioreactor for Advanced Wastewater Treatment. *Environmental Science & Technology* **43**(2): 380-385.

Yeon, K.M., Lee, C.H. and Kim, J. (2009b). Magnetic enzyme carrier for effective biofouling control in the membrane bioreactor based on enzymatic quorum quenching. *Environmental Science & Technology* **43**(19): 7403-7409.

Yigit, N.O., Harman, I., Civelekoglu, G., Koseoglu, H., Cicek, N. and Kitis, M. (2008). Membrane fouling in a pilot-scale submerged membrane bioreactor operated under various conditions. *Desalination* **231**(1-3): 124-132.

Yin, W.F., Tung, H.J., Sam, C.K., Koh, C.L. and Chan, K.G. (2012). Quorum Quenching *Bacillus sonorensis* isolated from Soya Sauce Fermentation Brine. *Sensors* **12**(4): 4065-4073.

Ying, Z. and Ping, G. (2006). Effect of powdered activated carbon dosage on retarding membrane fouling in MBR. *Separation and Purification Technology* **52**(1): 154-160.

Yogalakshmi, K.N. (2008). Performance of membrane bioreactor under shock load conditions. Ph.D. thesis, Anna University, Chennai, India.

Yoon, S.H., Kim, H.S. and Lee, S. (2004a). Incorporation of ultrasonic cell disintegration into a membrane bioreactor for zero sludge production. *Process Biochemistry* **39**(2): 1923-1929.

Yu, H.Y., Hu, M.X., Xu, Z.K., Wang, J.L. and Wang, S.Y. (2005a). Surface modification of polypropylene microporous membranes to improve their antifouling property in MBR: NH_3 plasma treatment. *Separation and Purification Technology* **45**(1): 8-15.

Yu, H.Y., Xie, Y.J., Hu, M.H., Wang, J.L., Wang, S.Y. and Xu, Z.K. (2005b). Surface modification of polypropylene microporous membrane to improve its antifouling property in MBR: CO_2 plasma treatment. *Journal of Membrane Science* **254**(1-2): 219-227.

Yun, W. (2016). Application of quorum quenching to control microbial biofouling in membrane bioreactors. Ph.D. thesis, National University of Singapore, Singapore.

Zahin, M., Hasan, S., Aqil, F., Khan, M.S., Husain, F.M. and Ahmad, I. (2010). Screening of certain medicinal plants from India for their anti-quorum sensing activity. *Indian Journal of Experimental Biology* **48**(12): 1219-1224.

Zeng, J., Gao, J.M., Chen, Y.P., Yan, P., Dong, Y., Shen, Y., Guo, J.S., Zeng, N. and Zhang, P. (2016). Composition and aggregation of extracellular polymeric substances (EPS) in hyperhaline and municipal wastewater treatment plants. *Scientific Reports* **6:** 26721.

Zhang, C., Zhan, S., Wang, J., Liu, Z., You, H. and Jia, Y. (2017). Isolation and characterization of seven quorum quenching bacteria for biofouling control in MBR. *Clean Technologies and Environmental Policy* **19**(4): 991-1001.

Zhang, C.Y., Ding, Yi, Yuan, L.M., Zhang, Y.Q. and Xi, D.L. (2007a). Characteristics of membrane fouling in an anaerobic- (Anoxic/Oxic)- MBR process. *Journal of China University of Mining and Technology* **17**(3): 387-392.

Zhang, G., Yang, J., Liu, H. and Zhang, J. (2009a). Sludge ozonation: disintegration, supernatant changes and mechanisms. *Bioresource Technology* **100**(3): 1505-1509.

Zhang, G., Zhang, P., Gao, J. and Chen, Y. (2008a). Using acoustic cavitation to improve the bio-activity of activated sludge. *Bioresource Technology* **99**(5): 1497-1502.

Zhang, H., Gao, Z., Zhang, L. and Song, L. (2014). Performance enhancement and fouling mitigation by organic flocculant addition in membrane bioreactor at high salt shock. *Bioresource Technology* **164:** 34-40.

Zhang, H., Xia, J., Yang, Y., Wang, Z. and Yang, F. (2009b). Mechanism of calcium mitigating membrane fouling in submerged membrane bioreactors. *Journal of Environmental Sciences* **21**(8): 1066-1073.

Zhang, H.F., Sun, B.S., Zhao, X.H. and Gao, Z.H. (2008b). Effect of ferric chloride on fouling in membrane bioreactor. *Separation and Purification Technology* **63**(2): 341-347.

Zhang, J., Loong, W.L.C., Chou, S., Tang, C., Wang, R. and Fane, A.G. (2012a). Membrane biofouling and scaling in forward osmosis membrane bioreactor. *Journal of Membrane Science* **403:** 8-14.

Zhang, K., Choi, H., Dionysiou, D.D., Sorial, G.A. and Oerther, D.B. (2006). Identifying pioneer bacterial species responsible for biofouling membrane bioreactors. *Environmental Microbiology* **8**(3): 433-440.

Zhang, M., Nguyen, Q.T. and Ping, Z. (2009c). Hydrophilic modification of poly (vinylidene fluoride) microporous membrane. *Journal of Membrane Science* **327**(1-2): 78-86.

Zhang, M., Zhang, K., Gusseme, B.D. and Verstraete, W. (2012b). Biogenic silver nanoparticles (bio-Ag^0) decrease biofouling of bio- Ag^0/PES nanocomposite membranes. *Water Research* **46**(7): 2077-2087.

Zhang, P., Zhang, G. and Wang, W. (2007b). Ultrasonic treatment of biological sludge: Floc disintegration, cell lysis and inactivation. *Bioresource Technology* **98**(1): 207-210.

Zhang, Y., Tian, J., Liang, H., Nan, J., Chen, Z. and Li, G. (2011). Chemical cleaning of fouled PVC membrane during ultrafiltration of algal-rich water. *Journal of Environmental Sciences* **23**(4): 529-536.

Zheng, Y.Y., Wang, X.B., Shang, L., Li, C.R., Cui, C., Dong, W.J., Tang, W.H. and Chen, B.Y. (2010). Fabrication of shape controlled Fe_3O_4 nanostructure. *Materials Characterization* **61**(4): 489-492.

Zhidong, L., Yong, Z., Xincheng, X., Lige, Z. and Dandan, Q. (2009). Study on anaerobic/aerobic membrane bioreactor treatment for domestic wastewater. *Polish Journal of Environmental Studies* **18**(5): 957-963.

Zhu, H., He, C.C. and Chu, Q.H. (2011). Inhibition of quorum sensing in *Chromobacterium violaceum* by pigments extracted from *Auricularia auricular*. *Letters in Applied Microbiology* **52**(3): 269-274.

Zhu, J., Dizin, E., Hu, X., Wavreille, A.S., Park, J. and Pei, D. (2003). S-Ribosylhomocysteine (LuxS) is a mononuclear iron protein. *Biochemistry* **42**(16): 4717-4726.

Zodrow, K., Brunet, L., Mahendra, S., Li, D., Zhang, A., Li, Q. and Alvarez, P.J. (2009). Polysulfone ultrafiltration membranes impregnate with silver

nanoparticles show improved biofouling resistance and virus removal. *Water Research* **43**(3): 715-723.

Publications in journals

1. **Kaur, J.** and Yogalakshmi K.N. (2018). Control of sludge microbial biofilm by novel quorum quenching bacteria *Pseudomonas nitroreducens* JYQ3 and *Pseudomonas* JYQ4 encapsulated sodium alginate- magnetic iron nanocomposites. *International Journal of Biodeterioration and Biodegradation* 134:68-75. (Impact factor: 3.824).

2. **Kaur, J.** and Yogalakshmi K.N. (2018). Screening of quorum quenching activity of the bacteria isolated from dairy industry waste activated sludge. *International Journal of Environmental Science and Technology* DOI 10.1007/s13762-018-1930-5. (Impact factor: 2.031).

3. **Kaur, J.** and Yogalakshmi K.N. (2017). Efficacy of quorum quenching bacteria *Bacillus cereus* 1306 encapsulated sodium alginate- magnetic iron nanocomposites in controlling quorum sensing mediated biofilm formation. Environment & We: An *International Journal of Science and Technology* 12(1-3): 29-36. (ISSN: 0975-7120).

4. **Kaur, J.** and Yogalakshmi K.N. (2013). Impact of treated industrial wastewater on crop productivity: A Mini Review. *International Journal of Environmental Research and Development* 3(6): 42-46. (ISSN: 2249- 3131).

Publications in conference proceedings

1. **Kaur, J.** and Yogalakshmi. K.N. (2016). Counteracting membrane biofouling through *Pseudomonas nitroreducens* JYQ3 encapsulated in sodium alginate-magnetic iron nanoparticle composites. Proceedings of International Conference on Water: From pollution to Purification, Inter University Instrumentation Centre, School of Environmental Sciences and Advanced Centre of Environmental Studies and Sustainable development, Mahatma Gandhi University, Kottayam, Kerala 12-15 December, 2016.

2. **Kaur, J.** and Yogalakshmi. K.N. (2013). Screening of Quorum Quenching Bacteria in Dairy Industry Wastewater. Proceedings of International conference on Health,

Environment and Industrial Biotechnology ICHEIB (BioSangham 2013), Department of Biotechnology, Motilal Nehru National Institute of Technology, Allahabad, 21-23 November 2013.

Book chapters

1. **Kaur, J.** and Yogalakshmi. K.N. (2018). Exploring the potential of carbohydrate rich algal biomass as feedstock for bioethanol production. In: Advances in Biofeedstocks and Biofuels; Volume 3: Liquid Biofuel production. Wiley Scrivener Publishing LLC, Salem. MA. https://doi.org/10.1002/9781119459866.ch5

List of conferences

Oral presentation

1. **Kaur, J.** and Yogalakshmi. K.N. (2016). Interruption of cell-to-cell communication through quorum quenching bacteria immobilized magnetic iron nanocomposite beads. National conference on Emerging Trends in biotechnology: A paradigm shift to cleaner and greener India at Khalsa college, Patiala held on 8th October, 2016.
2. **Kaur, J.** and Yogalakshmi. K.N. (2013). Impact of treated industrial wastewater on crop productivity: A Mini Review. International conference on Sustainable innovative techniques in Civil and Environmental Engineering (SITCEE 2013) at JNU, New Delhi held on 5-6th June 2013.

Poster presentation

1. **Kaur, J.** and Yogalakshmi. K.N. (2016). Counteracting membrane biofouling through *Pseudomonas nitroreducens* JYQ3 encapsulated in sodium alginate-magnetic iron nanoparticle composites. International Conference on Water: From pollution to Purification at Kottayam, Kerala held on 12-15th December, 2016.
2. **Kaur, J.** and Yogalakshmi K.N (2015). Germination behaviour of barley grains grown in Fertilizer industry wastewater. National Workshop on Advances in Agricultural Sciences & Biotechnology organized by DAV College, Jalandhar; February 28, 2015

3. **Kaur, J.** and Yogalakshmi. K.N. (2015). Removal of heavy metals from industrial wastewater using membrane filtration- A Review. One day National Workshop on Training the Trainers- Water quality and Health at Central University of Punjab, Bathinda held on 11th February, 2015.
4. **Kaur, J.** and Yogalakshmi. K.N. (2013). Screening of Quorum Quenching Bacteria in Dairy Industry Wastewater. International conference on Health, Environment and Industrial Biotechnology ICHEIB (BioSangham 2013) at Allahabad held on 21-23rd November 2013.
5. **J. Kaur**, Yogalakshmi. K. N and P. Ramarao (2011). Studies on effect of wastewater germination and growth of *Hordeum vulgare.* National Seminar on Environment and Health held at Central University of Punjab, Bathinda, September 2011.

Workshops/ Training programs/ Short term course/ Awareness programme

1. Attended Science Academics' Refresher course on "Plant Taxonomy, Phytogeography and Ecology" sponsored by Indian Academy of Sciences, Bangalore and organized by Central University of Punjab, Bathinda from 5th March to 20th March, 2019.
2. Attended one week short term course/ Faculty development program (TEQIP- III sponsored) on "Advances in Enzyme and Bioprocess Engineering" organized by Department of Biotechnology, Dr. BR Ambedkar National Institute of Technology, Jalandhar, Punjab from 7th February to 11th February, 2019.
3. Participated in the "Acquaintance Program of Inter University Accelerator Centre, New Delhi" organized by Central University of Punjab, Bathinda on 4th April, 2016.
4. Participated in a symposium on "Recent trends in Biological sciences" held at Centre for Animal Sciences, Central University of Punjab, Bathinda on 29th March, 2016.
5. Participated in one week training program on hands on "Analytical and molecular techniques "Biochemical based biorefineries for advanced biofuels and value added products" organized by Sardar Swaran Singh National Institute of Bioenergy, Kapurthala, Punjab from 14th to 18th March, 2016.

6. Participated in a seminar on “The evolving importance of intellectual property rights” organized by Intellectual Property Rights Cell (IPR Cell), Central University of Punjab, Bathinda on 30th January, 2016.
7. Attended Short term course on “Advances in Industrial Biotechnology” organized by Department of Biotechnology, Dr. BR Ambedkar National Institute of Technology, Jalandhar, Punjab from 30th November to 4th December, 2015.
8. Attended training programme on “Vermicomposting technology/ Apiculture” under the aegis of Community Development Cell of , Central University of Punjab, Bathinda from 12th April, 2015 to 31st October, 2015.
9. Attended one day awareness programme on “Biodiversity for Sustainable Development” organized by Centre for Environmental Science and Technology, Central University of Punjab, Bathinda in collaboration with Punjab Biodiversity Board and sponsored by National Biodiversity Authority, Govt. of India on 22nd May, 2015.
10. Attended 2-day training programme on “ArcGIS 10.3” held by ESRI India Pvt. Ltd. at Computer Centre, Central University of Punjab, Bathinda on 13th and14th May, 2015.
11. Participated in 13th Satellite Based Distance Learning Program on “Basics of remote sensing, GIS & GNSS” held at Central University of Punjab, Bathinda from 4th August to 14th November, 2014.
12. Participated in the 82nd BRNS-IANCAS National workshop on “Radiochemistry and Applications of Radioisotopes” conducted by Amity University, Haryana and Indian Association of Nuclear Chemists and Allied Scientists (IANCAS) from 12th to 20th March, 2013.